Title
Studies with calcium channel blockers

Author
Boyd, Rebecca A

Publication Date
1988

Peer reviewed|Thesis/dissertation

Studies with Calcium Channel Blockers: Molecular Pharmacology and Clinical Pharmacokinetics

by

Rebecca A. Boyd, B.Sc.(Pharm.), M.Sc., Dalhousie University

DISSERTATION

Submitted in partial satisfaction of the requirements for the degree of

DOCTOR OF PHILOSOPHY

in

Pharmaceutical Chemistry

in the

GRADUATE DIVISION

of the

UNIVERSITY OF CALIFORNIA

San Francisco

To my parents,

Ronald and Martha Boyd,

whose unfailing love, encouragement, and support

have made this possible.

Acknowledgements

There are many people who have played a part in the completion of this dissertation and to whom I am very grateful. In particular, I would like to express my deep appreciation:

To my advisor, Dr. Kathleen Giacomini. With her guidance, support and encouragement, and from her example, I have learned far more than what is contained in these pages.

To Dr. Leslie Benet and Dr. Bertram Katzung, whose valuable comments and criticism during the preparation of this dissertation resulted in significant improvements.

To Dr. Wendel Nelson for his help with the 1,4-dihydropyridine syntheses and the interpretation of the NMR and mass spectra of the products, and for providing me with compounds, in particular, the photoaffinity label studied in Chapter 5.

To Fee Mi Wong, Andrew Hui, Shu Chin, Donald Chang and Oluta Don-Pedro for their tremendous help in the laboratory.

To the staff of the Drug Studies Unit for their help with the clinical study.

To my family and friends, who were both far (my parents, my brother Malcolm and sister-in-law Marline, Dawn (Fig) Frail, Ingrid Sketris and Elizabeth Foy) and near (Anne Gillis, Ulf Eriksson, and, especially, Mathew Whittico) during these years of graduate study and whose support, encouragement and friendship meant a great deal to me.

To the University of California for the financial support I received in the form of a Regents Fellowship and a Chancellors Fellowship.

Table of Contents

Page

Dedication ii

Acknowledgements iii

List of Tables xi

List of Figures xiii

Abstract xvii

Chapter 1

Introduction - The Mechanism of Action of 1,4-Dihydropyridine Calcium Channel Blockers in Myocardium 1

Overall Goals 1

Background 1

History 1

The Role of Calcium in the Myocardium 3

Electrical Events 4

Mechanical Events 7

Mechanism of Action of the 1,4-Dihydropyridine Calcium Channel Blockers 7

Methods to Study the Mechanism of Action of the 1,4-Dihydropyridines 10

Radioligand Binding Experiments 10

Pharmacologic Response Experiments 11

Choice of Methods 12

Specific Objectives 13

Chapter 2

Synthesis of 1,4-Dihydropyridine Compounds 14

Introduction 14

Methods 15
Choice of Compounds 15
Synthesis 16
Confirmation of Structures 18
Chemicals 18
Results 19
Discussion 20

Chapter 3

Comparison of Binding Affinities and Negative Inotropic Potencies of the 1,4–Dihydropyridine Calcium Channel Blockers in Rabbit Myocardium 23
Introduction 23
Methods 24
Chemicals 24
Radioligand Binding Studies 25
Pharmacologic Response Studies 26
Data Analysis 27
Statistical Analysis 33
Results 33
Radioligand Binding Studies 33
Pharmacologic Response Studies 38
Discussion 41

Chapter 4

Species Differences in the Negative Inotropic Response of 1,4-Dihydropyridine Calcium Channel Blockers in Myocardium 54
Introduction 54
Methods 55
Chemicals 55

Radioligand Binding Studies 55
Pharmacologic Response Studies 56
Calcium Concentration-Response Studies 58
Data Analysis 58
Statistical Analysis 60
Results 60
Radioligand Binding Studies 60
Pharmacologic Response Studies 64
Discussion 65

Chapter 5

Characterization of Affinity Labels for the 1,4-Dihydropyridine Calcium Channel Blocker Receptor 75
Introduction 75
Background 76
Photoaffinity Labeling Studies 82
Background 82
Goals 85
Methods 86
Binding Characteristics of Nonphotoactivated GK-III-120D . 86
Photoactivation Procedures 88
Results 90
Binding Characteristics of Nonphotoactivated GK-III-120D . 90
Photoactivation Procedures 90
Discussion 100
Chemoaffinity Labeling Studies 109
Background 109
Goals 113

Methods 113
Chemicals 113
Sodium Dodecyl Sulfate Polyacrylamide Gel Electrophoresis (SDS-PAGE) 113
Preparation of Samples 114
Dissociation Experiments 115
Results 116
Discussion 120
Summary 122

Chapter 6

Introduction - The Pharmacokinetics and Pharmacodynamics of Diltiazem in Humans 127
Background 127
Clinical Pharmacology 129
Pharmacokinetics 130
Single Dose Pharmacokinetics 130
Absorption and Bioavailability 130
Distribution 135
Metabolism and Excretion 135
Clearance 137
Multiple Dose Pharmacokinetics 138
Pharmacokinetics in Renal Disease 140
Age-Related Pharmacokinetics 141
Pharmacodynamics 141
Summary 144
Specific Objectives of Part 2 145

Chapter 7

The Pharmacokinetics and Pharmacodynamics of Diltiazem and its Metabolites In Healthy Adults after a Single Oral Dose 146

Introduction 146

Methods 147

Clinical Protocol 147

Assay of Diltiazem and Metabolites in Biological Samples 149

Chemicals 149

HPLC System 149

Extraction Procedure 150

Validation of the Assay System 150

Plasma Protein Binding 151

Chemicals 151

Methods 151

Data Analysis 153

Pharmacokinetic Analysis 153

Pharmacodynamic Analysis 154

Plasma Protein Binding 154

Results 155

Validation of the HPLC Assay for Diltiazem, DAD and NDD 155

Results of the Clinical Study 159

Subject Characteristics 159

Pharmacokinetics 159

Plasma Protein Binding 166

Pharmacodynamics 168

Discussion 169

Pharmacokinetics 171

Pharmacodynamics 175

Chapter 8

Summary and Conclusions 178

Comparison of Binding Affinities and Negative Inotropic Potencies of the 1,4-Dihydropyridine Calcium Channel Blockers in Rabbit Myocardium 179

Species Differences in the Negative Inotropic Response of 1,4-Dihydropyridine Calcium Channel Blockers in Myocardium 180

Characterization of Affinity Labels for the 1,4-Dihydropyridine Calcium Channel Blocker Receptor 181

The Pharmacokinetics and Pharmacodynamics of Diltiazem and its Metabolites in Healthy Adults after a Single Oral Dose 183

References 186

Appendix A

NMR and Mass Spectra of Synthesized 1,4-Dihydropyridine Compounds 209

Appendix B

Derivation of Equations 219

Appendix C

Results of Computer Fits of Data from Radioligand Binding Experiments in Rabbit Ventricular Membrane Particulates 226

Appendix D

Results of Computer Fits of Data from Pharmacologic Response Experiments in Rabbit Right Ventricular Papillary Muscles 229

Appendix E

Results of Radioligand Binding and Pharmacologic Response Experiments in Rabbit Aorta 232

Appendix F

Results of Computer Fits of Data from Radioligand Binding Experiments in Rat Myocardial Membrane Particulates 233

Appendix G

Results of Computer Fits of Data from Pharmacologic Response Experiments in Rat Right Ventricular Strips 236

Appendix H

Summary of Calcium Concentration–Response Experiments 237

Appendix I

Chemical Structures of Additional 1,4-Dihydropyridine Compounds 240

Appendix J

SDS-PAGE Stock Solutions 242

Appendix K

Summary of Data for Each Volunteer in Diltiazem Study 246

List of Tables

Page

Table 1. The chemical structures of the 1,4-dihydropyridine compounds synthesized by the Hantzsch reaction. 17

Table 2. Melting points of synthesized 1,4-dihydropyridine compounds..... 19

Table 3. Results of computer fits of data from [^{3}H]nitrendipine saturation binding experiments in rabbit ventricular membrane particulates 34

Table 4. Chemical structures of the 1,4-dihydropyridine (DHP) compounds used in the binding and response studies. 36

Table 5. Mean IC_{50} values for inhibition of specific [^{3}H]nitrendipine binding and inhibition of isometric contractions in rabbit myocardium 38

Table 6. Results of computer fits of data from [^{3}H]nitrendipine saturation binding experiments in rabbit ventricular membrane particulates and rat myocardial membrane particulates 61

Table 7. Mean K_i values for inhibition of specific [^{3}H]nitrendipine binding in rat and rabbit myocardium 65

Table 8. Comparison of the negative inotropic response for selected 1,4-dihydropyridine compounds in rat and rabbit myocardium..... 67

Table 9. Summary of results of radiation inactivation target size analysis studies of the 1,4-dihydropyridine receptor from the literature..... 79

Table 10. Summary of results of studies in the literature identifying subunits of 1,4-dihydropyridine receptor/calcium channel after solubilization and purification..... 81

Table 11. Summary of results of photoaffinity labeling studies of the 1,4-dihydropyridine receptor from the literature 86

Table 12. Summary of results of chemoaffinity labeling studies of the 1,4-dihydropyridine receptor from the literature 111

Table 13. Summary of results of immunochemical studies of the 1,4-dihydropyridine receptor from the literature 125
Table 14. Summary of results of pharmacokinetic studies of diltiazem 132
Table 15. Between-day precision of standard curves for diltiazem, NDD and DAD in plasma and urine 157
Table 16. Accuracy and precision of the assay for diltiazem, NDD and DAD in plasma 158
Table 17. Accuracy and precision of the assay for diltiazem, NDD and DAD in urine 160
Table 18. Summary of subject characteristics 161
Table 19. Half-lives of diltiazem, NDD and DAD 163
Table 20. Area under the diltiazem plasma concentration-time curve 165
Table 21. Renal clearances of diltiazem, NDD and DAD 166
Table 22. Unbound fraction (fu) of diltiazem, NDD and DAD in plasma from six subjects 167
Table 23. Unbound renal clearances of diltiazem, NDD and DAD 168

List of Figures

Page

Figure 1. Chemical structures of the prototypical representatives of the three major chemical classes of calcium channel blockers..... 2

Figure 2. Schematic representation of a myocardial cell depicting the processes involved in cellular calcium regulation..... 5

Figure 3. The changes in the conductance of sodium and calcium underlying the action potential in a Purkinje fiber and the shape of action potentials from different regions of the heart..... 6

Figure 4. The mechanism by which calcium inititates the interaction between actin and myosin and the time course of mechanical activity in relation to the action potential..... 8

Figure 5. Mechanism of Hantzsch reaction for synthesis of 1,4-dihydropyridines..... 21

Figure 6. Example of a strip chart recording of isometric contractions of rabbit papillary muscle in the presence of cumulative concentrations of 2-MeO DHP..... 28

Figure 7. The time course of changes in isometric contraction of rabbit papillary muscle after addition of 1,4-dihydropyridine..... 29

Figure 8. Results of a control experiment in which contractions of a single rabbit papillary muscle were followed with time when no additions were made to the muscle bath..... 30

Figure 9. A representative saturation isotherm (25° C) of [^{3}H]nitrendipine binding in rabbit myocardial membrane particulates..... 35

Figure 10. Representative binding displacement and concentration-response curves in rabbit myocardium..... 37

Figure 11. Comparison of binding IC_{50} values and response IC_{50} values for

twelve 1,4-dihydropyridine compounds in rabbit myocardium..... 40

Figure 12. Data from a representative saturation binding experiment with high concentrations of [^{3}H]nitrendipine in rabbit myocardium..... 42

Figure 13. Schematic representations of the Hodgkin-Huxley gating theory for the sodium channel and of the modulated receptor hypothesis..... 47

Figure 14. Comparison of K_i values in rabbit myocardium and rabbit aorta for seven 1,4-dihydropyridine compounds..... 52

Figure 15. The time course of changes in isometric contractions of rat ventricular muscle in the presence or absence of 1,4-dihydropyridine..... 57

Figure 16. Representative saturation isotherms (25° C) of [^{3}H]nitrendipine binding in myocardial membrane particulates from rat and rabbit..... 62

Figure 17. Representative binding displacement and concentration-response curves in rat and rabbit myocardium..... 63

Figure 18. Comparison of binding K_i values for 12 DHP compounds in rat and rabbit myocardium..... 66

Figure 19. Data from a representative saturation binding experiment with high concentrations of [^{3}H]nitrendipine in rat myocardium..... 70

Figure 20. Data from representative calcium concentration-response experiments in myocardium from rabbit and rat..... 73

Figure 21. Chemical structure of GK-III-120D..... 87

Figure 22 Results of three experiments of displacement of specific [^{3}H]nitrendipine binding by GK-III-120D..... 91

Figure 23. UV spectrum of GK-III-120D prior to and after exposure to UV radiation at a wavelength of 254 nm..... 92

Figure 24. Results of a single photoactivation experiment in rat myocardial membrane particulates (100 mg/ml) after preincubation with GK-III-120D and exposure to 14 min of UV radiation (254 nm)..... 94

Figure 25. Results of a single photoactivation experiment in rat myocardial membrane particulates (100 mg/ml) after preincubation with GK-III-120D and exposure to UV radiation (254 nm) for 0, 10 and 30 min 95

Figure 26. Mean results of three photoactivation experiments (30 min UV exposure at 254 nm, 100 mg/ml tissue concentration) including a control for the effect of UV radiation on the tissue..... 96

Figure 27. Results of a single photoactivation experiment (30 min UV exposure at 254 nm, 50 mg/ml tissue concentration) including a control for the effect of UV radiation on the tissue and a nifedipine control..... 98

Figure 28. Results of two photoactivation experiments in which the tissue concentration was 20 mg/ml and the UV exposure was 15 min at 254 nm..... 99

Figure 29. Results of photoactivation experiments in which either GK-III-120D or nifedipine was incubated with tissue at a 10 or 20 mg/ml concentration and exposed to either 5 or 10 min of UV radiation (254 nm) 101

Figure 30. UV spectra of GK-III-120D and nifedipine prior to and after exposure to visible light (365 nm) 102

Figure 31. Results of two separate photoactivation experiments in which the light source was visible radiation at a wavelength of 365 nm..... 103

Figure 32. UV spectrum of nifedipine prior to and after exposure to UV radiation at a wavelength of 254 nm..... 108

Figure 33. UV spectra of nitrendipine and 2,6-Cl DHP prior to and after exposure to UV radiation at a wavelength of 254 nm..... 110

Figure 34. Chemical structure of *o*-NCS DHP 112

Figure 35. A representative polyacrylamide gel obtained after SDS-PAGE of solubilized rat myocardial membrane proteins. 117

Figure 36. Standard curve of log molecular weight of molecular weight markers *vs* migration relative to the bromophenol blue dye front on the poly-

acrylamide gel 118

Figure 37. Dissociation curves for specific binding of [^{3}H]*o*-NCS and [^{3}H]nitrendipine after the addition of 10^{-6} M nifedipine 119

Figure 38. Chemical structures of diltiazem and its two major metabolites, NDD and DAD 128

Figure 39. Qualitative comparison of the clinical cardiovascular properties of representative compounds from the three major classes of calcium channel blockers. 131

Figure 40. Representative HPLC chromatograms of diltiazem and its two major metabolites in plasma and urine 156

Figure 41. Semilogarithmic plots of the plasma concentrations of diltiazem, NDD and DAD *vs* time in six subjects after administration of 120 mg of diltiazem 162

Figure 42. Semilogarithmic plots of the plasma concentrations of diltiazem *vs* time in six subjects with the curves generated from the pharmacokinetic model of best fit 164

Figure 43. Plots of change in PR interval *vs* concentration of diltiazem for each of the six subjects 170

Abstract

Studies with Calcium Channel Blockers: Molecular Pharmacology and Clinical Pharmacokinetics

Rebecca A. Boyd

Calcium channel blockers are an important group of drugs in the therapy of cardiovascular disease. Despite widespread use, a number of questions remain unanswered regarding their molecular mechanism of action and their clinical use. The overall goal of the work presented in this dissertation was to study various aspects of the molecular pharmacology, pharmacokinetics and pharmacodynamics of selected calcium channel blockers to address some of these questions. First, the question of whether the high affinity binding site for the 1,4-dihydropyridine calcium channel blockers in myocardium is a receptor, based on classical receptor theory, was addressed. We studied both binding and negative inotropic response of a series of 1,4-dihydropyridine analogues *in vitro* in rabbit myocardium. A statistically significant rank order correlation between binding and response was found, but the potency of response of each compound was one to three orders of magnitude less than the binding affinity. Therefore, this binding site does not appear to conform to the classic definition of a receptor. Furthermore, the potency of response showed species differences. When we carried out similar studies in rat myocardium, the binding site appeared to be identical to that in rabbit myocardium, but the discrepancy between the binding affinities and potencies of response was greater. We were unable to detect a low affinity binding site for these compounds in myocardium from either species that could explain the discrepancy between binding affinities and potencies of response. Taken together, the results from the two species are consistent with several hypotheses. One possibility is that the activity of these compounds is governed by the modulated receptor hypothesis. Another is that these compounds possess agonistic as well as antagonistic properties.

In the study presented in the second part of this dissertation the pharmacokinetics

and pharmacodynamics of diltiazem, a benzothiazepine calcium channel blocker, and its two potentially active metabolites, N-monodemethyldiltiazem (NDD) and desacetyldiltiazem (DAD), were studied after a single 120 mg oral dose of diltiazem was administered to healthy humans. The specific goals of this clinical study were to obtain information about the pharmacokinetics of the metabolites and to determine whether the metabolites contribute to the effect of diltiazem. The results showed that these metabolites achieve significant plasma concentrations after a single oral dose of diltiazem and that they are eliminated with a half-life that is longer than that of diltiazem. Both diltiazem and NDD were found to be eliminated into the urine by net renal secretion. In addition, both metabolites bind to plasma proteins with unbound fractions similar to that of diltiazem. Neither blood pressure nor heart rate changed significantly after a single oral dose of diltiazem, but PR interval was significantly prolonged. The relationship between change in PR interval and plasma concentration of diltiazem changed with time, exhibiting a clockwise hysteresis in four of six subjects. This time-dependence is an indication of a number of phenomena, including the development of tolerance or the presence of an inhibitory metabolite.

CHAPTER 1

Introduction - The Mechanism of Action of 1,4-Dihydropyridine Calcium Channel Blockers in Myocardium

Overall Goals

The overall objective of this work was to study various aspects of the pharmacology, pharmacodynamics and pharmacokinetics of selected calcium channel blockers. The project was divided into two parts. The major objective of the first part was to answer questions regarding the site and mechanism of action of the 1,4-dihydropyridine calcium channel blockers in myocardium, using *in vitro* techniques. In this chapter, the first part is introduced. The specific studies of the first part are presented in Chapters 2 to 5. The major objective of the second part was to study the pharmacokinetics and pharmacodynamics of a specific calcium channel blocker, diltiazem, *in vivo* in humans. The second part is presented in Chapters 6 and 7.

Background

Calcium channel blockers are a chemically diverse group of compounds important in the treatment of various cardiovascular disorders, in particular, angina pectoris, certain cardiac arrhythmias, and hypertension. There are three major chemical groups of calcium channel blockers, the 1,4-dihydropyridines, the phenylalkylamines, and the benzothiazepines. Structures of the prototypical compounds from each chemical group are shown in Figure 1. The development of each of these groups occurred separately and predated the discovery of calcium channel blockade as the underlying mechanism of their therapeutic effects.

History

Verapamil was synthesized in the early 1960's at Knoll Pharmaceutical Company in

1,4-Dihydropyridines

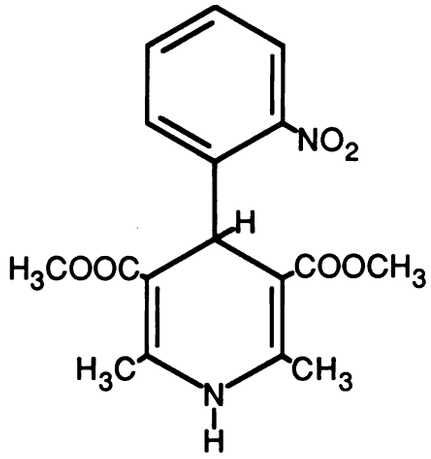

Nifedipine

Phenylalkylamines

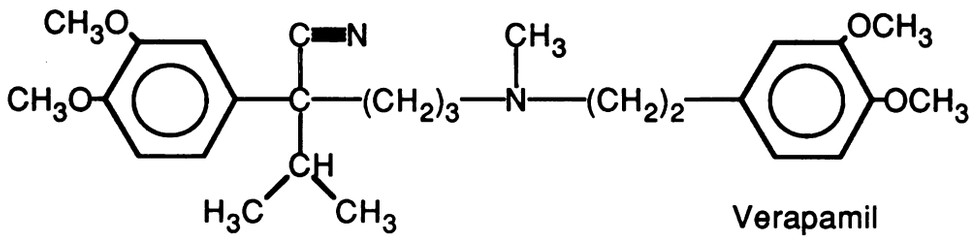

Verapamil

Benzothiazepines

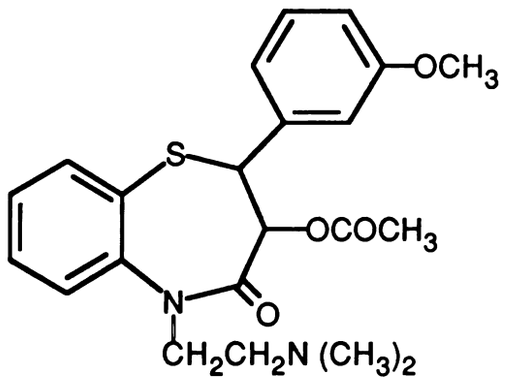

Diltiazem

Figure 1. Chemical structures of the prototypical representatives of the three major chemical classes of calcium channel blockers.

Germany (Haas and Härtfelder, 1962) and further developed for its potential coronary vasodilating effect. Because verapamil also had negative inotropic and chronotropic effects that were reversed by β-adrenoceptor agonists, it was initially believed to be a β-adrenoceptor blocking agent (Fleckenstein, 1977; Henry, 1980). However, unlike β-adrenoceptor antagonists, it also was capable of directly relaxing vascular smooth muscle and its activity could be reversed by increasing the concentration of calcium. Subsequent work by Fleckenstein (reviewed in Fleckenstein, 1977) demonstrated that the negative inotropic effect was achieved without an effect on the cardiac action potential and therefore that verapamil was acting as an uncoupler of excitation-contraction. This effect was attributed to an inhibition of the influx of calcium ions into myocardial cells and Fleckenstein, in 1967, was the first to apply the term "calcium antagonist" to verapamil. Several years later he determined that verapamil prevented the influx of calcium by reducing calcium conductance through channels in the cellular membranes of both cardiac and vascular smooth muscle (Fleckenstein, 1977).

Nifedipine also was developed in Germany, at Bayer Pharmaceutical Company, the result of traditional medicinal chemistry studies in search of a potent coronary vasodilating compound, and its discovery was first reported in 1971 (reviewed in Bossert, 1975). It also exhibited negative inotropic activity (reviewed in Kroneberg, 1975) and Fleckenstein later showed that the effect of nifedipine in both cardiac and vascular smooth muscle, like that of verapamil, could be attributed to an inhibition of transmembrane calcium influx (Fleckenstein, 1977). The discovery of potent coronary vasodilating properties of diltiazem also was reported in the early 1970's (Sato *et al.*, 1971). Its development is discussed in Chapter 6.

The Role of Calcium in the Myocardium

To understand the pharmacologic effects of calcium channel blockers in the heart, it is necessary to understand the role of calcium ions in the regulation of normal myocardial function. Calcium is essential in the myocardium for both electrical and mechanical activa-

tion and therefore myocardial concentrations of calcium are carefully regulated.

In the resting state of myocardial cells, the free ionic calcium concentration in the cytoplasm is maintained at a low level with respect to extracellular fluid, due in part to the low permeability of the cellular membrane to calcium ions. In addition, there are a number of routes by which calcium is removed from the cytoplasm, either to the extracellular fluid or into intracellular organelles (sarcoplasmic reticulum and mitochondria). These include both active processes (requiring ATP) and exchange mechanisms with protons or sodium ions. Figure 2 shows a schematic representation of a myocardial cell depicting the processes involved in the regulation of cytoplasmic calcium concentrations.

Electrical Events

The electrical potential across the membrane of a typical resting myocardial cell is about -90 mV, with the inside of the cell negative with respect to the outside. After a stimulus, the cell is depolarized by a rapid influx of sodium ions through sodium-selective channels (macromolecular pores) in the cellular membrane. As a result, the membrane potential rapidly reaches positive values. After a short time, sodium channels close and calcium-selective channels (represented by a rectangle across the cellular membrane in Figure 2) open, allowing an influx of calcium ions into the cell. This inward calcium current is partially responsible for maintenance of a prolonged period of depolarization characteristic of heart muscle. The time course of changes in membrane potential is referred to as the cardiac action potential. Figure 3A shows the action potential in a Purkinje fiber as well as the underlying changes in sodium and calcium conductances.

The action potential differs in various regions of the heart, as illustrated in Figure 3B. Of note is the different shape of the action potential in the sinoatrial (SA) and atrioventricular (AV) nodes of the heart. The resting membrane potential of these cells is more positive and the rate of depolarization is slower. In these cells initiation of depolarization is due primarily to the smaller inward calcium current rather than the larger sodium current. Calcium is therefore of primary importance in controlling the electrical activity of the

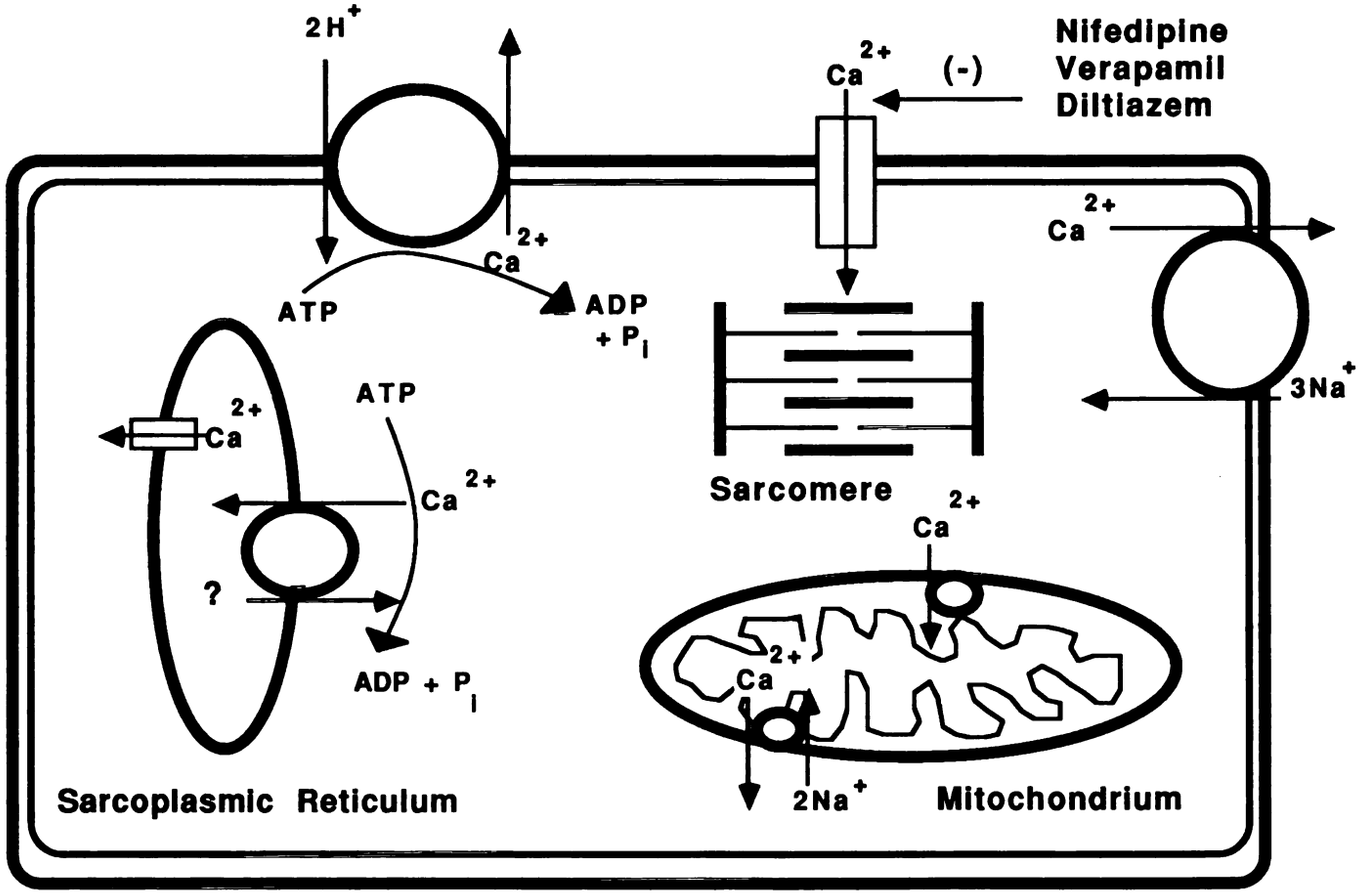

Figure 2. Schematic representation of a myocardial cell depicting the processes involved in cellular calcium regulation. Shown are exchange mechanisms (represented by circles across the membranes), including both active (requiring ATP) and passive processes. Calcium movement through channels is represented by a rectangle across the membrane.

A

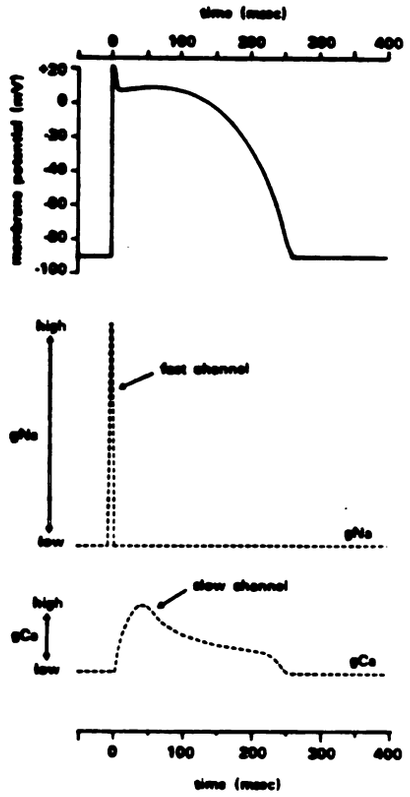

B

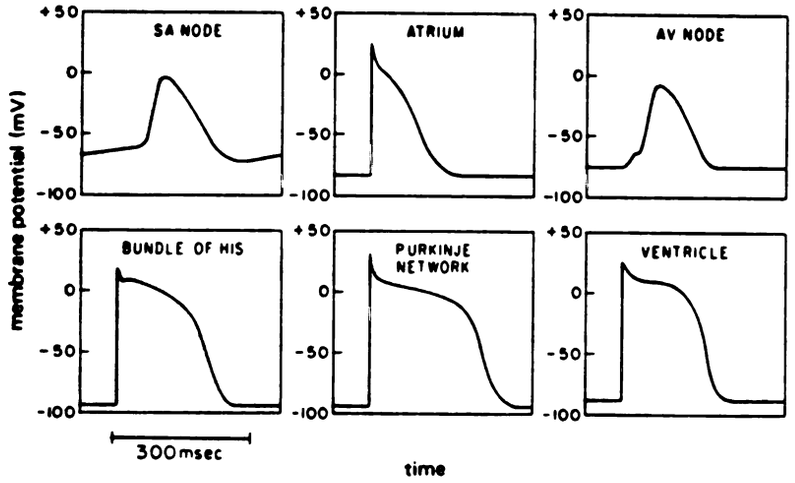

Figure 3. **A.** The changes in the conductance of sodium (gNa) (middle panel) and calcium (gCa) (lower panel) underlying the action potential (upper panel) in a Purkinje fiber **B.** Action potentials from different regions of the heart (from Katz, 1977)

pacemaker cells of the SA node and the conducting cells of the AV node (Antman *et al.*, 1980; Henry, 1980; Janis and Triggle, 1983; Katz, 1977).

Mechanical Events

In contracting myocardial cells, the influx of calcium through calcium channels is also responsible for initiation of a series of events leading to muscle contraction. On the molecular level, contraction is the result of an interaction between actin and myosin filaments in the sarcomere. In the resting cell, this interaction is inhibited by the attachment of actin to the protein tropomyosin by the troponin complex protein (Figure 4 A, left). When intracellular free calcium concentrations increase, calcium is available to bind to one subunit of troponin complex, removing its inhibitory effect and allowing actin to interact with myosin, resulting in a shortening of the sarcomere (Figure 4 A, right). The calcium influx initiates muscle contraction either by directly providing the calcium that interacts with these proteins, or by triggering the release of additional calcium from intracellular stores, in particular, the sarcoplasmic reticulum. The source of the calcium for contraction depends on the region of the heart and the species. Figure 4 B shows the time course of cardiac muscle contraction (lower panel) related to the time course of electrical events (upper panel).

Mechanism of Action of the 1,4-Dihydropyridine Calcium Channel Blockers

There are a number of mechanisms by which a compound could interfere with the action of calcium on the electrical and mechanical activity of the heart. These include: 1) inhibition of the influx of extracellular calcium, 2) inhibition of release of calcium from intracellular stores, 3) inhibition of calcium efflux from cells, 4) inhibition of calcium uptake or binding to intracellular stores, and 5) interference with the action of calcium on the proteins regulating muscle contraction. The primary action of calcium channel blockers in the myocardium is believed to be inhibition of influx of extracellular calcium through calcium channels, although the exact molecular site and mechanism of this effect have not been fully elucidated. This inhibitory effect results in a significant decrease in myocardial

A

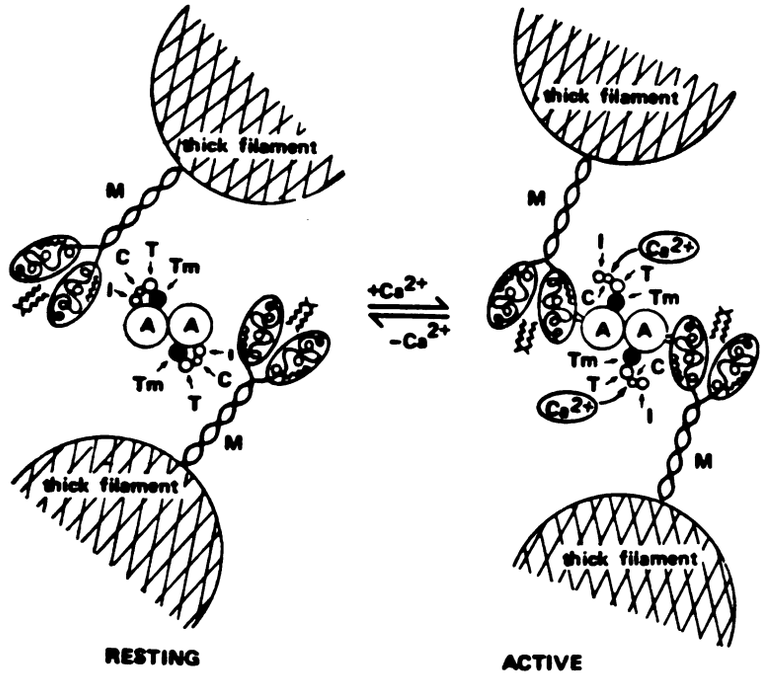

B

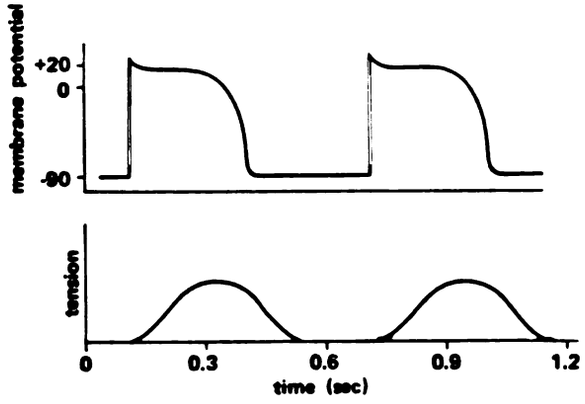

Figure 4. **A.** The mechanism by which calcium inititates the interaction between actin (A) and myosin (M). In the resting cell (left panel), the attachment of the proteins tropomyosin and troponin (consisting of subunits T, C and I) to actin prevents its interaction with myosin. When calcium concentrations increase in the active cell (right panel), calcium binds to the C subunit of troponin which results in conformational changes that detach subunit I from actin, thereby removing the inhibitory effect. **B.** Time course of mechanical activity (bottom) in relation to the action potential (top) in myocardial tissue (from Katz, 1977)

contractility with only a minimal effect on electrical excitability in contracting myocardial cells, thus justifying their characterization as "uncouplers" of excitation-contraction. In contrast, in those cells that depend on calcium influx for initiation and propagation of the action potential, calcium channel blockers can have a significant effect on electrical activity.

The site and mechanism of the effect of the 1,4-dihydropyridine calcium channel blockers in myocardium are of particular interest. Although the 1,4-dihydropyridines exhibit more potent negative inotropic, chronotropic and dromotropic effects *in vitro* than the other two classes of calcium channel blockers, these effects are not seen clinically (Antman *et al.*, 1980; Henry, 1980; Schwartz and Triggle, 1984; Stone *et al.*, 1980). In addition, the cardiac effects of the 1,4-dihydropyridine compounds occur at concentrations greater than those required to relax vascular muscle, making these compounds highly selective for vascular smooth muscle (Antman *et al.*, 1980; Henry, 1980). In contrast, the phenylalkylamines and the benzothiazepines are equally active in cardiac and vascular smooth muscle, with significant effects on the electrical system of the heart. Interestingly, however, a single high affinity binding site for 1,4-dihydropyridine compounds has been characterized in myocardium by a number of investigators (reviewed in Janis and Triggle, 1984). For several of these compounds, the K_d of this site was reported to be several orders of magnitude lower than the concentrations required to elicit an effect in myocardium. Although the characteristics of this binding site suggest that it may be a receptor for the pharmacologic effect of the 1,4-dihydropyridine calcium channel blockers, the discrepancy between binding affinity and potency of response must be explained.

Consequently, major questions that remain unanswered regarding the site and mechanism of action of the 1,4-dihydropyridine calcium channel blockers in myocardium are: 1) is the high affinity binding site in myocardium a receptor for the activity of 1,4-dihydropyridine calcium channel blockers, based on the classic criteria (Burt, 1985)? 2) can a low affinity binding site responsible for pharmacologic effect be identified? 3) what are the structure-activity relationships of the 1,4-dihydropyridines in terms of binding and

pharmacologic response in myocardium? and 4) what are the molecular characteristics of the putative myocardial receptor? The work presented in Part 1 of this dissertation focuses on these questions.

Methods to Study the Mechanism of Action of the 1,4-Dihydropyridines

To determine if a binding site is a receptor, one useful method is to compare the characteristics of binding for a large number of compounds using radioligand binding techniques and to determine if these are consistent with their pharmacological effects. In the case of the 1,4-dihydropyridine calcium channel blockers, *in vivo* systems are inappropriate for evaluation of direct myocardial effects because of reflex sympathomimetic activity triggered by vasodilation. *In vitro* systems are therefore more useful in mechanistic studies because these confounding influences are eliminated. There are a number of pharmacologic effects of the 1,4-dihydropyridine calcium channel blockers that can be monitored at the tissue or cellular levels. These include: 1) negative inotropy, 2) inhibition of $^{45}Ca^{2+}$ influx and 3) inhibition of the inward calcium current using electrophysiologic techniques (Chin, 1986; Spedding and Cavero, 1984). These binding and response techniques are discussed below.

Radioligand Binding Experiments

Radioligand binding studies in disrupted membrane preparations have contributed significantly to our knowledge of opiate, muscarinic and adrenergic receptors (Creese and Snyder, 1975; Maguire *et al.*, 1976; Mukherjee *et al.*, 1976). If pharmacologic response is mediated through a specific receptor, the binding characteristics of drugs for this receptor can be studied, providing a high affinity radioligand of high specific activity is available. When radiolabeled nitrendipine (Table 4, Chapter 3) became available in 1981, and was shown to have an affinity in the nanomolar range for binding sites in myocardium (Bellemann *et al.*, 1981), it became an important tool for subsequent studies of the characteristics of the putative 1,4-dihydropyridine receptor. Using tritiated nitrendipine and other

radiolabeled 1,4-dihydropyridine compounds, a high affinity binding site has been identified in a number of different tissues (Bolger *et al.*, 1982, 1983; Ehlert *et al.*, 1982; Fosset *et al.*, 1983). However, radioligand binding studies can provide valuable information on the mechanism and site of action only if the binding site being characterized is actually a receptor. For this to be confirmed, the binding affinity of ligands to the site should show a correlation with potency of pharmacologic response. This has not been demonstrated for the 1,4-dihydropyridine compounds in myocardium.

Pharmacologic Response Experiments

Negative Inotropy. The negative inotropic effect of the 1,4-dihydropyridines on myocardium is easily studied in isolated, electrically paced cardiac muscle strips or in the isolated spontaneously beating whole heart, known as the Langendorff preparation (Kitchen, 1984). The former technique has the advantage that the rate of pacing and the duration of the pulses can be controlled experimentally. By monitoring the isometric force of contraction in the presence of various concentrations of 1,4-dihydropyridines, concentration-response curves can be generated and a quantitative measure of potency obtained.

Inhibition of Calcium Current. The development of electrophysiologic voltage clamp techniques has allowed the inward sodium and calcium currents in the myocardium to be separated, and the calcium current to be both qualitatively and quantitatively studied. These techniques have been used to study the effects of 1,4-dihydropyridine compounds on calcium currents in whole tissue (Sanguinetti and Kass, 1984), and with the more recent development of patch clamp techniques, in isolated individual cells (Bean, 1984; Uehara and Hume, 1985) and in individual channels (Hess *et al.*, 1984). Application of voltage clamp techniques has provided very detailed and valuable information on the activation and inactivation properties of calcium channels, and the manner in which these calcium channel blockers affect these processes. However, measurement of inward calcium current using voltage clamp techniques is somewhat more difficult than measurement of negative inotropy.

Inhibition of $^{45}Ca^{2+}$ Influx. The effect of calcium channel blockers on the uptake of radiolabeled calcium ion ($^{45}Ca^{2+}$) is another technique that has been used to measure response. This type of study has most often been applied to vascular smooth muscle because, until recently, electrophysiologic techniques had not been perfected for use in this tissue. These experiments can be difficult to perform in cardiac tissue because of the many routes of calcium influx and efflux in cardiac cells (Figure 2) and great care must be taken to isolate the calcium influx through calcium channels (Spedding and Cavero, 1984).

Choice of Methods

We chose to address the question of whether there was a specific receptor for 1,4-dihydropyridine compounds in myocardium by characterizing their binding to sites labeled by tritiated nitrendipine and by evaluating their negative inotropic effect on isolated cardiac muscle strips. Although negative inotropy is further removed from the interaction between drug and calcium channel than inhibition of calcium influx, previous studies have demonstrated that the potency of response of the 1,4-dihydropyridines is similar for both pharmacologic endpoints (Fleckenstein, 1985; Janis and Triggle, 1984). In addition, the previously described discrepancy between binding affinity and potency of response was reported both for negative inotropic effect (DePover *et al.*, 1982, 1983; McBride *et al.*, 1984; Millard *et al.*, 1983) and for inhibition of calcium current (Lee and Tsien, 1983). An additional factor involved in our choice was that inhibition of contraction was the effect measured in a similar study in ileal smooth muscle, where a 1:1 correlation between binding affinities and potencies of pharmacologic response for a series of 1,4-dihydropyridines was observed (Bolger *et al.*, 1983). Using inhibition of myocardial contraction as a response would allow us to make comparisons with these data.

Finally, to obtain further information on the molecular characteristics of the binding site and putative receptor for the 1,4-dihydropyridines in myocardium, we carried out a series of studies to characterize and assess the usefulness of affinity labels to be used as covalently linked probes. It was hoped that such compounds could be used in *in vitro*

experiments designed to isolate and characterize the receptor molecule. These methods are described further in Chapter 5.

Specific Objectives

1. To synthesize a number of 1,4-dihydropyridine compounds with low affinity for the binding sites in myocardium, thereby extending the range of affinities of a series of compounds over several orders of magnitude. (Chapter 2)

2. To address the question of whether the high affinity binding site for the 1,4-dihydropyridine calcium channel blockers in myocardium is a receptor, based on classical receptor theory, by comparing the binding affinities and potencies of negative inotropic response for a series of 1,4-dihydropyridine compounds in rabbit myocardium. In addition, the following questions were addressed. Can a low affinity binding site be identified? In comparing the results in myocardium and vascular smooth muscle, are specific 1,4-dihydropyridine compounds more selective for vascular smooth muscle? If so, which structural features determine this selectivity? (Chapter 3)

3. To determine whether there are differences between rat and other mammalian species in myocardial binding or response of the 1,4-dihydropyridine calcium channel blockers, by comparing the binding and response for a series of 1,4-dihydropyridine compounds in rat and rabbit myocardium. (Chapter 4)

4. To characterize potential chemoaffinity and photoaffinity labels for the 1,4-dihydropyridine putative receptor to determine their usefulness as probes for the eventual isolation and characterization of the receptor molecule. (Chapter 5)

CHAPTER 2

Synthesis of 1,4-Dihydropyridine Compounds

Introduction

Demonstration of saturable, reversible, stereoselective, high affinity binding of a drug in a tissue is insufficient evidence that the binding site is a receptor for that drug. Binding to such a site also must result in some physiological response. One method to establish that a drug binding site is a receptor is to demonstrate a correlation between binding affinities for the site and potencies of pharmacologic effect for a series of analogues having a range of potencies (Burt, 1985; Laduron, 1984). Such studies have played an integral part in the identification of muscarinic receptors (Yamamura and Snyder, 1974), opiate receptors (Creese and Snyder, 1975) and β-adrenergic receptors (Maguire *et al.*, 1976; Mukherjee *et al.*, 1976). Because we were interested in examining the question of whether the binding site for the 1,4-dihydropyridine calcium channel blockers in myocardium was the receptor for pharmacologic response, we wanted to carry out both binding and response studies. To do this, it first was necessary to obtain a series of 1,4-dihydropyridine analogues.

At the time our studies began, the only 1,4-dihydropyridine calcium channel blocker available clinically was nifedipine. However, a number of pharmaceutical companies were in various development stages with other 1,4-dihydropyridine compounds, and we were able to obtain samples of some of these. The individual compounds and their sources are listed in Chapter 3. These 1,4-dihydropyridines were expected to be of high potency, and high affinity binding in myocardium had been demonstrated for several of them (Holck *et al.*, 1982; Janis *et al.*, 1982, 1984b). Therefore, we needed to obtain analogues with lower potencies and, presumably, lower binding affinities, to extend our range of compounds. Two compounds were provided to us by Dr. Wendel L. Nelson of the

Department of Medicinal Chemistry, University of Washington. These compounds were 2-Cl DHP and MR-I-12 (see Chapter 3 for full chemical names and structures). MR-I-12 was a precursor for the putative photoaffinity compound GK-III-120D (see Chapter 5). To obtain additional compounds, we first had to select the compounds, based on available structure-activity relationship (SAR) data in the literature, and then synthesize them. The synthetic method for the production of 1,4-dihydropyridine compounds is well established (Eisner and Kuthan, 1972; Bossert *et al.* 1981) and is easily carried out.

Methods

Choice of Compounds

A number of reports of the activity of synthesized 1,4-dihydropyridine compounds had appeared in the literature prior to our studies (Bolger *et al.*, 1983; Loev *et al.*, 1974; Meyer *et al.*, 1981; Rodenkirchen *et al.*, 1979). These provided SAR information that enabled us to choose potential low-potency compounds to synthesize. In general, whether the target tissue was vascular smooth muscle (Loev *et al.*, 1974; Meyer *et al.*, 1981), cardiac muscle (Rodenkirchen *et al.*, 1979), or ileal smooth muscle (Bolger *et al.*, 1983), a number of relationships between the structure of 1,4-dihydropyridine compounds and potency of response were evident:

1) a phenyl ring at the 4 position of the 1,4-dihydropyridine ring was optimal for activity
2) ortho or meta substitution on the phenyl ring increased potency, with ortho substitution being more potent; para substitution decreased or had no effect on potency
3) the potency of response was independent of the electronic properties of aryl substituents, but size appeared to be important, with bulkier substituents conferring greater potency on the compounds
4) methyl groups at the 2 and 6 positions of the 1,4-dihydropyridine ring were

optimal for activity

5) substitution on the nitrogen atom decreased activity

6) electron-withdrawing substituents at the 3 and 5 positions were important for activity, with carboxy groups being the best; activity was inversely associated with the size of the carboxy esters, with methyl and ethyl substitution resulting in the highest potency

7) other things being equal, compounds asymmetrically substituted at the 3 and 5 positions were more potent than those symmetrically substituted

Accordingly, we chose to synthesize five achiral 1,4-dihydropyridine compounds to bring our total number of compounds to 12. The compounds and their structures are shown in Table 1. Each of these compounds was included in one of the previous SAR studies (Loev *et al.*, 1974; Rodenkirchen *et al.*, 1979) and demonstrated a potency less than that of the compounds obtained from pharmaceutical manufacturers. By choosing compounds with substituents at various positions on the aryl ring, their potencies would be expected to vary significantly.

Synthesis

Five achiral 1,4-dihydropyridine compounds were synthesized in our laboratory by the method of Hantzsch (Bossert *et al.*, 1981; Eisner and Kuthan, 1972; Meyer *et al.*, 1981). The reaction is a "one-pot" condensation of an aldehyde, a β-ketoester (in this case, an ester of acetoacetic acid) and ammonia (in the form of ammonium hydroxide) in the molar ratio of 1:2:1 to produce a symmetrically substituted 1,4-dihydropyridine, as depicted in Scheme 1.

Specifically, the aldehyde was a substituted benzaldehyde, and a methyl or ethyl ester of acetoacetic acid was used. The procedure was as follows. To a 200 ml round bottomed flask in a fume hood was added: 0.1 moles of the benzaldehyde derivative, 0.2 moles of the acetoacetic acid ester and 10 ml of ammonium hydroxide. Approximately 10 ml of absolute ethanol per 5 g of solid was added as a solvent. A magnetic stirrer was

Table 1. The chemical structures of the 1,4-dihydropyridine compounds synthesized by the Hantzsch reaction.

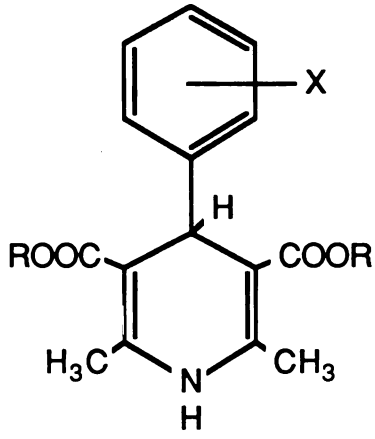

Compound	X	R
2,6-Cl DHP	2,6 -Cl	ethyl
2-MeO DHP	2-OCH_3	methyl
3-MeO DHP	3-OCH_3	methyl
4-Cl DHP	4-Cl	methyl
4-Me DHP	4-CH_3	methyl

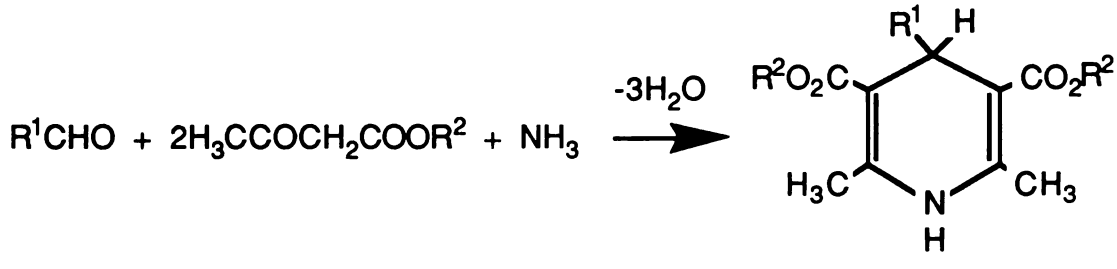

Scheme 1

added and the flask was attached to a reflux apparatus. The whole system was covered with aluminum foil and the flask was placed in a heating mantle on a stirring apparatus. The heating mantle was set at low and the mixture was allowed to reflux overnight (≈12 hours). After refluxing, the contents of the flask were added to a separatory funnel containing 200 ml of distilled water. A 200 ml volume of dichloromethane was added and the mixture was shaken well. The dichloromethane layer was removed and a second extraction with 200 ml of dichloromethane was carried out. The two dichloromethane extracts were combined into a round bottomed flask covered with aluminum foil and evaporated on a rotary evaporator (RotaVAPOR <R>, Büchi, Switzerland) under subdued light. The resulting oily residue was recrystallized in approximately 200 ml of hot n-hexane to which a small volume of dichloromethane (about 10 ml) was added to ensure dissolution.

Confirmation of Structures

The melting points of the resulting crystals were obtained on a Thomas-Hoover Capillary Melting Point Apparatus (Arthur H. Thomas Co., Philadelphia, PA). These were used as a measure of purity and to compare to values in the literature. The structures of the compounds were confirmed by their nuclear magnetic resonance (NMR) spectra and by mass spectrometry (MS) analysis. Both were done in the laboratory of Dr. Wendel L. Nelson, Department of Medicinal Chemistry, University of Washington. The NMR spectra were obtained in a solution of d_6 acetone or a mixture of d_6 acetone/$CDCl_3$ on a Varian T-60 or a Varian HA-100 spectrometer. Chemical shifts are expressed as parts per million (δ) relative to $(CH_3)_4Si$ as the internal standard. The MS analysis was performed by low resolution chemical ionization (in methane) on a VG-7070 mass spectrometer using a direct insertion probe.

Chemicals

The benzaldehyde derivatives, 2,6-dichlorobenzaldehyde, 4-chlorobenzaldehyde, 2-methoxybenzaldehyde (also known as *o*-anisaldehyde), 3-methoxybenzaldehyde (also known as *m*-anisaldehyde), and 4-methylbenzaldehyde (also known as *p*-tolualdehyde),

and the acetoacetate esters were obtained from Aldrich Chemical Company, Inc. (Milwaukee, WI). Ethanol (200 proof) was purchased from Gold Shield Chemical Co. (Hayward, CA). Concentrated ammonium hydroxide was obtained from Fisher Scientific (Fair Lawn, NJ). Dichloromethane and n-hexane were obtained from Mallinckrodt Inc. (Paris, KY). All chemicals were of the highest available grade.

Results

The syntheses resulted in yellow crystals in all cases. The yields for each compound were not calculated because we were interested in obtaining only a small amount of each compound, sufficient to carry out both receptor binding and pharmacologic response experiments. The melting points of the five 1,4-dihydropyridine compounds are shown in Table 2. The melting points suggest that the compounds were pure. Unfortunately, al-

Table 2. Melting points of synthesized 1,4-dihydropyridine compounds.

Compound	Observed Melting Point (°C)	Reported Melting Point (°C)
2,6-Cl DHP	131.5-133.5	133-135[1]
2-MeO DHP	196-198	na[2]
3-MeO DHP	167.5-169.5	na
4-Cl DHP	187-188.5	na
4-Me DHP	165.5-168.5	na

[1]Loev *et al.*, 1974

[2]not reported in the literature

though all of these compounds had been used in previous binding and/or response experiments, details of the synthesis for only one of the compounds, 2,6-Cl DHP, were available in the literature (Loev *et al.*, 1974). For this compound, the melting point we obtained

(131.5-133.5°C) was very close to the reported value (133-135°C). For the other four compounds, we were unable to compare their melting points with values in the literature.

Appendix A contains the NMR and mass spectra obtained for each compound. NMR and mass spectra were consistent with the assigned structures. Therefore, we were confident that we had obtained the compounds listed in Table 1.

Discussion

The synthesis of achiral 1,4-dihydropyridine compounds was first described by Hantzsch in 1882 as an intermediate step in the synthesis of pyridines, which previously had to be extracted from coal tar (Bossert *et al.*, 1981; Meyer *et al.*, 1985; Eisner and Kuthan, 1972). Further interest in dihydropyridine compounds was generated by the discovery in the 1930's that NADH, a dihydronicotinamide derivative, was an important coenzyme in biochemical oxidation-reduction reactions. Renewed interest in simpler "Hantzsch-type" dihydropyridine compounds occurred in the late 1960's and early 1970's when several were discovered to have pharmacologic properties, specifically, coronary vasodilating activity (Loev *et al.*, 1974). Since that time, their mechanism of action as calcium channel blockers has been established and a great number of 1,4-dihydropyridine derivatives have been produced, with many having achieved clinical importance as antianginal and antihypertensive agents.

The mechanism of the Hantzsch synthetic reaction is shown in Figure 5 (Eisner and Kuthan, 1972). The reaction includes a primary Knoevenagel condensation of an aldehyde (**2**) with one molecule of an acetoacetate ester (**1**) to yield an aralkylidene-acetoacetate (**4**), followed by a Michael addition of the aminocrotonate (**5**), formed from the second acetoacetate molecule (**1**) and ammonia (**3**), to yield a highly reactive tautomeric system (**6,7**). This compound undergoes cyclization to the hydroxytetrahydropyridine (**8**) followed by the loss of water to form the 1,4-dihydropyridine (**9**). A modification of this reaction is used to produce chiral 1,4-dihydropyridine compounds. The aminocrotonic acid ester (**5**)

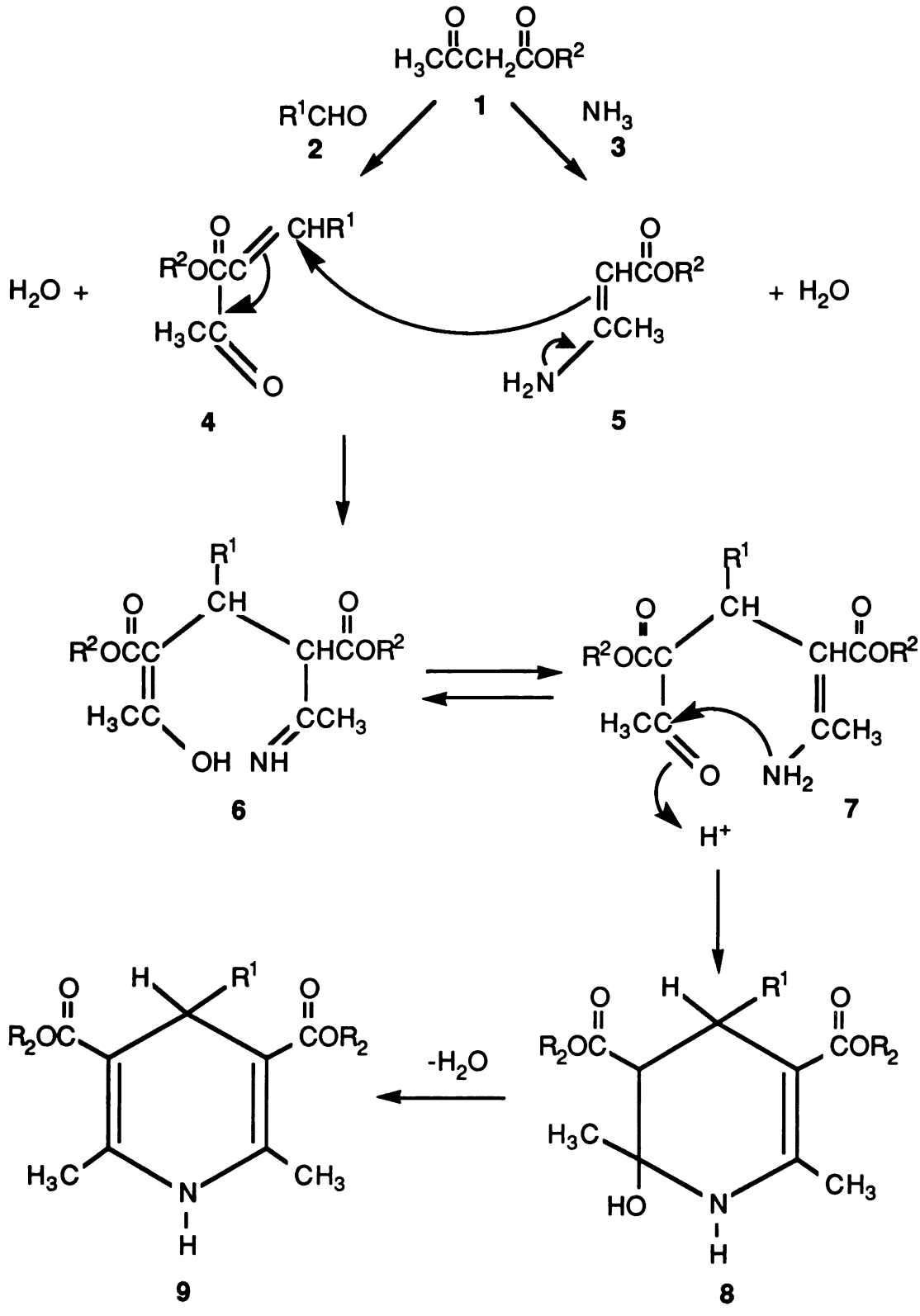

Figure 5. Mechanism of Hantzsch reaction for synthesis of 1,4-dihydropyridines.

is preformed from an acetoacetic acid ester plus ammonia. This is reacted with an aldehyde and a different ester of acetoacetic acid ester to yield a 1,4-dihydropyridine that is asymmetrically substituted at the 3 and 5 positions.

We applied this simple reaction to successfully produce a series of five 1,4-dihydropyridine compounds that, along with the two compounds we received from Dr. Wendel Nelson, would have lower potency in receptor binding and pharmacologic response experiments than the compounds we obtained from commercial sources. This enabled us to carry out the studies in Chapters 3 and 4.

CHAPTER 3

Comparison of Binding Affinities and Negative Inotropic Potencies of the 1,4–Dihydropyridine Calcium Channel Blockers in Rabbit Myocardium

Introduction

A number of criteria have been established to confirm that a tissue binding site for a drug, identified in radioligand binding studies, is a receptor (Burt, 1985; Laduron, 1984). The binding of the radioligand should be saturable, reversible, and of high affinity. In addition, the specificity and stereoselectivity of binding should be demonstrated using a series of analogues, including pairs of enantiomers. These criteria have been met for the 1,4-dihydropyridine (DHP) calcium channel blockers in several tissues. A number of studies have demonstrated the presence of a specific, saturable, high affinity binding site for the 1,4-dihydropyridine compounds in membrane particulates prepared from myocardium (Bolger *et al.*, 1982; Ehlert *et al.*, 1982; Murphy and Snyder, 1982), smooth muscle (Bolger *et al.*, 1983; Ehlert *et al.*, 1982; Sarmiento *et al.*, 1984; Triggle *et al.*, 1982), skeletal muscle (Ferry and Glossmann, 1982; Fosset *et al.*, 1983) and brain (Murphy and Snyder, 1982; Marangos *et al.*, 1982).

An additional requirement is demonstration of a correlation between binding affinities and pharmacologic potencies in identical tissue preparations (same tissue, same species) for a series of structural analogues having a wide potency range. Such a correlation for the 1,4-dihydropyridines has been found in guinea pig ileal smooth muscle (Bolger *et al.*, 1983; Wei *et al.*, 1986), in guinea pig bladder smooth muscle (Yousif *et al.*, 1985), in rat tail artery (Wei *et al.*, 1986), and in rabbit aorta (Gordon *et al.*, 1986). In one study in guinea pig ileum, an excellent 1:1 correlation between binding affinities and response potencies was demonstrated for a series of 1,4-dihydropyridine compounds. In other studies, either a weaker correlation or a slight deviation from a 1:1 correlation was found,

perhaps because fewer compounds were studied. Such a correlation has not been demonstrated in myocardial tissue, although some investigators have attempted to correlate binding affinities in one tissue with response potencies in a different species and/or tissue, including myocardium (Bellemann *et al.*, 1983; Janis *et al.*, 1982, 1984b; Sarmiento *et al.*, 1984).

Furthermore, myocardium is of special interest because it has been observed for several 1,4-dihydropyridine compounds that concentrations that inhibit contraction (DePover *et al.*, 1982, 1983; McBride *et al.*, 1984; Millard *et al.*, 1983) or slow inward calcium current (Lee and Tsien, 1983) are 100 to 1000 times greater than those that inhibit 1,4-dihydropyridine radioligand binding. The reason for this discrepancy in myocardium has not been determined, although several theories have been proposed.

Because no correlation between binding data and pharmacologic response data in myocardium has been demonstrated, debate continues over whether the previously identified high affinity binding site specific for the 1,4-dihydropyridine calcium channel blockers in myocardium represents a receptor. The goal of this investigation, therefore, was to examine in detail both the binding and the pharmacologic response of a series of 1,4-dihydropyridines in myocardium of the rabbit, a species in which myocardial function is similar to that in humans (Fox, 1984), and to determine if a correlation exists similar to that found in smooth muscle.

Methods

Chemicals

[^{3}H]Nitrendipine (specific activity, 79.0 or 87.0 Ci/mmol) was obtained from New England Nuclear (Boston, MA). Nifedipine was purchased from Sigma Chemical Co.(St. Louis, MO). Nitrendipine, nimodipine and nisoldipine were generously donated by Dr. Alexander Scriabine (Miles Pharmaceuticals, West Haven, CT). Nicardipine HCl was a gift of Syntex (Palo Alto, CA). The remainder of the 1,4-dihydropyridine compounds

were synthesized in our laboratories using the method of Hantzsch (Bossert *et al.*, 1981) (see Chapter 2). Structures were confirmed by nuclear magnetic resonance and mass spectrometry analysis. All other chemicals were obtained from commercial sources and were of the highest grade available.

Radioligand Binding Studies

Male New Zealand White rabbits (3-3.5 kg) were sacrificed by decapitation. The heart was removed and immediately perfused with ice-cold buffer (50 mM tris(hydroxymethyl)aminomethane (Tris) HCl; pH 7.4, 22° C). This buffer was used for all subsequent steps in the binding experiments. After the heart was trimmed of fat, exposed vessels and the atria, the ventricles were weighed and placed in sufficient ice-cold buffer to achieve a concentration of 100 mg wet weight tissue/ml buffer. The tissue was minced with scissors and then homogenized with a Brinkmann Polytron (Brinkmann Instruments, Westbury, NY) at setting 8, using 3 x 5 sec bursts. The homogenate was centrifuged at 48,000g for 15 min at 5° C in a Beckman Model J2-21 centrifuge using a JA-20 rotor (Beckman Instruments, Palo Alto, CA), after which the supernatant was discarded. The same volume of buffer was added to the pellet and it was resuspended with the Brinkmann Polytron and centrifuged as above. These steps were repeated once more. The pellet was then resuspended to a final concentration of 40 mg original wet weight tissue/ml buffer.

Aliquots (100 µl) of the final membrane particulate suspension were incubated in 12 x 75 mm disposable borosilicate glass culture tubes (Fisher Scientific Co., Springfield, NJ) with [^{3}H]nitrendipine in buffer at 25° C for 90 min. To prevent light-catalyzed oxidation of the 1,4-dihydropyridines, incubations were carried out in the dark. The total volume of incubate was 2 ml. These incubation conditions were established previously in our laboratories. Experiments were repeated at least three times and in each experiment all data points were determined in triplicate. Saturation experiments were performed with concentrations of [^{3}H]nitrendipine ranging from 0.02 to 1.0 nM or from 10 to 1000 nM. For displacement experiments, the concentration of [^{3}H]nitrendipine was 0.05 nM and the incuba-

tion mixtures contained concentrations of unlabeled 1,4-dihydropyridine compounds ranging from 3.2×10^{-13} M to 10^{-4} M. Stock solutions (1 mM) of the 1,4-dihydropyridine compounds were prepared in absolute ethanol, protected from light, and refrigerated. Dilutions were made in 50 mM Tris HCl buffer. The final concentration of ethanol in the incubation mixture was low and in preliminary control experiments, ethanol in buffer, in a concentration equivalent to the highest concentration expected in the incubation mixture, was substituted for 1,4-dihydropyridine solution and found to have no effect on [^{3}H]nitrendipine binding.

Incubations were terminated by rapid vacuum filtration over Whatman GF/B filters (Whatman International Ltd., Maidstone, England) followed by 3 x 4 ml washes with ice-cold buffer. The filter apparatus was either a filter manifold (Hoeffer Scientific, San Francisco, CA) containing 2.5 cm filters, or a cell harvester (Brandel Biomedical Research & Development Labs, Gaithersburg, MD) containing filter strips. Bound radioactivity was determined by liquid scintillation counting of the filters which were placed in 10 ml of either ACS (Amersham Corporation, Des Plaines, IL) or Scintiverse II (Fisher Scientific Co., Springfield, NJ) as the liquid scintillant. A Beckman Model LS7800 liquid scintillation counter (Beckman Instruments, Palo Alto, CA) was used. Counting efficiency ranged from 14 to 42%. Nonspecific binding was defined as the amount of [^{3}H]nitrendipine bound in the presence of 1 μM nifedipine and, in the displacement experiments, accounted for an average of 22 ± 8 (S.D.) % of total binding. Protein concentrations were determined by the method of Lowry *et al.* (1951) using bovine serum albumin as the standard. The protein concentration of the final incubation mixture in the saturation experiments was 0.09 ± 0.006 (S.D.) mg/ml (n=3).

Pharmacologic Response Studies

Papillary muscles (≈ 1 mm x 6 mm) from the right ventricle of rabbit heart, isolated as described above, were fixed at the ventricular end and suspended in a 20 ml jacketed muscle bath (Harvard Apparatus, South Natick, MA) containing 25 ml of isotonic Krebs-

Henseleit buffer of the following composition (mM): NaCl, 118.2; KCl, 4.6; KH_2PO_4, 1.2; $MgSO_4$, 1.2; $NaHCO_3$, 24.8; $CaCl_2$, 2.5; glucose, 10. The temperature of the buffer was maintained at 30° C and the buffer was aerated continuously with 95% O_2: 5% CO_2 and maintained at pH 7.4. The tendinous end of the papillary muscle was attached to a Grass FT 03 force-displacement transducer (Grass Instrument Company, Quincy, MA). Contractions were induced by field stimulation at a rate of 1 Hz with a Grass Model SD9 stimulator. Contraction signals were amplified and recorded on a Grass Model 7 polygraph and peak heights were measured by hand. A preload tension of 0.5 g was applied to the tissue and maintained during an equilibration period of 90 to 120 min that was necessary to achieve steady baseline contractions. Figure 6 shows an example of a strip chart recording from an experiment in a single papillary muscle.

Cumulative concentration-response curves for inhibition of isometric contractions were obtained by adding increasing amounts of the 1,4-dihydropyridine compounds to the muscle bath, contained in 250 µl volumes, corresponding to final concentrations of 10^{-10} M to 10^{-4} M. Response was measured after an incubation time of 30 min for each concentration. Preliminary studies indicated that 30 min was sufficient to attain maximum effect (Figure 7, upper and lower panels) and that tissue viability was maintained for the duration of the experiment (Figure 8). At least three curves were obtained for each compound, each the result of an experiment with a papillary muscle from a different rabbit. Stock solutions of the compounds (10 mM) were prepared in polyethylene glycol (PEG) 400 and stored protected from light. Dilutions were made in Krebs-Henseleit buffer. The solvent, PEG 400, had no effect on muscle contraction at the highest concentration present (1%) (Figure 7, lower panel). All experiments were carried out under subdued lighting.

Data Analysis

The data from individual saturation experiments were expressed as amount bound (B) and plotted against the concentration of [^{3}H]nitrendipine. To obtain the K_d and B_{max} (maximum number of binding sites) of nitrendipine, the data were fit to the following

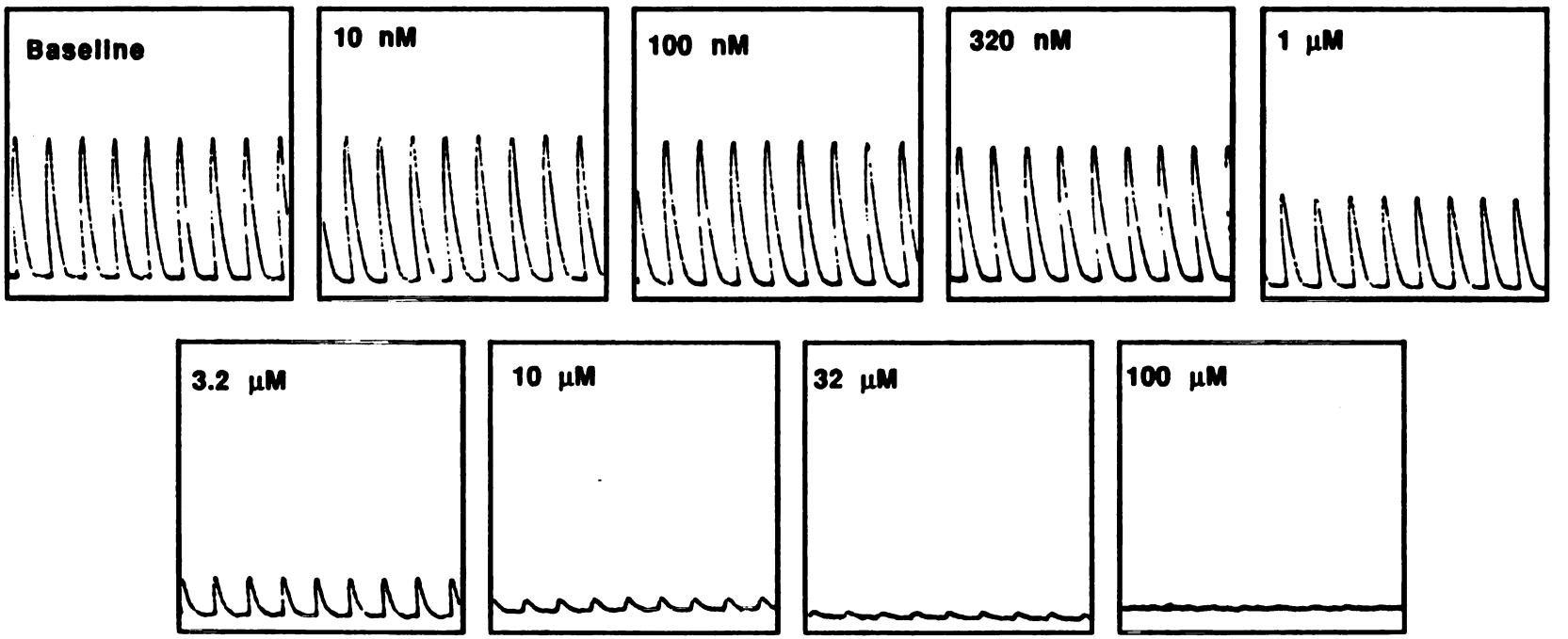

Figure 6. Examples of the strip chart recording of isometric contractions of rabbit papillary muscle from a single experiment. The panels represent the contractions before (baseline) and after 30 min incubations of cumulative concentrations of 2-Meo DHP.

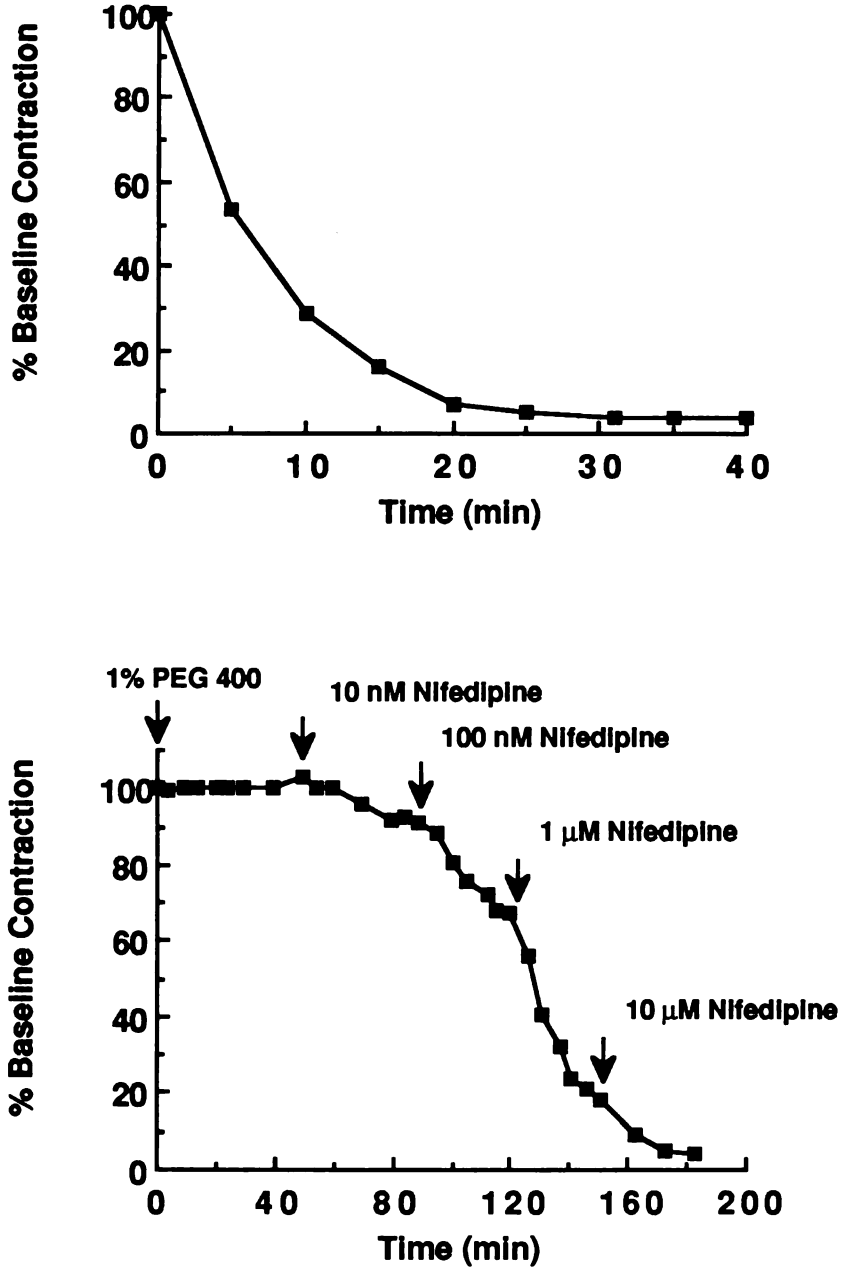

Figure 7. Results of representative experiments designed to determine the time of incubation for each concentration of 1,4-dihydropyridine added to the muscle bath. The upper panel shows the decrease in force of contraction with time after the addition of a single concentration of nifedipine (10 μM). The lower panel shows the effect on force of contraction of 1% PEG 400 followed by increasing concentrations of nifedipine.

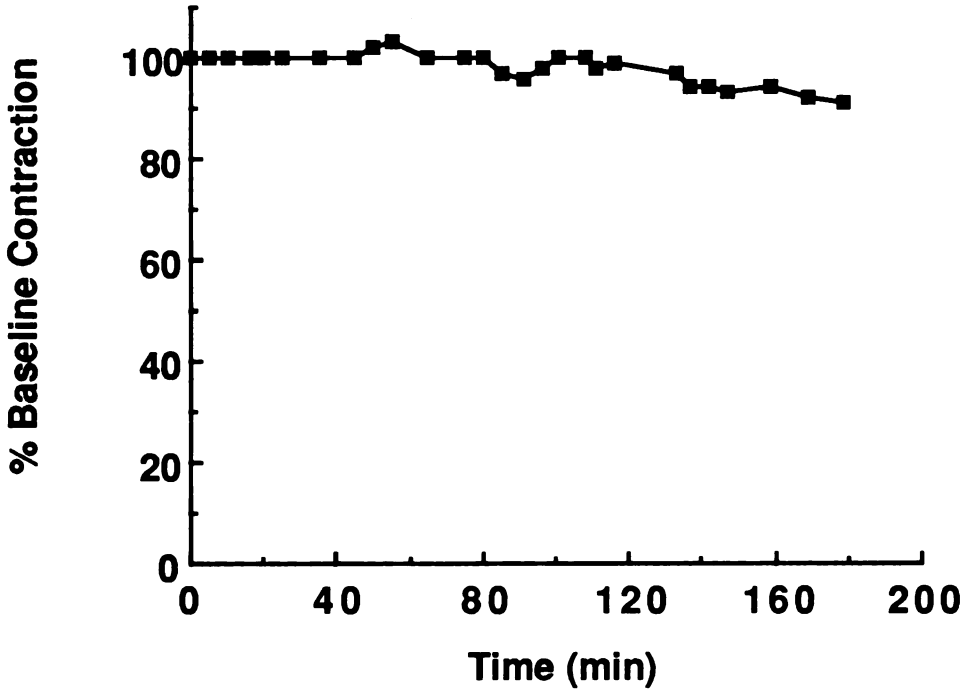

Figure 8. Results of a control experiment in which contractions of a single rabbit papillary muscle were followed with time when no additions were made to the muscle bath.

equation using FITFUN, the iterative nonlinear least squares regression program on the National Institutes of Health PROPHET system (Bolt Beranek and Newman Inc., Cambridge, MA):

$$B = \frac{B_{max} * C}{K_d + C} + K_{ns} * C \qquad \text{(Equation 1)}$$

where C is the total concentration of [^{3}H]nitrendipine in the incubation mixture and K_{ns} is the nonspecific binding constant. Weights equal to the reciprocal of the square of the observed values were used. Because the total amount of [^{3}H]nitrendipine bound to membrane particulates was less than 10% of added radioligand, total concentrations approximated free concentrations.

The data from individual displacement experiments were expressed as total amount of [^{3}H]nitrendipine bound and plotted against the logarithm of the concentration of displacing compound. The data were fit with the following four parameter logistic function (De Lean *et al.*, 1978), using FIT FUNCTION, another version of the PROPHET iterative nonlinear least squares regression program, to obtain estimates of nonspecific binding (B_{ns}), maximum specific binding (B_o-B_{ns}), IC_{50} and n, the slope factor:

$$B = B_{ns} + \frac{B_o - B_{ns}}{1 + \left(\frac{C}{IC_{50}}\right)^n} \qquad \text{(Equation 2)}$$

The data were then converted to percentage of maximum specific binding (($B_{observed}/B_o$-B_{ns})*100) and plotted against the logarithm of the concentration of the displacing compound. K_i values for the twelve 1,4-dihydropyridine compounds were calculated from IC_{50} estimates using the Cheng and Prusoff equation (Cheng and Prusoff, 1973):

$$K_i = \frac{IC_{50}}{1+\left(\frac{[L]}{K_d}\right)} \qquad \text{(Equation 3)}$$

where [L] is the concentration of [^{3}H]nitrendipine in the inhibition experiments and K_d is the mean dissociation constant of [^{3}H]nitrendipine obtained from the saturation binding experiments.

The data from individual pharmacologic response experiments were normalized to initial baseline contraction amplitude, expressed as percentage baseline contraction, and plotted *vs* the logarithm of the concentration of the 1,4-dihydropyridine compound. The data were fit by a sigmoidal inhibitory E_{max} model (Holford and Sheiner, 1981), using FIT FUNCTION, to obtain estimates of IC_{50} and n. The form of the equation was as follows:

$$E = \frac{E_o}{1 + \left(\frac{C}{IC_{50}}\right)^n} \qquad \text{(Equation 4)}$$

where E is the effect, E_o is the initial effect, C is the 1,4-dihydropyridine concentration and n is the slope factor. The assumption made when applying this model was that the contractions could be inhibited completely at high concentrations of 1,4-dihydropyridines. This was true for the most potent compounds, but because of solubility limitations, complete inhibition of contractions could not be demonstrated for the least potent compounds. Because there was no reason to assume that these analogues would behave differently, the same model was applied. The data were then converted to percentage of initial effect (obtained from the computer estimates) and plotted against the logarithm of the concentration of 1,4-dihydropyridine compound. In all cases, data from individual experiments were analyzed by computer and the results expressed as the mean ± S.D. of the resulting estimated parameters. The derivations for the equations used in the data analysis can be found in Appendix B.

Statistical Analysis

In general, only data with fits that resulted in statistically significant parameter estimates were included. Using this criterion, data from 10% of the radioligand binding experiments were discarded (4 out of 40). For the pharmacologic response experiments, this value was somewhat higher (33% or 18 out of 55 experiments). Statistical comparisons of estimated parameters were made using the unpaired Student's t-test. A statistically significant correlation was indicated by a correlation coefficient significantly different from zero. In all cases, a p-value less than 0.05 was considered an indication of statistical significance.

Results

Radioligand Binding Studies

Table 3 shows the parameter estimates from the weighted computer fits, using equation 1, of the data from three [^{3}H]nitrendipine saturation binding experiments in rabbit ventricular membrane particulates. Included are the estimates of K_{ns}, B_{max}, and K_d, as well as the p-values for each parameter, generated from tests of the null hypotheses that each parameter is equal to zero. The data fit well to the equation incorporating a saturable and a nonsaturable component. The mean K_d and B_{max} ($\pm$ S.D.) were 0.15 ($\pm$ 0.06) nM and 247 ($\pm$ 150) fmol/mg protein (n=3). The K_d is in good agreement with the IC_{50} for displacement of [^{3}H]nitrendipine by unlabeled nitrendipine (0.43 nM) in the same preparation (Table 5), and the values for both K_d and B_{max} are similar to those found in the rabbit ventricle by others (Janis *et al.*, 1984b). A representative saturation isotherm demonstrating high affinity [^{3}H]nitrendipine binding to rabbit ventricular membrane particulates is shown in Figure 9.

The 1,4-dihydropyridine compounds used in the displacement experiments are listed in Table 4, along with their chemical structures. Several representative displacement curves from individual experiments are shown (Figure 10, upper panel), illustrating the range of binding affinities obtained. Both the experimental points and computer-generated

Table 3. Results of computer fits of data from [^{3}H]nitrendipine saturation binding experiments in rabbit ventricular membrane particulates

Experiment	K_{ns} (fmol/mg protein/nM) (p-value)	B_{max} (fmol/mg protein) (p-value)	K_d (nM) (p-value)
1	208 (0.001)	416 (0.0001)	0.19 (0.0005)
2	81 (0.012)	195 (0.0001)	0.17 (0.0001)
3	499 (0.0001)	130 (0.001)	0.077 (0.008)
Mean	**263**	**247**	**0.15**
S.D.	**214**	**150**	**0.06**

curves are included. The slopes of the curves are approximately parallel and steep, with slope factors (n) not significantly different from 1 (mean ± S.D. from all experiments; 1.27 ± 0.34), suggesting competitive displacement of [^{3}H]nitrendipine from a single binding site.

Table 5 lists the computer estimates of IC_{50} for inhibition of [^{3}H]nitrendipine binding by these compounds. The binding affinities ranged over several orders of magnitude and generally agreed with the results of binding of a series of 1,4-dihydropyridine compounds in guinea pig ileal smooth muscle membranes (Bolger *et al.*, 1983) and rabbit ventricular membranes (Janis *et al.*, 1984b). The parameter estimates obtained from the computer fits of data from individual experiments are shown in Appendix C.

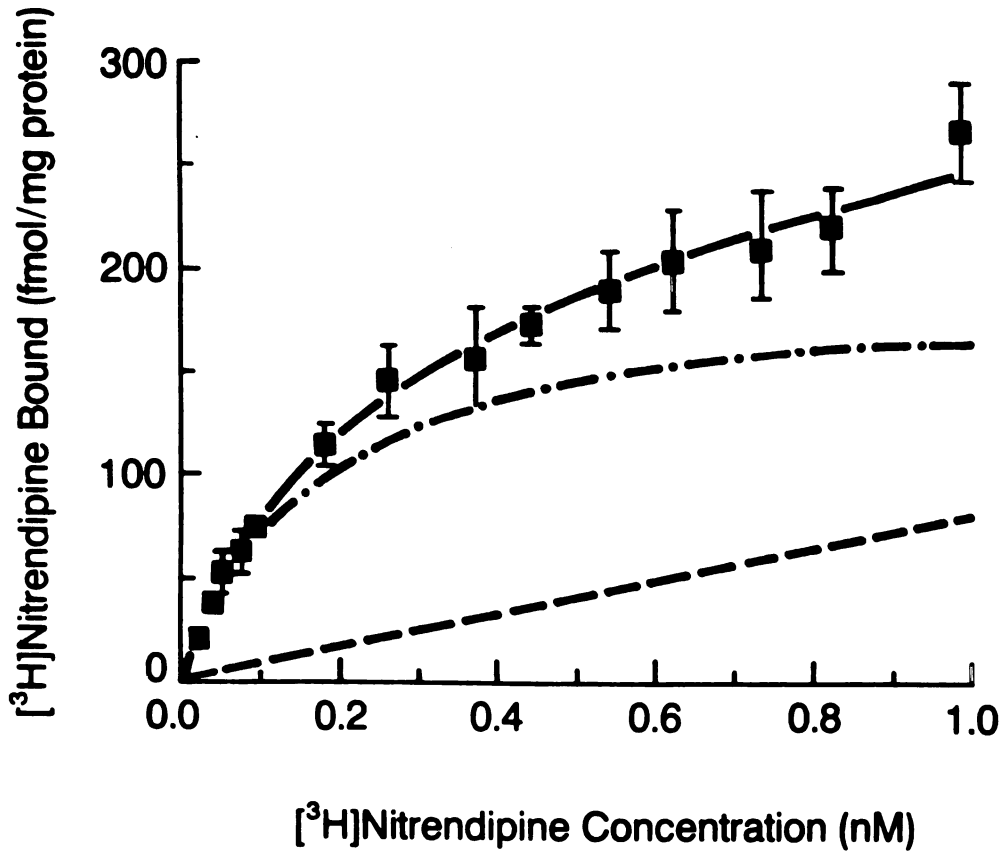

Figure 9. A representative saturation isotherm (25° C) of [^{3}H]nitrendipine binding in rabbit myocardial membrane particulates. Shown are the experimental points for total binding (± S.D.) (■), the computer-generated fit of the total data to Equation 1 (—), and the computer-generated curves for the nonspecific (– – –) and specific (• — • — •) binding. The K_d and B_{max} estimated from this experiment are 0.17 nM and 195 fmol/mg protein.

Table 4. Chemical structures of the 1,4-dihydropyridine (DHP) compounds used in the binding and response studies.

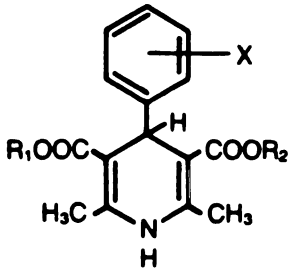

COMPOUND	X	R_1	R_2
Nifedipine	2-NO_2	CH_3	CH_3
Nitrendipine	3-NO_2	CH_3	C_2H_5
Nimodipine	3-NO_2	$CH(CH_3)_2$	$(CH_2)_2OCH_3$
Nicardipine (HCl)	3-NO_2	CH_3	$(CH_2)_2N(CH_3)CH_2C_6H_5$
Nisoldipine	2-NO_2	CH_3	$CH_2CH(CH_3)_2$
2-Cl DHP	2-Cl	CH_3	CH_3
4-Cl DHP	4-Cl	CH_3	CH_3
2,6-Cl DHP	2,6-Cl	C_2H_5	C_2H_5
MR-I-12	2-NO_2, 5-CL	CH_3	CH_3
2-MeO DHP	2-OCH_3	CH_3	CH_3
3-MeO DHP	3-OCH_3	CH_3	CH_3
4-Me DHP	4-CH_3	CH_3	CH_3

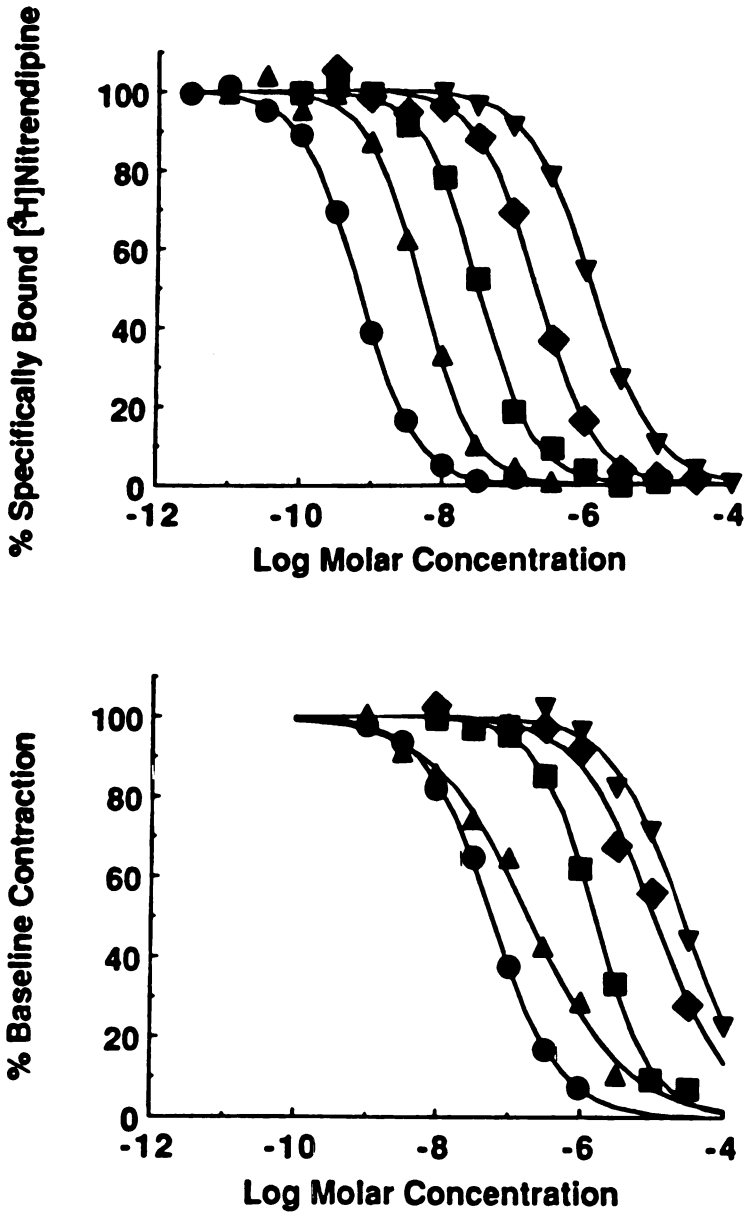

Figure 10. *Upper panel:* Data from representative experiments of displacement of specifically bound [^{3}H]nitrendipine (0.05 nM) by various 1,4-dihydropyridine compounds in membrane particulates from rabbit ventricles. The compounds are nifedipine (●), MR-I-12 (▲), 2-MeO DHP (■), 2-Cl DHP (◆), and 4-Me DHP (▼). The curves were generated by computer fit of the data using Equation 2. *Lower panel:* Representative concentration-response curves for the same five compounds shown in the upper panel. The data were fit by Equation 4 and represent percentage of baseline contractions of electrically stimulated (1 Hz) papillary muscle from rabbit right ventricle.

Table 5. Mean IC_{50} values for inhibition of specific [^{3}H]nitrendipine binding and inhibition of isometric contractions.

Compound	-Log Binding IC_{50} (M) (Mean ± S.D.) (n=3)	-Log Response IC_{50} (M) (Mean ± S.D.) (n=3-4)
Nifedipine	8.99 ± 0.17	7.32 ± 0.22
Nitrendipine	9.37 ± 0.32	6.24 ± 0.30
Nimodipine	8.75 ± 0.07	5.96 ± 0.07
Nicardipine (HCl)	8.86 ± 0.07	5.76 ± 0.40
Nisoldipine	8.86 ± 0.10	7.10 ± 0.34
2-Cl DHP	6.76 ± 0.06	5.23 ± 0.26
4-Cl DHP	6.61 ± 0.08	4.79 ± 0.07
2,6-Cl DHP	7.75 ± 0.34	5.86 ± 0.13
MR-I-12	8.33 ± 0.02	6.31 ± 0.48
2-MeO DHP	7.39 ± 0.16	5.86 ± 0.08
3-MeO DHP	7.20 ± 0.10	5.89 ± 0.35
4-Me DHP	5.88 ± 0.07	4.92 ± 0.46

Pharmacologic Response Studies

Pharmacologic response data were obtained for all the 1,4-dihydropyridine compounds included in the radioligand binding displacement experiments. The characteristics of the resulting response curves are illustrated by representative curves for the same five compounds included in the upper panel of Figure 10 (Figure 10, lower panel). Generally, the slopes of the curves for these compounds are approximately parallel and steep, with slope factors not significantly different from 1 (mean ± S.D. from all experiments; 0.73 ± 0.22). However, in comparison to the binding curves, the response curves are shifted to

the right by one to three orders of magnitude. The computer estimates of IC_{50} for inhibition of baseline contraction for all of the 1,4-dihydropyridine compounds are summarized in Table 5. The parameter estimates from the computer fits of data from individual experiments are shown in Appendix D. For all compounds, the IC_{50} for response was greater than the IC_{50} for binding. However, there was a statistically significant correlation between the binding IC_{50} values and response IC_{50} values ($r = 0.79$, $p < .005$) (Figure 11). In addition, there was a statistically significant rank order correlation (Spearman Rank Correlation Coefficient (r_s) = 0.78, $p < .005$).

Four of the compounds (nitrendipine, nimodipine, nicardipine and nisoldipine) were racemates, and might be expected to exhibit somewhat different binding and response characteristics in comparison to the achiral compounds. Therefore, we compared the binding and response parameters for these compounds with those obtained for the achiral compounds. We observed that the slopes of the concentration-response curves for the racemic compounds were more shallow than the slopes for the achiral compounds. When the slopes were compared for these two groups of compounds, there was a statistically significant difference (0.57 ± 0.11 for the racemic compounds *vs* 0.80 ± 0.22 for the achiral compounds; $p < .003$). In contrast, the slopes of the [^{3}H]nitrendipine displacement curves for these four compounds were not significantly different from those of the achiral compounds. For three of the racemic compounds, nitrendipine, nimodipine and nicardipine, there appeared to be a greater discrepancy between their binding IC_{50} values and their response IC_{50} values in comparison to the other 1,4-dihydropyridines. The ratio of the mean IC_{50} value for response over the mean IC_{50} for binding was significantly greater for this group of three compounds compared to the other nine compounds (mean $\pm$ S.D. of the ratios = 1090 ± 374 *vs* 50 ± 30; $p < .001$). For nisoldipine, however, there was no greater discrepancy than for the nonracemic compounds.

Additional saturation binding experiments were undertaken to determine if a low affinity site could be detected in the myocardial particulates, in addition to the high affinity

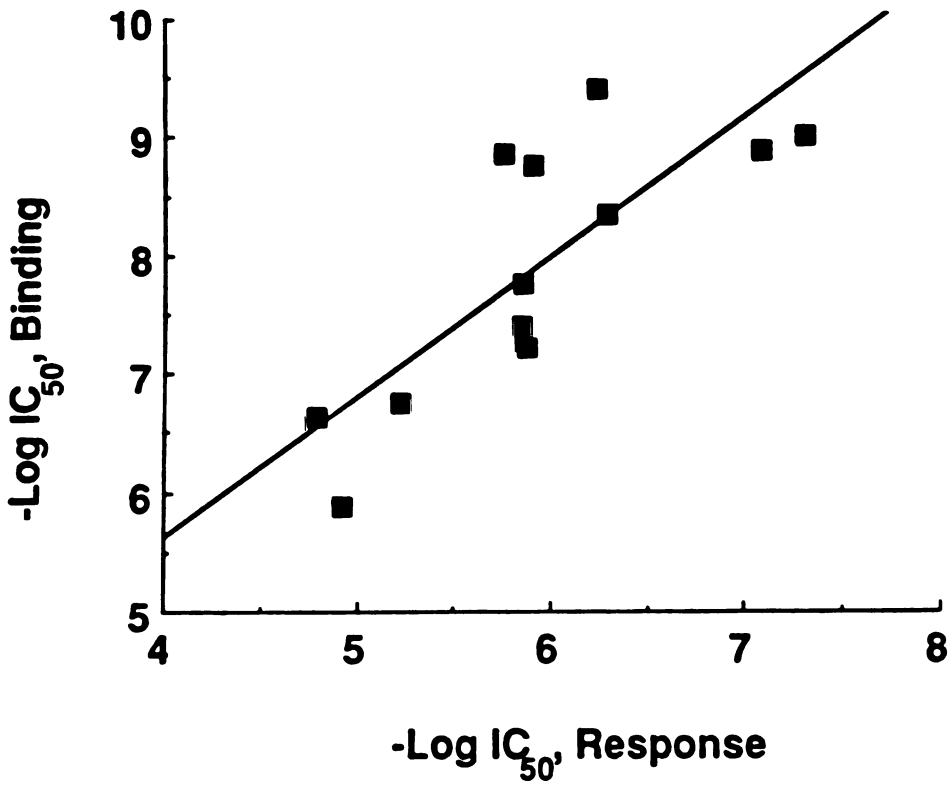

Figure 11. Comparison of binding IC_{50} values and response IC_{50} values for twelve 1,4-dihydropyridine compounds with least squares linear fit ($r = 0.79$, $p < .005$; slope = 1.17; $r_s = 0.78$, $p < .005$).

site already characterized (Figure 9). The concentrations of [^{3}H]nitrendipine in these experiments (n=3) ranged from 10 to 1000 nM. The results of a representative experiment are shown in Figure 12. No saturable binding could be discerned under these experimental conditions and the data were most appropriately fit by a straight line.

Discussion

Controversy still exists over whether the high affinity binding site in myocardium, identified in previous radioligand binding studies (Bolger *et al.*, 1982; Ehlert *et al.*, 1982; Murphy and Snyder, 1982) and characterized in this study (Figures 9 and 10; Table 3), is the receptor for the pharmacologic action of the 1,4-dihydropyridine calcium channel blockers in the heart. Although the binding properties of saturability, reversibility, high affinity, specificity and stereoselectivity of binding have been observed for 1,4-dihydropyridine compounds in myocardium (present study and Bolger *et al.*, 1982; Ehlert *et al.*, 1982; Murphy and Snyder, 1982), a correlation of binding data with biological response data has not been established. A good correlation has been found in guinea pig ileal smooth muscle (Bolger *et al.*, 1983; Wei *et al.*, 1986), in guinea pig bladder smooth muscle (Yousif *et al.*, 1985), in rat tail artery (Wei *et al.*, 1986), and in rabbit aorta (Gordon *et al.*, 1986).

Previous studies have addressed the question of whether the 1,4-dihydropyridine binding site in myocardium is a receptor. Some studies have been carried out by determining binding in one species and response in a different species (Janis *et al.*, 1984b; Rodenkirchen *et al.*, 1979). Studies in the same species have used either too few 1,4-dihydropyridine compounds with a narrow range of potencies (Goll *et al.*, 1986) or a number of calcium channel blockers from different chemical classes (Holck *et al.*, 1983).

In this study, we examined both binding and response potencies of a series of 1,4-dihydropyridine analogues in rabbit myocardium. We used [^{3}H]nitrendipine as the radioligand to characterize 1,4-dihydropyridine binding. The results of our saturation binding

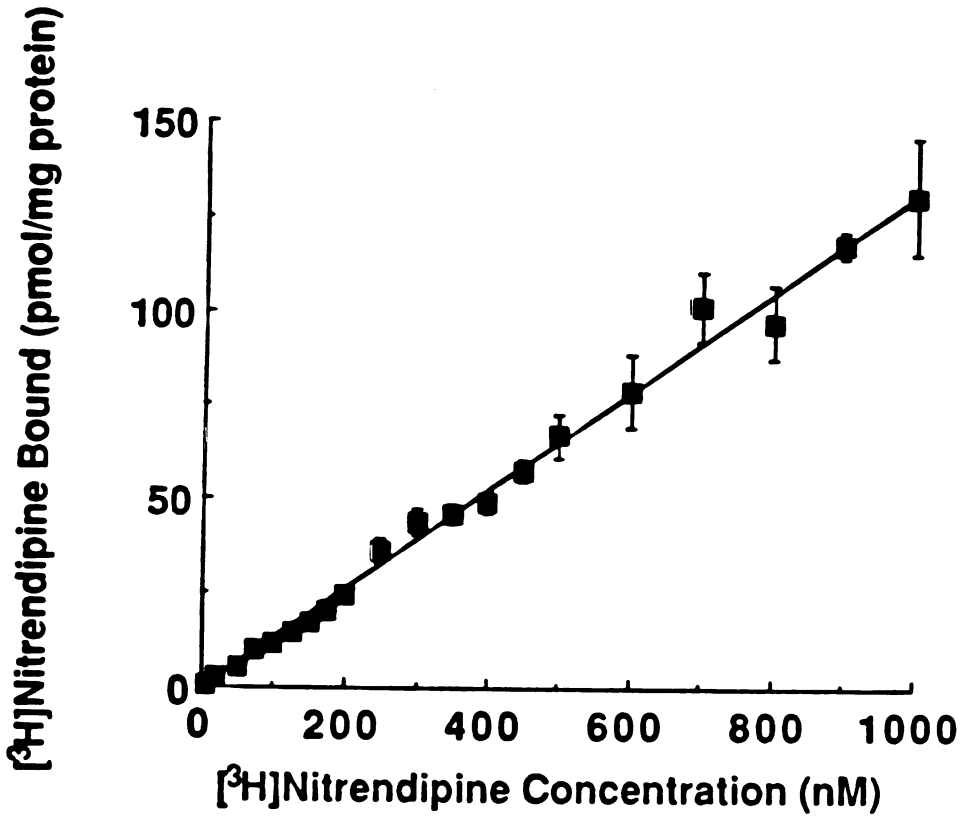

Figure 12. Data from a representative saturation binding experiment with high concentrations of [^{3}H]nitrendipine. Shown are the experimental points for total binding (± S.D.) and the linear fit that was obtained.

experiments with [^{3}H]nitrendipine agree well with those of Janis *et al.* (1984b), who also examined binding in rabbit myocardium, using similar methods. However, McBride *et al.* (1984) and Bristow *et al.* (1984) reported a K_d that is at least an order of magnitude higher than the K_d obtained in the present study. This discrepancy may be due to differences in experimental conditions such as the temperature and time of incubation. Holck *et al.* (1982) examined the binding of [^{3}H]nifedipine in rabbit ventricular homogenates and found a K_d of 1.8 nM. This value agrees with the binding affinity for unlabeled nifedipine found in the present study.

The 1,4-dihydropyridine analogues used in our study can be divided into two series. The compounds in one group all contain a 2- or 3-nitrophenyl group and various ester substituents. In the second group, the position and type of phenyl substituent varies and the ester substituents are either methyl or ethyl groups. In addition, four of the compounds, nitrendipine, nimodipine, nisoldipine and nicardipine, are racemic mixtures of enantiomers (Table 4). Binding affinities for all of these compounds were obtained from displacement experiments using [^{3}H]nitrendipine, and a wide range of values was obtained (Table 5; Figure 10, upper panel).

We next evaluated pharmacologic potencies using negative inotropy as the pharmacologic response. The question of whether negative inotropy is an appropriate variable can be addressed by referring to previous studies. Contraction in the myocardium of the rabbit was found to be more highly dependent on the influx of extracellular calcium than on the release of calcium from intracellular stores (Bodem and Sonnenblick, 1975; Sutko and Willerson, 1980). Fleckenstein (1985) demonstrated a linear relationship, in the presence of calcium channel blockers, between the decrease in calcium influx, measured electrophysiologically, and the decrease in isometric force of contraction in guinea pig papillary muscle. Also, as pointed out by Janis and Triggle (1984), when they examined the data from a number of studies, there is a reasonably good correlation between the concentration of 1,4-dihydropyridine compound needed to inhibit calcium current in the myocardium and

that needed to inhibit myocardial contraction.

Our data from the pharmacologic response experiments show a range of potencies of negative inotropic response (Table 5; Figure 10, lower panel). However, notably, we observed a shift in the potencies of response when compared to the binding affinities, the potencies of negative inotropic response being lower then the binding affinities for all the compounds. Despite the discrepancy between the absolute values for binding affinity and response potency, there is a good linear fit of the data and a statistically significant correlation between the binding and response potencies for the twelve 1,4-dihydropyridine compounds (Figure 11). Our studies are the first to compare the binding affinities and response potencies of a large series of 1,4-dihydropyridine compounds in myocardium of a single species. We have found a statistically significant rank order correlation between the binding affinities and pharmacologic potencies of the twelve 1,4-dihydropyridine compounds, but have observed a large discrepancy between the absolute values of these potencies, confirming previous reports for a few of these compounds (DePover *et al.*, 1982, 1983; McBride *et al.*, 1984; Millard *et al.*, 1983) and extending the finding to many more compounds. A similar rank order correlation between binding affinities and pharmacologic potencies was found in cat myocardium for a series of 13 phenylalkylamine derivatives (Goll *et al.*, 1986). These investigators also demonstrated a discrepancy of from one to two orders of magnitude between the absolute values of the binding affinities and pharmacologic potencies.

We considered a number of theories that might explain this discrepancy. We first examined the possibility that calcium in the physiological buffer may have been responsible. No statistically significant difference in the K_d or B_{max} of [^{3}H]nitrendipine was noted in saturation binding experiments carried out in physiologic Krebs-Henseleit buffer containing 2.5 mM calcium ($K_d = 0.07 \pm 0.04$ nM; $B_{max} = 54 \pm 24$ fmol/mg protein; n = 3) compared to those conducted in Tris buffer containing no calcium ($K_d = 0.15 \pm 0.06$ nM; $B_{max} = 247 \pm 150$ fmol/mg protein; n = 3), although the mean K_d and B_{max} were lower in

the physiologic buffer. The apparent K_d would be expected to be higher if calcium were inhibiting the binding of these compounds and a decrease in B_{max} would not explain the difference between binding affinity and potency of response. The lack of a significant effect of low concentrations of calcium on 1,4-dihydropyridine binding in isolated rabbit myocardial membranes has been demonstrated previously (Bristow *et al.*, 1984; Holck *et al.*, 1983).

Two major hypotheses have been proposed previously to explain the observed discrepancy between binding and response potencies in myocardium. The first is that two binding sites exist, one a high affinity site and the other a low affinity site, and the latter is responsible for pharmacologic effect (Marsh *et al.*, 1983; Vaghy *et al.*, 1984, 1985). A number of investigators, using radiolabeled 1,4-dihydropyridines, have reported finding two binding sites of different affinities for the 1,4-dihydropyridine compounds in myocardial membranes from guinea pig (Bellemann *et al.*, 1981), rat (Kenessey *et al.*, 1984; Rogart *et al.*, 1986), rabbit (Janis *et al.*, 1984a) and dog (McBride *et al.*, 1984; Vaghy *et al.*, 1984, 1985), as well as in cultured embryonic chick ventricular cells (Marsh *et al.*, 1983). All of the membrane preparations were similar in purity to our preparation except that of Vaghy *et al.* (1984, 1985) which consisted of purified sarcolemmal membranes. The affinity of nitrendipine for the low affinity site was found to agree fairly well with its response potency in two studies (Marsh *et al.*, 1983; Vaghy *et al.*, 1984). Most investigators, however, have found only a single, high affinity binding site for the 1,4-dihydropyridine compounds in a variety of tissues from a number of species.

We examined the binding of [^{3}H]nitrendipine at higher concentrations, but did not observe a low affinity binding site (Figure 12). It is possible that a low affinity site exists in our preparation, and that it is the pharmacologic receptor for the 1,4-dihydropyridines, but it would be difficult to detect and characterize. The mean response IC_{50} we obtained for nitrendipine was 5.75×10^{-7} M. If a low affinity binding site had a similar K_d, and the association rate was assumed to be diffusion limited (a minimum rate constant of approxi-

mately 10^7 $M^{-1}sec^{-1}$) (Rhodes *et al.*, 1985), the resulting dissociation rate constant and half-life of dissociation would be 5.8 sec^{-1} and 0.12 sec, respectively. This high dissociation rate, coupled with the high level of nonspecific binding at high radioligand concentrations, would make it difficult to characterize such a low affinity binding site as a pharmacologic receptor (Bennett and Yamamura, 1985).

The second theory is that the modulated receptor hypothesis, first proposed to explain the effects of local anesthetic compounds on the sodium channel (Hille, 1977; Hondeghem and Katzung, 1977), is applicable to the action of the 1,4-dihydropyridine compounds on the calcium channel (Hondeghem and Katzung, 1984). The assumption made when applying this theory is that the regulation of the calcium channel can be described by the classic Hodgkin-Huxley gating theory developed for the sodium channel (Figure 13A). That is, the calcium channel can exist in three states, resting, open and inactivated, controlled by membrane potential (Hondeghem and Katzung, 1977). The modulated receptor hypothesis states that the 1,4-dihydropyridine compounds will have different affinities for these three states of the calcium channel (Hondeghem and Katzung, 1984) (Figure 13B). Therefore, the binding and activity of these compounds in myocardium depend on the state of the calcium channel, which is determined by membrane potential and frequency of stimulation. Specifically, the theory suggests that these drugs bind with high affinity to the inactivated (depolarized) state of the calcium channel and with low affinity to the resting state. In the disrupted membrane particulates used in the radioligand binding experiments, no membrane potential exists and the channel is presumably in the inactivated, high affinity state. In intact tissue, however, the channel is cycling among the resting, open and inactivated states, with the majority of time spent in the resting, low affinity state. High concentrations are therefore necessary to produce a significant response.

There is considerable evidence in support of the modulated receptor hypothesis from recent electrophysiological studies (Bean, 1984; Hamilton *et al.*, 1987; Sanguinetti and Kass, 1984a; Uehara and Hume, 1985), in which it was demonstrated that the con-

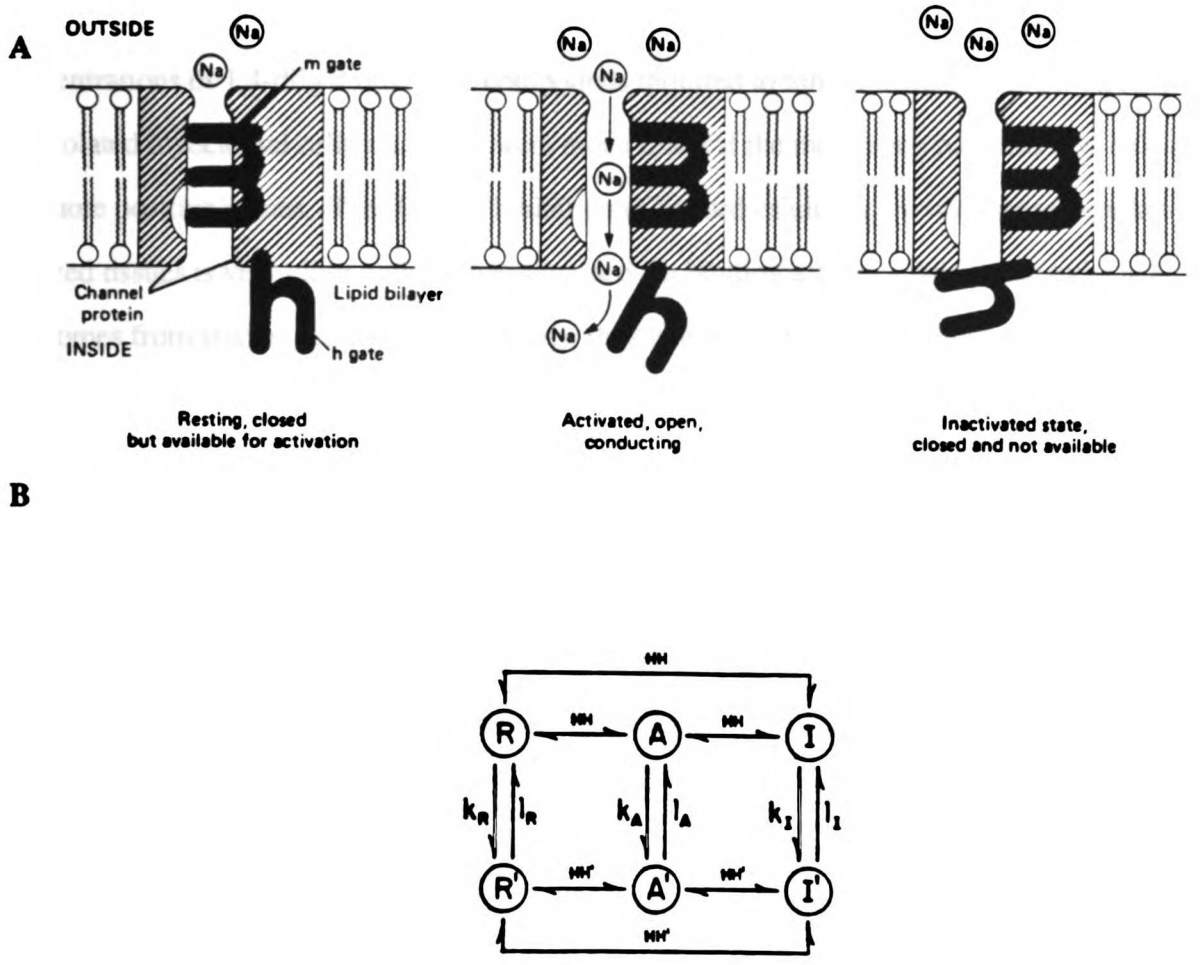

Figure 13. **A.** The three states of the sodium channel, determined by membrane potential. In the resting state (left panel), the membrane is polarized, the activation (m) gate is closed, the inactivation (h) gate is open, and the channel is available for opening. In the open state (middle panel), the m and h gates are open and the membrane is being depolarized. In the inactivated state (right panel), the membrane is depolarized, the h gate is closed, the m gate is open, and the channel is unavailable for opening (from Hondeghem and Mason, 1987). **B.** Schematic diagram of the modulated receptor hypothesis. R, A and I refer to the resting, activated and inactivated states of the channel. R', A' and I' refer to the corresponding drug-associated states. HH and HH' refer to the Hodgkin-Huxley kinetic parameters governing conversion between states in the absence or presence of drug. k and l refer to the association and dissociation rate constants of a drug from each state (from Hondeghem and Katzung, 1977).

centrations of 1,4-dihydropyridine compounds required to inhibit inward calcium current in isolated myocardial cells and tissue were much lower if the membrane potential was held at more positive values. The IC_{50} for inhibition of inward calcium current in these depolarized tissues is very close to the values obtained for binding affinity. Additional evidence comes from studies demonstrating voltage-dependent binding of 1,4-dihydropyridine compounds in isolated cardiac cells (Green *et al.*, 1985; Porzig *et al.*, 1987; Reuter *et al.*, 1985). In these studies either an increased affinity (Porzig *et al.*, 1987; Reuter *et al.*, 1985) or an increased number of high affinity binding sites (Green *et al.*, 1985) was found when cells were depolarized.

Our data are consistent with the modulated receptor hypothesis if one assumes that in the isolated papillary muscle, stimulated at a rate of 1 Hz, the channels are in the inactivated high affinity state for a small percentage of the time compared to time spent in the resting, low affinity state. There would therefore be little observable effect resulting from interaction with the inactivated channel. Inasmuch as binding experiments are conducted in depolarized tissue, the modulated receptor hypothesis suggests that only high affinity binding would occur. This theory is compatible with our inability to discern a low affinity binding site in saturation experiments using high concentrations of [^{3}H]nitrendipine.

Another possible explanation for the very low potency of negative inotropic effect involves the pharmacology of these compounds. There have been a number of reports of agonistic properties for nitrendipine (Brown *et al.*, 1986; Hess *et al.*, 1984; Thomas *et al.*, 1984), nimodipine (Schwartz *et al.*, 1984) and nicardipine (Razzetti *et al.*, 1984; Thomas *et al.*, 1984), as well as for nifedipine (Strauer, 1974; Thomas *et al.*, 1984). Although we did not observe any apparent agonistic properties of any of the compounds, it is possible that all the 1,4-dihydropyridine compounds have both agonistic and antagonistic properties, and the rightward shift in the concentration-response curves reflects this balance.

Of particular interest are three of the 1,4-dihydropyridine compounds included in our study, nitrendipine, nimodipine and nicardipine, for which a much greater discrepancy

between binding affinities and response potencies appears to exist. Such a low potency in myocardium has been reported previously for nitrendipine, nimodipine and nicardipine (Bristow *et al.*, 1984; DePover *et al.*, 1982, 1983; Janis and Triggle, 1983; Nakayama *et al.*, 1985; Rodenkirchen *et al.*, 1979; Velena *et al.*, 1985), although there also have been reports of higher potency (McBride *et al.*, 1984). In contrast, in a single study, nisoldipine did not demonstrate this low potency (Kazda *et al.*, 1980).

To explain the apparent deviation of these three compounds, one must look for chemical features that they share but that are absent in the compounds that exhibited a similar high affinity for the binding site in disrupted membranes. These features may be responsible for the very low potency in myocardium, by affecting either the affinity of these 1,4-dihydropyridines for the receptor in intact tissue, or the efficacy of their response. The explanation given for the deviation of nimodipine and nitrendipine in the study by Janis and Triggle (1983) was that these two compounds were the only ones in the group that contained large ester functions. Another possibility is that these compounds are racemic mixtures and that one of the two enantiomers could be inactive, or have agonistic properties (Hof *et al.*, 1985; Williams *et al.*, 1985), resulting in a lower potency. Neither of these possibilities may explain the deviation we found, however, because the binding and response potencies of nisoldipine, a racemic compound with a large ester function, did not deviate to a greater extent than most of the 1,4-dihydropyridines, including nifedipine. The second possibility may, however, provide an explanation for the shallow concentration-response curves that were observed for all the racemic compounds, including nisoldipine.

A further possible explanation for the large discrepancy is that the phenyl substitution is important in determining activity or receptor affinity in intact myocardial tissue. Nitrendipine, nicardipine and nimodipine all have a nitro substituent in the meta position, whereas the nitro group is in the ortho position in nisoldipine and nifedipine. It is possible that a meta nitro substituent confers on the compound a very poor affinity for the receptor or a greatly reduced efficacy of response compared to compounds with an ortho nitro sub-

stituent.

Two previous studies in cat papillary muscle have attempted to determine qualitative structure-activity relationships for the negative inotropic response of 1,4-dihydropyridine analogues (Goll *et al.*, 1986; Rodenkirchen *et al.*, 1979). From the structure-activity studies of Rodenkirchen *et al.* (1979), it was concluded that as the size of the ester substituents increased, the negative inotropic effect decreased, and that the order of potency for substituents on the phenyl ring was ortho > meta > para. Because a limited series of analogues was used, the relative importance of these two substituents for myocardial activity is unknown. Goll *et al.* (1986) determined both the binding affinities and the negative inotropic potencies of eight 1,4-dihydropyridine compounds, including nifedipine, nimodipine and niludipine. All of the compounds showed weak activity in the heart, and there was no correlation between binding affinities and response potencies for these compounds, probably because the range of potencies was very narrow, and the investigators were unable to make any firm conclusions about the structure-activity relationships.

Perhaps of greater interest is a comparison of the potency of negative inotropic effect and the potency of smooth muscle relaxation. Certain 1,4-dihydropyridine analogues undergoing clinical investigation are very potent vascular smooth muscle relaxants and are used primarily in the treatment of angina pectoris and hypertension. Compounds that possess high potency in relaxing vascular smooth muscle and low potency in exerting a negative inotropic response, an undesirable effect, would have the highest therapeutic index. Identification of structural features that could predict such vascular selectivity would be important for designing better antihypertensive and antianginal analogues.

A detailed structure-activity study of the *in vivo* antihypertensive effect of a number of 1,4-dihydropyridine compounds in dogs was carried out by Loev *et al.* (1974), who found that by increasing the size of the ester substituents, the oral potency was increased. Subsequent *in vitro* studies in vascular and nonvascular smooth muscle confirm the finding that 1,4-dihydropyridine compounds with large ester functions are very potent smooth

muscle relaxants (Bolger *et al.*, 1983; McBride *et al.*, 1984; Kazda *et al.*, 1980; Razzetti *et al.*, 1984). Another *in vivo* study examined the coronary vasodilating and antihypertensive effect of a series of 3-nitrophenyl derivatives with various ester substituents (Meyer *et al.*, 1981). In general, it appeared that asymmetrically substituted derivatives were more potent than the corresponding symmetrically substituted compounds, but that there was no consistent relationship to the size of the ester functions.

In a recent report from our laboratories, results of a series of binding and response studies for a number of 1,4-dihydropyridine analogues in rabbit aorta were presented (Gordon *et al.*, 1986). The results are summarized in Appendix E. When the binding affinities for seven 1,4-dihydropyridine compounds in rabbit myocardium (present study) and aorta (Gordon *et al.*, 1986) were compared, there was an excellent 1:1 correlation (Figure 14; $r = 0.93$, $p < .005$; $r_s = 0.89$, $p < .007$), suggesting that the binding site is the same in the two tissues. When potencies of response in the two tissues were compared, again there was a good correlation, but the potencies in the heart were less than in the aorta. Of note is the observation that nitrendipine and nimodipine were the most potent compounds in the aorta and therefore demonstrated the greatest degree of vascular smooth muscle selectivity.

Several explanations for the higher response potency of 1,4-dihydropyridines in vascular smooth muscle can be offered. One is an extension of the modulated receptor hypothesis. Because the resting membrane potential in vascular smooth muscle cells is much more positive than in myocardial cells (Schwartz and Triggle, 1984), a high affinity state of the 1,4-dihydropyridine receptor may predominate in intact vascular smooth muscle tissue. Alternatively, the depolarized state occurring during vascular smooth muscle contraction may be maintained for a much longer period of time than that in myocardium (Bean, 1984). A second hypothesis is a corollary of the two binding site theory in myocardium. That is, only a high affinity site exists in vascular smooth muscle and it represents the receptor. However, a low affinity binding site for 1,4-dihydropyridine has been reported in bovine

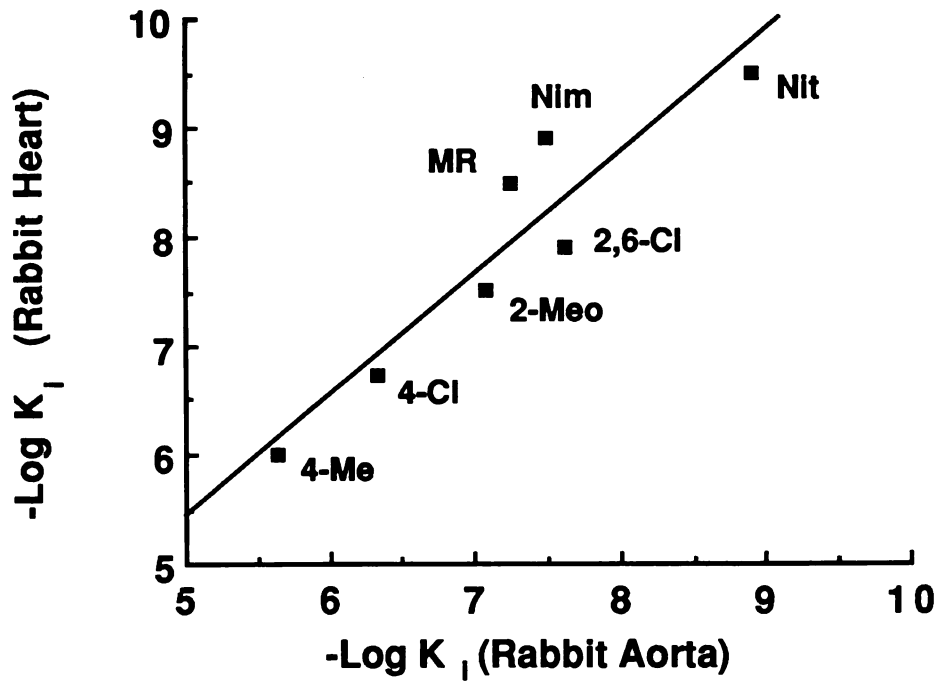

Figure 14. Comparison of K_i values in rabbit myocardium and rabbit aorta for seven 1,4-dihydropyridine compounds with least squares linear fit ($r = 0.93$, $p < .005$; slope = 1.11; $r_s = 0.89$, $p < .007$). Data in rabbit aorta were obtained from Gordon *et al.* (1986). The compounds are: Nit, nitrendipine; Nim, nimodipine; MR, MR-I-12; 2,6-Cl, 2,6-Cl DHP; 2-MeO, 2-MeO DHP; 4-Cl, 4-Cl DHP and 4-Me, 4-Me DHP.

aorta (Rogart *et al.*, 1986).

Another possible explanation for the differences in potency between the two tissues would be a difference in lipid composition between vascular smooth muscle cell membranes and myocardial cell membranes. The 1,4-dihydropyridines are believed to approach the receptor from within the membrane phase (Rhodes *et al.*, 1985). If they had a higher solubility in vascular smooth muscle cell membranes, the local concentration at the receptor site would be higher and the apparent potency of response would be greater. However, although differences in lipid composition of cell membranes from different organs in the same species are common (Harrison and Lunt, 1980), one would expect such differences to be reflected by differences in binding affinities, but these were very similar in the two tissues (Figure 14).

In summary, we have studied both the binding and response of a series of 1,4-dihydropyridine analogues in myocardium of the rabbit. The compounds bind to a single, high affinity site and the data provide no evidence for a low affinity binding site. Although we have confirmed the existence of a discrepancy between potencies of negative inotropic response and binding affinities and extended this finding to many more compounds, we also found a statistically significant rank order correlation. We are unable to distinguish among several possible hypotheses that could explain the discrepancy between binding and response. Three compounds demonstrated a much weaker negative inotropic effect than was expected. Structural features that favor this very low myocardial potency could include the presence of a meta nitro substituent on the phenyl ring and/or the size of the ester substituents. Structure-activity studies, with a larger number and wider variety of analogues, will be necessary to elucidate the reason for the high vascular smooth muscle selectivity of these compounds.

CHAPTER 4

Species Differences in the Negative Inotropic Response of 1,4-Dihydropyridine Calcium Channel Blockers in Myocardium

Introduction

In our previous study (Chapter 3), we demonstrated that the 1,4-dihydropyridine calcium channel blockers exert negative inotropic effects on rabbit myocardium at concentrations one to three orders of magnitude greater than their binding affinities to the high affinity binding site. As pointed out in that study, this discrepancy between binding and response is not present in other tissues, such as vascular smooth muscle or guinea pig ileum. Unlike smooth muscle, there is evidence that the myocardium functions differently in different species (Bers, 1985). In particular, there is considerable evidence that rat myocardium is different from other mammalian myocardium in that: 1) it exhibits a negative force-frequency relationship, whereas a positive relationship exists for most other mammals and 2) its action potential is of a shorter duration, with a rapid repolarization phase followed by a slower repolarization phase at more negative potentials (Forester and Mainwood, 1974). The long plateau at positive potentials occurring in most other mammals is absent. These differences between the rat and other mammals are believed to arise from a greater dependence in rat myocardium on intracellular stores of calcium (*ie*, from sarcoplasmic reticulum) for contraction than in most other species (Bers, 1985; Bodem and Sonnenblick, 1975; Siegl and McNeill, 1980; Sutko and Willerson, 1980). Because of these differences, comparative studies of the activity of the 1,4-dihydropyridine compounds in myocardium of rat and other species might provide more information on their mechanism of action.

In this study we examined both the binding and negative inotropic response of the

1,4-dihydropyridine calcium channel blockers in rat myocardium and compared the results to our previous findings in rabbit myocardium (Chapter 3). The results demonstrate that the binding site for 1,4-dihydropyridine calcium channel blockers appears to be identical in rat and rabbit myocardium, but the potency of the 1,4-dihydropyridines in eliciting a negative inotropic response is significantly lower in rat myocardium.

Methods

Chemicals

[^{3}H]Nitrendipine (specific activity, 79.0 to 87.0 Ci/mmol) was obtained from New England Nuclear (Boston, MA). The unlabeled 1,4-dihydropyridine compounds were obtained or synthesized as described in Chapters 2 and 3 (see Table 4, Chapter 3). All other chemicals were obtained from commercial sources and were of the highest grade available.

Radioligand Binding Studies

Male Sprague-Dawley rats (250-350 g) were killed by cervical dislocation. A membrane particulate suspension was prepared as described for rabbit myocardium in Chapter 3, with the exception that both atria and ventricles were used. Incubations of the final rat myocardial particulate suspension with [^{3}H]nitrendipine were carried out as for rabbit myocardium except that saturation experiments were performed with concentrations of [^{3}H]nitrendipine ranging from 0.01 to 1.0 nM or from 1.0 to 500 nM. The conditions for the displacement experiments were identical. Incubations were terminated by rapid vacuum filtration over 2.5 cm Whatman GF/B filters, using a filter manifold (Hoeffer Scientific Instruments, San Francisco, CA), followed by 3 x 4 ml washes with ice-cold buffer. Bound radioactivity was determined by liquid scintillation counting of the filters as described in Chapter 3. Counting efficiency ranged from 35 to 40%. Nonspecific binding was defined as the amount of [^{3}H]nitrendipine bound in the presence of 1 μM nifedipine and, in the displacement experiments, accounted for an average of 32 (± 8)% in rat myocardium. Protein concentrations were determined by the method of Lowry et al. (1951)

using bovine serum albumin as the standard. The protein concentration of the final incubation mixture in the low concentration saturation experiments was 0.12 (± 0.025) mg/ml.

Pharmacologic Response Studies

Longitudinal strips (≈ 2 mm x 8 mm) from the right ventricle of rat heart were fixed at one end and suspended in a 100 ml jacketed muscle bath containing isotonic Krebs-Henseleit buffer under the same conditions used for rabbit papillary muscles. The other end of the ventricle strip was attached to a Grass FT 03 force-displacement transducer. Contractions were induced by field stimulation at a rate of 1 Hz with a Grass Model SD9 stimulator. Contraction signals were amplified and recorded on a Grass Model 7 polygraph and peak heights were measured by hand. A preload tension of 1.0 g was applied to the muscle, which was then allowed an equilibration period to achieve steady baseline contractions, usually 60 to 120 min.

Cumulative concentration-response curves for inhibition of isometric contractions were obtained for five of the 1,4-dihydropyridine compounds (nifedipine, nitrendipine, nisoldipine, nimodipine and nicardipine) by adding increasing amounts of the compounds to the muscle bath, contained in 1.0 ml volumes, corresponding to final concentrations of 3.2×10^{-14} to 10^{-4} M. Response was measured after an incubation time of 30-40 min for each concentration. Preliminary experiments similar to those described for rabbit papillary muscle in Chapter 3 were conducted to determine the incubation period and to demonstrate the viability of the tissue for the duration of the experiments (Figure 15). At least three curves were obtained for each compound, each the result of an experiment in a muscle from a different animal. Stock solutions of the compounds (10 mM) were prepared in polyethylene glycol (PEG) 400 and stored protected from light. Dilutions were made in Krebs-Henseleit buffer. The solvent, PEG 400, had no effect on muscle contraction at the highest concentration present (1%). All experiments were carried out under subdued lighting.

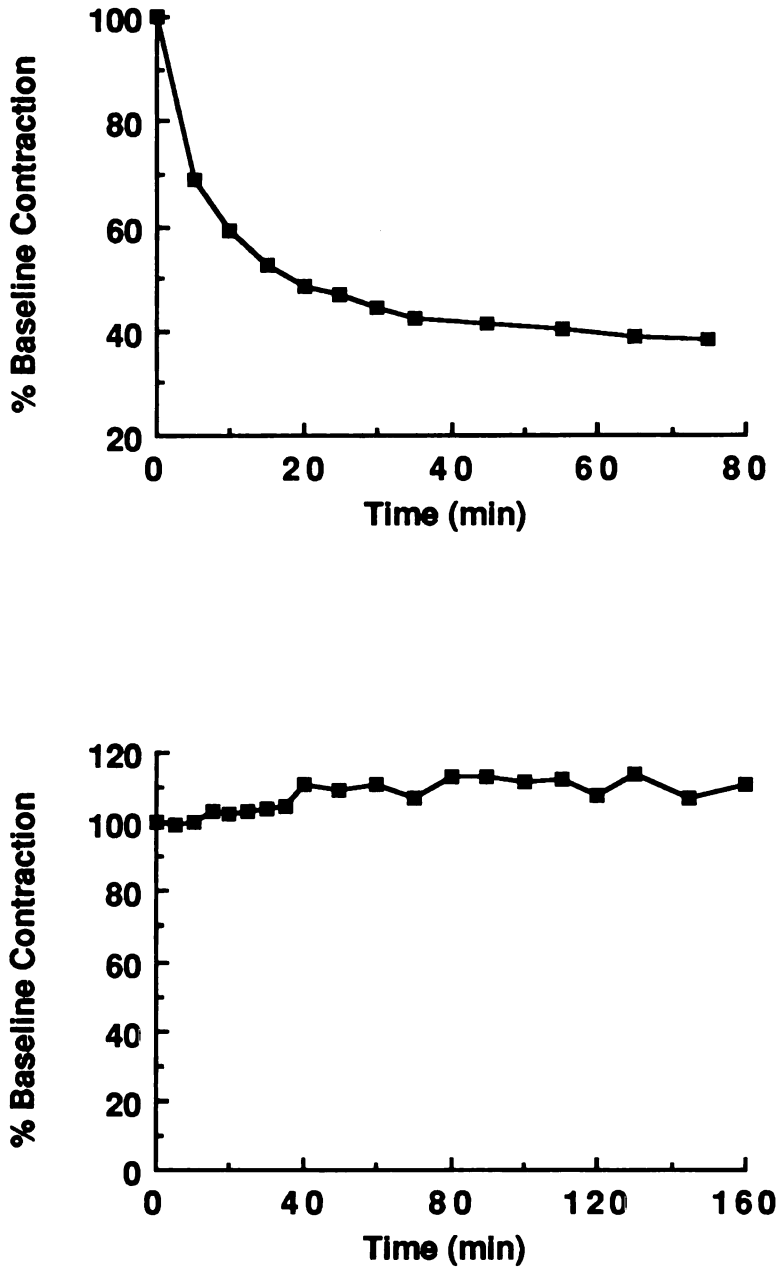

Figure 15. *Upper panel.* Results of a representative experiment showing the decrease in force of contraction of a rat ventricle strip with time after the addition of a single concentration of nifedipine (1 μM). *Lower panel.* Data from a representative control experiment showing the force of contraction of a rat ventricle strip over time when no additions were made to the muscle bath.

Calcium Concentration-Response Studies

Papillary muscles from the right ventricle of rabbit myocardium or longitudinal strips from the right ventricle of rat myocardium were isolated and mounted as described above with the exception that the buffer contained only a low concentration of calcium (0.5-1.0 mM). After steady baseline contractions were achieved with electrical stimulation at a rate of 1 Hz, additional calcium was added to the muscle bath via aliquots of a 50 mM stock solution of $CaCl_2$, resulting in final concentrations of from 1.0 to 5.4 mM. Each concentration was incubated for 10 min and the peak heights of the recorded contraction signals were then measured. The experiment was performed five times for each species.

Data Analysis

The data from individual saturation experiments in rabbit and rat myocardium were expressed as amount bound (B) and plotted against the concentration of [^{3}H]nitrendipine. Because the total amount of [^{3}H]nitrendipine bound to membrane particulates was less than 10% of added radioligand, total concentrations approximated free concentrations. To obtain the K_d and B_{max} of nitrendipine, the data were fit to Equation 1 (Chapter 3) using FIT FUNCTION. Because of the somewhat increased variability in the data from rat myocardium compared to the data for rabbit myocardium, some of the estimated parameters were not statistically significant ($p>0.05$). Therefore, K_{ns} was obtained from the slope of the linear regression of the nonspecific binding data and included in Equation 1 as a constant, rather than estimated from the computer fit of the total binding data. For the purpose of comparison, the saturation binding data from rabbit myocardium were reanalyzed by this method.

The data from individual displacement experiments were expressed as total amount of [^{3}H]nitrendipine bound and plotted against the logarithm of the concentration of displacing compound. The data were fit with Equation 2 (Chapter 3), using FIT FUNCTION, to obtain estimates of IC_{50} and n, the slope factor. The data were then converted to percentage of maximum specific binding (using the computer estimates for B_o and

B_{ns}) and plotted against the logarithm of the concentration of the displacing compound. The K_i values for the twelve 1,4-dihydropyridine compounds in rat and rabbit myocardium were calculated from IC_{50} estimates using the Cheng and Prusoff equation (Cheng and Prusoff, 1973) (Equation 3, Chapter 3), where [L] is the concentration of [^{3}H]nitrendipine in the inhibition experiments and K_d is the mean dissociation constant of [^{3}H]nitrendipine obtained from the saturation binding experiments in the corresponding tissue.

The data from individual pharmacologic response experiments were normalized to initial baseline contraction amplitude, expressed as percentage of baseline contraction, and plotted *vs* the logarithm of the concentration of the 1,4-dihydropyridine compound. The data were fit to the sigmoidal inhibitory E_{max} model (Equation 4, Chapter 3), using FIT FUNCTION, to obtain estimates of IC_{50} and n. The assumption made when applying this model was that the contractions could be completely inhibited at high concentrations of 1,4-dihydropyridine. The data were then converted to percentage of initial effect (using the computer estimate for E_o) and plotted against the logarithm of the concentration of 1,4-dihydropyridine compound.

The peak heights in each calcium concentration-response experiment were normalized relative to the initial peak height at the lowest calcium concentration and then fit to the sigmoidal E_{max} model (Holford and Sheiner, 1981) to obtain estimates of EC_{50} and n. The form of the equation was:

$$E = \frac{E_{max} * C^n}{C^n + EC_{50}{}^n} \qquad \text{(Equation 5)}$$

where E is the effect, E_{max} is the maximum effect, C is the calcium concentration, EC_{50} is the calcium concentration resulting in 50% of the maximum effect and n is the slope factor. The data in each experiment were then converted to percentage of the estimated E_{max} and plotted *vs* the calcium concentration.

In all cases, data from individual experiments were analyzed by computer and the results expressed as the mean ± S.D. of the resulting estimated parameters.

Statistical Analysis

In the binding experiments in myocardial membrane particulates from rat, only data with fits that resulted in statistically significant parameter estimates ($p < .05$) were included. Using this criterion, data from only one out of 37 experiments in rat myocardium were discarded. Because of the low potency of these compounds in rat myocardium, coupled with their low aqueous solubility, computer fits of the pharmacologic response data often resulted in parameter estimates with p-values greater than 0.05. These data were not discarded because we felt that under these conditions, more reliable parameter estimates would be difficult to obtain. The rejection rates for data from binding and response experiments in rabbit myocardium were reported in Chapter 3.

Statistical comparisons of estimated parameters were made using the unpaired Student's t-test. A paired Student's t-test was used in comparing the IC_{50} values for response of the individual compounds in rat and rabbit myocardium (Table 8). In Figure 18, a correlation coefficient significantly different from zero was an indication of a statistically significant correlation. In all cases, a p-value less than 0.05 was considered an indication of statistical significance.

Results

Radioligand Binding Studies

Table 6 shows the parameter estimates from the computer fits, using Equation 1 (Chapter 3), of the data from three [^{3}H]nitrendipine saturation binding experiments in both rabbit ventricular membrane particulates and rat myocardial particulates. In each species, the data were fit well by Equation 1. The K_d and B_{max} (mean ± S.D.) from three experiments were 0.19 ± 0.02 nM and 157 ± 29 fmol/mg protein in rat and 0.14 ± 0.06 nM

Table 6. Results of computer fits of data from [^{3}H]nitrendipine saturation binding experiments in rabbit ventricular membrane particulates and rat myocardial membrane particulates

Experiment	Rabbit			Rat		
	K_{ns}[1]	B_{max}[2] (p-value)	K_d[3]	K_{ns}[1]	B_{max}[2] (p-value)	K_d[3]
1	250 (0.0001)	358 (0.0001)	0.14 (0.003)	268 (0.0001)	153 (0.0001)	0.16 (0.0001)
2	107 (0.0001)	213 (0.0001)	0.20 (0.0001)	237 (0.0001)	131 (0.0001)	0.20 (0.0005)
3	167 (0.0001)	109 (0.0001)	0.073 (0.0005)	289 (0.0001)	188 (0.0001)	0.20 (0.001)
Mean	**175**	**227**	**0.14**	**265**	**157**	**0.19**
S.D.	**72**	**125**	**0.06**	**26**	**29**	**0.02**

[1](fmol/mg protein/nM), obtained from linear regression analysis of nonspecific binding data

[2](fmol/mg protein)

[3](nM)

and 227 ± 125 fmol/mg protein in rabbit. There was no statistically significant difference between the two species for either parameter. Figure 16 shows representative saturation isotherms demonstrating high affinity binding of [^{3}H]nitrendipine to rat myocardial membrane particulates (upper panel) and rabbit myocardial particulates (lower panel).

Radioligand binding displacement experiments were carried out for twelve 1,4-dihydropyridine compounds in both rat and rabbit myocardial membrane particulates. Figure 17 shows representative displacement curves for three compounds, nifedipine, nisoldipine and nicardipine, in myocardial membrane particulates from rat (A) and rabbit (B). Both

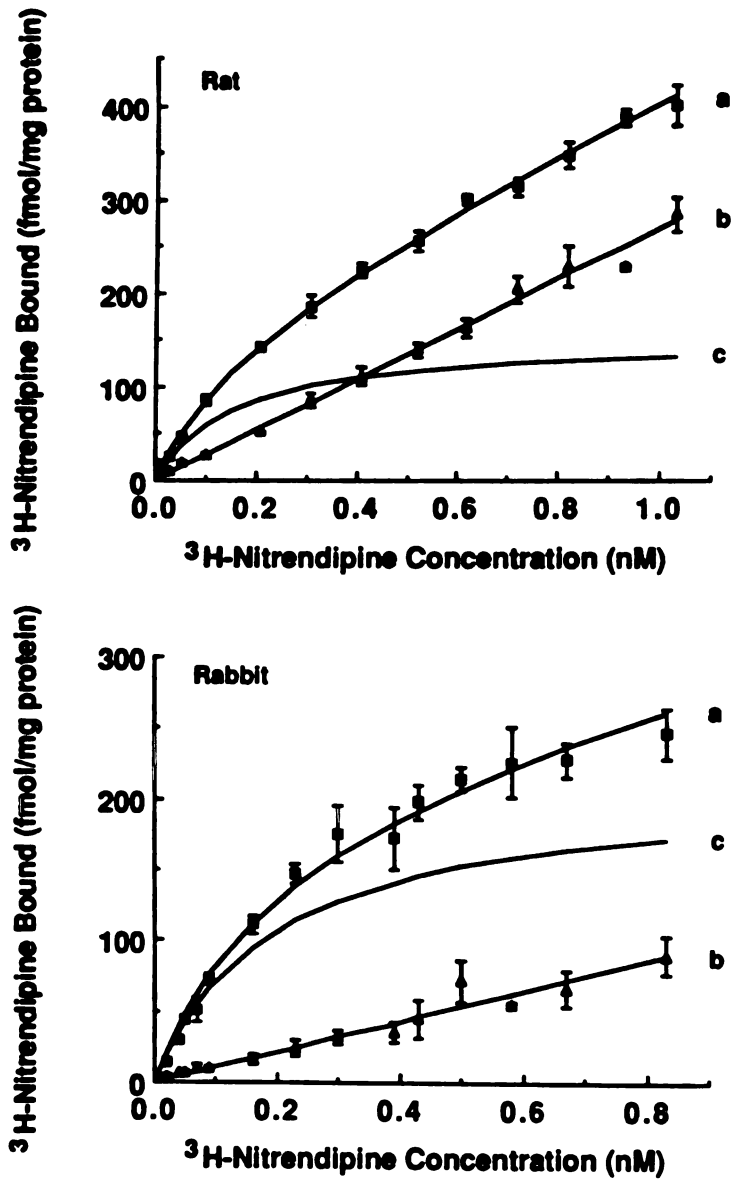

Figure 16. Representative saturation isotherms (25° C) of [^{3}H]nitrendipine binding in myocardial membrane particulates from rat (upper panel) and rabbit (lower panel). Each point represents the mean ± S.D. of 3 replicate determinations of total (■) and nonspecifically (▲) bound [^{3}H]nitrendipine at each concentration. The curves represent: (a) the computer-generated fit of the total data to Equation 1 (see text); (b) the least squares linear regression of the nonspecific binding; and (c) the computer-generated curve for the specific binding. The K_{ns}, K_d and B_{max} estimates from these experiments were, respectively, 268 fmol/mg protein/nM, 0.16 nM and 153 fmol/mg protein for rat myocardium and 107 fmol/mg protein/nM, 0.20 nM and 213 fmol/mg protein for rabbit myocardium.

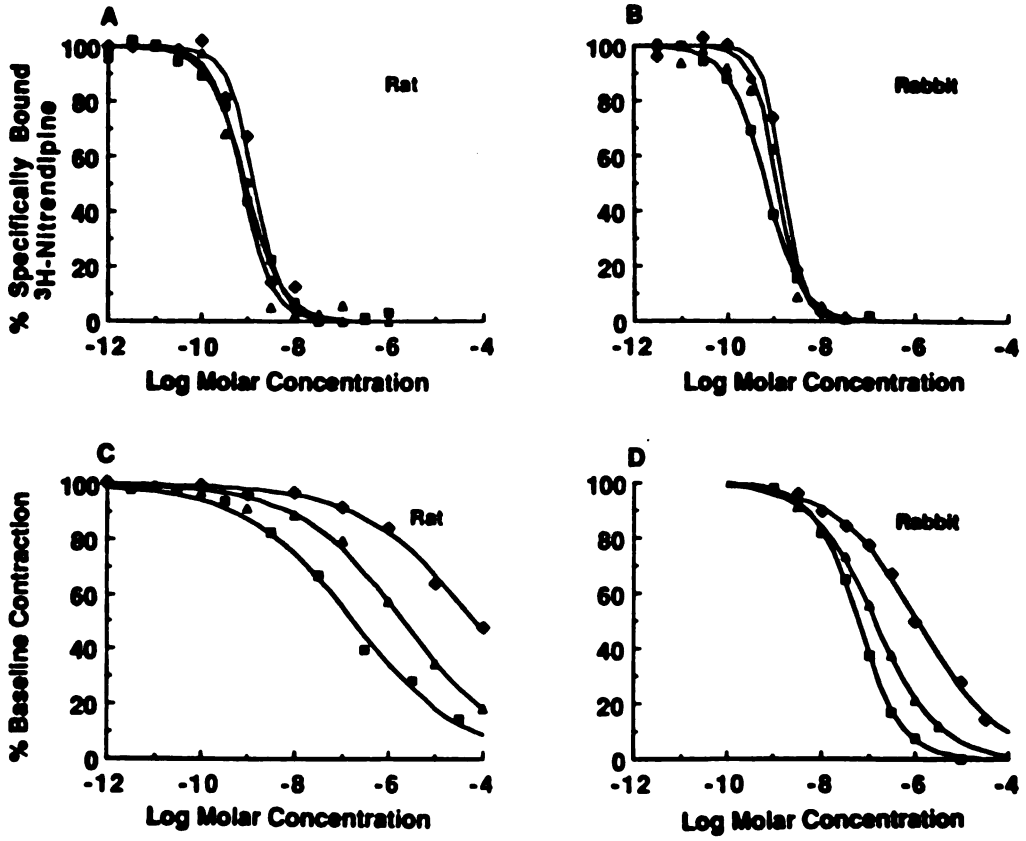

Figure 17. **A,B.** Results of representative experiments of inhibition of specifically bound [^{3}H]nitrendipine in rat (A) and rabbit (B) myocardial membrane particulates. The compounds are nifedipine (■), nisoldipine (▲), and nicardipine (◆). The curves were generated by computer fit of the data using Equation 2 (Chapter 3). **C,D.** Representative concentration-response curves for the same three compounds in rat (C) and rabbit (D) myocardium. The data were fit to Equation 4 (Chapter 3).

the experimental values and computer-generated curves of best fit are shown. The slopes of the curves were approximately parallel and steep, with slope factors (n) not significantly different from 1. No statistically significant difference between the slopes obtained in the two species was found (mean ± S.D. from all experiments; 1.18 ± 0.29 in rat and 1.27 ± 0.34 in rabbit). These results suggest competitive displacement of [^{3}H]nitrendipine from a single binding site in both species. Results of the computer fits of the data from radioligand binding experiments for all the 1,4-dihydropyridine compounds in rat myocardial membrane particulates can be found in Appendix F. The results of all of the displacement experiments are summarized in Table 7 as the mean estimates of K_i, expressed as the mean negative logarithm, for inhibition of [^{3}H]nitrendipine binding for the 12 compounds in myocardial membrane particulates from both rat and rabbit. There was an excellent 1:1 correlation between the binding K_i values for these 12 compounds in the two species ($r = 0.99$, $p < .001$) (Figure 18).

Pharmacologic Response Studies

Pharmacologic response data were obtained in both rat and rabbit myocardium for five of the 1,4-dihydropyridine compounds included in the radioligand binding displacement experiments. The characteristics of the resulting response curves are illustrated by representative curves for three of the compounds (Figure 17, C and D), the same three compounds included in the representative binding displacement curves in Figures 17 A and 17 B. Data for all the compounds are summarized in Appendix G. The response curves were less steep than the binding displacement curves and were shifted to the right. There was a distinct difference, however, in the characteristics of response to the 1,4-dihydropyridines between rat and rabbit myocardium. The mean slope factor (n) from all experiments for the five compounds was 0.62 (± 0.15) in rabbit and 0.38 (± 0.24) in rat. This represents a statistically significant difference ($p < .002$). In addition, these compounds were less potent in rat than in rabbit myocardium. Table 8 shows the mean computer estimates of IC_{50}, expressed as the mean negative logarithm, for these five compounds in

Table 7. Mean K_I values for inhibition of specific [^{3}H]nitrendipine binding in rat and rabbit

Compound	-Log K_I (M), Rat (Mean ± S.D.) (n=3)	-Log K_I (M), Rabbit (Mean ± S.D.) (n=3)
Nitrendipine	9.32 ± 0.12	9.50 ± 0.30
Nifedipine	9.10 ± 0.06	9.13 ± 0.19
Nisoldipine	9.12 ± 0.13	8.98 ± 0.10
Nicardipine (HCl)	8.94 ± 0.08	8.98 ± 0.08
Nimodipine	9.00 ± 0.16	8.90 ±0.09
2-NO_2, 5-Cl DHP	8.40 ± 0.11	8.48 ± 0.02
2,6-Cl DHP	7.99 ± 0.21	7.90 ± 0.31
2-OCH_3 DHP	7.42 ± 0.07	7.51 ± 0.15
3-OCH_3 DHP	7.26 ± 0.02	7.35 ± 0.07
2-Cl DHP	6.77 ± 0.02	6.90 ± 0.09
4-Cl DHP	6.71 ± 0.12	6.73 ± 0.08
4-CH_3 DHP	5.85 ± 0.03	6.00 ± 0.08

rabbit and rat myocardium. For each compound, the IC_{50} of response was higher in rat myocardium than in rabbit myocardium ($p < .003$).

Discussion

Many of the initial studies characterizing the high affinity binding site for 1,4-dihydropyridines in myocardium were carried out in rat (Bolger *et al.*, 1982; Ehlert *et al.*, 1982; Murphy and Snyder, 1982), although no corresponding response studies were reported.

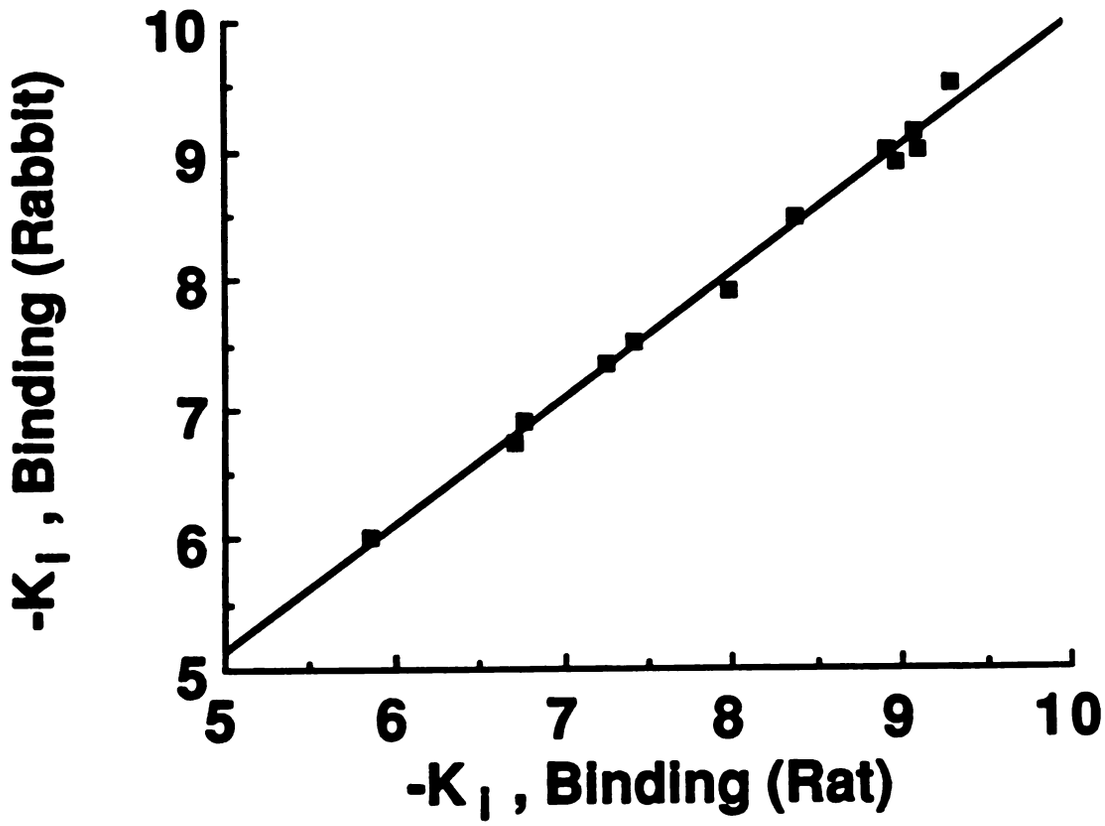

Figure 18. Comparison of binding K_i values for 12 DHP compounds in rat and rabbit myocardium using least squares linear regression analysis ($r = 0.997$, $p < .001$).

Table 8. Comparison of the negative inotropic response for selected 1,4-dihydropyridine compounds in rat and rabbit

Compound	-Log IC_{50} (M), Rat (Mean ± S.D.) (n=3)	-Log IC_{50} (M), Rabbit (Mean ± S.D.) (n=3)
Nifedipine	5.99 ± 1.01	7.32 ± 0.22
Nisoldipine	5.77 ± 0.17	7.10 ± 0.34
Nimodipine	5.21 ± 0.54	5.96 ± 0.07
Nitrendipine	4.21 ± 1.33	6.24 ± 0.30
Nicardipine (HCl)	4.05 ± 0.12	5.76 ± 0.40

It appears that the K_d for binding of [^{3}H]nitrendipine in rat myocardium is similar to that in other species (Janis *et al.*, 1984b; Sarmiento *et al.*, 1984; Gould *et al.*, 1984), but this has not been examined in detail. Although the question of differences in binding affinities of a number of 1,4-dihydropyridine analogues in different tissues within the same species has been addressed (Gould *et al.*, 1984), little attention has been paid to species differences in either binding affinities or potency of response in the same tissue. To address the question of whether species differences exist in response to calcium channel blockers and whether this is due to a difference in the 1,4-dihydropyridine binding site, we examined both binding affinities and response potencies of a series of 1,4-dihydropyridine compounds in rabbit and rat myocardium.

We used [^{3}H]nitrendipine as the radioligand to characterize 1,4-dihydropyridine binding. The results of our saturation binding experiments indicate that there appears to be no difference in the characteristics of the binding site for [^{3}H]nitrendipine in rabbit and rat heart. This is further confirmed by the results of the [^{3}H]nitrendipine binding displacement

experiments carried out with the 12 unlabeled 1,4-dihydropyridine compounds. The K_i values in rat and rabbit myocardium for each compound were almost identical and there was an excellent 1:1 correlation when the data for all of the compounds were compared (Figure 18). It therefore appears that the binding site is the same in the two tissues.

We next evaluated pharmacologic potencies of five compounds using negative inotropy as the pharmacologic response. Results of experiments in rabbit heart with all 12 of the 1,4-dihydropyridine compounds were reported previously (Chapter 3). However, when similar experiments were conducted in rat myocardium, we noted that the resulting concentration-response curves were very shallow and shifted even farther to the right than in rabbit heart. To obtain reliable estimates of IC_{50}, we therefore studied the compounds with the highest binding affinities - nifedipine, nisoldipine, nimodipine, nitrendipine and nicardipine - and response curves for these compounds were compared in rat and rabbit myocardium. These compounds were significantly less potent in rat heart than in rabbit heart (Table 8), suggesting a species difference with respect to the negative inotropic potencies of these compounds. Furthermore, the characteristics of negative inotropic response were different in the two species. In rat myocardium, the slopes of the response curves were significantly more shallow than in rabbit myocardium suggesting that different mechanisms may be involved.

Because no previous studies have examined the species differences of response to 1,4-dihydropyridine calcium channel blockers we could not compare our results to data in the literature. However, calcium channel blockers from the phenylalkylamine class have been found to be less effective in rat myocardium than in other species. D600 had less negative inotropic activity in rat left papillary muscle than in cat papillary muscle (Willerson *et al.*, 1978). In a comparison of the effect of D600 in rat, guinea pig and rabbit cardiac preparations, it was least effective in rat papillary muscle and the concentration-response curve in rat myocardium was more shallow than in rabbit or guinea pig myocardium (Siegl and McNeill, 1980). In contrast, Quinn *et al.* (1981) examined the effect of verapamil on

calcium concentration-response curves in cat, rabbit and rat myocardium and found the opposite order of sensitivity, the rat being the most sensitive and the rabbit the least sensitive to verapamil. It is not known why these results differ from the findings with D600, but it may be due to the difference in the pharmacologic endpoint, or to the presence of atenolol, a ß-adrenergic receptor blocker, in the physiological buffer used by Quinn *et al.* (1981).

There are a number of possible explanations for the species differences in the pharmacologic potency of 1,4-dihydropyridine calcium channel blockers in rat myocardium compared to rabbit myocardium. The first hypothesis is that the high affinity binding site for these compounds represents the receptor for pharmacologic activity and that it is different in the two species. The results of our binding experiments indicate that the binding site appears to be identical in myocardium from rat and rabbit (Figure 18), arguing against this explanation.

The second possibility is that there is a low affinity binding site responsible for pharmacologic effect in both tissues, but the affinity of 1,4-dihydropyridines for this site is lower in rat compared to rabbit. Two previous investigators have reported finding both a high and a low affinity binding site in membrane particulates and homogenates of rat myocardium (Kenessey *et al.*, 1984; Rogart *et al.*, 1986). However, when we examined the binding of high concentrations of [^{3}H]nitrendipine in rat (Figure 19) and rabbit (Figure 12, Chapter 3) myocardium we did not observe a low affinity binding site. Furthermore, to attribute the pharmacologic potencies of the 1,4-dihydropyridines to interactions at a low affinity site, one would have to postulate that the site differs between rat and rabbits. This would seem unlikely, given that the high affinity binding site appears to be identical in myocardium from the two species.

A third hypothesis is that the action of 1,4-dihydropyridine compounds on the calcium channel is governed by the modulated receptor hypothesis (Bean, 1984; Hondeghem and Katzung, 1984; Sanguinetti and Kass, 1984a; Uehara and Hume, 1985). This hypothesis suggests that these drugs bind with high affinity to the inactivated (depolarized)

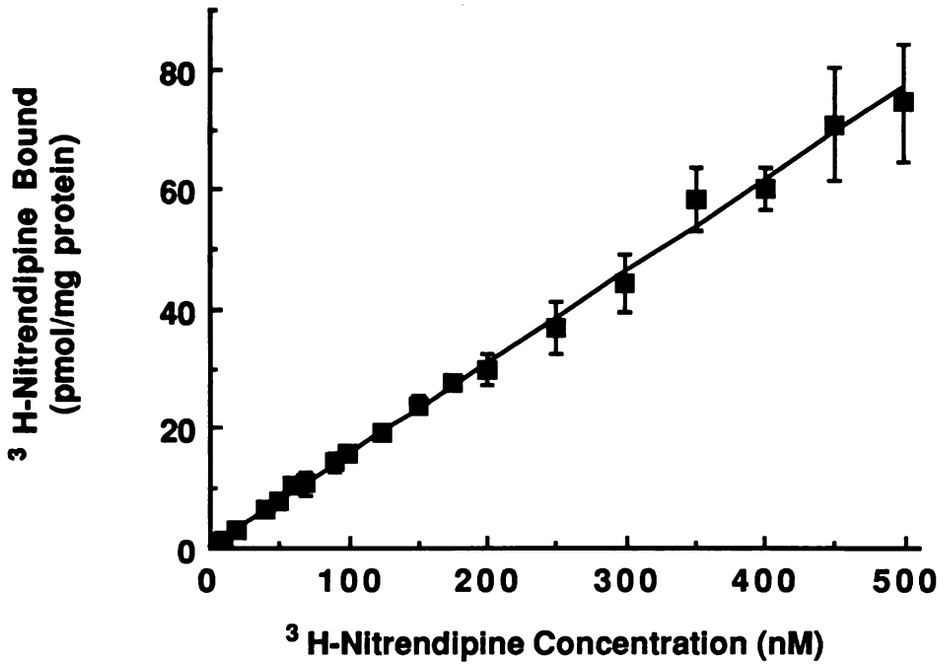

Figure 19. Data from a representative saturation binding experiment with high concentrations of [^{3}H]nitrendipine in rat myocardium. Shown are the experimental points for total binding (± S.D.) and the linear fit that was obtained.

state of the calcium channel, the state in disrupted membrane particulates used in the radioligand binding experiments, but in intact tissue, the majority of time is spent in the resting (polarized) state, to which these compounds bind with low affinity. Because of the abbreviated action potential in rat myocardium and its very rapid repolarization (Forester and Mainwood, 1974; Kelly and Hoffman, 1960), even less time would be spent in the depolarized state, so these compounds would be interacting almost entirely with the low affinity, polarized state and therefore higher concentrations would be necessary to elicit an effect.

A further possible explanation for the very low potency of 1,4-dihydropyridine calcium channel blockers in rat myocardium in comparison to rabbit myocardium is based on the fact that contraction in rat myocardium is more dependent on intracellular stores of calcium than on the influx of extracellular calcium (Bers, 1985). Rabbit myocardium, on the other hand, is highly dependent on the influx of extracellular calcium as the source of calcium for contraction (Bers, 1985; Bodem and Sonnenblick, 1975; Sutko and Willerson, 1980). Inhibition of calcium entry into rat myocardial cells could therefore have less effect on myocardial contractility.

Contraction is dependent on release of calcium from sarcoplasmic reticulum to a greater or lesser extent in the myocardium of all species (Bers, 1985). There are two mechanisms proposed for the release of this calcium: (1) calcium-induced calcium release (Fabiato and Fabiato, 1978) and (2) depolarization-induced calcium release (Winegrad, 1982). Currently, evidence appears to be more convincing for the first mechanism. If this is the operative mechanism, blockade of calcium influx would inhibit the release of calcium, and calcium channel blockers should effectively inhibit contraction, even in those species highly dependent on intracellular stores of calcium for contraction. On the other hand, if the second mechanism is operative, a decoupling of calcium entry and contraction would occur, and 1,4-dihydropyridine calcium channel blockers would be expected to have little effect on myocardial contractility in species that rely mostly on an intracellular source

of calcium for contraction.

Evidence in support of the former mechanism is the finding that lanthanum, an inorganic calcium channel blocker, inhibited steady state contractions equally in rabbit and rat myocardium (Bers, 1985). In addition, we carried out calcium concentration-response experiments in both rat and rabbit myocardium, and found no differences in the dependence of the force of myocardial contraction on external calcium concentrations under our experimental conditions. Figure 20 shows representative results from these experiments. The mean (± S.D.) EC_{50} and n were 2.43 (± 2.05) mM and 2.06 (± 0.75) for rabbit myocardium and 1.98 (± 0.90) mM and 2.31 (± 0.67) for rat myocardium (see Appendix H for the results of individual experiments). Thus it appears that steady state myocardial contractions are dependent on external calcium in both species. However, these experiments do not distinguish whether this calcium is acting as a trigger for release of calcium from intracellular organelles in rat myocardium, or is simply responsible for filling intracellular stores. If the latter case is true, it is possible that calcium cycles between sarcoplasmic reticulum and cytoplasm without being affected by the influx of external calcium.

We are unable to distinguish between the modulated receptor hypothesis and the special dependence of myocardial contractility on intracellular calcium in the rat as explanations for our findings. Additional support for both hypotheses comes from a study by Sutko and Willerson (1980). They found that when rat papillary muscle was depolarized with a high extracellular concentration of potassium, and mechanical and electrical function were restored with isoproterenol, D600 was very effective in abolishing contraction in the presence of a high concentration of ryanodine, an inhibitor of release of calcium from sarcoplasmic reticulum. In contrast, D600 was relatively ineffective in normally polarized rat papillary muscle (Willerson *et al.*, 1978). Further work will be necessary to separate the influence of membrane potential and source of calcium on the action of 1,4-dihydropyridine calcium channel blockers in rat myocardium and to determine if either is responsible for their low potency in this tissue.

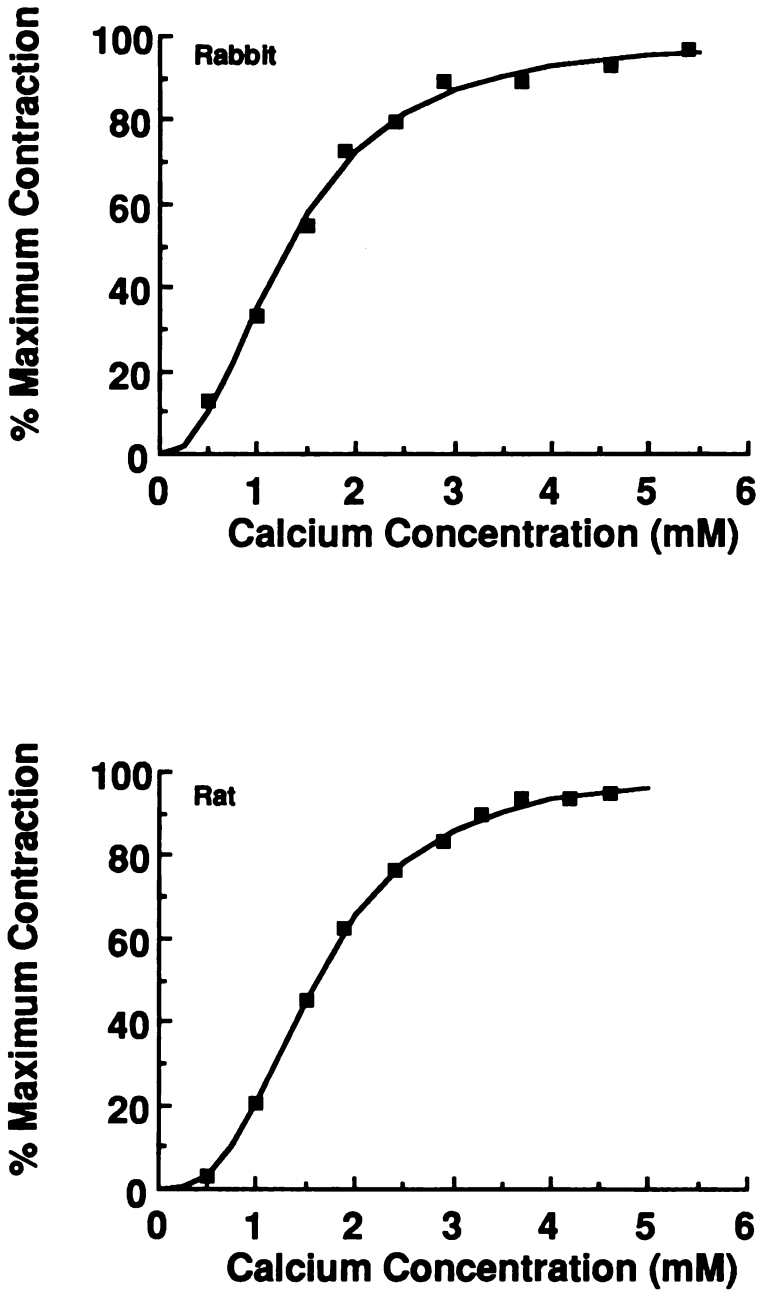

Figure 20. Data from representative calcium concentration-response experiments in myocardium from rabbit (upper panel) and rat (lower panel). Shown are the experimental points and the computer fits of the data using Equation 5. The EC_{50} and n estimated from these experiments were 1.3 mM and 2.29 in rabbit myocardium and 1.60 mM and 2.89 in rat myocardium.

A final possible explanation for the low potency in rat myocardium is that these agents have greater agonist potency (relative to antagonist potency) in rat than in rabbit myocardium. Although we did not observe any apparent agonistic properties of any of the 1,4-dihydropyridine compounds in either rat or rabbit myocardium, agonistic properties of some of these compounds have been demonstrated in myocardium from cat (Strauer *et al.*, 1974), guinea pig (Brown *et al.*, 1986; Hess *et al.*, 1984; Razzetti *et al.*, 1984; Thomas *et al.*, 1984) and rat (Schwartz *et al.*, 1984). However, not enough data are available from these studies to determine if differences in potency exist between species. Therefore we cannot rule out this possibility as an explanation for our data.

In summary, we have studied the binding and negative inotropic response of a series of 1,4-dihydropyridine analogues in myocardium from both rat and rabbit. When negative inotropic response of five of these compounds was compared in the two species, the potency was significantly lower for each compound in rat myocardium. This difference cannot be explained by a difference in the binding site because the compounds bind to a single, high affinity site that appears to be identical in both species. In addition, a low affinity site was not detected in either rat or rabbit myocardium. Rat myocardium differs from other mammalian myocardium in several ways that may explain the low potency of organic calcium channel blockers, but further work is necessary to elucidate which property is responsible. Other species may exhibit these properties to a greater or lesser extent, and it is therefore important to consider species differences when examining the effect of calcium channel blockers and when making comparisons with receptor binding.

CHAPTER 5

Characterization of Affinity Labels for the 1,4-Dihydropyridine Calcium Channel Blocker Receptor

Introduction

Receptor binding and pharmacologic response studies, together with electrophysiologic studies, have provided much information on the mechanism and site of action of the 1,4-dihydropyridine calcium channel blockers and on the physiologic and pharmacologic properties of the calcium channel. However, to fully understand the molecular mechanism of action of the 1,4-dihydropyridines, it is important to be able to isolate and characterize the macromolecules to which these compounds are binding and then to be able to relate information on the molecular structure of these macromolecules to the activity of this group of calcium channel blockers.

Most of the initial work on the molecular characterization of the 1,4-dihydropyridine receptor (binding site) was carried out in brain (Curtis and Catterall, 1983; Ferry *et al.*, 1983b; Norman *et al.*, 1983), ileal smooth muscle (Venter *et al.*, 1983) and skeletal muscle (Ferry *et al.*, 1983a; Glossmann and Ferry, 1983; Goll *et al.*, 1983; Norman *et al.*, 1983). Skeletal muscle was a particularly attractive choice for molecular characterization studies because the density of 1,4-dihydropyridine binding sites is much greater in this tissue than in any other tissue (Fosset *et al.*, 1983). However, no pharmacologic response to the 1,4-dihydropyridines is evident in skeletal muscle or brain (Miller and Freedman, 1984), and the binding sites in these tissues may be different from the receptors in tissues in which a pharmacologic response can be demonstrated (heart and vascular smooth muscle). For example, the K_d of radiolabeled 1,4-dihydropyridines in skeletal muscle has generally been reported to be an order of magnitude greater than in myocardium (Fosset *et al.*, 1983).

Therefore, we were interested in the isolation and molecular characterization of the

1,4-dihydropyridine receptor in myocardium, both to better understand the mechanism of action of the 1,4-dihydropyridines, and to address the question of why there was a discrepancy between binding and response potencies for these compounds in myocardium. Because it was assumed that the 1,4-dihydropyridine receptor site is associated with the calcium channel, we also anticipated that molecular characterization could provide information on the structure and function of the calcium channels themselves. In addition, we hoped that these studies would serve as a starting point for a comparison of the molecular characteristics of the 1,4-dihydropyridine receptor in myocardium with those of the receptor in other tissues, in particular, in vascular smooth muscle where there is a good correlation between binding and response potencies (Gordon *et al.*, 1986). In particular, we wished to examine the hypothesis that a difference in receptor structure could explain these differences in potency of response. At the time our studies began (1984), only a few preliminary attempts had been made to determine the molecular properties of the 1,4-dihydropyridine receptor in myocardial tissue (Campbell *et al.*, 1984; Horne *et al.*, 1984; Venter *et al.*, 1983) and there had been no such studies in vascular smooth muscle.

Specifically, our objective was to use affinity labels to obtain information on the molecular characteristics of the 1,4-dihydropyridine receptor in myocardium. Our studies were divided into two parts. In the first part, we conducted studies with a potential 1,4-dihydropyridine photoaffinity label that was synthesized for us, with the objective of ascertaining whether it was a specific, high affinity photoaffinity label for the 1,4-dihydropyridine receptor and therefore a viable tool with which to isolate and characterize this receptor. These studies were carried out between June and October of 1984. In the second part (began in February of 1986) we used a commercially available, radiolabeled, potential chemoaffinity label for this receptor. Each part will be discussed separately.

Background

There are a number of experimental methods that can be used to obtain preliminary

information on the molecular structure of membrane proteins such as receptors or ion channels. Each method represents only an initial step toward the ultimate goals of isolation, purification and reconstitution of the receptor/ion channel complex to the fully functioning state by incorporation into artificial lipid membranes or cellular membranes, followed by identification and sequencing of the amino acids that form the polypeptide receptor/channel subunits and finally, determination of the relationship between structure and function. Each method provides different types of information. These methods include: 1) chemical and enzymatic modification of the membrane and receptor protein; 2) radiation inactivation target size analysis; 3) solubilization of the receptor with detergents followed by analysis and purification; and 4) affinity labeling of the receptor, followed by isolation and purification. These methods previously have been applied to studies of the sodium channel (Catterall, 1982; Talvenheimo, 1985) and to studies of various drug receptors (Ferry *et al.*, 1983a, 1983b; Homcy and Graham, 1985; Takemori and Portoghese, 1985; Venter *et al.*, 1983; Wouters and Laduron, 1985). However, none of these methods is useful without a sensitive, specific assay system with which to detect the receptor. The development of high affinity radiolabeled 1,4-dihydropyridine compounds made possible the application of these methods to obtain information on the molecular characteristics of the 1,4-dihydropyridine calcium channel blocker receptor.

Initial chemical and enzymatic modification of the 1,4-dihydropyridine binding site in guinea pig brain and rabbit skeletal muscle provided evidence that binding sites are membrane proteins, possibly glycoproteins, sensitive to their phospholipid environment (Fosset *et al.*, 1983; Glossmann *et al.*, 1982). The first estimates of the molecular size of the calcium channel/1,4-dihydropyridine receptor came from radiation inactivation studies in a number of tissues (Ferry *et al.*, 1983a, 1983b; Goll *et al.*, 1983; Norman *et al.*, 1983; Venter *et al.*, 1983). In these studies, membrane preparations were irradiated with high energy electrons and the destruction of the receptor monitored by the decrease in number of binding sites for a radiolabeled 1,4-dihydropyridine compound, measured as a function of

radiation dose. Theoretically, when proteins (receptors or enzymes) are exposed to high energy ionizing radiation (x-rays, γ-rays or high energy electrons), the protein activity is destroyed in proportion to the radiation dose. Assuming that damage to any part of the protein will destroy activity, the larger the protein, the greater its chance of being damaged, and the smaller the radiation dose necessary to cause a given degree of destruction (Kempner and Schlegel, 1979; Lo *et al.*, 1982).

The theory predicts that the activity (number of radioligand binding sites) will decrease exponentially as the radiation dose increases and therefore, the logarithm of the activity will be a linear function of radiation dose. The slope of this inactivation curve is proportional to the molecular weight of the macromolecule and the molecular weight of the receptor can be estimated by comparing this slope to the slopes of inactivation curves of proteins of known molecular weight (Lo *et al.*, 1982). Alternatively, the dose of radiation resulting in a decrease in activity to 37% of control (D_{37}) can be related to molecular weight by an empirical formula (Kempner and Schlegel, 1979). The results of these studies are summarized in Table 9.

Although this method offers the advantages of giving an estimate of the molecular size of the receptor *in situ* in membranes and not requiring a highly purified preparation, the estimates represent the size of the active unit of the 1,4-dihydropyridine binding site. It is not known whether this structure is just a subunit containing the 1,4-dihydropyridine binding site or an oligomeric protein composed of closely associated subunits. It also is not known if this structure represents the size of the entire calcium channel or just a part of the channel.

Another approach to obtaining an estimate of the size of a receptor complex is solubilization of the receptor proteins with nonionic detergents followed by size determinations using gel filtration chromatography and sucrose density gradient centrifugation. Subunits are not separated by this method because no denaturing agents are used. Therefore, this method gives an estimate of the total (polymeric) size of the receptor complex. In addi-

Table 9. Summary of results of radiation inactivation target size analysis studies of the 1,4-dihydropyridine receptor from the literature

Tissue	Radioligand[1]	Molecular Weight of Receptor	Reference
Guinea pig brain	[^{3}H]nimodipine	185,000	Ferry *et al.*, 1983b
Rat cortical synaptic membranes	[^{3}H]nitrendipine	210,000	Norman *et al.*, 1983
Guinea pig ileum	[^{3}H]nitrendipine	278,000	Venter *et al.*, 1983
Rabbit skeletal muscle transverse tubules	[^{3}H]nitrendipine	210,000	Norman *et al.*, 1983
Guinea pig skeletal muscle	[^{3}H]nimodipine	178,000	Ferry *et al.*, 1983a
	[^{3}H]PN 200-110[2]	136,000	Goll *et al.*, 1983
Guinea pig heart	[^{3}H]nimodipine	184,000	Glossmann *et al.*, 1985
Rat heart	(+)[^{3}H]PN 200-110	185,000	Doble *et al.*, 1985

[1] Radioligand used to measure activity of protein

[2] The chemical structure of PN 200-110 is shown in Appendix I

tion, these procedures result in purification of the receptor complex. Additional purification and characterization can be achieved by the use of ion exchange chromatography and lectin affinity chromatography.

Activity of a solubilized receptor is monitored by radioligand binding, either by following radioactivity when a radioligand is added before the solubilization procedure, or by performing binding assays with the solubilized receptor. Further analysis is possible by treating the solubilized, purified receptor complex with denaturing agents and determining the molecular weight of the subunits using sodium dodecyl sulfate polyacrylamide gel electrophoresis (SDS-PAGE). This method is very useful for obtaining purified receptors that can be used in reconstitution studies. It also allows identification of subunits present in purified fractions. However, because the radiolabeled ligand will be removed by the de-

naturing step, it does not allow identification of the subunit to which the ligand is binding.

A number of investigators have worked on the solubilization and purification of the 1,4-dihydropyridine receptor (Borsotto *et al.*, 1984a, 1984b, 1985; Curtis and Catterall, 1983, 1984; Glossmann and Ferry, 1983; Rengasamy *et al.*, 1985). Some have solubilized a receptor-radiolabeled 1,4-dihydropyridine complex (Curtis and Catterall, 1983, 1984; Rengasamy *et al.*, 1985) while others have solubilized the receptor complex alone and monitored the binding activity of the solubilized receptor with a number of 1,4-dihydropyridine radioligands (Borsotto *et al.*, 1984a, 1984b, 1985; Glossmann and Ferry, 1983). The methods have varied, making use of different detergents and different combinations of purification steps. The results of those studies that identified the subunits present in purified fractions of radiolabeled 1,4-dihydropyridine binding activity are shown in Table 10.

A final and important method used to obtain information on subunit structure of a receptor is affinity labeling (Singer *et al.*, 1973). This method involves direct chemical identification of a binding site *in situ* by covalent labeling with a radiolabeled affinity analogue of a normal ligand. The covalently bound radioligand then can be followed through denaturation and gel electrophoresis procedures. This method offers an advantage over the previous method in that it allows the identification of the specific subunit to which a ligand is binding, and not just the subunits that comigrate with ligand-binding activity during purification steps (Cavalla and Neff, 1985).

There are two general types of affinity labels: chemoaffinity and photoaffinity labels (Singer *et al.*, 1973). Chemoaffinity labels are analogues of normal ligands containing an unmasked highly reactive electrophilic functional group that can react with certain nucleophilic chemical groups at the specific binding site to form a covalent bond. A photoaffinity label, on the other hand, contains a photosensitive functional group that is normally chemically inactive, but that becomes chemically reactive and capable of forming a covalent bond at the binding site upon photoactivation. Before photoactivation, the photoaffinity label

Table 10. Summary of results of studies in the literature identifying subunits of 1,4-dihydropyridine receptor/calcium channel after solubilization and purification

Tissue	Radioligand	Molecular Weight of Subunits[1]	Reference
Rabbit skeletal muscle t-tubules	[^{3}H]nitrendipine	130,000 50,000 33,000	Curtis and Catterall, 1984
	(+)[^{3}H]PN 200-110	142,000 33,000 32,000	Borsotto *et al.*, 1984a
Chick heart membranes	(+)[^{3}H]PN 200-110	60,000 54,000 34,000	Rengasamy *et al.*, 1985
Rabbit skeletal muscle membranes	(+)[^{3}H]PN 200-110	137,000 30,500 30,000	Borsotto *et al.*, 1985
Chick skeletal muscle membranes	(+)[^{3}H]PN 200-110	135,000 30,500 30,000	Borsotto *et al.*, 1985
Frog skeletal muscle membranes	(+)[^{3}H]PN 200-110	141,000 56,000	Borsotto *et al.*, 1985
Rabbit skeletal muscle t-tubules	[^{3}H]nitrendipine or (+)[^{3}H]PN 200-110	142,000[2] 56,000[2] 30,000[2]	Flockerzi *et al.*, 1986a
Chick cardiac membranes	(+)[^{3}H]PN 200-110	170,000[2] 140,000	Cooper *et al.*, 1987

[1] SDS-PAGE carried out under reducing conditions unless otherwise indicated

[2] SDS-PAGE carried out under nonreducing conditions

behaves like a normal reversible ligand, with both high affinity for the binding site, and biological activity. The following discussion will focus on the use of photoaffinity labels

in general, and on our studies, in particular. This will be followed by a discussion of our chemoaffinity labeling studies.

Photoaffinity Labeling Studies

Background

A photoaffinity label is a compound that will bind specifically to the receptor of interest and form a covalent bond at that site after photoactivation. There are a number of properties that define a useful photoaffinity label (Cavalla and Neff, 1985; Fedan *et al.*, 1984; Guillory and Jeng, 1983; Singer *et al.*, 1973). First, it should have a high affinity for the binding site and bind reversibly prior to photoactivation. However, the affinity should be slightly lower than that of the normal ligand because this is an indication that the photoactive substituent is attached to a part of the ligand important for binding to the receptor. Second, upon photoactivation, it should form a covalent attachment at or near the binding site. This should occur at a wavelength long enough (or at short enough times) to avoid damage to the receptor. Third, the rate and extent of this covalent insertion should decrease if a competing ligand is present during photoactivation. Fourth, if photoactivated prior to exposure to the biological sample, the photoaffinity label should be unable to form covalent bonds.

Scheme 2 demonstrates the reaction of a photoaffinity label and a receptor (Cavalla and Neff, 1985; Hanstein, 1979; Singer *et al.*, 1973). In this scheme, R is the receptor, L is the photoaffinity ligand, "R-L" represents a noncovalent association, "L*" designates the highly reactive photoactivated compound, and "R—L*" represents a covalent association. For this reaction to occur, the compound must be capable of activation while in the vicinity of the receptor and the reaction between the activated compound and an amino acid substituent in the binding site to form the covalent bond must be faster than dissociation of the activated compound from the receptor ($k_3 >> k_4$) (Singer *et al.*, 1973; Turro, 1980).

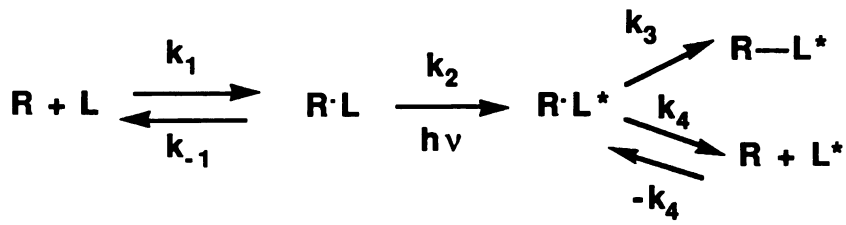

Scheme 2

Theoretically, photoaffinity labels should react very specifically and to a great extent with the receptor because of the following properties (Bayley and Knowles, 1977; Cavalla and Neff, 1985; Hanstein, 1979; Singer *et al.*, 1973): 1) very reactive functional groups can be generated that will react with most chemical groups in the vicinity, including CH bonds; 2) the binding and response of the compound can be characterized before photoactivation to demonstrate site-specificity of the ligand analogue and to allow design of optimum conditions for photolabeling experiments; 3) the investigator has control over when covalent binding will occur, allowing study of the binding under various time-dependent experimental conditions; and 4) various techniques can be used to achieve high specificity (low nonspecific binding) such as the addition of scavengers or the inclusion of a washing procedure before photoactivation. In addition, because equilibrium is achieved before photoactivation, a high concentration of photoaffinity label at the receptor site can be achieved.

A number of photosensitive substituents have been used on photoaffinity labels. Most of these compounds are azido or arylazido derivatives (RN_3). The photoactivation of the azido compound occurs as shown in the following scheme (Cavalla and Neff, 1985; Guillory and Jeng, 1983; Hanstein, 1979; Singer *et al.*, 1973):

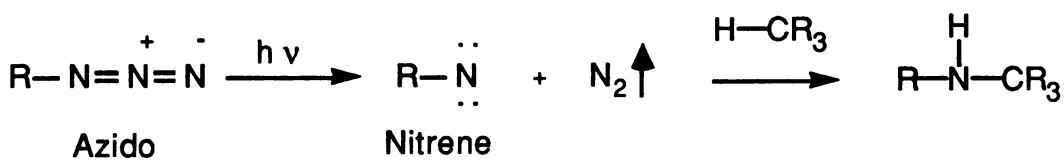

Scheme 3

A nitrene is the reactive substituent that reacts with a chemical group in its vicinity, forming a covalent bond. Arylazido derivatives offer a number of advantages as photoaffinity labels (Bayley and Knowles, 1977; Cavalla and Neff, 1985; Guillory and Jeng, 1983): 1) they absorb light, and therefore can be activated, in the visible region of the electromagnetic spectrum, thereby simplifying the photoactivation procedure and minimizing possible damage to the biological system, 2) they are chemically stable in the absence of light and 3) they are less subject to intramolecular rearrangement after photoactivation, which would reduce the amount of compound available for binding to macromolecules. One disadvantage of arylazido compounds is that the reactive substituent is less reactive than some other photoactive functional groups and will not react as readily with amino acid residues in the binding site. However, the presence of an electron-withdrawing group (*eg.* NO_2) on the aryl ring will increase the reactivity of the nitrene and increase the wavelength of maximum absorption (λ_{max}) to longer wavelengths, but decrease the stability of the unreacted compound to heat and light. Addition of an NO_2 group will also increase the electrophilicity of the compound, thereby increasing the possibility of reaction with nucleophilic groups such as solvent water, and decreasing reactions with receptor CH bonds. The addition of electrophilic groups also decreases the possibility of intramolecular rearrangement. The overall result will be low specific labeling levels, but at the the same time, nonspecific labeling of a reactive compound that is formed in solution (pseudophotoaffinity labeling) will be reduced.

At the time our studies began, a few attempts at photoaffinity labeling of the 1,4-dihydropyridine receptor had been made. The first photoaffinity label to be used to identify the 1,4-dihydropyridine receptor was [^{3}H]azidopine (Appendix I) (Ferry *et al.*, 1984). With this compound, a binding site of molecular weight 145,000 was identified. This value was larger than other reports of the 1,4-dihydropyridine subunit size. Because the photoreactive substituent (N_3) of azidopine is located at the end of a long ester side chain, it is possible that this compound is covalently binding to a protein other then the 1,4-dihy-

dropyridine binding subunit (Bayley and Knowles, 1977). Previous structure activity studies have shown that the size of the ester function does not affect affinity of binding as much as substitution of the 4-phenyl ring (Rodenkirchen *et al.*, 1979). Ferry *et al.* (1985) further studied the binding of [^{3}H]azidopine in guinea pig, rabbit, chicken and frog skeletal muscle membranes and again, reported large molecular weights for subunits to which [^{3}H]azidopine was attached (Table 11).

Finally, a report of the use of [^{3}H]nitrendipine as a photoaffinity label had been published (Campbell *et al.*, 1984) before our studies began. It is not clear what mechanism would be involved in the covalent binding of nitrendipine after exposure to UV radiation. Nevertheless, canine myocardial membranes were irradiated with UV light in the presence of [^{3}H]nitrendipine and subsequent gel electrophoresis revealed radioactivity in a band corresponding to a molecular weight of 32,000. However, this peak of radioactivity was only partially reduced when light exposure occurred in the presence of a high concentration of unlabeled nitrendipine. Therefore, it is uncertain whether the 1,4-dihydropyridine binding site had been labeled in these studies. A summary of these results is given in Table 11.

Goals

A potential 1,4-dihydropyridine photoaffinity compound, GK-III-120D (2,6-dimethyl-3,5-dicarbomethoxy-4-(2-nitro,5-azidophenyl)-1,4-dihydropyridine) (Figure 21), was synthesized by Dr. Wendel Nelson of the Department of Medicinal Chemistry, School of Pharmacy, University of Washington and made available to us for characterization. This compound appeared to be promising because it was an aryl azide with an electron withdrawing NO_2 substituent. The specific objectives of our studies with this compound were: 1) to determine if GK-III-120D was a suitable candidate as a photoaffinity label for the 1,4-dihydropyridine receptor and 2) if the preliminary results were positive, to have the compound radiolabeled and then use it to further characterize the calcium channel blocker receptor in myocardium and vascular smooth muscle.

Table 11. Summary of results of photoaffinity labeling studies of the 1,4-dihydropyridine receptor from the literature

Tissue	Affinity Label	Molecular Weight of Subunit[1]	Reference
Guinea pig skeletal muscle t-tubules	[^{3}H]azidopine[2]	145,000	Ferry *et al.*, 1984
Rabbit and guinea pig skeletal muscle t-tubules	[^{3}H]azidopine	240,000[3] 158,000[3] 99,000[3]	Ferry *et al.*, 1985
Chicken and frog skeletal muscle t-tubules	[^{3}H]azidopine	158,000[3]	Ferry *et al.*, 1985
Canine myocardium	[^{3}H]nitrendipine	32,000	Campbell *et al.*, 1984
Rabbit skeletal muscle t-tubules	(+)[^{3}H]PN 200-110	170,000	Galizzi *et al.*, 1986
Bovine myocardium, bovine aorta, and chicken skeletal muscle	[^{125}I]Bay P 8857[2]	33-35,000	Sarmiento *et al.*, 1986
Guinea pig skeletal muscle t-tubules	(-)[^{3}H]azidopine	155,000[3]	Striessnig *et al.*, 1986
Guinea pig, chick, and rat myocardium	(-)[^{3}H]azidopine	155,000[3]	Ferry *et al.*, 1986 Glossmann *et al.*, 1987

[1] SDS-PAGE carried out under reducing conditions unless otherwise indicated

[2] Chemical structure shown in Appendix I

[3] SDS-PAGE carried out under nonreducing conditions

Methods

Binding Characteristics of Nonphotoactivated GK-III-120D

Radioligand binding experiments were carried out with GK-III-120D and [^{3}H]nitrendipine in a rat myocardial membrane particulate suspension. The membrane

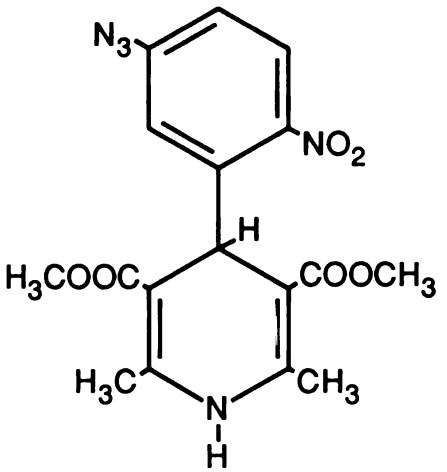

GK-III-120D

Figure 21. Chemical structure of GK-III-120D (2,6-dimethyl-3,5-dicarbomethoxy-4-(2-nitro,5-azidophenyl)-1,4-dihydropyridine)

suspension was prepared as described in Chapter 4. The experimental methods were the same as those used for displacement experiments with other unlabeled 1,4-dihydropyridine compounds in Chapters 3 and 4. Briefly, the [^{3}H]nitrendipine concentration in the incubate was 0.05 nM and the incubation mixture contained concentrations of unlabeled GK-III-120D ranging from 10^{-11} to 10^{-6} M. The experiment was carried out three times and in each experiment, each data point was determined in triplicate.

The data from individual displacement experiments were expressed as total dpm of [^{3}H]nitrendipine bound and plotted against the logarithm of molar concentration of GK-III-120D.The data were fit to the four parameter logistic function (equation 2, Chapter 3) using FIT FUNCTION to obtain estimates of IC_{50}, n (the slope factor), nonspecific binding (B_{ns}), and maximum specific binding (B_o-B_{ns}). The data were then replotted as percentage of maximum specific binding (obtained from the computer estimates) versus the logarithm of molar concentration of GK-III-120D.

Photoactivation Procedures

A control UV spectral scan of GK-III-120D (3.2×10^{-5} M) in absolute ethanol was obtained using an Ultraspec 4050 spectrophotometer (LKB Biochrom Ltd., Gaithersburg, MD). The range of wavelengths scanned was 201 nm to 450 nm. In preliminary experiments, no absorbance was observed at wavelengths from 451 nm to 900 nm. The solution of GK-III-120D was then exposed to UV radiation at a wavelength of 254 nm using an UVSL-25 Mineralight (115 volts, 60 Hz, 0.16 amps) (Ultra-Violet Products, Inc., San Gabriel CA) in quartz cuvettes for various periods of time at a distance of 2 cm. A UV spectral scan was obtained after each exposure time. A wavelength of 254 nm was chosen for the photoactivation procedure because there was significant absorbance by GK-III-120D at that wavelength and because a light source of that wavelength, suitable for these studies, was readily available. In addition, it has been reported that aryl azide compounds show higher labeling efficiencies at 254 nm than at longer wavelengths and the rate of photoactivation at this wavelength occurs faster than the rate of destruction of the biological

system (Bayley and Knowles, 1977).

The basic procedure for determining if GK-III-120D was covalently bound was an indirect method because the compound was not radiolabeled. Similar methods have been used to characterize the covalent binding of a 1,4-dihydropyridine chemoaffinity compound (Venter *et al.*, 1983) and an α_1-adrenergic antagonist photoaffinity label (Hess *et al.*, 1983). The compound was incubated with the membrane suspension in the dark until equilibrium was achieved and then the incubate was exposed to UV radiation. The unbound compound was washed out and the binding of a single concentration of [^{3}H]nitrendipine was determined and compared with a number of controls. If GK-III-120D had covalently bound, the specific binding of [^{3}H]nitrendipine would be reduced.

Because a very large loss of specific binding sites occurred in tissue that underwent the initial incubation and the washing procedure compared to tissue that had not been subjected to these manipulations, considerable time was spent on optimizing the conditions of these experiments before the photoactivation was attempted. The effects of Polytron speed, number of washes, initial tissue concentration and volume of washing buffer were varied to find conditions that minimized the loss of binding sites, maximized the ratio of specific to nonspecific binding and facilitated removal of noncovalently bound GK-III-120D.

The membrane particulate fraction of rat myocardium was prepared as described for the radioligand binding experiments except that the tissue concentration in the final resuspension was 100 mg original wet weight/ml buffer. A 1.9 ml aliquot of this turbid membrane suspension was incubated with 100 µl of a solution of GK-III-120D in buffer to achieve a final concentration of 10^{-6} M. This 2 ml volume was incubated in the dark for 60 min at 25° C. At the end of this incubation, for those samples to be exposed to UV radiation, the incubation volumes were transferred to quartz cuvettes and exposed to 254 nm radiation at a distance of 2 cm for the specified time. After exposure of the appropriate samples to UV radiation, each incubation volume was transferred to a centrifuge tube and 18 ml of ice-cold Tris buffer was added. The mixture was vortexed, allowed to stand for

10 min, and then centrifuged at 28,000 g (15,000 rpm) at 5° C for 10 min in a Beckman Model J2-21 centrifuge using a JA-20 rotor. The supernatant was discarded, the pellet re-suspended in 20 ml Tris buffer with a Brinkmann Polytron (setting 6) and the suspension allowed to stand for 10 min before the next centrifugation. This centrifugation-resuspension procedure was carried out a total of three times, with the final resuspension in 4.75 ml of buffer to give a tissue concentration of 40 mg original wet weight /ml buffer. A 200 µl aliquot of this final suspension was incubated with [^{3}H]nitrendipine (0.05 nM) for 60 min at 25° C in a total volume of 2 ml. Additionally, half of the incubates contained 10^{-6} M nifedipine to define nonspecific binding. The incubations were terminated by rapid vacuum filtration and the radioactivity trapped on the filters was determined by liquid scintillation counting. All determinations were carried out in triplicate.

Results

Binding Characteristics of Nonphotoactivated GK-III-120D

The results of the radioligand displacement experiments with GK-III-120D are shown in Figure 22. Both the experimental points (± S.D.) and the computer fits of the data are shown. The mean estimate of the IC_{50} from the three experiments was 3.84 (± 0.35) x 10^{-9} M. Using the equation of Cheng and Prusoff (19), with a radioligand concentration of 0.05 nM and a K_d for [^{3}H]nitrendipine of 0.32 nM (Chapter 4), we obtained a K_i of 3.32 x 10^{-9} M. The mean slope factor (n) was 0.96 ± 0.13. Nonspecific binding accounted for a mean of 29 ± 4 % of the total binding under these experimental conditions.

Photoactivation Procedures

Figure 23 A shows a UV spectrum of GK-III-120D both before exposure to UV radiation and after 15 min exposure to 254 nm at a distance of 2 cm. Figure 23 B includes the changes in the spectrum at intermediate exposure times. An exposure time of 14 min at a distance of 2 cm initially was chosen for photoactivation in the membrane suspension because, under these conditions, a significant change had occurred in the UV spectrum of GK-III-120D.

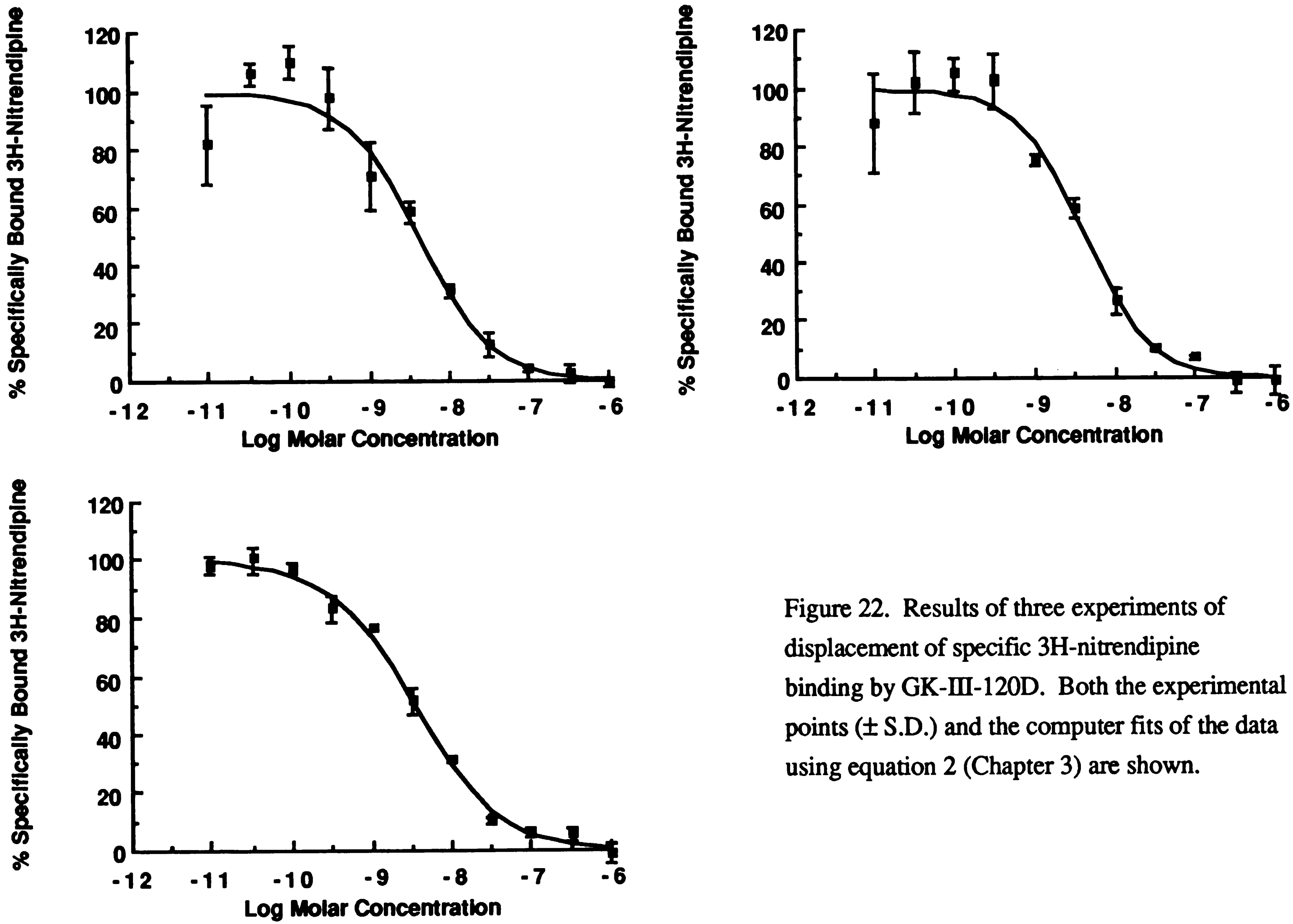

Figure 22. Results of three experiments of displacement of specific 3H-nitrendipine binding by GK-III-120D. Both the experimental points (± S.D.) and the computer fits of the data using equation 2 (Chapter 3) are shown.

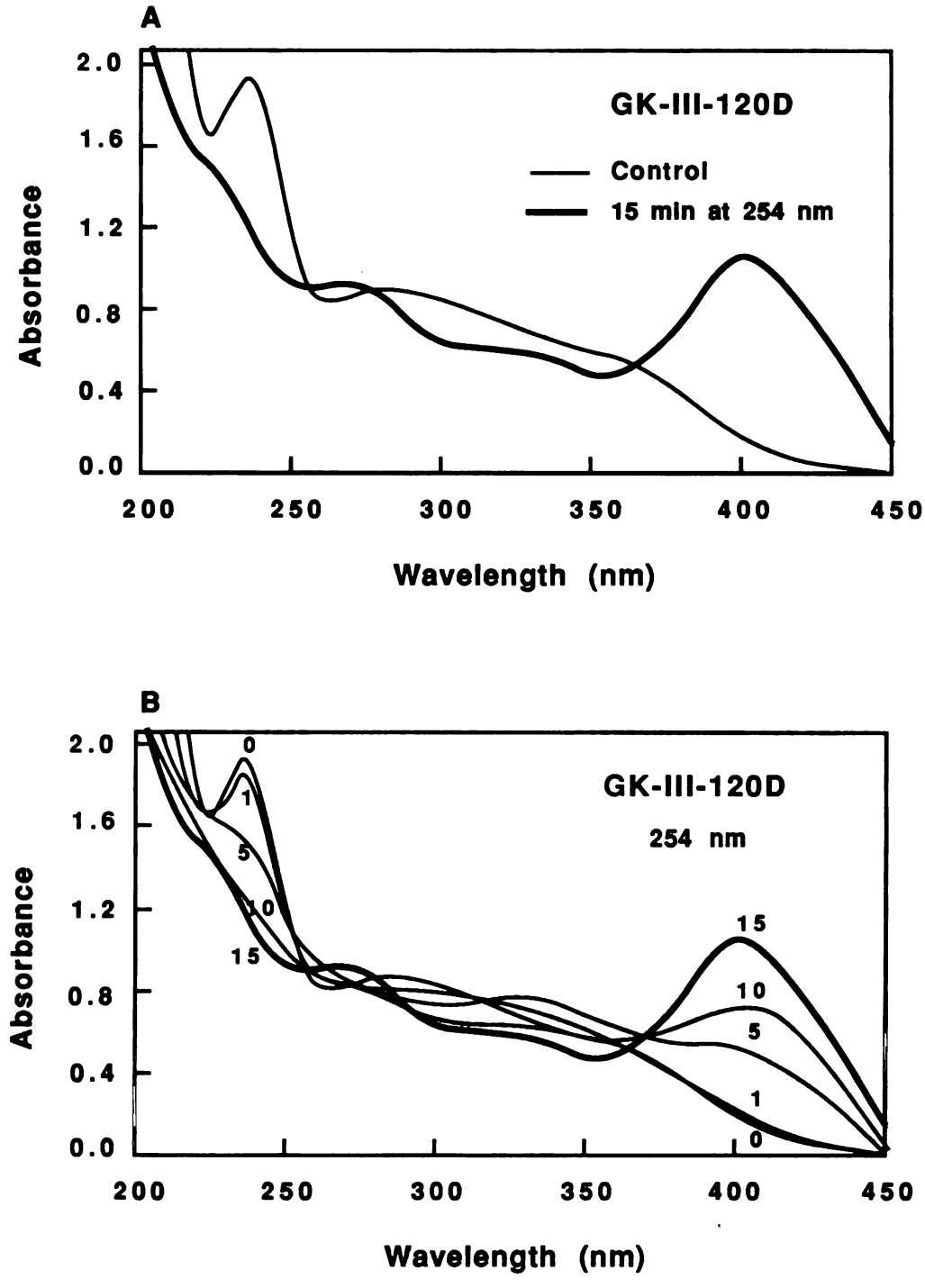

Figure 23. **A.** UV spectrum of GK-III-120D (3.2×10^{-5} M) in absolute ethanol prior to (——) and after (——) 15 min exposure to UV radiation at a wavelength of 254 nm. **B.** As in **A**, with the addition of spectra obtained at intermediate exposure times as indicated on figure.

Initial results from a single experiment with a 14 min UV exposure are shown in Figure 24. The figure demonstrates the apparent decrease in specific [^{3}H]nitrendipine binding in tissue incubated with GK-III-120D that had been exposed to UV radiation. In addition, however, there was a large decrease in specific binding after incubation of tissue with GK-III-120D that had not been exposed to UV radiation. We considered the following explanations for this observation: 1) noncovalently associated GK-III-120D was not being washed out with this procedure or 2) GK-III-120D was covalently bound without exposure to UV light. Subsequent experiments were designed to distinguish between these possibilities. In addition, the effect of UV light, alone, on specific [^{3}H]nitrendipine binding was examined to determine if the decrease in specific binding after incubation with GK-III-120D and exposure to UV radiation was due to covalent binding of the photoactivated compound, or due to destruction of binding sites by the UV radiation. The experimental conditions that were altered in these studies included tissue concentration, UV exposure time, and UV wavelength.

With the goal of further increasing the apparent photoactivation of GK-III-120D, the next experiment examined the effect of different UV exposure times. Because a very significant reduction in specific binding of [^{3}H]nitrendipine was found after a 30 min exposure of GK-III-120D to UV radiation (Figure 25), this exposure time was used for the next group of experiments. Figure 26 shows the mean results from three of these experiments. Included was a control for the effect of UV radiation on [^{3}H]nitrendipine binding sites in the absence of GK-III-120D. After a 30 min UV exposure, three major problems were evident: 1) the UV exposure appeared to have a destructive effect on the tissue, 2) again, a significant amount of the unexposed GK-III-120D either was not washed out or was covalently bound in the absence of light, and 3) the large reduction in specific binding of [^{3}H]nitrendipine observed in the initial experiment after a 30 min UV exposure of GK-III-120D (Figure 25) was not reproducible.

All of the previous experiments were carried out with tissue concentrations of 100

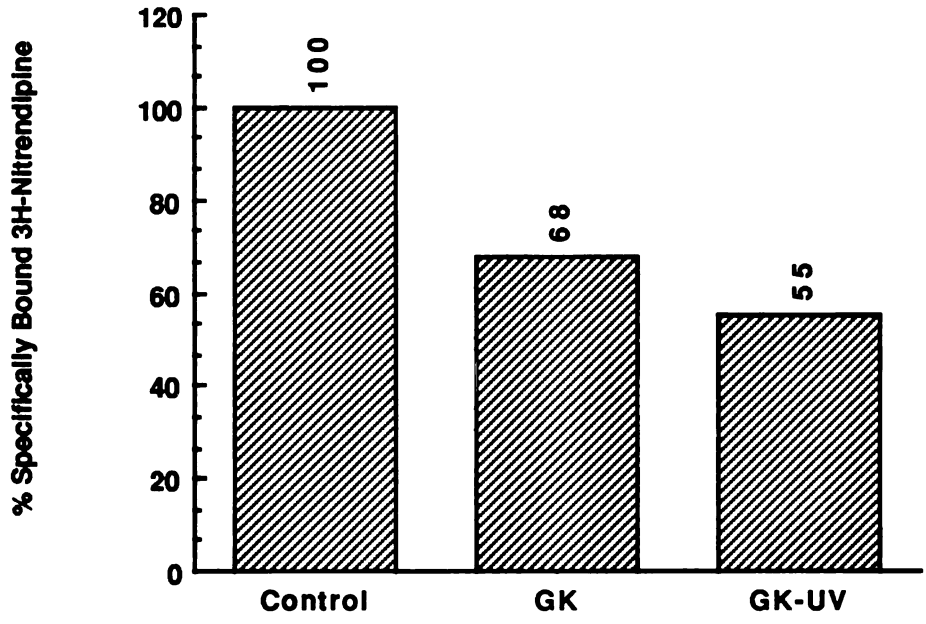

Figure 24. Results of a single experiment showing specifically bound [^{3}H]nitrendipine in rat myocardial membrane particulates after preincubation with GK-III-120D and exposure to 14 min of UV radiation (254 nm) (GK-UV) or no UV radiation exposure (GK), relative to control tissue with no GK-III-120D present and no exposure to UV radiation. The tissue concentration in all cases was 100 mg/ml.

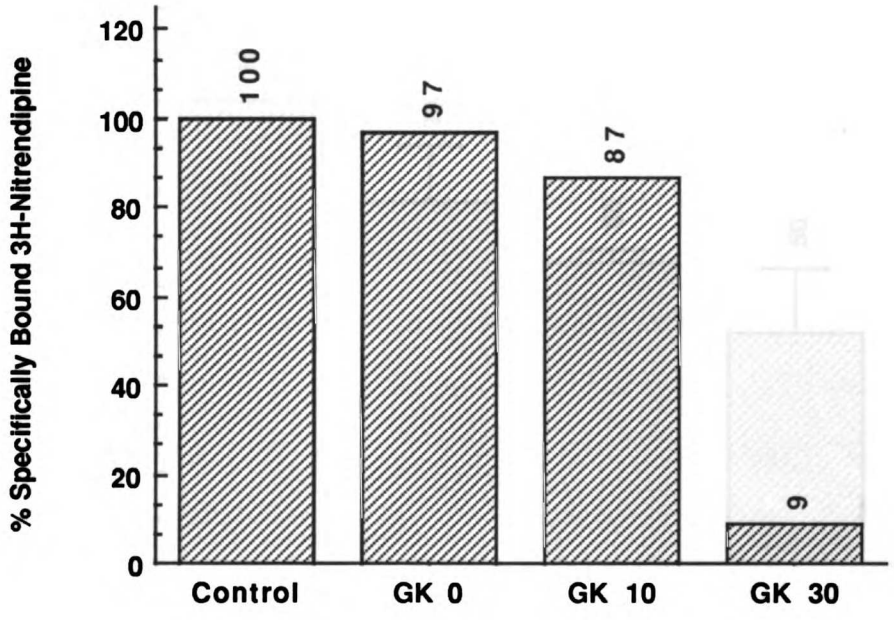

Figure 25. Results of a single experiment showing specifically bound [^{3}H]nitrendipine in rat myocardial membrane particulates after preincubation with GK-III-120D and exposure to UV radiation (254 nm) for 0, 10 and 30 min, relative to control tissue with no GK-III-120D present and no exposure to UV radiation. The tissue concentration was 100 mg/ml.

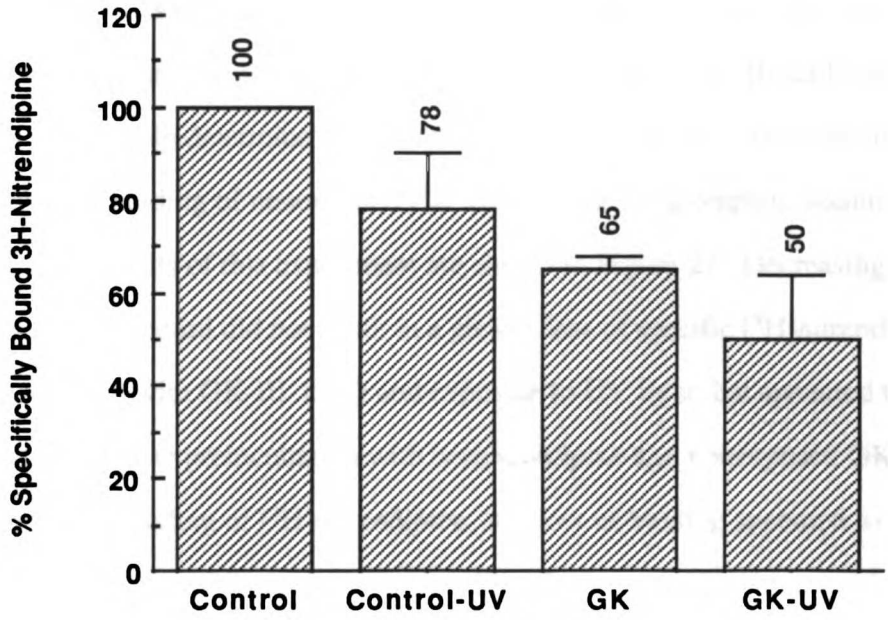

Figure 26. Mean results of three experiments showing specifically bound [^{3}H]nitrendipine after preincubation with GK-III-120D and exposure to 30 min of UV radiation (254 nm) (GK-UV) or no UV radiation exposure (GK), relative to control tissue with no GK-III-120D present and no UV exposure (Control) or 30 min of UV exposure (Control-UV). The tissue concentration was 100 mg/ml. The error bars represent the S.E.M.

mg/ml. It was possible that this concentration was too high, thus preventing optimum exposure of GK-III-120D to the light and also preventing the noncovalently bound GK-III-120D from being washed out. In the next experiment, the tissue concentration was halved to 50 mg/ml. In addition, a nifedipine control was added in which tissue was incubated with nifedipine, but not exposed to UV light. Because nifedipine differs from GK-III-120D only in the absence of the photoactive substituent, it would be expected to have binding characteristics similar to GK-III-120D, except that it would not covalently bind. Therefore, comparison of results with nifedipine with those of GK-III-120D not exposed to UV light should help determine whether the decrease in specific [^{3}H]nitrendipine binding is due to covalent binding of nonexposed GK-III-120D or to incomplete washing out of the compound. The results of this experiment are shown in Figure 27. Decreasing the tissue concentration to 50 mg/ml did not result in a greater loss of specific [^{3}H]nitrendipine binding after incubation with GK-III-120D and exposure to UV light, but appeared to decrease the loss. Also, because preincubation with both nifedipine and nonexposed GK-III-120D decreased specific binding of [^{3}H]nitrendipine, this loss of binding appeared to be due to noncovalent association of these compounds. Also demonstrated in this experiment was the apparently greater destruction of binding sites by UV light at this lower tissue concentration.

In an attempt to improve the washing out of noncovalently bound compound, the tissue concentration was decreased further to 20 mg/ml. At the same time, the UV exposure time was reduced to 15 min. An additional control was included in which tissue was preincubated with nifedipine and exposed to UV radiation. The results of two of these experiments are shown in Figure 28. At this tissue concentration, it appeared that GK-III-120D and nifedipine not exposed to UV radiation were almost completely washed out. In addition, under these conditions, there was a significant loss of specific [^{3}H]nitrendipine binding after preincubation with GK-III-120D and exposure to UV radiation. However, because this loss also occurred in those samples exposed to UV radiation and preincubated

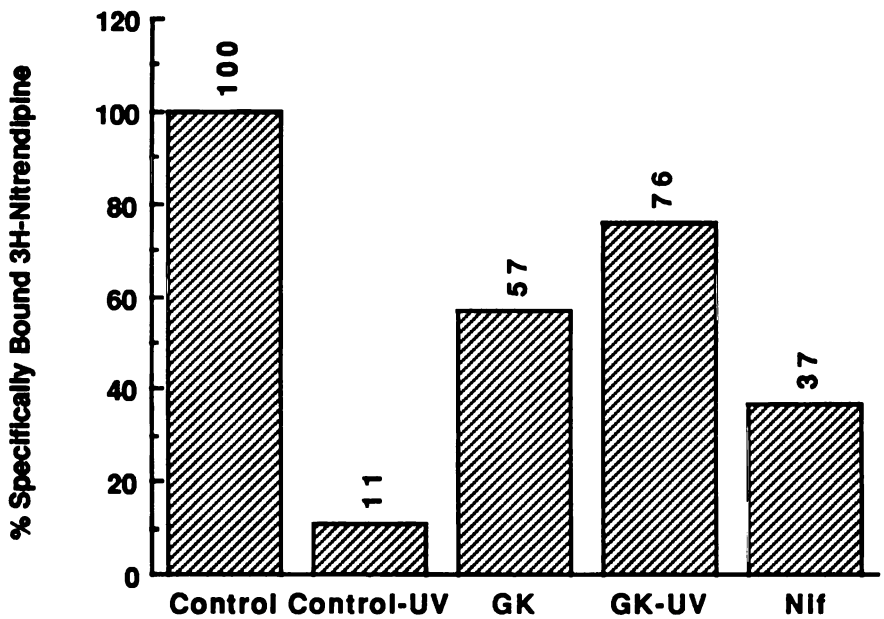

Figure 27. Results of a single experiment showing specifically bound [^{3}H]nitrendipine after preincubation with GK-III-120D and exposure to 30 min UV radiation (254 nm) (GK-UV) or no UV radiation exposure (GK), relative to control tissue with no GK-III-120D present and no UV exposure (Control) or 30 min UV exposure (Control-UV) and to tissue incubated with nifedipine (10^{-6} M) and no exposure to UV radiation (Nif). The tissue concentration in this experiment was 50 mg/ml.

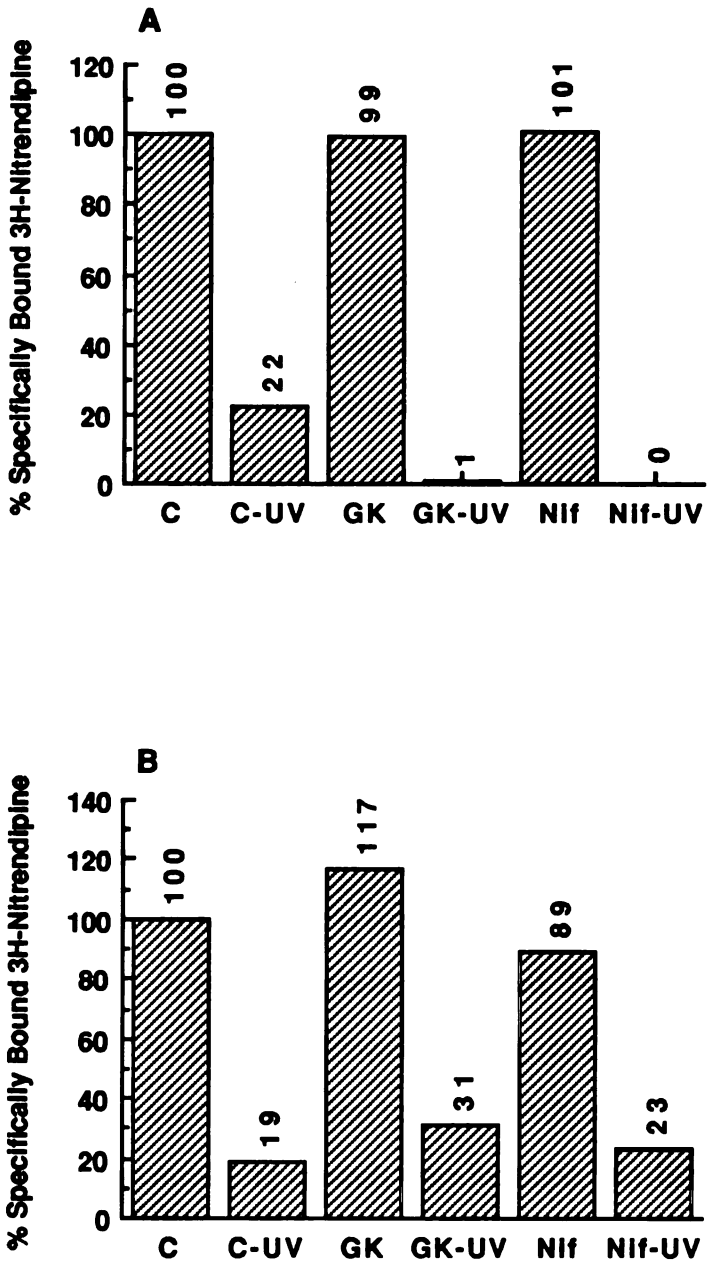

Figure 28. A and B. Results of two separate experiments in which the tissue concentration was 20 mg/ml and the UV exposure time was 15 min. An additional control was included in which tissue was preincubated with nifedipine and exposed to UV radiation (Nif-UV). Otherwise, the conditions were the same as in the previous figure (C= control).

with either nifedipine or no compound, it appeared that most of the loss of specific binding due to GK-III-120D in the presence of UV radiation could be accounted for by the effect of UV exposure alone. Further shortening of the UV exposure time to 5 or 10 min reduced the effect on specific binding sites (Figure 29 A), but with a tissue concentration of 10 mg/ml, a 10 min exposure resulted in a loss of specific binding similar to what occurred after a 15 min exposure at a 20 mg/ml tissue concentration (Figure 29 B).

Further evidence that the decrease in specific binding sites after preincubation with GK-III-120D and exposure to UV radiation was due to the UV radiation alone comes from experiments in which a wavelength in the visible region (365 nm) was used. Visible light should not be harmful to biological samples and initial studies indicated that exposure to this wavelength had a profound effect on GK-III-120D in solution (Figure 30). Therefore, we speculated that exposure to this wavelength might result in photoactivation and covalent binding of GK-III-120D, without causing damage to the tissue. In the experiment depicted in Figure 31A, a tissue concentration of 100 mg/ml and radiation exposure times of 10 and 30 min were used. The greatest decrease in specific binding occurred with unexposed GK-III-120D, probably because it was not entirely washed out. No decrease occurred with exposed GK-III-120D, and no significant deleterious effect on tissue was evident. In a further experiment, the tissue concentration was decreased to 20 mg/ml, exposure times of 15 and 30 min were used, and nifedipine controls were included. No decrease in specific binding could be demonstrated under these conditions (Figure 31 B).

Discussion

GK-III-120D initially appeared to be a promising candidate as a photoaffinity label for the 1,4-dihydropyridine receptor. It bound reversibly to the 1,4-dihydropyridine binding site with an affinity very close to that of its parent compound, nifedipine (an IC_{50} of 3.84 nM vs 1.00 nM), and it appeared to be activated promptly in solution after exposure to UV radiation at a wavelength of 254 nm. In addition, at a concentration of 10^{-6} M, GK-III-120D should have been able to occupy all of the receptors so that, theoretically, after

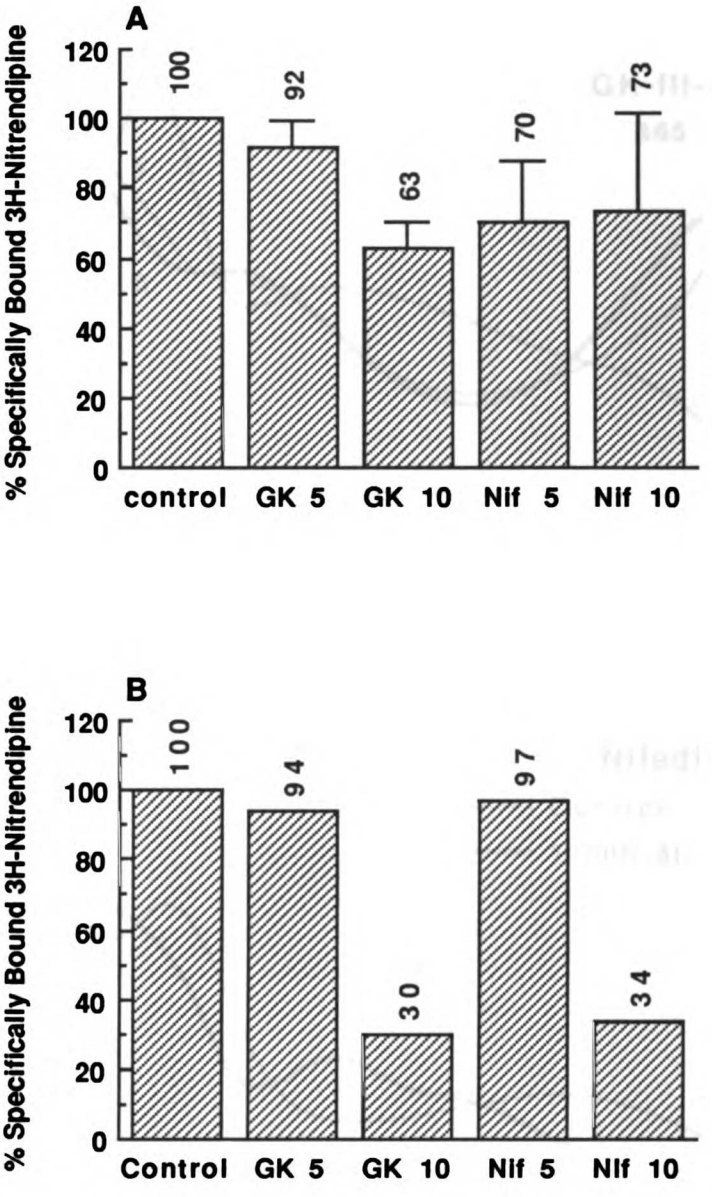

Figure 29. **A.** Mean results of three experiments showing specifically bound [^{3}H]nitrendipine after preincubation with either GK-III-120D or nifedipine and exposure to either 5 or 10 min of UV radiation (254 nm), relative to control tissue with no compound present and no UV exposure. The tissue concentration was 20 mg/ml. The error bars represent the S.E.M. **B.** Same as in **A**, except that the tissue concentration was 10 mg/ml and the results are from a single experiment.

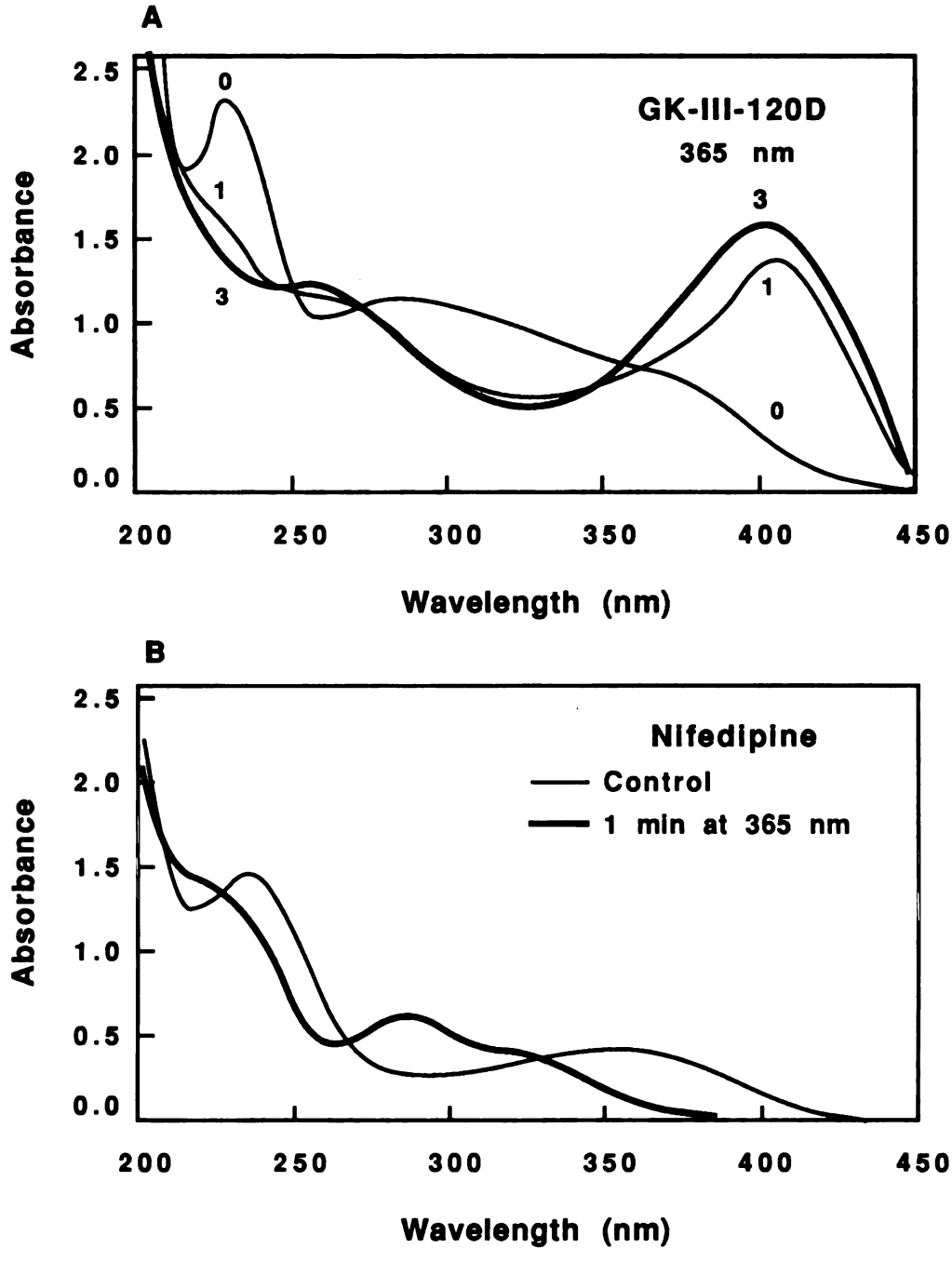

Figure 30. UV spectrum of GK-III-120D (3.2×10^{-5} M) (**A**) and nifedipine (3.2×10^{-5} M) (**B**) in absolute ethanol prior to (——) and after (▬) exposure to visible light (365 nm) for the times indicated in the figure.

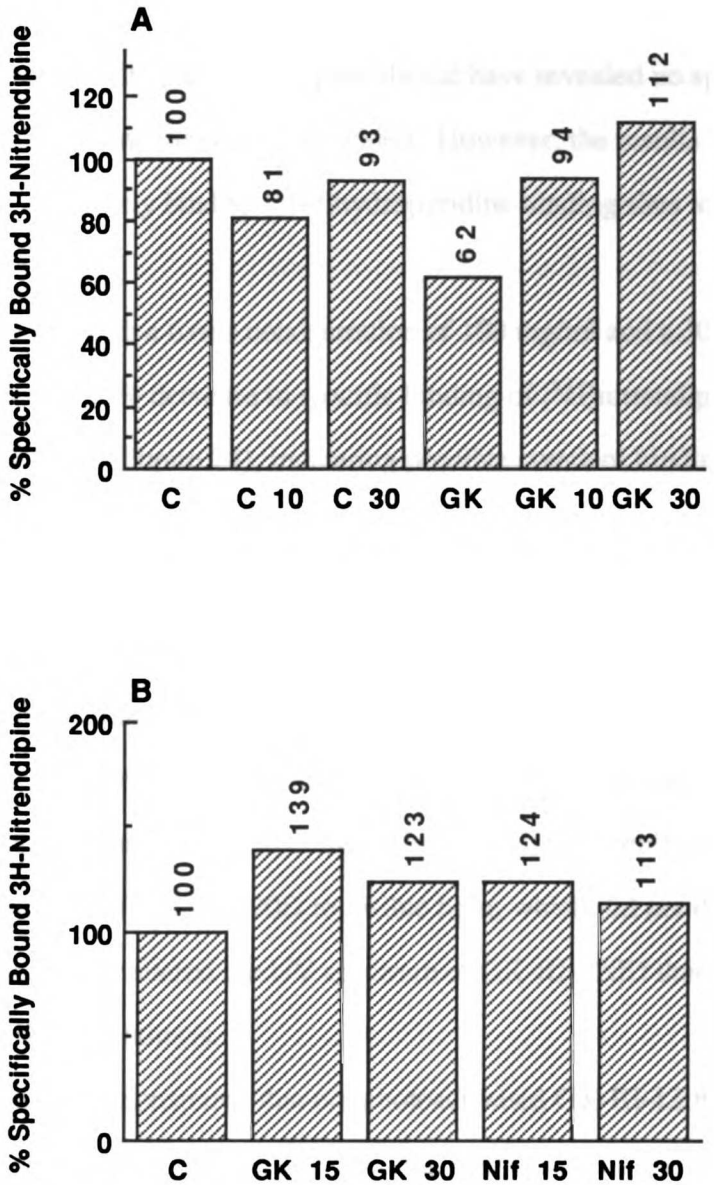

Figure 31. Results of two separate experiments in which the light source was visible radiation at a wavelength of 365 nm. **A.** Tissue concentration was 20 mg/ml. Light exposure was for 10 or 30 min. **B.** Tissue concentration was 10 mg/ml. Light exposure was for 15 or 30 min. The graph labels are the same as for previous figures.

photoactivation, all sites should have had a covalently bound molecule of GK-III-120D and subsequent incubation with [^{3}H]nitrendipine should have revealed no specific binding compared to tissue with no GK-III-120D added. However, the results indicated that GK-III-120D did not covalently bind to 1,4-dihydropyridine binding sites to an appreciable extent.

Initial studies with a tissue concentration of 100 mg/ml and a 30 min UV exposure demonstrated about a 50% decrease in specific binding of [^{3}H]nitrendipine after photoactivation of GK-III-120D (Figure 24), indicating possible covalent binding. However, subsequent work demonstrated that the disappearance of specific [^{3}H]nitrendipine binding probably could be attributed to a combination of a direct destructive effect of the UV radiation on the binding sites and incomplete washing out of noncovalently bound compound. Both the tissue concentration and the length of UV exposure influenced the extent of tissue damage, with the most dramatic destruction occurring with low tissue concentrations and long exposure times. Our inability to demonstrate any loss of specific [^{3}H]nitrendipine binding after exposure of GK-III-120D to visible light, which did not damage tissue but which more dramatically altered the UV spectrum of GK-III-120D than did UV radiation, further supports this hypothesis.

Initial studies demonstrated that nonphotoactivated GK-III-120D caused a significant decrease in specific [^{3}H]nitrendipine binding, suggesting the possibility that it was acting as a chemoaffinity label. Because this loss of specific binding also occurred with nifedipine, a compound with no photoactive group, and disappeared at lower tissue concentrations, the effect could best be explained by the failure of the washing procedure to remove the noncovalently associated GK-III-120D. Therefore, despite the theoretical specificity of this type of label, the extent or efficiency of covalent binding was not sufficient to warrant its ultimate use to help isolate and identify the 1,4-dihydropyridine binding site in the myocardium.

Similar problems have been reported with the use of photoaffinity labels for other

receptors, and for enzymes and transport proteins (Bayley and Knowles, 1977; Cavalla and Neff, 1985; Singer *et al.*, 1973). A number of explanations have been proposed for failures of other compounds that might explain the apparent inability of GK-III-120D to be photoactivated. First, it is possible that GK-III-120D was not (or less rapidly) photoactivated in the presence of the binding site compared to when it was in solution (Singer *et al.*, 1973). This could have been because of energy transfer to some other chromophore at or near the binding site, or because the turbidity of the tissue suspension prevented adequate exposure to the UV radiation (Fedan *et al.*, 1984; Hanstein, 1979). The latter explanation is unlikely because although the loss of specific [^{3}H]nitrendipine binding was greater when the tissue concentration was decreased, this also occurred in the absence of any compound, or in the presence of nifedipine. Second, it is possible that the nitrene formed was in a triplet state (two unpaired electrons) instead of the singlet state. This excited state does not form covalent bonds but, instead, abstracts protons or reacts with other radicals (Guillory and Jeng, 1983; Hanstein, 1979; Singer *et al.*, 1973). Probably the most likely explanation is that GK-III-120D was photoactivated in both its bound and free states, but the nitrene did not react rapidly enough in the active site and first dissociated from the site ($k_4 >> k_3$ in Scheme 2) (Bayley and Knowles, 1977; Cavalla and Neff, 1985; Guillory and Jeng, 1983; Hanstein, 1979; Singer *et al.*, 1973; Turro, 1980; Westheimer, 1980).

Little is known about the chemistry of nitrenes, but the lifetime of an aryl nitrene has been estimated to be from 100 ns (Guillory and Jeng, 1983) to 1 ms (Westheimer, 1980). The rate of covalent insertion is presumed to be faster than this (Guillory and Jeng, 1983; Turro, 1980), so the factor determining whether covalent binding will occur is the rate of dissociation of the nitrene from the receptor (Bayley and Knowles, 1977). Because the K_i of GK-III-120D is 3.32 nM and the association rate can be assumed to be diffusion limited and therefore a maximum of 10^9 M^{-1} sec^{-1} (Hanstein, 1979; Westheimer, 1980), the fastest dissociation rate would be estimated to be 0.18 sec, which is slow enough to allow covalent binding to occur. However, this K_i is that of the azide, not of the nitrene.

The dissociation rate of the nitrene is not known and could be greater.

We could not distinguish among these explanations for the failure to demonstrate covalent binding of GK-III-120D. However, consideration of its dissociation rate is complicated by the fact that the parent compound, nifedipine, is photosensitive. In the presence of light it undergoes disproportionation to the 4-(2-nitrosophenyl) pyridine (Berson and Brown, 1955; Ebel *et al.*, 1978) (Scheme 4). Although binding studies have not been carried out with this compound, it has been demonstrated that the nitropyridine derivative is at least two orders of magnitude less effective as a negative inotropic agent in isolated papillary muscle (Mannhold *et al.*, 1982) and that the effect of the photodecomposition products of nifedipine and nisoldipine have only a fraction of the activity of the parent compounds in inhibiting calcium current (Sanguinetti and Kass, 1984b). In addition, the effect of the parent compounds of nifedipine and nisoldipine on calcium current and muscle contraction could be reversed in seconds after exposure to intense pulses of light (Gurney *et al.*, 1985; Morad *et al.*, 1983; Nerbonne *et al.*, 1985). These effects could be explained either by a

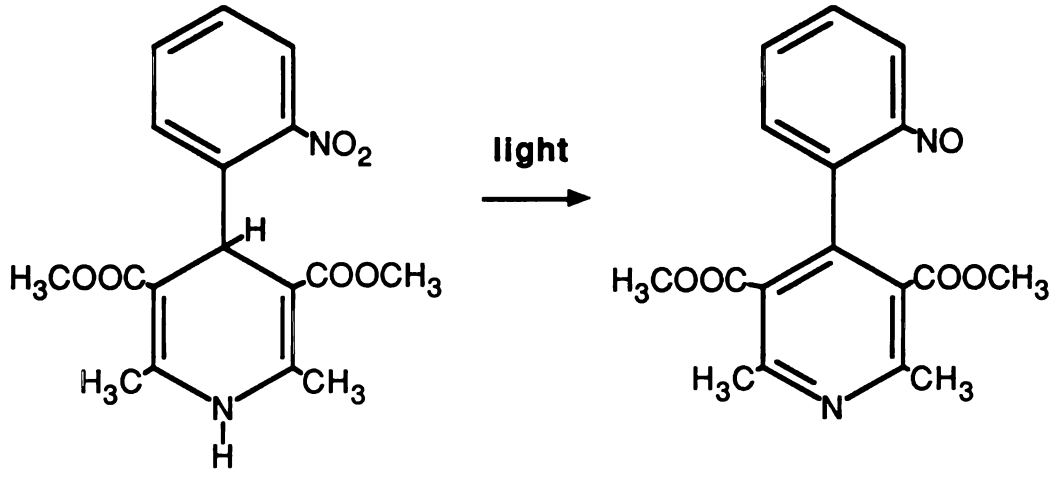

Nifedipine **Nitrosopyridine**

Scheme 4

decrease in the affinity of the photodegradation products or by a decrease in their effect with no change in binding affinity (Sanguinetti and Kass, 1984b). However, the fact that only the photodegradation products could be effectively washed out of the preparations suggested that a decrease in affinity was the explanation (Sanguinetti and Kass, 1984b). In addition, various pyridine derivatives of nitrendipine were found to be inactive in a radioreceptor binding assay in concentrations as high as 100 nM (Janis *et al.*, 1983).

We obtained a UV spectrum of nifedipine before and after exposure to UV radiation of wavelength 254 nm (Figure 32 A and B). After 15 min of exposure, the spectrum resembled that of the nitrosopyridine derivative with characteristic absorption peaks at about 280 nm and 320 nm (Berson and Brown, 1955; Ebel *et al.*, 1978; Morad *et al.*, 1983). The progression of these changes with time is shown in Figure 32 B. When these spectra were compared to those of GK-III-120D (Figure 23 A and B), there appeared to be a similar time dependence and the 15 min spectrum of GK-III-120D showed evidence of characteristic nitrosopyridine peaks.

Based on these results, it appears that GK-III-120D may have been degraded to the nitrosopyridine derivative, in addition to being photoactivated, and therefore removed too rapidly from the binding site to undergo covalent binding. Additional support for this theory can be obtained from the experiments using visible light. Exposure of both GK-III-120D and nifedipine to light of a wavelength of 365 nm resulted in changes in the UV spectra similar to those occurring after exposure to UV radiation, but much more rapid (Figure 30 A and B). However, unlike UV radiation, light of this wavelength did not cause tissue damage (Figure 31 A). Therefore, if the spectral changes were indicative of photoactivation, one would expect a much a greater loss of specific binding sites with GK-III-120D exposed to 365 nm. Instead, exposure of GK-III-120D to light of this wavelength resulted in no loss of specific binding (Figure 31 A and B). The spectral changes were therefore probably indicative of photodegradation to the 4-(2-nitrosophenyl) pyridine.

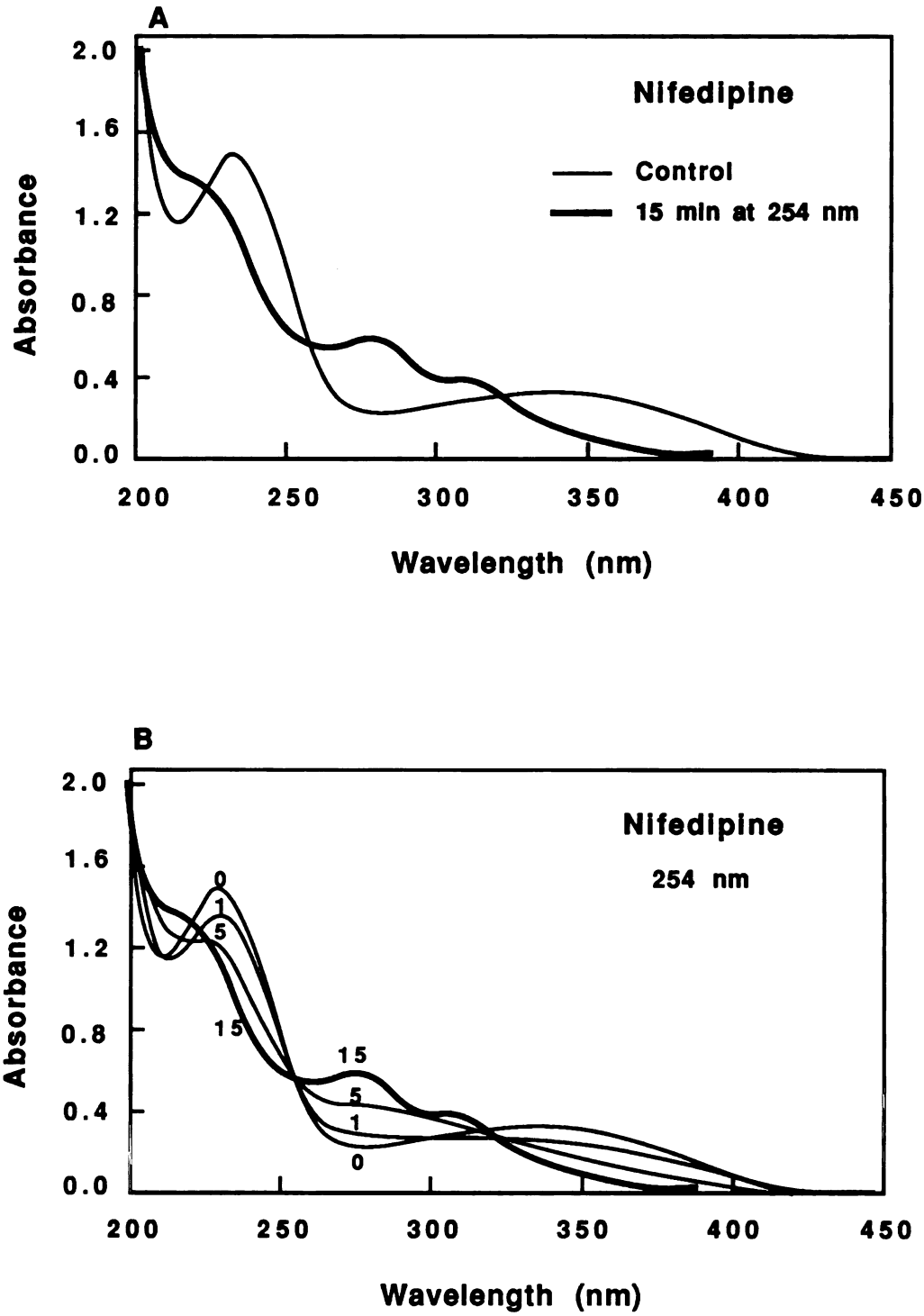

Figure 32. **A.** UV spectrum of nifedipine (3.2×10^{-5} M) in absolute ethanol prior to (——) and after (——) 15 min exposure to UV radiation at a wavelength of 254 nm. **B.** As in **A**, with the addition of spectra obtained at intermediate exposure times.

Perhaps a more suitable 1,4-dihydropyridine photoaffinity label would be a similar azido derivative of a 4-(3-nitrophenyl)-1,4-dihydropyridine compound. These compounds have been reported to be less sensitive to photodegradation (Berson and Brown, 1955; Morad *et al.*, 1983; Sanguinetti and Kass, 1984b). To confirm this, we irradiated nitrendipine for 15 min at 254 nm and noted only a very minor change in the UV spectrum (Figure 33 A). A better candidate may be a 1,4-dihydropyridine derivative substituted on the phenyl ring with a substituent other than NO_2 since 15 min irradiation of 2,6-Cl DHP (Figure 33 B) and 3-MeO DHP (not shown) resulted in no change in the UV spectrum.

Chemoaffinity Labeling Studies

Background

A chemoaffinity label is an analogue of a normal ligand with a reactive electrophilic function that is capable of reacting with nucleophilic groups (*eg.* SH, OH, and NH functions and aromatic systems) to form a covalent bond (Bayley and Knowles, 1977; Singer *et al.* 1973; Hanstein, 1979). This reaction is shown in the following scheme:

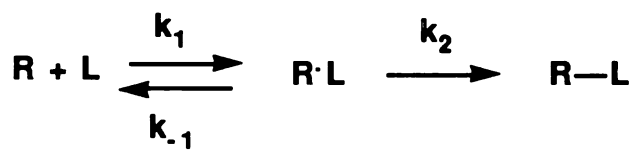

Scheme 5

Chemoaffinity labels have traditionally been used in drug-receptor studies but they have several drawbacks: 1) the reactivity of the active substituent is limited because it must not react with the solvent before it reaches the binding site, 2) there may be a lack of specificity (and therefore a high level of nonspecific binding) because the reactive group is free to react with many sites, and 3) there must be a nucleophilic group present (SH, NH, OH or aromatic group) in the binding site. These disadvantages prompted the development

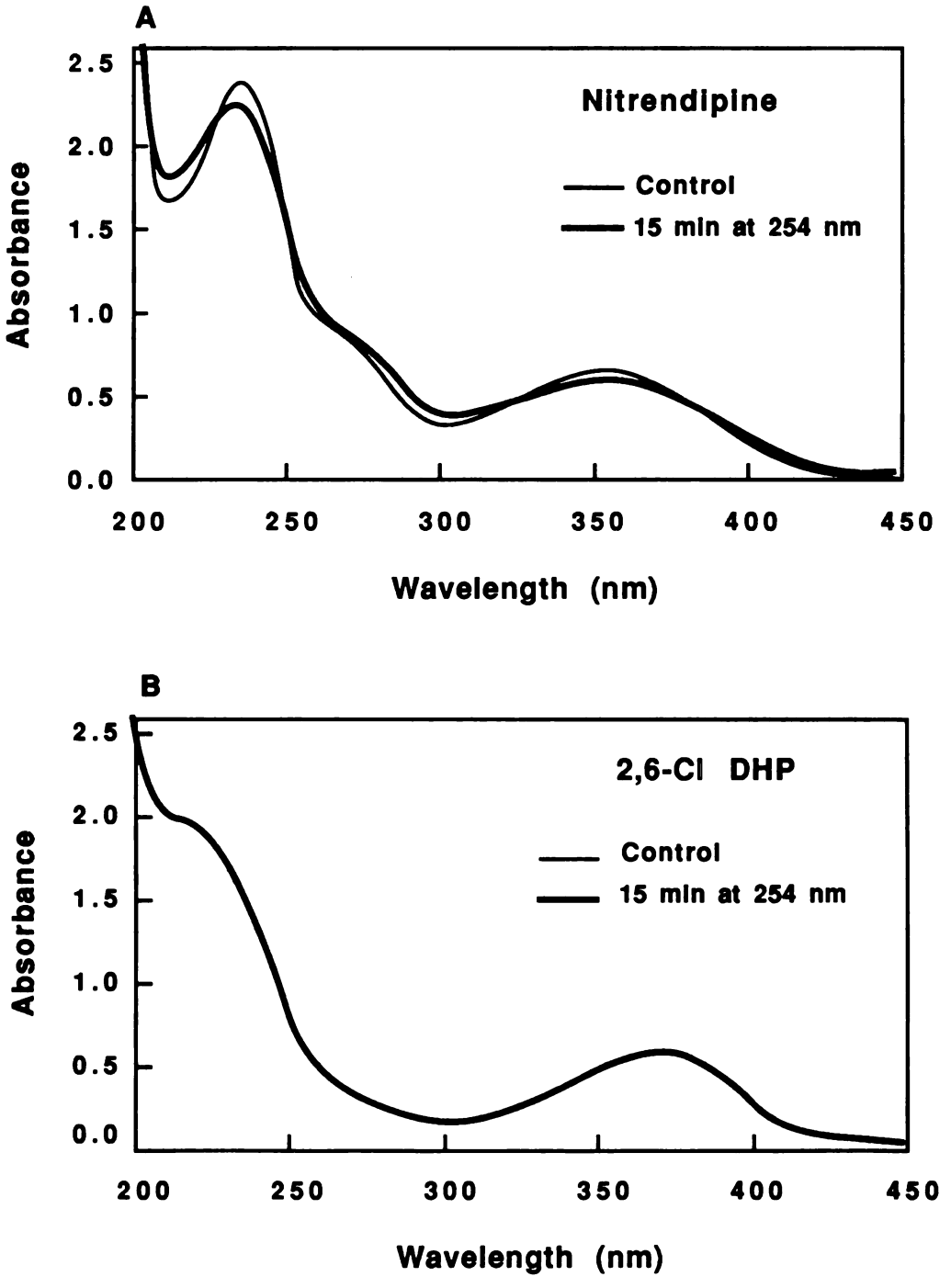

Figure 33. UV spectrum of nitrendipine (**A**) and 2,6-Cl DHP (**B**) (3.2×10^{-5} M in absolute ethanol) prior to (——) and after (——) 15 min exposure to UV radiation at a wavelength of 254 nm.

of photoaffinity labels, which, ideally, should overcome these drawbacks. Nevertheless, chemoaffinity labels have been used successfully in studies of receptors (Homcy and Graham, 1985; Takemori and Portoghese, 1985).

A number of investigators have attempted chemoaffinity labeling of the 1,4-dihydropyridine receptor. The first report was by Venter *et al.* (1983). They used a radiolabeled isothiocyanate 1,4-dihydropyridine derivative (Figure 34) as a chemoaffinity label to identify the 1,4-dihydropyridine receptor in guinea pig ileum and rat myocardium. A subunit with a molecular weight of 45,000 was identified in both tissues. Subsequently, the same compound was used to identify subunits in canine cardiac membranes (Horne *et al.*, 1984) and in rabbit skeletal muscle transverse tubules (Kirley and Schwartz, 1984). In the latter two cases, however, the data did not provide convincing evidence that this compound was specifically labeling the 1,4-dihydropyridine binding site. These results are summarized in Table 12.

Table 12. Summary of results of chemoaffinity labeling studies of the 1,4-dihydropyridine receptor from the literature

Tissue	Affinity Label	Molecular Weight of Subunit[1]	Reference
Guinea pig ileum	[^{3}H] *o*-NCS	45,000	Venter *et al.*, 1983
Rat myocardium	[^{3}H] *o*-NCS	45,000	Venter *et al.*, 1983
Canine myocardium	[^{3}H] *o*-NCS	42,000	Horne *et al.*, 1984
Rabbit skeletal muscle transverse tubules	[^{3}H] *o*-NCS	36,000	Kirley and Schwartz, 1984

[1] SDS-PAGE carried out under reducing conditions

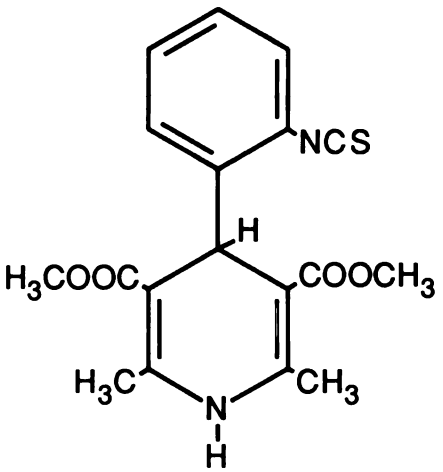

o-NCS DHP

Figure 34. Chemical structure of *o*-NCS DHP (2,6-dimethyl-3,5-dicarbomethoxy-4-(2-isothiocyanatophenyl)-1,4-dihydropyridine)

Goals

When we were unable to demonstrate that the potential photoaffinity label, GK-III-120D, was covalently binding to the 1,4-dihydropyridine receptor, we began studies with the chemoaffinity label, dihydropyridine isothiocyanate (*o*-NCS). The goals with this compound were similar to those for the photoaffinity label, specifically, to covalently label and identify the 1,4-dihydropyridine binding site in rat myocardium. Because radiolabeled *o*-NCS was available, it could be used directly in experiments to isolate and identify the 1,4-dihydropyridine receptor, using sodium dodecyl sulfate polyacrylamide gel electrophoresis (SDS-PAGE).

Methods

Chemicals

Tritium labeled dihydropyridine isothiocyanate (2,6-dimethyl-3,5-dicarbomethoxy-4-(2-isothiocyanatophenyl)-1,4-dihydropyridine) ([^{3}H]*o*-NCS) of specific activity 76.6 or 79.4 Ci/mmol was obtained from New England Nuclear (Boston, MA). Molecular weight markers for SDS-PAGE were obtained from Sigma (St. Louis, MO) as a kit (MW-SDS-70L). All other chemicals used in the preparation and running of the polyacrylamide gels also were purchased from Sigma.

Sodium Dodecyl Sulfate Polyacrylamide Gel Electrophoresis (SDS-PAGE)

SDS-PAGE is a procedure designed to separate proteins into their polypeptide subunits and determine their molecular weights. A protein mixture is denatured and solubilized by heating in a solution of the anionic detergent, SDS, and 2-mercaptoethanol, to reduce disulfide bonds. The denatured proteins, associated with the SDS, migrate on the polyacrylamide gel in an electric field according to their respective molecular weights, with proteins of lowest molecular weight migrating the farthest. The molecular weight of an unknown protein can be determined by the simultaneous use of protein standards of known molecular weight and by using the empirical linear relationship between the logarithm of the molecular weight and the mobility on the gel. In our experiments, the proteins used for

molecular weight standards (and their molecular weights) were: α-lactalbumin (14,200), trypsin inhibitor (20,100), trypsinogen (24,000), carbonic anhydrase (29,000), glyceraldehyde 3-phosphate dehydrogenase (36,000), ovalbumin (45,000) and bovine albumin (66,000).

In these experiments, the Bio-Rad Protean II Slab Cell System (Bio-Rad, Richmond, CA) was used. The polyacrylamide gel was a 20 cm x 20 cm slab of 1 mm thickness and consisted of a large pore stacking gel (3% polyacrylamide) polymerized on top of a small pore separating gel (10% polyacrylamide). This gel system was used with the discontinuous buffer system developed by Laemmli (1970) and adapted to slab gels by Studier (1973) and Ames (1974). Briefly, this system consists of a Tris-glycine buffer (pH 8.3) in the electrode reservoirs, a Tris buffer of pH 6.8 in the stacking gel and a Tris buffer of pH 8.8 in the separating gel. With this buffer system, the proteins are forced into narrow zones during migration through the stacking gel, which results in improved resolution of their separation in the 10% polyacrylamide gel. The methods for preparation of the stock solutions and the polyacrylamide gels are detailed in Appendix J.

After separation in this electrophoretic system under a constant current of 16 mA in the stacking gel and 24 mA in the separating gel, proteins were stained by soaking the gel in a Coomassie Blue solution, followed by a destaining solution, and the gel then was dried. Dried gel also was sliced (4 mm), and the slices were solubilized overnight at 37° C in either Protosol (New England Nuclear):water (9:1) or 30% hydrogen peroxide, and then subjected to liquid scintillation counting.

Preparation of Samples

Rat myocardial membrane particulates were initially prepared as described previously in Chapter 4, with the exception that the tissue concentration in the final resuspension was 44.4 mg original wet weight/ml buffer. In preliminary experiments, aliquots of this suspension were incubated in buffer either alone, or with [^{3}H]*o*-NCS (10 nM), in the absence or presence of 10^{-6} M nifedipine. The final tissue concentration in the incubate was

40 mg wet weight/ml buffer. All samples were incubated in the dark for 60 min at 25° C. At the end of the incubation period, the membrane particulates were combined with an equal volume of solubilizing buffer containing SDS and 2-mercaptoethanol to achieve final concentrations of 2% and 5%, respectively. Bromophenol blue was included as the tracking dye. The mixture was heated at 100° C for 5 min and aliquots applied to the gels.

Although this procedure was successful in solubilizing and allowing detection of membrane proteins, no radioactivity was associated with any of these bands. We therefore altered the procedure in an attempt to optimize covalent labeling. After Horne *et al.* (1984) reported that Tris buffer reacts with [^{3}H]*o*-NCS and reduces the efficiency of labeling, but phosphate buffer (50 mM NaH_2PO_4, pH 7.2) does not, we substituted 50 mM phosphate buffer for 50 mM Tris buffer in all steps of the sample preparation. In addition, we halved the tissue concentration to 20 mg wet weight/ml buffer and reduced the incubation time to 10 min or 30 min to follow the procedures used in the literature (Horne *et al.*, 1984; Kirley and Schwartz, 1984; Venter *et al.*, 1983). At the end of the incubation, the suspension was centrifuged at 48,000 g for 15 min at 5° C. The supernatant was discarded, the pellet washed in cold phosphate buffer and then resuspended in solubilizing buffer and treated as before.

Dissociation Experiments

Rat membrane particulates were prepared as described in Chapter 4 except that 50 mM NaH_2PO_4 buffer, pH 7.2, was substituted for 50 mM Tris buffer in all steps of the procedures. A 0.1 ml aliquot of the final tissue suspension was incubated in a total volume of 2 ml with either [^{3}H]nitrendipine or [^{3}H]*o*-NCS (0.05 nM) with or without 10^{-6} M nifedipine. The samples were incubated in the dark at 25° C for 40 to 60 min. At the end of the incubation period, 0.1 ml of a nifedipine solution was added to achieve a final concentration of 10^{-6} M. Samples then were filtered at various times after addition of nifedipine through Whatman GF/B filters and washed with 3 x 4 ml of ice-cold phosphate buffer. Radioactivity trapped on the filters was determined by liquid scintillation counting.

Results

A representative gel obtained after electrophoresis of solubilized membrane proteins alone, along with the molecular weight standards, is shown in Figure 35. Lanes 1 and 6 contained the standards. A 30 µl aliquot of the final solution of solubilized proteins, prepared by the initial procedure described above, was added to lanes 2 to 5. A standard curve of log molecular weight of the standards in lane 6 plotted against their migration relative to the bromophenol blue dye front is shown in Figure 36.

As discussed above, when the same procedure was used with [^{3}H]*o*-NCS present, no radioactivity above background could be detected in any of the lanes. When the new procedures were applied, again, no radioactivity could be detected (results not shown). However, there was significant radioactivity in the solutions applied to the gels. Because no radioactivity appeared to be covalently associated with the membrane proteins, we questioned whether [^{3}H]*o*-NCS was actually covalently binding. To examine this possibility, we carried out preliminary dissociation experiments with [^{3}H]*o*-NCS (Weiland and Molinoff, 1981). A reversible 1,4-dihydropyridine radioligand present in a low concentration would be expected to be displaced from its specific binding sites in the presence of a high concentration of nifedipine.

The results with [^{3}H]*o*-NCS were difficult to interpret because of the high level of nonspecific binding with this compound. Nevertheless, it appeared to be dissociating in the presence of excess nifedipine. The results of one such experiment with [^{3}H]*o*-NCS, along with a dissociation curve for [^{3}H]nitrendipine obtained in the same tissue sample on the same day, are shown in Figure 37 A and B. In this experiment, the dissociation rate constant (k_{-1}) for [^{3}H]*o*-NCS was 0.040 min^{-1}, corresponding to a half-life of dissociation of 17.3 min. The corresponding k_{-1} for [^{3}H]nitrendipine was 0.134 min^{-1} and the half-life was 5.2 min. This value is consistent with the K_d of [^{3}H]nitrendipine and a diffusion limited association rate constant. It also agrees well with values reported in the literature (Bolger *et al.*, 1983; Janis *et al.*, 1984).

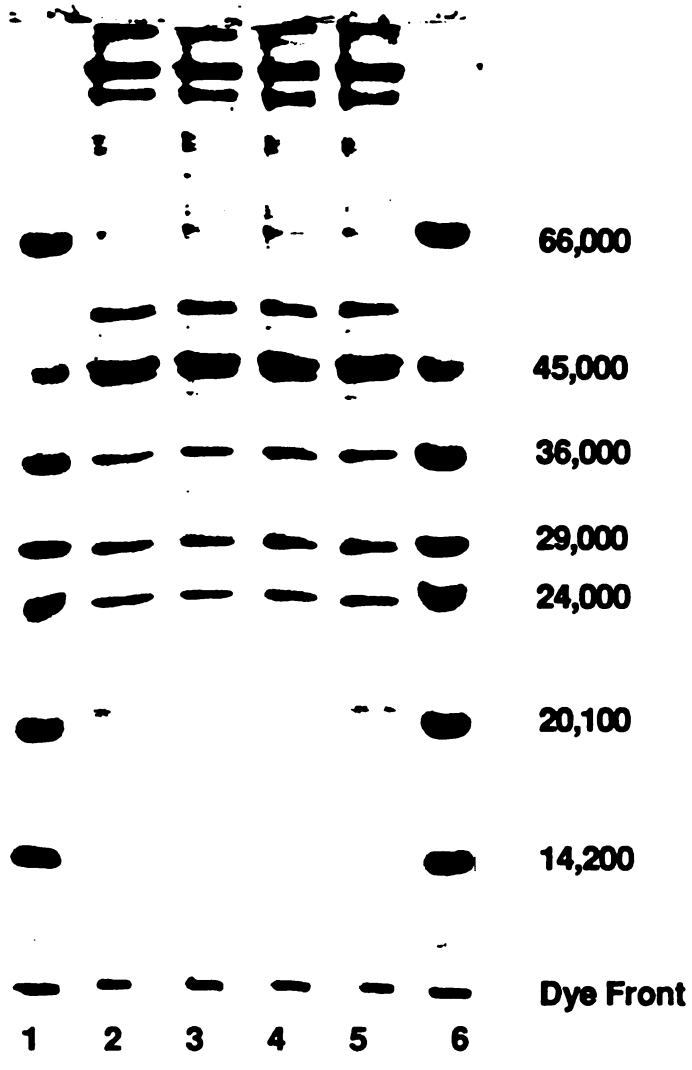

Figure 35. A representative polyacrylamide gel obtained after SDS-PAGE of solubilized rat myocardial membrane proteins. Membrane proteins are shown in lanes 2 to 5. Molecular weight standards are shown in lanes 1 and 6.

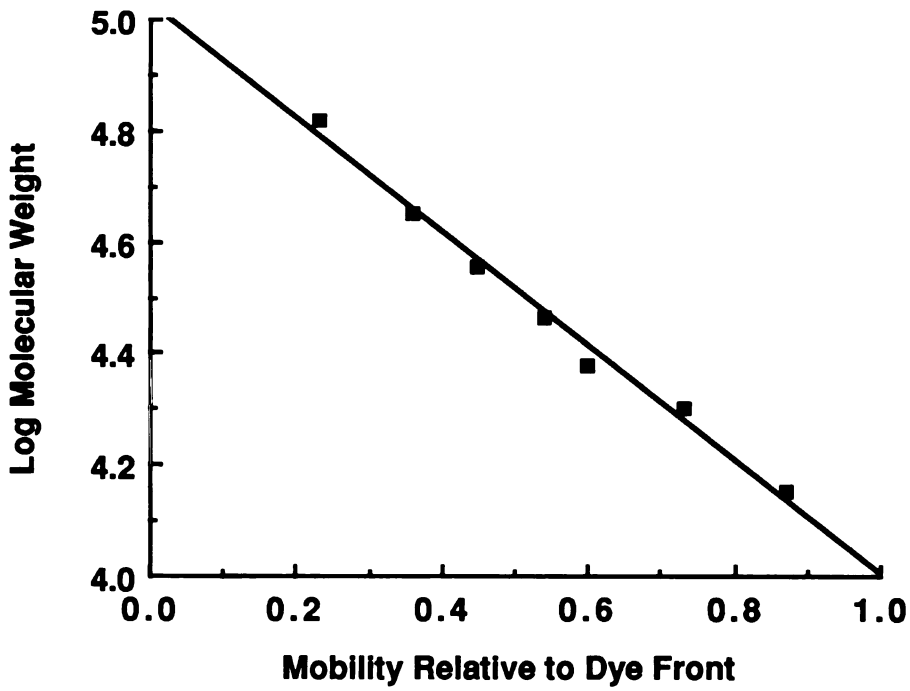

Figure 36. Standard curve of log molecular weight versus migration relative to the bromophenol blue dye front for the molecular weight markers in lane 6 of Figure 35.

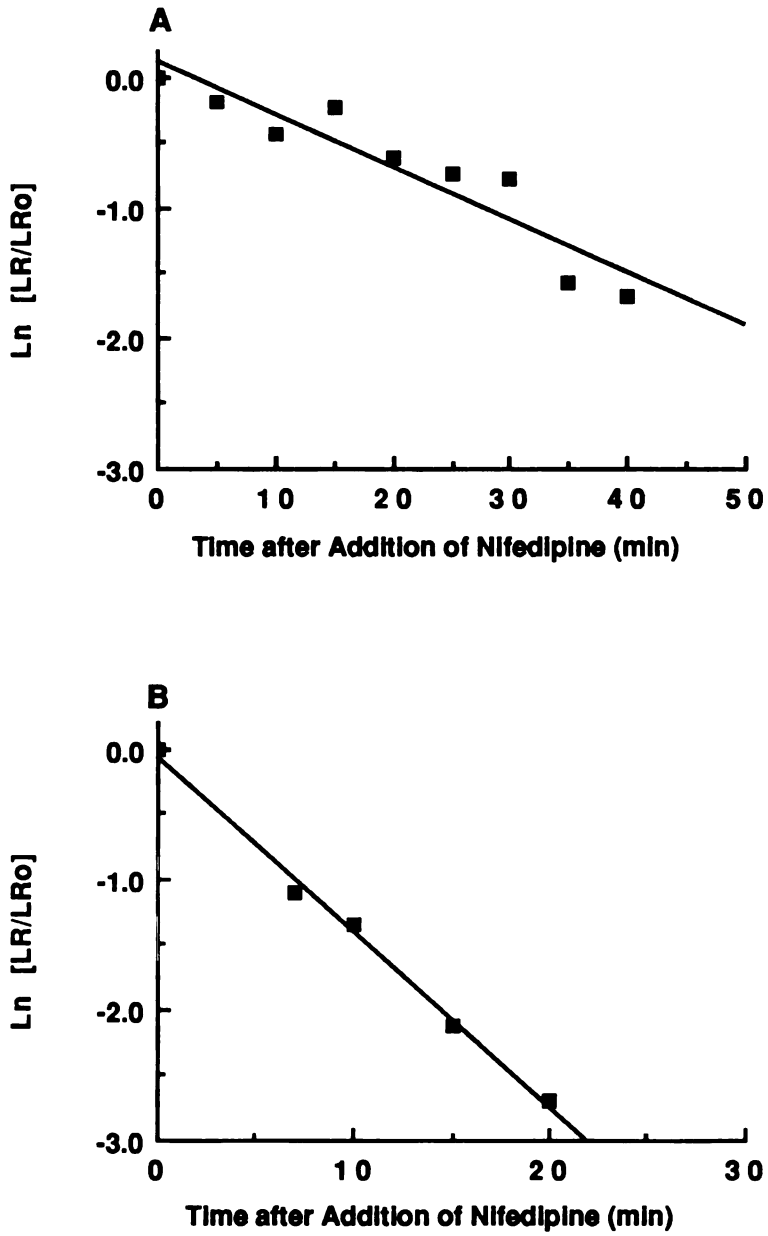

Figure 37. Dissociation curves for specific binding of [^{3}H]*o*-NCS (**A**) and [^{3}H]nitrendipine (**B**) after the addition of 10^{-6} M nifedipine. LR_0 is the specific binding before addition of nifedipine and LR is the specific binding at various times after the addition of nifedipine.

Discussion

Although there have been a number of reports of the successful affinity labeling of the 1,4-dihydropyridine binding site in various tissues with *o*-NCS (Horne *et al.*, 1984; Kirley and Schwartz, 1984; Venter *et al.*, 1983), we were unable to detect this in our studies. Upon reexamination of those original studies, the evidence supporting covalent binding was not very convincing. Using 2 x 10^{-6} M unlabeled *o*-NCS in a preincubation step with guinea pig ileal muscle strips, Venter *et al.* (1983) demonstrated a 76% decrease in specific [^{3}H]nitrendipine binding to guinea pig ileal membranes, prepared after a two hour washing procedure of the muscle strips involving solution changes every 15 min. Such results could be explained by very tight, noncovalent binding of *o*-NCS that was not removed by the washing procedure. In addition, the amount of radioactivity associated with a protein in guinea pig ileum upon SDS-PAGE was very low. Further experiments by this group (Horne *et al.*, 1984) demonstrated a much higher radioactivity peak associated with a protein of molecular weight 42,000 when canine cardiac membranes were incubated with 10 nM [^{3}H]*o*-NCS in a phosphate buffer instead of the Tris buffer used in the previous study. However, this peak was decreased by only about 50% in the presence of excess unlabeled *o*-NCS and about 70% by nicardipine so it is questionable whether this peak represented specific binding of [^{3}H]*o*-NCS to the 1,4-dihydropyridine binding site. Finally, Kirley and Schwartz (1984) found radioactivity associated with a protein of 36,000 molecular weight in skeletal muscle t-tubular membranes after incubation with an unspecified concentration of [^{3}H]*o*-NCS in a sodium borate buffer. Although it was stated that the inclusion of unlabeled 1,4-dihydropyridine did not affect a peak at 115,000 daltons, the effect on the major peak at 36,000 daltons was not specified.

At the same time, another group reported its inability to covalently incorporate [^{3}H]*o*-NCS into guinea-pig skeletal muscle or myocardial membranes, even in amine-free buffer (Ferry *et al.*, 1984; Ferry *et al.*, 1986). Two subsequent groups of investigators also have reported their inability to demonstrate covalent binding of [^{3}H]*o*-NCS

(Greenberg *et al.*, 1985; Kozlowski *et al.*, 1986). Greenberg *et al.* (1985) reported that, in contrast to results in guinea pig ileum, in rat brain membranes [^{3}H]*o*-NCS bound reversibly. They attributed the difference in binding properties to possible structural variations in voltage-dependent calcium channels in the two tissues. They incubated [^{3}H]nitrendipine and [^{3}H]*o*-NCS with brain tissue at 25° C for 60 min in the dark, then added nifedipine at a concentration of 100 nM. Dissociation of specifically bound [^{3}H]*o*-NCS followed first order kinetics with a k_{-1} of 0.046 min^{-1}, corresponding to a half-life of about 15 min, almost identical to our preliminary results. Similar results were obtained when dissociation was induced by dilution, and when the experiments were carried out in Tris, phosphate or HEPES (4-(2-hydroxyethyl)-1-piperazine-ethanesulfonic acid) buffer. In addition, a saturation isotherm for [^{3}H]nitrendipine in the presence of unlabeled *o*-NCS revealed a decrease in the apparent K_d for [^{3}H]nitrendipine but no change in the B_{max}.

Kozlowski *et al.* (1986) demonstrated similar properties of [^{3}H]*o*-NCS binding in guinea pig cardiac membranes, using a phosphate buffer. Dissociation of [^{3}H]*o*-NCS after addition of 10^{-6} M nifedipine at 37° C resulted in dissociation with a half-life of 3.2 min. In addition, they demonstrated concentration-dependent inhibition of [^{3}H]*o*-NCS binding by nifedipine after preincubation of the membranes with [^{3}H]*o*-NCS (0.5 nM), yielding an IC_{50} for nifedipine of 3.19 nM. Also, they could detect no radioactivity peaks after SDS-PAGE. They also carried out pharmacologic studies with this compound, demonstrating a duration of action longer than that of other 1,4-dihydropyridines and showing that eventually the effect could be washed out, or reversed by the calcium agonist, BAY K 8644. They speculated that it was possible that *o*-NCS binds reversibly to the 1,4-dihydropyridine receptor, but also accumulates nonspecifically in lipid membrane, providing a long-lasting depot of drug to occupy the receptor and maintain the activity.

Our preliminary results confirm the reversibility of [^{3}H]*o*-NCS binding in myocardium of another species, the rat. Taken together, the results of our studies and those of Greenberg *et al.* (1985) and Kozlowski *et al.* (1986) suggest that the isothiocyanate dihy-

dropyridine is not an effective affinity label to study the molecular characteristics of the 1,4-dihydropyridine receptor.

Summary

Many approaches have been used to study the molecular characteristics of the 1,4-dihydropyridine receptor. When our studies began, it appeared that photoaffinity or chemoaffinity labels would be valuable tools to identify the specific protein to which 1,4-dihydropyridine compounds were binding. Unfortunately, suitable photoaffinity or chemoaffinity labels have yet to be developed. Since our studies were completed, no new studies demonstrating successful use of the chemoaffinity label, *o*-NCS, have been published. However, there have been several additional reports of photoaffinity labeling of the 1,4-dihydropyridine receptor (Galizzi *et al.*, 1986; Sarmiento *et al.*, 1986; Striessnig *et al.*, 1986). One of these groups has again made use of azidopine, this time as the (-) isomer, to label the 1,4-dihydropyridine receptor in guinea pig skeletal muscle t-tubules (Striessnig *et al.*, 1986). Under nonreducing conditions, SDS-PAGE revealed that (-) azidopine was bound to a protein of molecular weight 155,000. This value is similar to previous findings with the racemate of this compound, determined either under reducing or nonreducing conditions (Ferry *et al.*, 1984, 1985). Again, because of the position of the azido substituent on the molecule, it is uncertain whether covalent binding is actually occurring at the receptor site.

In contrast, in two other studies, 1,4-dihydropyridine compounds with no obvious photolabile substituents, (+)[^{3}H]PN 200-110 and Bay P 8857 (Appendix I) were used as photoaffinity labels (Galizzi *et al.*, 1986; Sarmiento *et al.*, 1986). Interestingly, in both studies, SDS-PAGE was carried out under reducing conditions but a small polypeptide (33-35,000) was labeled by Bay P 8857 (Sarmiento *et al.*, 1986) and a large polypeptide (170,000) was labeled by (+)[^{3}H]PN 200-110 (Galizzi *et al.*, 1986).

Therefore, the subunit to which 1,4-dihydropyridine compounds are binding has

not yet been identified unequivocally. This information probably will be obtained only by the development of a photoaffinity label – similar to GK-III-120D – with an azido substituent on the phenyl ring, and its use in a highly purified preparation of 1,4-dihydropyridine receptor.

Although the specific binding site for 1,4-dihydropyridines has not yet been identified, considerable progress has been made in the isolation of the proteins that make up the calcium channel/1,4-dihydropyridine receptor. Despite the use of different detergents and purification steps, the results of most of the initial purification studies are in general agreement. That is, after reduction of disulfide bonds, there are two proteins copurifying with 1,4-dihydropyridine binding in skeletal muscle and cardiac membranes from a number of species; one with a molecular weight of approximately 130-142,000 and another with a molecular weight of about 30-33,000 (Curtis and Catterall, 1984; Borsotto *et al.*, 1984a, 1985) (Table 10) More recent purification studies appear to confirm these results (Flockerzi *et al.*, 1986a; Cooper *et al.*, 1987) and also provide evidence that these two subunits are joined by a disulfide bond *in vivo* (Cooper *et al.*, 1987).

Another method used recently to identify the membrane proteins associated with 1,4-dihydropyridine binding is immunochemical detection (Cooper *et al.*, 1987; Norman *et al.*, 1987; Schmid *et al.*, 1986a, 1986b; Vandaele *et al.*, 1987). This technique involves the production of either polyclonal or monoclonal antibodies directed against the purified components of the 1,4-dihydropyridine receptor that are then used as immunological probes for the identification of 1,4-dihydropyridine receptor proteins in other tissues. These antibodies are used to precipitate the 1,4-dihydropyridine receptor proteins in a purified preparation of interest before separation on SDS-PAGE or are incubated with proteins previously separated by SDS-PAGE and transferred to nitrocellulose. The bound antibodies are then detected by one of a number of radiochemical or fluorochemical procedures.

This method has both very high sensitivity and specificity for detection of receptor proteins and therefore is very useful for studies in tissue where the 1,4-dihydropyridine re-

ceptor density is low, such as cardiac and vascular smooth muscle. In addition, it can be used to probe for immunological differences between tissues and species. In all of the immunochemical studies to date, the antibodies have been raised against the 1,4-dihydropyridine receptor in purified rabbit skeletal muscle t-tubules and used to detect 1,4-dihydropyridine receptor proteins in a number of tissues from various species (Table 13). In every case, antibodies have identified a protein with a molecular weight of about 170,000 when SDS-PAGE was run under nonreducing conditions (Cooper *et al.*, 1987; Norman *et al.*, 1987; Schmid *et al.*, 1986a, 1986b; Takahashi and Catterall, 1987; Vandaele *et al.*, 1987). In most cases, antibodies from various antisera recognized proteins of about 140,000 and 30,000 daltons under reducing conditions. Furthermore, these anti-140,000 and anti-30,000 antibodies also recognized the 170,000 dalton protein, suggesting that at least part of the 1,4-dihydropyridine receptor consists of two subunits with molecular weights of 140,000 and 30,000, joined by a disulfide bond. These results agree well with most of the estimates of subunit size from solubilization and purification studies (Borsotto *et al.*, 1984a, 1985; Curtis and Catterall, 1984; Flockerzi *et al.*, 1986a; Cooper *et al.*, 1987). It therefore appears that the proteins necessary for 1,4-dihydropyridine binding have been identified and that they are very similar between tissues within a species and between species.

It remains to be seen whether the 170,000 dalton protein comprises the entire calcium channel. The finding that both diltiazem and desmethoxyverapamil binding also were associated with these proteins (Galizzi *et al.*, 1986; Vandaele *et al.*, 1987) provides evidence supporting this hypothesis. In addition, in preliminary studies, the solubilized, purified 1,4-dihydropyridine receptor from skeletal muscle t-tubules has been reconstituted into phospholipid vesicles (Curtis and Catterall, 1986; Horne *et al.*, 1986) and into phospholipid bilayer membranes at the tip of a glass patch pipette (Flockerzi *et al.*, 1986b). In the vesicle studies, the reconstituted receptor was shown to have calcium channel blocker binding properties similar to the membrane-bound receptor (Curtis and Catterall, 1986;

Table 13. Summary of results of immunochemical studies of the 1,4-dihydropyridine receptor from the literature

Tissue	Antibody[1]	Molecular Weight of Subunits-Nonreducing Conditions	Molecular Weight of Subunits-Reducing Conditions	Reference
Rabbit skeletal muscle membranes	Polyclonal	170,000	140,000 32,000 29,000 25,000	Schmid *et al.*, 1986a
Rabbit cardiac membranes	Polyclonal	176,000	34,000 32,000 29,000	Schmid *et al.*, 1986a
Rabbit intestinal smooth muscle membranes	Polyclonal	170,000	32,000 29,000	Schmid *et al.*, 1986a
Rabbit brain synaptosomes	Polyclonal	170,000	140,000 32,000 29,000	Schmid *et al.*, 1986b
Rabbit skeletal muscle t-tubules	Monoclonal	170,000	140,000 30,000 26,000	Vandaele *et al.*, 1987
Chick cardiac membranes	Polyclonal and monoclonal	170,000	140,000 32,000 29,000	Cooper *et al.*, 1987
Skeletal muscle of rabbit, rat, mouse and frog	Monoclonal	330,000 310,000[2] 170,000	140,000	Norman *et al.*, 1987
Rabbit brain and cardiac membranes	Monoclonal		140,000	Norman *et al.*, 1987
Rabbit skeletal muscle	Polyclonal	163,000	135,000	Takahashi and Catterall, 1987
Rabbit brain		169,000	140,000	
Rabbit cardiac membranes		170,000	141,000	

[1] All antibodies were raised against 1,4-dihydropyridine receptors in rabbit skeletal muscle

[2] Not found in frog skeletal muscle

Horne *et al.*, 1986). In addition, specific $^{45}Ca^{2+}$ transport into the vesicles, regulated by calcium channel blockers, was mediated by these reconstituted receptors (Curtis and Catterall, 1986). Reconstituted receptor in the lipid bilayer also demonstrated a number of the electrophysiologic and pharmacologic properties of a functional calcium channel (Flockerzi *et al.*, 1986b). On the other hand, the results of the radiation inactivation studies (Table 9) and one of the immunochemical studies (Norman *et al.*, 1987) suggest that the protein making up the calcium channel may be larger than 170,000 daltons. Further work aimed at sequencing, synthesizing and reconstituting these proteins to form a functioning calcium channel will be necessary to answer these questions.

In addition, further study with specific affinity labels will be necessary to determine the exact binding site of the 1,4-dihydropyridines and other calcium channel blockers on these proteins. It is interesting to note that of all the photoaffinity and chemoaffinity labels used to specifically label the 1,4-dihydropyridine binding site, the ones that bound to proteins corresponding most closely in size to those isolated in purification or immunochemical studies were small 1,4-dihydropyridine derivatives with no traditional photolabile substituents but that were used as photoaffinity labels ((+)[^{3}H]PN 200-110 (Galizzi *et al.*, 1986), [^{3}H]nitrendipine (Campbell *et al.*, 1984) and Bay P 8857 (Sarmiento *et al.*, 1986)). Perhaps future affinity labels should be modeled after these compounds. In addition to identification of the calcium channel blocker binding sites, further study will be necessary to determine the molecular mechanism by which these compounds control calcium channel gating.

CHAPTER 6

Introduction - The Pharmacokinetics and Pharmacodynamics of Diltiazem in Humans

Background

Diltiazem (*d-cis*-3-acetoxy-5-[2-(dimethylamino)ethyl]-2,3-dihydro-2-(*p*-methoxyphenyl)-1,5-benzothiazepin-4(5H)-one HCl), also known as CRD-401, was developed by the Japanese pharmaceutical company, Tanabe Seiyaku Co., Ltd., in the early 1970's. Its chemical structure is shown in Figure 38. Among a series of 1,5-benzothiazepine derivatives synthesized for potential antidepressant activity (Kugita *et al.*, 1971), diltiazem instead was found to have potent coronary and peripheral vasodilating activity in the anesthetized dog (Sato *et al.*, 1971; Nagao *et al.*, 1972). Additionally, weak negative chronotropic, negative inotropic and hypotensive effects were observed (Sato *et al.*, 1971). Subsequent work in isolated cardiac muscles from various species examined the effect of diltiazem on both the action potential and muscle contraction. Because diltiazem exerted a negative inotropic effect without dramatically affecting the action potential, thereby acting as an uncoupler of excitation-contraction, its mechanism of action was believed to be an inhibition of the slow calcium current into the myocardium (Nabata, 1977; Nakajima *et al.*, 1975, 1976; Saikawa *et al.*, 1977). This mechanism of action was later confirmed by voltage clamp experiments in isolated myocardial muscle (Kanaya and Katzung, 1984; Kanaya *et al.*, 1983; Tung and Morad, 1983) and in single myocardial cells (Lee and Tsien, 1983). At about the same time, Cauvin *et al.* (1983) demonstrated that the vasodilating action of diltiazem was due to inhibition of the influx of calcium into vascular smooth muscle cells.

The activity of diltiazem, like that of the 1,4-dihydropyridines, appears to be receptor-mediated. Early studies demonstrated the pronounced stereospecific activity of the

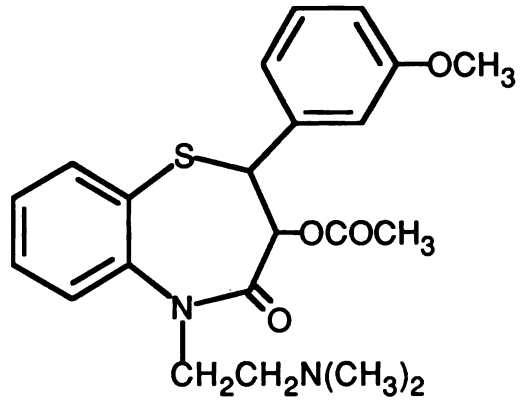

Diltiazem

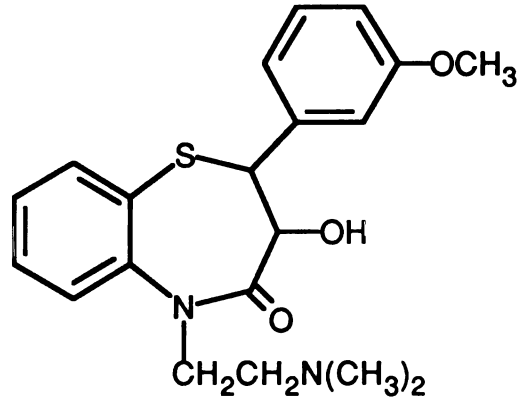

DAD

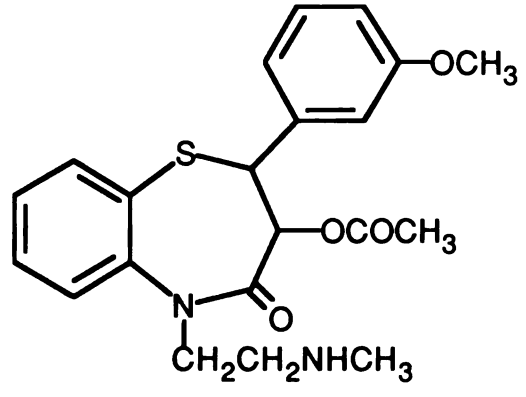

NDD

Figure 38. Chemical structures of diltiazem and its two major metabolites, desacetyldiltiazem (DAD), and N-monodemethyldiltiazem (NDD).

d-cis isomer (Sato *et al.*, 1971; Nagao *et al.*, 1972). More recently, a saturable, reversible, stereoselective, moderately high affinity binding site has been identified in cardiac sarcolemma from several species in radioligand binding experiments using [^{3}H]diltiazem (Balwierczak and Schwartz, 1985; Balwierczak *et al.*, 1987; Garcia *et al.*, 1986). The results from these studies have been in fairly good agreement and the reported K_d has ranged from 58 to 115 nM, and the B_{max} from 1.95 to 2.3 pmol/mg protein. This binding site appears to be distinct from those for the 1,4-dihydropyridines and the phenylalkylamines, although the three binding sites seem to be coupled in a temperature-dependent manner, allowing both negative and positive allosteric interactions among the three classes of calcium channel blockers (Garcia *et al.*, 1986). Evidence that the binding site for diltiazem is a receptor comes from examination of these interactions. Both 1,4-dihydropyridines and phenylalkylamines influence the negative inotropic effect of diltiazem in a manner that is consistent with their effect on diltiazem binding (Garcia *et al.*, 1986).

Clinical Pharmacology

The clinical pharmacology of diltiazem has been reviewed extensively (Feld and Singh, 1985; Chaffman and Brogden, 1985). The observed clinical effects of diltiazem result from a combination of its actions on vascular smooth muscle and myocardial cells, as well as from the body's autonomic reflex responses to the resulting changes. The major clinical effect of diltiazem is vasodilation of coronary arteries and peripheral arterioles. Its primary usefulness, therefore, is in the treatment of angina pectoris, especially the more recalcitrant varieties such as Prinzmetal's angina, and it is currently approved for use in the U.S. only as an antianginal agent. However, the peripheral vasodilating effect also results in a decreased blood pressure, and the potential effectiveness of diltiazem for the treatment of hypertension has been studied. Diltiazem also affects the electrophysiology of the heart by slowing AV conduction and reducing the rate of SA node activation, evident as a prolongation of the PR interval of the electrocardiogram and a decreased heart rate, respec-

tively. It therefore has been used successfully for the treatment of certain cardiac arrhythmias, specifically, supraventricular tachycardias. Only a weak negative inotropic effect of diltiazem has been observed *in vivo*. A qualitative comparison of the cardiovascular properties of diltiazem and representative compounds from the 1,4-dihydropyridine and phenylalkylamine classes of calcium channel blockers, nifedipine and verapamil, respectively, is presented in Figure 39.

Pharmacokinetics

Despite the wide clinical use of diltiazem, its pharmacokinetics have been poorly studied. Although the half-life has been reported in a number of studies, detailed pharmacokinetic data are limited. Most information comes from studies in which single oral or intravenous doses were administered to healthy subjects or patients with arrhythmias or hypertension. Pharmacokinetic evaluation of multiple dose therapy has been limited. Table 14 summarizes the results of the major pharmacokinetic studies of diltiazem. In addition, the subject has been reviewed recently (Echizen and Eichelbaum, 1986).

Single Dose Pharmacokinetics

Absorption and Bioavailability

Peak plasma concentrations of diltiazem after a single oral dose of a tablet formulation occur at 1.7 to 4.7 hours, most often at about 3 to 3.5 hours (Bighley *et al.*, 1980; Hermann *et al.*, 1983; Kinney *et al.*, 1983; Koiwaya *et al.*, 1981a,b; Montamat and Abernethy, 1987; Ochs and Knüchel, 1984; Rovei *et al.*, 1980; Smith *et al.*, 1983). The bioavailability of diltiazem after an oral dose has been estimated in only four studies and was reported to be 33% for a solution formulation (Ochs and Knüchel, 1984) and from 38% to 44% for a tablet formulation in three studies (Hermann *et al.*, 1983; Ochs and Knüchel, 1984; Smith *et al.*, 1983) and 64% in another study (Schwartz and Abernethy, 1987). The generally low bioavailability is believed to be due to first pass metabolism because diltiazem is almost entirely eliminated by metabolism with a high total plasma clear-

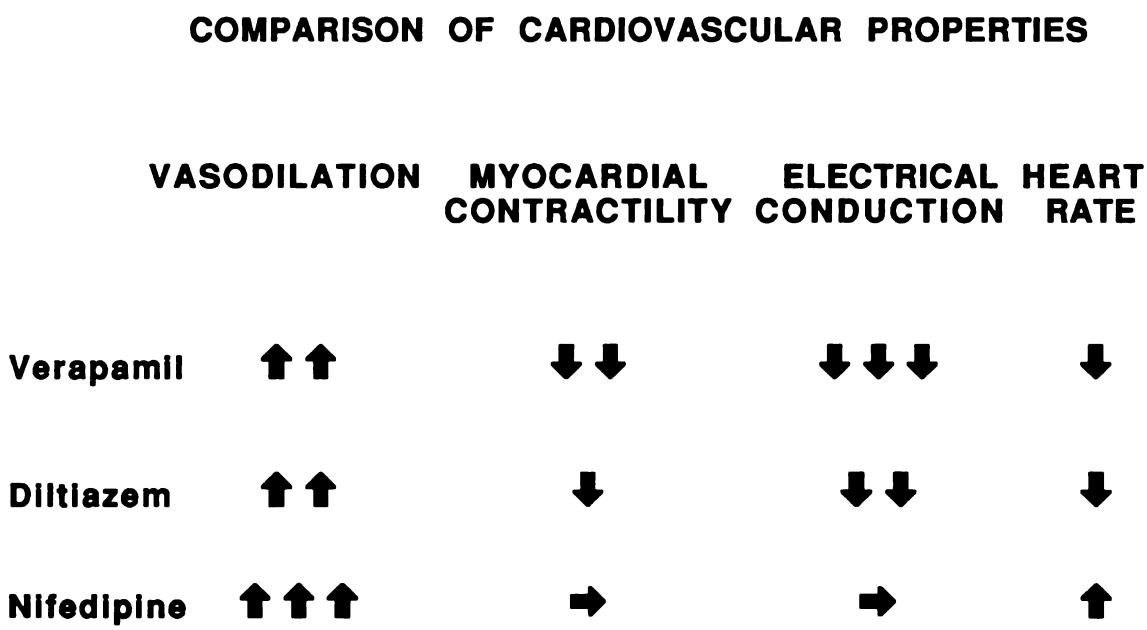

Figure 39. Qualitative comparison of the clinical cardiovascular properties of representative compounds from the three major classes of calcium channel blockers.

Table 14. Summary of results of pharmacokinetic studies of diltiazem

Reference	N[1]	Dose and Route[2]	t1/2 (h)	V_d[3,4] (L)	Cl[4] (ml/min)	t_{peak} (h)	F (%)
Single Dose Studies							
Bighley *et al.*, 1980	6, healthy	60 mg po (caps and tabs)				1.5-3.3	
Rovei *et al.*, 1980	3, healthy	60-210 mg po (caps and tabs)	4.4-6.9			1.0-3.7	
Kinney *et al.*, 1981	13, healthy	30-120 mg po (tabs)	4.1-5.6			3.3-4.0	
Koiwaya *et al.*, 1981a	9, healthy	90 mg po (tabs)				2.0-3.0	
Koiwaya *et al.*, 1981b	10, coronary artery disease	90 mg po (tabs)				4.0	
Hermann *et al.*, 1983	12, healthy	60 mg po (tabs)	3.2			2.8	
		15 mg iv	3.1	371	1491		42
Smith *et al.*, 1983	8, paroxysmal atrial tachycardia	20 mg iv	4.5	370	828		
		60 or 90 mg po (tabs)	3.7			1.8-4.7	38
Pozet *et al.*, 1983	9, severe renal failure	120 mg po (tabs)	3.4			2.0-3.0	
Ochs and Knüchel, 1984	6, healthy	20 mg iv	11.2	777	805		
		120 mg po (soln)	11.2			0.63	44
		120 mg po (tabs)	8.2			2.75	33

Table 14. Summary of results of pharmacokinetic studies of diltiazem (cont'd)

Reference	N[1]	Dose and Route[2]	t1/2 (h)	V_d[3,4] (L)	Cl[4] (ml/min)	t_{peak} (h)	F (%)
Finch and Johnston, 1985	6, healthy	60-180 mg po	5.0			3.0	
Montamat and Abernethy, 1987	12 young hypertensives	21.8 mg iv	3.69	271	873		
	12 elderly hypertensives	21.8 mg iv	3.78	289	892		
Schwartz and Abernethy, 1987	10 young hypertensives	25 mg iv	3.3	364[5]	1610		
		50 mg iv	3.8	378[5]	1484		
		120 mg po (tabs)	3.3	931[5]		3.3	64
	13 elderly hypertensives	25 mg iv	4.5	315[5]	882		
		50 mg iv	4.5	315[5]	1085		
		120 mg po (tabs)	4.7	686[5]		3.3	64
Fu *et al.*, 1987	10, healthy	138-187 mg po (soln)	3.8			0.54	
Multiple Dose Studies							
Rovei *et al.*, 1980	4, healthy	60 mg po t.i.d x 6 days (caps)	4.6			2.0	
Smith *et al.*, 1983	8, paroxysmal atrial tachycardia	60 or 90 mg q 6 h x 4 days	4.85				90

Table 14. Summary of results of pharmacokinetic studies of diltiazem (cont'd)

Reference	N[1]	Dose and Route[2]	t1/2 (h)	V_d[3,4] (L)	Cl[4] (ml/min)	t_{peak} (h)	F (%)
Ellenbogen *et al.*, 1986	8, healthy	iv infusion (10 mg/h) x 15 min-48 h	4.2	380	1149		
Montamat and Abernethy, 1987	12 young hypertensives	60 mg po q 12 h x 7 days, then 120 mg q 12 h x 7 days	5.2				
	12 elderly hypertensives	same	5.96				

[1] number of subjects

[2] po = oral, iv = intravenous, tabs = tablets, caps = capsules, soln = solution

[3] $V_{d\ area}$ unless otherwise indicated

[4] based on a 70 kg person

[5] $V_{d\ ss}$

ance (see below). In addition, wide interpatient variability in the estimates of bioavailability have been reported in all these studies, consistent with significant first pass metabolism. No saturation in first pass metabolism was apparent after single oral doses as high as 210 mg (Kinney *et al.*, 1981; Rovei *et al.*, 1980).

Distribution

Diltiazem is a weak base (pK_a of 7.7) with an octanol/water coefficient of 158 (Ochs and Knüchel, 1984). The volume of distribution of diltiazem is large, as expected for a nonpolar, basic compound, with estimates after intravenous doses ranging from 271 to 777 L, based on a 70 kg person (see Table 14). Plasma concentration-time profiles of diltiazem after intravenous doses have exhibited both two- and three-compartment characteristics (Hermann *et al.*, 1983; Montamat and Abernethy, 1987; Ochs and Knüchel, 1984; Schwartz and Abernethy, 1987; Smith *et al.*, 1983).

Diltiazem is reported to be 69 to 87% bound to protein in plasma (Morselli *et al.*, 1979; Rovei *et al.*, 1980) and in serum (Bloedow *et al.*, 1982; Kwong *et al.*, 1985; Pieper, 1984), with most estimates being about 78 to 81%. In one study, the percentage bound of diltiazem in plasma was reported to be lower, ranging from 55 to 65% (Nakamura *et al.*, 1987). Because the concentrations of diltiazem studied extended from 0.3 to 30 μg/ml, saturation of binding sites may have occurred at the higher concentrations. Binding of diltiazem appears to be independent of concentration over the range of concentrations of 30 ng/ml to 2 μg/ml (Bloedow *et al.*, 1982; Pieper, 1984; Rovei *et al.*, 1980).

Diltiazem binds to α_1-acid glycoprotein and lipoproteins, and, to a lesser extent, to albumin (Kwong *et al.*, 1985; Morselli *et al.*, 1979; Nakamura *et al.*, 1987; Pieper, 1984). It has been suggested that the variability in the percentage bound found among individuals is due to variability in α_1-acid glycoprotein and lipoprotein concentrations (Kwong *et al.*, 1985; Pieper, 1984).

Metabolism and Excretion

Diltiazem is extensively metabolized, primarily by deacetylation and N- and O-

demethylation. The first group of investigators to study the metabolism of diltiazem in humans (Rovei *et al.*, 1980) positively identified four metabolites in the urine using mass spectrometry. These metabolites were desacetyldiltiazem (DAD or M_1) (see Figure 38), N-demethyldesacetyldiltiazem (M_2), O-demethyldesacetyldiltiazem (M_4), and N,O-demethyldesacetyldiltiazem (M_6), as well as conjugates of M_4 and M_6. An additional metaboite was tentatively identified as N,N-demethyldesacetyldiltiazem (M_8). The alpha-numeric designations refer to the labels given the metabolites in the first animal study of metabolism (Meshi *et al.*, 1971).

A more quantitative study of the metabolism of diltiazem was carried out by Sugihara *et al.* (1984). Like Rovei *et al.* (1980), they recovered the metabolites DAD, M_2, M_4, and M_6, as well as conjugates of M_2, M_4, and M_6 in the urine. A fifth metabolite also was identified. This new metabolite was determined to be N-monodemethyldiltiazem (NDD or M_A) (Figure 38). At about the same time, a report appeared in which the authors claimed to have detected six metabolites and a small amount of unchanged diltiazem in the urine of two patients (Clozel *et al.*, 1984). The metabolites included DAD, M_2, M_4, M_6, and the N-oxide derivatives of DAD and M_4. These two N-oxide derivatives previously had been detected as metabolites in rats (Meshi *et al.*, 1971). All of the metabolites were highly conjugated and the major metabolites appeared to be M_6 and the N-oxide of DAD. No NDD was detected. However, in contrast to the previous study in which the identity of the metabolites was confirmed by mass spectrometry, the metabolites were identified only on the basis of retention times in an HPLC system.

The recovery of unchanged drug and DAD in the urine after an oral dose of 60 to 210 mg accounted for only 0.1-4% and 0.3-0.8% of the dose, respectively, in the study by Rovei *et al.* (1980). The proportion of the dose represented by the other metabolites was not reported. Sugihara *et al.*, (1984) found that urinary recovery of diltiazem and NDD each accounted for about 5% of a 30 mg dose and M_2 accounted for 0.75% of the dose. Unconjugated forms of the other three metabolites, DAD, M_4, and M_6, were de-

tected, but were below the limit of determination of the assay.

In plasma, only one metabolite (DAD) was detected by Rovei *et al.* (1980). It reached concentrations that were 10-30% of diltiazem concentrations for the first 6-8 hours after a single oral dose in capsule form and about the same as those of diltiazem at 24 hours. Only NDD was detected in addition to diltiazem in plasma by Sugihara *et al.* (1984). In patients who were taking 60 mg of diltiazem three times daily, NDD plasma concentrations reached levels about one third those of diltiazem. Subsequent studies have demonstrated that DAD achieves significant plasma levels after both a single oral or intravenous dose of diltiazem (Schwartz and Abernethy, 1987) and after multiple oral or intravenous dosing (Ellenbogen *et al.*, 1986; Smith *et al.*, 1983). However, when an assay method that detected NDD in addition to DAD was used, NDD was found to be the major metabolite of diltiazem appearing in the plasma (Goebel and Kölle, 1985; Montamat and Abernethy, 1987).

Clearance

Controversy exists over the value for total plasma clearance of diltiazem. In three studies, the mean total plasma clearance of diltiazem has been estimated to range from 800-900 ml/min (based on a 70 kg person) (Montamat and Abernethy, 1987; Ochs and Knüchel, 1984; Smith *et al.*, 1983). In three other studies, however, the mean estimated plasma clearance was as high as 1150 to 1600 ml/min (Ellenbogen *et al.*, 1986; Hermann *et al.*, 1983; Schwartz and Abernethy, 1987).

Because diltiazem is almost entirely eliminated by hepatic metabolism, its total clearance can be approximated by hepatic clearance. Therefore, the well-stirred physiological model (Rowland *et al.*, 1973; Wilkinson and Shand, 1975) can be used to describe the clearance of diltiazem from blood, assuming that the drug in the liver is in equilibrium with the venous blood. Because the blood to plasma concentration ratio for diltiazem is equal to 1 (Kölle *et al.*, 1983), blood clearance is equal to plasma clearance.

In two studies, (Hermann *et al.*, 1983; Schwartz and Abernethy, 1987), the esti-

mates of plasma clearance are inconsistent with the bioavailabilities reported. Because F = 1- E = 1- Cl/Q, where Q is the hepatic blood flow, (or less than this value if the drug is not absorbed intact from the gastrointestinal tract), the bioavailability would be expected to approach zero, assuming a hepatic blood flow of 1500 ml/min, with the total clearances of 1491 and 1610 ml/min reported by Hermann *et al.* (1983) and Schwartz and Abernethy (1987), respectively. Instead, the corresponding values for bioavailability in these two studies were 42% and 64%. The lower estimates of clearance obtained in other studies are in better agreement with reported bioavailabilities. The reason for the discrepancy in the estimates of total plasma clearance in these studies is not known. Not enough data were presented to determine if reliable estimates of the AUC, from which Cl was calculated, were obtained.

Half-lives have been reported from many more studies and have ranged from 3.1 to 11.2 h in single dose studies, most being about 5 h (see Table 14). Possible reasons for this wide range of values are discussed in Chapter 7 with reference to our results.

Multiple Dose Pharmacokinetics

The pharmacokinetics of diltiazem have been studied after multiple oral dosing to steady state (Smith *et al.*, 1983; Montamat and Abernethy, 1987) and after long-term intravenous infusion (Ellenbogen *et al.*, 1986), with conflicting results. Smith *et al.*, (1983) examined the areas under the concentration-time curve (AUC) after a single oral dose ($AUC_{0\rightarrow\infty}$) and at steady state ($AUC_{0\rightarrow\tau}$) and demonstrated a mean ratio of 2.39 for $AUC_{0\rightarrow\tau}/AUC_{0\rightarrow\infty}$. No increase in AUC after chronic dosing was noted by Montamat and Abernethy (1987), and Ellenbogen *et al.* (1986) did not study single doses.

Because AUC = F*D/Cl, where F is the bioavailability, D is the dose and Cl is the total plasma clearance, the increase in AUC after chronic dosing theoretically could be due to an increase in F or a decrease in Cl. Furthermore, applying the well-stirred physiological model for clearance as discussed under Single Dose Pharmacokinetics, and assuming that diltiazem is completely absorbed intact from the gastrointestinal tract, AUC_{oral} =

$D/(Cl_i * fu)$ where Cl_i is the intrinsic metabolic clearance and fu is the unbound fraction in plasma. Consequently, the increased AUC after chronic oral dosing could be due to a decreased intrinsic clearance or a decreased unbound fraction. The latter is unlikely inasmuch as it would require an increased apparent binding affinity to plasma proteins, an increased number of binding sites per protein molecule, or an increased concentration of plasma proteins. Although diltiazem binds to α_1-acid glycoprotein and the concentrations of this plasma protein could increase, no changes in α_1-acid glycoprotein levels have been reported as a consequence of chronic oral therapy with diltiazem. On the other hand, decreased intrinsic clearance could be due to concentration-dependent effects (saturation of hepatic metabolism) or time-dependent effects (inhibition of metabolizing enzymes by diltiazem or its metabolites). The second possibility is discussed in more detail below.

Alternatively, the assumption of complete absorption of intact diltiazem from the gastrointestinal tract may be incorrect. Although greater than 90% of an oral dose of radiolabeled diltiazem was recovered within 72 hours in the rat (Meshi *et al.*, 1971), the extent of recovery of an oral dose in humans has not been reported. In addition, pre-hepatic metabolism of diltiazem cannot be ruled out. Therefore, increased absorption of intact drug could also explain the increased AUC after chronic oral dosing.

There is contradictory evidence concerning half-life increases of diltiazem with multiple dosing. Rovei *et al.* (1980) and Smith *et al.* (1983) found no statistically significant increase in half-life after multiple oral dosing to steady state, although this trend was apparent. On the other hand, Montamat and Abernethy (1987), who included more subjects in their study, did find a significantly longer half-life at steady state, which they attributed to a decreased clearance because they assumed no change in distribution with chronic dosing ($t1/2 = 0.693 * V/Cl$, where t1/2 is the plasma half-life and V is the volume of distribution).

Because diltiazem has been reported to inhibit hepatic oxidative metabolism both *in vitro* (Renton, 1985) and *in vivo* (Bauer *et al.*, 1986; Carrum *et al.*, 1986), it is possible

that it may inhibit its own metabolism with chronic therapy, thus decreasing intrinsic clearance and increasing half-life. Alternatively, the hepatic blood flow may be altered, or the accumulated metabolites could inhibit the metabolism of diltiazem. However, it is also possible that the fraction unbound has also increased, either due to saturable plasma protein binding or displacement by metabolites, resulting in an increased volume of distribution ($V = V_T * fu/fu_T$, where V_T is the tissue volume and fu_T is the unbound fraction in the tissue) and an increased half-life. The plasma protein binding has not been measured in any of these pharmacokinetic studies.

Of these possible explanations for the observed increase in half-life, only a decrease in intrinsic clearance is compatible with the observed increase in AUC with chronic oral dosing, assuming that the relationship between AUC_{oral}, Cl_i and fu described above is correct. Clearly, more study of the multiple-dose pharmacokinetics of diltiazem is needed to explain the conflicting reports of increased half-life and AUC, and to determine the underlying mechanisms.

The pharmacokinetics of the metabolites, DAD and NDD, have been examined only after chronic oral dosing of diltiazem (Montamat and Abernethy,1987; Goebel and Kölle, 1985). After chronic oral therapy with diltiazem for 14 days, the half-lives of diltiazem, NDD and DAD were 5.2, 7.4 and 8.3 hours in a group of young hypertensive patients and 5.96, 10.37 and 10.92 hours in a group of elderly hypertensive patients (Montamat and Abernethy, 1987). When the AUC over a single dosing interval of each metabolite was compared to that of diltiazem as a measure of the amount of each metabolite appearing in plasma, the AUC of NDD was about 50 % and the AUC of DAD about 20% of the AUC of diltiazem in the young group and about 30% and 15% in the elderly group. After multiple oral dosing of five subjects for two days, the half-lives of diltiazem, DAD and NDD were determined to be 6.4, 8.7 and 9.0 h (Goebel and Kölle, 1985).

Pharmacokinetics in Renal Disease

Only one study has examined the effect of renal dysfunction on the pharmacokinet-

ics of diltiazem (Pozet *et al.*, 1983). When a single 120 mg oral dose of diltiazem was administered to nine patients with severe renal dysfunction, no significant alterations in the pharmacokinetics were apparent when compared to parameters reported in the literature for healthy subjects (see Table 14). The half-life was unchanged, the concentrations of DAD reached levels about 26% of those of diltiazem, and 1.35% of the dose appeared in the urine as unchanged diltiazem. No measurements of plasma protein binding were made. To date, there has been no published report of the pharmacokinetics of diltiazem in hepatic disease.

Age-Related Pharmacokinetics

Montamat and Abernethy (1987) and Schwartz and Abernethy (1987) have examined the pharmacokinetics of diltiazem in both young and elderly hypertensives (see Table 14). Schwartz and Abernethy (1987) found that the clearance of diltiazem was significantly lower in the elderly group after single intravenous doses of 25 and 50 mg, infused over 10 min. The half-life was significantly longer in the elderly only after the 50 mg intravenous dose. There was no statistically significant difference between the two groups for volume of distribution. Montamat and Abernethy (1987), on the other hand, found no statistically significant differences between the young and elderly groups for any of the pharmacokinetic parameters of diltiazem, DAD or NDD, estimated after multiple oral dosing or a single intravenous dose (diltiazem only). However, there was a tendency for the half-life to increase with age for the two metabolites. No measurements of plasma protein binding were made but the volume of distribution after the intravenous dose was not significantly different in the two groups.

Pharmacodynamics

Despite the fact that there are well defined and easily measured pharmacologic endpoints for diltiazem (decreased blood pressure and heart rate, prolonged AV conduction), there is no detailed information about the relationship between these pharmacologic effects

and plasma concentrations of diltiazem. Although pharmacologic responses were monitored in a number of the pharmacokinetic studies, either no attempt was made to relate them quantitatively to plasma concentrations, or no effects were noted (Finch and Johnston, 1985; Hermann *et al.*, 1983; Kinney *et al.*, 1981; Koiwaya *et al.*, 1981a,b; Smith *et al.*, 1983).

The only consistent effect observed after diltiazem administration has been a change in PR interval (Ellenbogen *et al.*, 1986; Fu *et al.*, 1987; Joyal *et al.*, 1986; Schwartz and Abernethy, 1987; Smith *et al.*, 1987). This was especially evident in the study by Fu *et al.* (1987) in which a high dose of an oral solution of diltiazem was administered to healthy subjects. All developed at least first degree heart block. The investigators stated that there was no correlation between the degree of PR interval prolongation and the plasma concentration of diltiazem, but no data were shown.

The only study in which there was a detailed quantitative evaluation of the relationship between plasma concentrations of diltiazem and pharmacologic effect using a pharmacodynamic model was that of Schwartz and Abernethy (1987). They reported a significant correlation between the change in PR interval and plasma concentration of diltiazem after a 25 mg or 50 mg intravenous dose or a 120 mg oral dose, and used a linear pharmacodynamic model to describe the relationship. However, although the mean parameters estimated from this model were reported, no concentration-effect data were presented. Changes in heart rate and blood pressure were observed in some cases, but were not analyzed using a pharmacodynamic model.

In other studies in which both PR interval and plasma concentrations of diltiazem were measured, significant changes in PR interval were noted, but quantitative data describing the relationship between changes in PR interval and plasma concentrations of diltiazem were not presented. Ellenbogen *et al.*(1986) reported a correlation between the prolongation of the PR interval and plasma concentrations of diltiazem after the termination of a long-term intravenous infusion. No correlations were seen at any time during the infu-

sion. Data on which this correlation was based were not presented. Joyal *et al.* (1986) found a significant linear correlation between a single concentration of diltiazem, 15 min after initiation of an intravenous infusion, and change in blood pressure and left ventricular work index in 14 patients with stable effort angina.

Smith *et al.* (1983) also noted a prolonged PR interval after both a single oral dose and a short intravenous infusion over 10 min and they observed a counterclockwise hysteresis after the intravenous dose. A similar delay in maximal response after attainment of peak concentration was reported by Joyal *et al.* (1986).

The pharmacological activity of the metabolites of diltiazem have been determined only in animal tissues, both *in vitro* and *in vivo*. DAD was found to possess about 40 to 50% of the activity of the diltiazem in producing hemodynamic effects in several species of anesthetized animals (Cavero *et al.*, 1979). In anesthetized dogs and in blood-perfused canine papillary muscles, the cardiovascular effects of NDD, DAD, M_2, M_4, and M_6 were studied and found to be qualitatively similar to those of diltiazem but of lower potency (Yabana *et al.*, 1985). DAD had about 50% and NDD about 20% of the effect of diltiazem in increasing coronary flow in the whole animal and in the isolated preparation. However, the pharmacologic effect of diltiazem and NDD lasted longer than that of DAD. In lowering blood pressure, DAD had an effect equivalent to diltiazem and NDD had about 33% of the effect of diltiazem. The negative inotropic activity of diltiazem and the metabolites was very weak, but followed the same potency order. Because the determination of relative potencies in these preparations was based on doses rather than on concentrations, it is not known to what extent the differences in potency or duration can be explained by differences in pharmacokinetic properties.

Narita *et al.* (1986) administered diltiazem, DAD and NDD separately to both conscious and anesthetized spontaneously hypertensive rats (SHR) and monitored heart rate and mean blood pressure. In conscious SHR, the hypotensive effects of diltiazem and DAD were equivalent and NDD had about one third of their activity. Again, diltiazem and

NDD had a longer duration of action than DAD. In conscious SHR, the heart rate first increased then decreased with diltiazem and DAD, but only increased with NDD. Similar results were found in anesthetized SHR, but at lower doses. However, under these conditions, the heart rate decreased with all three compounds, with NDD being much less potent than diltiazem and DAD. Again, the relative potencies were based on doses rather than on concentrations of these compounds.

The antagonistic activities of diltiazem and its metabolites on phasic contractions of the rat portal vein were determined and compared with their binding affinities for the [^{3}H]diltiazem binding site in rat cerebral cortex (Schoemaker *et al.*, 1987). The order of potency for binding was diltiazem > DAD > NDD > M_2 > M_4 > M_6. The order of potency for inhibition of vascular smooth muscle contraction was DAD ≥ diltiazem > NDD ≥ M_2 > M_4 >> M_6, with the potency of NDD being about 25% of that of diltiazem. These results agree well with those of the previous studies.

Summary

The pharmacokinetics and pharmacodynamics of diltiazem are not well characterized. Several inconsistencies in reports of its pharmacokinetic parameters after both single and multiple doses remain to be reconciled. A significant problem is the relatively recent discovery of a metabolite, NDD (Sugihara *et al.*, 1984), that appears to be the major metabolite of diltiazem and that accumulates in the plasma, especially after chronic oral dosing (Goebel and Kölle, 1985; Montamat and Abernethy, 1987). Because most of the pharmacokinetic data on diltiazem were obtained with assays that did not detect NDD, little is known about its pharmacokinetic properties.

For the same reason, the available pharmacodynamic data for diltiazem may be unreliable. Both DAD and NDD may have pharmacologic effects, although this has not yet been demonstrated in humans, and their contribution to the pharmacologic effect of diltiazem is unknown. It is therefore necessary to examine diltiazem pharmacodynamic data for

the presence of a hysteresis effect. Dose- and time-dependence in the concentration-effect relationship could be an indication of the presence of active or inhibitory metabolites, as well as such phenomena as a delay in the drug reaching the effect site, or the development of tolerance or sensitization. There is some evidence that a hysteresis effect may occur with diltiazem (Smith *et al.*, 1983), but this has not been well characterized.

Another factor that has been ignored in considerations of the pharmacodynamics of diltiazem is its binding to plasma proteins. Because it is generally believed that only unbound drug is capable of exerting a pharmacologic effect, it is important to relate unbound plasma concentrations to pharmacologic effect. Diltiazem has been shown to be about 80% bound to plasma proteins (Bloedow *et al.*, 1982; Kwong *et al.*, 1985; Pieper, 1984; Rovei *et al.*, 1980). There is only one report on the extent of binding of DAD to plasma proteins (about 85% at 22 ° C) (Morselli *et al.*, 1979) and there is no information on the plasma protein binding of NDD.

In light of these problems, the goal of the second part of this dissertation was to study the pharmacokinetics and pharmacodynamics of diltiazem. In these studies, we addressed some of the deficiencies of the previous work. Specifically, we used an HPLC assay that simultaneously measures diltiazem, DAD and NDD in plasma and urine. Also, we carried out plasma protein binding studies of diltiazem, DAD and NDD so that pharmacologic effects could be related to unbound concentrations. Finally the concentration-effect data was analyzed using the appropriate pharmacodynamic model (Holford and Sheiner, 1981).

Specific Objectives of Part 2 (Chapter 7)

1. To study the pharmacokinetics and pharmacodynamics of diltiazem after a single oral dose in healthy adult volunteers.

2. To determine the plasma protein binding of diltiazem, DAD and NDD in plasma from healthy adult volunteers.

CHAPTER 7

The Pharmacokinetics and Pharmacodynamics of Diltiazem and its Metabolites In Healthy Adults after a Single Oral Dose

Introduction

Despite the widespread use of diltiazem in the therapy of a variety of cardiovascular disorders, there are surprising gaps in our knowledge of its pharmacokinetics and pharmacodynamics. Although the pharmacokinetics of diltiazem have been studied after both oral and intravenous doses (Hermann *et al.*, 1983; Montamat and Abernethy, 1987; Ochs and Knüchel, 1984; Schwartz and Abernethy, 1987; Smith *et al.*, 1983), there are major discrepancies in reports of estimated pharmacokinetic parameters. There is even less information on the relationship between plasma concentrations of diltiazem and pharmacologic response. Diltiazem is used therapeutically for its ability to relax vascular smooth muscle and slow AV conduction in the heart. These effects are measured clinically by monitoring changes in blood pressure, heart rate and the PR interval of the electrocardiogram and they can be related to the plasma concentrations of diltiazem to describe the pharmacodynamics of this compound. However, a quantitative description of the relationship between the plasma concentration of diltiazem and pharmacologic response has been reported only for prolongation of the PR interval (Ellenbogen *et al.*, 1986; Schwartz and Abernethy, 1987; Smith *et al.*, 1983), and detailed data were not presented.

A potential complicating factor in examining the pharmacodynamics of diltiazem is that it is extensively metabolized and two of the metabolites, desacetyldiltiazem (DAD) and N-demethyldiltiazem (NDD) (see Chapter 6, Figure 38 for structures) may have pharmacologic activity. DAD possessed from 40 to 100% and NDD from 20 to 30% of the activity of diltiazem on a number of hemodynamic parameters in animals, both *in vivo* and *in vitro* (Cavero *et al.*, 1979; Schoemaker *et al.*, 1987; Yabana *et al.*, 1985). There is no in-

formation on their pharmacologic activity in man and limited pharmacokinetic data are available but both metabolites are present in significant concentrations in plasma after oral administration of diltiazem (Goebel and Kölle, 1985; Montamat and Abernethy, 1987; Smith *et al.*, 1983; Sugihara *et al.*, 1984). It is therefore possible that these metabolites contribute to the pharmacologic effect of diltiazem, but this possibility has not been explored.

The goal of this investigation was to address some of these unanswered questions by studying the pharmacokinetics and pharmacodynamics of diltiazem and its two metabolites, NDD and DAD, after an oral dose of diltiazem. Specifically, the following questions were addressed. How do the pharmacokinetics of NDD and DAD compare with the pharmacokinetics of diltiazem? Is there a quantitative relationship between pharmacologic response and plasma concentration of diltiazem? Is there any evidence for a hysteresis effect that might suggest the contribution of a metabolite to the response? To carry out these studies, we used a sensitive HPLC assay that allowed us to simultaneously measure the concentrations of diltiazem, NDD and DAD in both plasma and urine for 24 hours after the dose. The results demonstrate that there appears to be an interesting relationship between electrophysiologic response and plasma concentration of diltiazem that may indicate that the metabolites influence the response.

Methods

Clinical Protocol

The study protocol was approved by the Committee on Human Research of the University of California San Francisco. Six healthy male volunteers between the ages of 22 and 40 years, weighing between 62.6 and 95.1 kg were included in the study. All were in good health on the basis of history, physical examination, urinalysis and blood chemistry. None had a history of cardiovascular, renal, hepatic, gastrointestinal, respiratory, hematological or other diseases that could affect the absorption, distribution, metabolism or

excretion of the study drug. Informed consent was obtained after the purpose, procedures, and risks of the study were explained to the volunteers. The volunteers were instructed to avoid any other drugs, including alcohol, for two weeks prior to the study and during the study day.

On the study day, volunteers entered the Drug Studies Unit of the University of California San Francisco at 7:00 am after an overnight fast from 10:00 pm the previous evening. An indwelling polyethylene catheter capped with a Teflon obturator (Angiocath 20 G 1-1/4 in, Deseret Medical, Inc., Becton Dickinson and Company, Sandy, UT) was inserted into a forearm vein for blood withdrawal. A half-hour before drug administration, a 40 ml blood sample and a urine sample were collected, and supine blood pressure, heart rate and ECG measurements were made. Blood pressure (systolic, diastolic and mean arterial pressure) and heart rate were measured with a Dura-Cuf attached to a Dinamap-845XT Vital Signs Monitor (Critikon, Tampa, FL). ECG measurements were made using a 3-lead Lifepak 6 Cardiac Monitor (Physio-Control Corporation, Redmond, WA). Blood samples were collected in 10 ml plastic syringes and immediately transferred to heparinized (143 USP Units of Na Heparin) stoppered glass tubes (Vacutainer Green Top, Becton-Dickinson, Rutherford, NJ). Two 60 mg tablets of diltiazem (Cardizem™, Marion Laboratories, Kansas City, MO) then were administered with 240 ml of water.

Ten milliliter blood samples were collected at the following times after drug administration: 0.5, 0.75, 1, 1.5, 2, 3, 4, 6, 8, 10, 12, and 24 hours. Blood pressure and heart rate were measured at each blood sampling time. An ECG was displayed continuously on an oscilloscope for four hours after the dose and recorded on a strip chart at a paper speed of 25 mm/sec at each blood sampling time thereafter. Urine was collected over the following intervals: from 0.5 hr before the dose to 0.5 hr after the dose, and then from 0.5-1.5, 1.5-2.5, 2.5-3.5, 3.5-5, 5-7, 7-9, 9-11, 11-13, and 13-24 hr. After each urine collection period, each subject was asked to drink 240 ml of water to maintain adequate urine output. A light meal was given at lunch time (at least four hours after drug administration).

Blood was centrifuged at 1000 g immediately after collection and the plasma was transferred to screw-top glass vials. The volume and pH of each urine sample were recorded and a 20 ml aliquot from each collection period was saved in a screw-top glass scintillation vial. Plasma and urine samples were stored at -20° C until analysis.

Assay of Diltiazem and Metabolites in Biological Samples

Concentrations of diltiazem and its two metabolites, DAD and NDD, in plasma and urine were assayed by an HPLC method that is a modification of the assay of Goebel and Kölle (1985). The procedure is detailed in the following sections.

Chemicals

Methanol, acetonitrile, triethylamine, methyl-*tert*-butyl ether, all of HPLC grade, and ammonium bromide, hydrochloric acid, and sodium hydroxide, all of analytical-reagent grade, were obtained from Fisher Scientific Co. (Fair Lawn, NJ). Diltiazem HCl and verapamil HCl (the internal standard) were obtained from Sigma Chemical Co. (St. Louis, MO). The metabolites, desacetyldiltiazem HCl (DAD) and N-monodemethyldiltiazem fumarate (NDD), were generously provided by Dr. Darrell Abernethy, Division of Clinical Pharmacology, Brown University.

Aqueous stock solutions of diltiazem, DAD, NDD, and verapamil (10 mg base/100 ml) were prepared and stored in amber glass containers at 4° C. Concentrations were monitored periodically and the solutions of metabolites showed no degradation over a period of six months. Fresh stock solutions of diltiazem and verapamil were prepared every two months.

HPLC System

The instrumentation used included a Waters Model M-45 Solvent Delivery System (Waters Associates, Inc., Milford, MA) or a Beckman Model 110A Solvent Metering Pump (Beckman Instruments, Inc., Palo Alto, CA), a Rheodyne Model 7125 Sample Injector (Rheodyne Incorporated, Cotati, CA) with a 200 µl sample loop, a Waters Lambda-Max Model 481 UV detector, set at 237 nm, and an OmniScribe B-5000 Strip Chart

Recorder (Houston Instruments, Austin, TX). A reverse-phase C_{18} column was used (Beckman Ultrasphere ODS, 5 μm particle size, 4.6 mm O.D. x 15 cm, Beckman Instruments, Inc., San Ramon, CA).

The mobile phase consisted of methanol:0.04 M ammonium bromide in water:acetonitrile (40:36:24). Triethylamine was added to adjust the pH to 8.5. The solvent mixture was filtered and degassed under vacuum. Mobile phase was pumped at a flow rate of 1.2 ml/min.

Extraction Procedure

The extraction procedure for plasma is outlined as follows. A 4 μl aliquot of the verapamil stock solution was added to a 1 ml plasma sample in a 16 x 125 mm borosilicate disposable glass culture tube (Fisher Scientific Co., Pittsburgh, PA). Five milliliters of methyl-*tert*-butyl ether was added to the tube, which was then capped with a Tainer Top (Fisher Scientific Co.) and mixed for 20 min on a Waring Tube Rotator (Scientific Equipment Products, Baltimore, MD). After centrifugation at 1200 g for 10 min, the organic layer was transferred to a 12 x 75 mm borosilicate disposable glass culture tube containing 100 μl of 0.01 M HCl. The tube was capped, vortexed for 45 s and centrifuged again for 10 min. The organic layer was removed and discarded, and a 50 μl aliquot of the aqueous layer was injected directly into the HPLC system. Plasma samples were assayed on the same day that they were extracted. The extraction procedure for urine was similar, with the exception that 0.4 ml of 0.1 N NaOH was added to the urine sample to increase the pH and improve the extraction efficiency. In addition, aliquots of from 50 to 250 μl of urine from the subjects were assayed, after adding sufficient blank urine from a healthy male volunteer to bring the volume to 1 ml.

Validation of the Assay System

Plasma standard curves were constructed by assaying 1 ml blank plasma samples spiked with aliquots of stock solutions of diltiazem, DAD, NDD, and verapamil. The concentrations for diltiazem were 5, 10, 25, 50, 100, 200 and 300 ng/ml. For DAD and NDD,

the concentrations were 5, 10, 25, 50, 75 and 100 ng/ml. Peak-height ratios were plotted against concentrations and least squares linear regression analysis performed. The accuracy of the method was determined by comparing the theoretical concentrations with the concentrations predicted by the equation of the linear regression and expressed as percentage error. The between-day variability was assessed by comparing the slopes and intercepts of the linear regression equations determined from standard curves performed on 4 different days. The within-day variability was assessed by assaying six samples containing a low concentration of diltiazem and metabolites (10 ng/ml) and six samples containing a high concentration of diltiazem and metabolites (100 ng/ml) on the same day. In addition, the recovery of each compound was calculated by comparing the absolute peak heights from these samples with the absolute peak heights of samples of the same concentrations prepared in 0.01 M HCl and not subjected to the extraction procedure. The same procedures were used for the validation of the assay of urine samples except that the concentrations included in the standard curves were 10 to 400 ng/ml for NDD.

A new standard curve was constructed from blank plasma or urine each day that unknown samples were assayed. In addition, a blank plasma sample from each subject was assayed to check for interference from endogenous compounds.

Plasma Protein Binding

Chemicals

[^{3}H]Diltiazem (specific activity, 60.5 Ci/mmol) was obtained from New England Nuclear (Boston, MA). Potassium phosphate and sodium phosphate were obtained from Mallinckrodt (Paris, KY) and Sigma Chemical Co. (St. Louis, MO), respectively. The sources of all other chemicals were previously listed in the section describing the HPLC assay of diltiazem and its metabolites.

Methods

The binding of diltiazem, NDD and DAD to plasma proteins in blank plasma from each volunteer was determined by equilibrium dialysis. The system consisted of 2 ml

Teflon dialysis cells (Dianorm System, Spectrum Medical, Los Angeles, CA) separated into two 1 ml compartments by a cellulose membrane (Spectra/Por 2, Spectrum Medical) with a molecular weight cutoff of 12,000-14,000. Duplicate 1 ml blank plasma samples from each volunteer were dialyzed against 1 ml of isotonic Sorensen's phosphate buffer (0.13 M, pH 7.4) containing 125 ng of either diltiazem, NDD or DAD. Dialysis was carried out at 37° C for 4 h and the cells were gently rotated throughout the dialysis period. In preliminary studies using blank pooled plasma from healthy volunteers, 4 h was found to be a sufficient time for equilibrium to be reached for all three compounds. Further preliminary studies on the concentration dependence of diltiazem binding established that the unbound fraction (fu) does not change up to concentrations of 630 ng/ml.

The concentration of diltiazem in buffer and plasma was determined by adding approximately 82.9 pg of [^{3}H]diltiazem to the solution of unlabeled diltiazem in the buffer compartment. Immediately after dialysis, 0.5 ml aliquots from the plasma and buffer compartments were added to 10 ml Scintiverse II (Fisher Scientific, Springfield, NJ) and the radioactivity determined in a Beckman LS 1801 Scintillation Counter (Beckman Instruments, Palo Alto, CA). The recovery of [^{3}H]diltiazem from the dialysis system was determined from mass balance equations using the radioactivity in the buffer before dialysis and the radioactivity in the buffer and plasma after dialysis, with corrections for changes in volume (Tozer *et al.*, 1983). To confirm the stability of [^{3}H]diltiazem during the dialysis procedure, a triplicate determination of the protein binding of diltiazem in pooled plasma from healthy volunteers was carried out in the absence of [^{3}H]diltiazem and the concentrations of diltiazem in plasma and buffer were analyzed by HPLC as described below for the metabolites.

The concentrations of NDD and DAD in plasma and buffer were determined by the HPLC method described above. The extraction procedure for buffer was the same as that used for plasma. After dialysis, 0.5 ml aliquots from the plasma and buffer compartments were frozen at -20° C until analysis, a period of less than 10 days. On the day of analysis,

standard curves were prepared by spiking 1 ml of blank plasma or 1 ml of Sorensen's phosphate buffer with known concentrations of NDD and DAD. The volume of the unknown samples was brought to 1 ml with either blank plasma or blank buffer before analysis.

To determine the extent of volume shift during dialysis (Giacomini *et al.*, 1984; Tozer *et al.*, 1983), the concentration of protein in the plasma from each subject before and after dialysis was determined by the method of Lowry (1951). Triplicate samples of plasma before dialysis and duplicate samples of plasma from each of two dialysis cells after dialysis were analyzed for each subject.

Data Analysis

Pharmacokinetic Analysis

The logarithm of the concentrations of diltiazem, DAD and NDD in plasma were plotted *vs* time for each subject. The half-lives of NDD and DAD were obtained from the least squares linear regression of all points after the peak concentration on the ln concentration-time plot as $t_{1/2} = 0.693/\text{slope}$. Because the declining concentration-time data for diltiazem showed possible multiexponential characteristics, a model-independent half-life for diltiazem was determined from least squares linear regression of the final three points. In addition, the diltiazem concentration-time data were fit by both one- and two-compartment pharmacokinetic models with zero order or first order input by weighted nonlinear regression using DRUGFUN on the PROPHET system (Holford, 1982a). Weights of $1/y^2$ were used. A lag time estimate was included in each model. The Schwartz-Leonard criterion was used to choose the best fit of the data (Holford, 1982b) and the half-life was calculated as $0.693/\lambda_z$, where λ_z was the estimated disposition rate constant of the terminal exponential phase.

The area under the diltiazem concentration-time curve from 0 to 1440 min ($AUC_{0\rightarrow1440}$) was calculated using the linear trapezoidal rule for increasing concentrations and the logarithmic trapezoidal rule for declining concentrations. The extrapolated area un-

der the curve (AUC_{extrap}) was calculated by both model-dependent and model-independent methods and added to $AUC_{0\rightarrow1440}$ to obtain $AUC_{0\rightarrow\infty}$. In the former method, AUC_{extrap} was calculated as C_{est}/λ_z, where C_{est} is the concentration at 1440 min estimated from the equation of best fit of the data and λ_z is the terminal elimination rate constant obtained from the curve fitting. In the second method, AUC_{extrap} was calculated as C/k, where C is the measured concentration at 1440 min and k is the slope obtained from least squares linear regression of the terminal points. Apparent oral clearance (Cl/F) was calculated as Dose/$AUC_{0\rightarrow\infty}$, where $AUC_{0\rightarrow\infty}$ was obtained by the second method described above.

Renal clearances of diltiazem and its metabolites were calculated by plotting the excretion rate (concentration in urine sample x volume of urine collected in interval/time of interval) against the plasma concentration obtained at the midpoint of each urine collection interval. The slope of the linear least-squares regression fit (forced through the origin) is the renal clearance.

Pharmacodynamic Analysis

The PR interval was measured by hand from the strip chart recordings taken at each blood sampling time. The mean of the PR intervals from five consecutive heart beats (expressed in msec) was used as the measure of electrophysiologic effect at each time point. The change in PR interval was then calculated by subtracting the baseline PR interval from the PR interval at each sampling time. The pharmacologic measurements of change in PR interval, blood pressure, and heart rate were each plotted against the concentration of diltiazem to determine if a relationship existed and if the data could be fit by a pharmacodynamic model. The points on these plots also were linked in chronological order to determine if any time-dependencies existed.

Plasma Protein Binding

The unbound fraction (fu) of each compound in each volunteer was calculated using the following equation (Giacomini *et al.*, 1984):

$$\frac{C'_b}{C'_{bnd}(1+\delta)+C'_b} \qquad \text{(Equation 6)}$$

where C'_b is the concentration of compound in the buffer after dialysis and is equivalent to the unbound concentration in the plasma; C'_{bnd} is the bound concentration after dialysis, calculated as the total concentration in the plasma compartment after dialysis minus the concentration in buffer; and δ is the fractional increase in volume of the plasma due to the osmotic water shift. δ is determined from the protein concentration in plasma before (P) and after (P') dialysis as $\delta = (P/P')-1$ (Giacomini *et al.*, 1984). The equation is derived in Appendix B.

Results

Validation of the HPLC Assay for Diltiazem, DAD and NDD

Representative chromatograms from blank plasma (A), plasma spiked with diltiazem, NDD, DAD and verapamil (B), blank urine (C) and spiked urine (D) are shown in Figure 40. The peaks were sharp, symmetrical and well separated. Diltiazem, NDD, DAD and verapamil eluted with retention times of 6.2, 8.2, 10.6 and 14.6 min, respectively. No endogenous substance in plasma or urine from the six subjects interfered with any of these peaks. However, as noted by others (Montamat *et al.*, 1987; Rovei *et al.*, 1977; Verghese *et al.*, 1983), after storage of the blank blood bank plasma for several months, an endogenous peak appears that elutes immediately before DAD and overlaps the DAD peak. This was not a problem with the clinical samples because they were analyzed within four weeks of collection.

The standard curves for diltiazem and the two metabolites in plasma and urine were linear over the range of concentrations added and reproducible from day to day. Table 15 shows the variability in the slopes and intercepts of standard curves in plasma and urine obtained on four different days. The coefficient of variation of the slope was less than 10% in all cases and the mean intercept was not significantly different from zero. Table 16

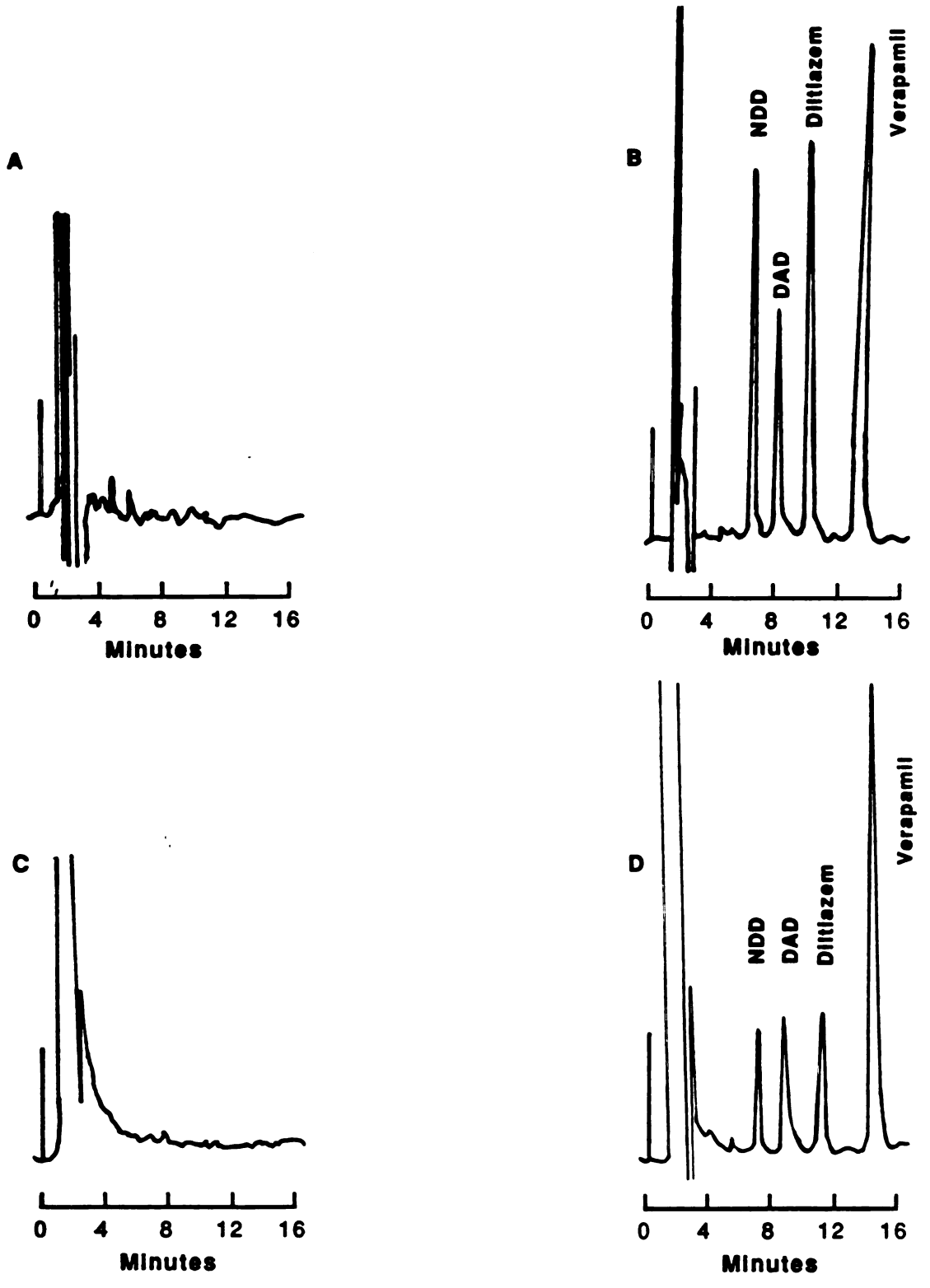

Figure 40. Representative chromatograms of blank plasma (A); plasma spiked with 100 ng of diltiazem, 75 ng of NDD and DAD, and 400 mg of verapamil (B); blank urine (C); and urine spiked with 50 ng of diltiazem, NDD and DAD and 400 mg of verapamil.

Table 15. Between-day precision of standard curves for diltiazem, NDD and DAD in plasma and urine from determinations on four different days

Compound	Mean Slope (± S.D.)	Mean Intercept[1] (± S.D.)	Mean Correlation Coefficient (r) (± S.D.)
Plasma			
Diltiazem	0.0077 (±0.0005)	-0.0102 (±0.0098)	0.9997 (±0.0003)
NDD	0.0105 (±0.0005)	-0.0105 (±0.0079)	0.9994 (±0.0005)
DAD	0.0061 (±0.0003)	-0.0099 (±0.0044)	0.9988 (±0.0004)
Urine			
Diltiazem	0.0087 (±0.0007)	-0.0400 (±0.0150)	0.9980 (±0.0004)
NDD	0.0081 (±0.0007)	-0.0258 (±0.0274)	0.9990 (±0.0001)
DAD	0.0067 (±0.0004)	-0.0125 (±0.0092)	0.9975 (±0.0020)

[1]Not significantly different from zero

shows the variability in the concentrations calculated from these standard curves. The coefficients of variation were less than or equal to 10% for all concentrations. The calculated concentrations for all three compounds were within 10% of the theoretical concentra-

Table 16. Accuracy and precision of the assay for diltiazem, NDD and DAD in plasma

Theoretical Concentration (ng/ml)	Mean Calculated Concentration (ng/ml)[1]	Coefficient of Variation (C.V.)	% Error
Diltiazem			
5	5.89	9.54	17.80
10	10.7	8.98	7.20
25	24.3	2.08	-2.93
50[2]	47.5	5.41	-5.08
100	100	2.27	0.49
200	201	2.48	0.54
300	300	1.22	-0.18
NDD			
5	5.67	9.74	13.30
10	10.3	5.17	3.30
25	23.3	4.53	-6.87
50	50.4	2.35	0.75
75	75.7	1.72	0.92
100	99.7	1.05	-0.34
DAD			
5	6.28	10.04	25.55
10	10.7	3.64	7.18
25	22.5	1.31	-9.91
50	50.4	3.75	0.72
75[2]	74.0	2.56	-1.32
100	101	1.43	0.86

[1]Mean of measurements on four different days

[2]Only three measurements were made

tions except for the 5 ng/ml concentration, which was somewhat overestimated.

In urine, the results were similar to plasma for NDD and DAD except for greater

variability in estimating the lowest concentration (Table 17). For diltiazem, there was a much greater overestimation of the 5 and 10 ng/ml concentrations. However, this did not affect the estimates of urine concentrations because the lowest concentration estimated in the clinical samples was 22.4 ng/ml.

The within-day variability in six replicate samples of 10 ng/ml and 100 ng/ml of diltiazem, NDD and DAD in plasma and urine was similar to the between-day variability, with coefficients of variation ranging from 0.92% to 10.59%. The average recoveries of 100 ng of diltiazem, NDD and DAD, and 400 ng of verapamil from 1 ml of plasma were 88.8%, 88.4%, 93.8% and 86.4%. The corresponding recoveries of the same amounts from 1 ml of urine were 83.2%, 54.0%, 84.5% and 92%.

Results of the Clinical Study

Subject Characteristics

A summary of subject characteristics for the six male volunteers included in the study is shown in Table 18. All subjects tolerated the 120 mg dose of diltiazem well. The only adverse effect noted was a headache, by subjects 1 and 2. In subject 1 the headache was mild and of short duration. In subject 2, who had the highest plasma concentrations of diltiazem among the six subjects, the headache required the administration of 500 mg of acetaminophen, nine hours after the dose of diltiazem had been given.

Pharmacokinetics

Plasma concentration-time profiles for diltiazem, NDD and DAD in each subject are shown in Figure 41. The measured concentrations are tabulated in Appendix K. The peak concentration of diltiazem ranged from 97.9 to 304 ng/ml and occurred between 1.5 and 4.25 hours after the dose. Peak concentrations of NDD and DAD ranged from 29.8 to 53.7 ng/ml and from 11.2 to 20.1 ng/ml, respectively, and occurred between 1.5 and 6 hours after the dose for NDD and between 3 and 6 hours after the dose for DAD. As has been demonstrated in recent studies, NDD is the major metabolite of diltiazem appearing in the plasma.

Table 17. Accuracy and precision of the assay for diltiazem, NDD and DAD in urine

Theoretical Concentration (ng/ml)	Mean Calculated Concentration (ng/ml)[1]	Coefficient of Variation (C.V.)	% Error
Diltiazem			
5	9.39	11.29	87.85
10	14.0	3.71	40.35
25	27.5	4.72	10.10
50	44.6[2]	5.68	-10.70
100	86.6	3.63	-13.38
200	205	2.19	2.59
300	301	0.86	0.42
NDD			
10	12.2	23.98	21.78
25	25.5	7.60	1.82
50	50.7	5.01	1.37
100	89.2[2]	3.32	-10.81
200	208	2.36	3.79
300	297	3.01	-1.15
400	401	1.28	0.16
DAD			
5	6.15	18.02	23.00
10	11.1	6.93	10.75
25	23.8	3.99	-4.78
50	47.0	5.05	-5.99
75	76.3	4.77	1.79
100	101	2.46	0.62

[1]Mean of measurements on four different days

[2]Only three measurements were made

Table 18. Summary of subject characteristics

Subject	Age	Weight (kg)	Height (cm)	Baseline Vital Signs BP[1]	HR[2]	MAP[3]
1 (D.S.)	26	75.5	179	117/76	64	83
2 (J.S.)	25	66.1	167	122/61	59	81
3 (J.D.)	22	95.1	192	119/66	56	85
4 (M.N.)	22	62.6	174	131/69	77	81
5 (L.K.)	40	70.6	177	115/79	53	86
6 (A.D.)	28	79.5	171	115/78	55	89

[1]Blood pressure (mm Hg)

[2]Heart rate (beats/min)

[3]Mean arterial pressure (mm Hg)

The half-lives estimated for diltiazem, NDD and DAD by model-independent methods are summarized in Table 19. When the concentration-time data for diltiazem were fit by various pharmacokinetic models, zero order input provided a better fit than first order input in five of six subjects. Therefore, for the purposes of comparison, zero order input was subsequently used to fit the data of all the subjects. No inferences about the mechanism of the absorption of diltiazem should be made from this procedure. In four out of six subjects, a one-compartment model provided the better fit of the data. In the other two subjects, the data were better fit by a two-compartment model. However, in all but one subject there was evidence of a second compartment. The curves of best fit are shown in Figure 42 and the model-dependent estimates of half-life are included in Table 19.

Table 20 shows the $AUC_{0\rightarrow 1440}$ and the $AUC_{0\rightarrow\infty}$, calculated by two methods, in six subjects. The values for $AUC_{0\rightarrow\infty}$ calculated by each method were similar in each individual, except in subject 6. AUC_{extrap} represented 0.5 to 83% of $AUC_{0\rightarrow\infty}$ using the model-dependent method of calculation and 3.7 to 10.5% of $AUC_{0\rightarrow\infty}$ using the model-

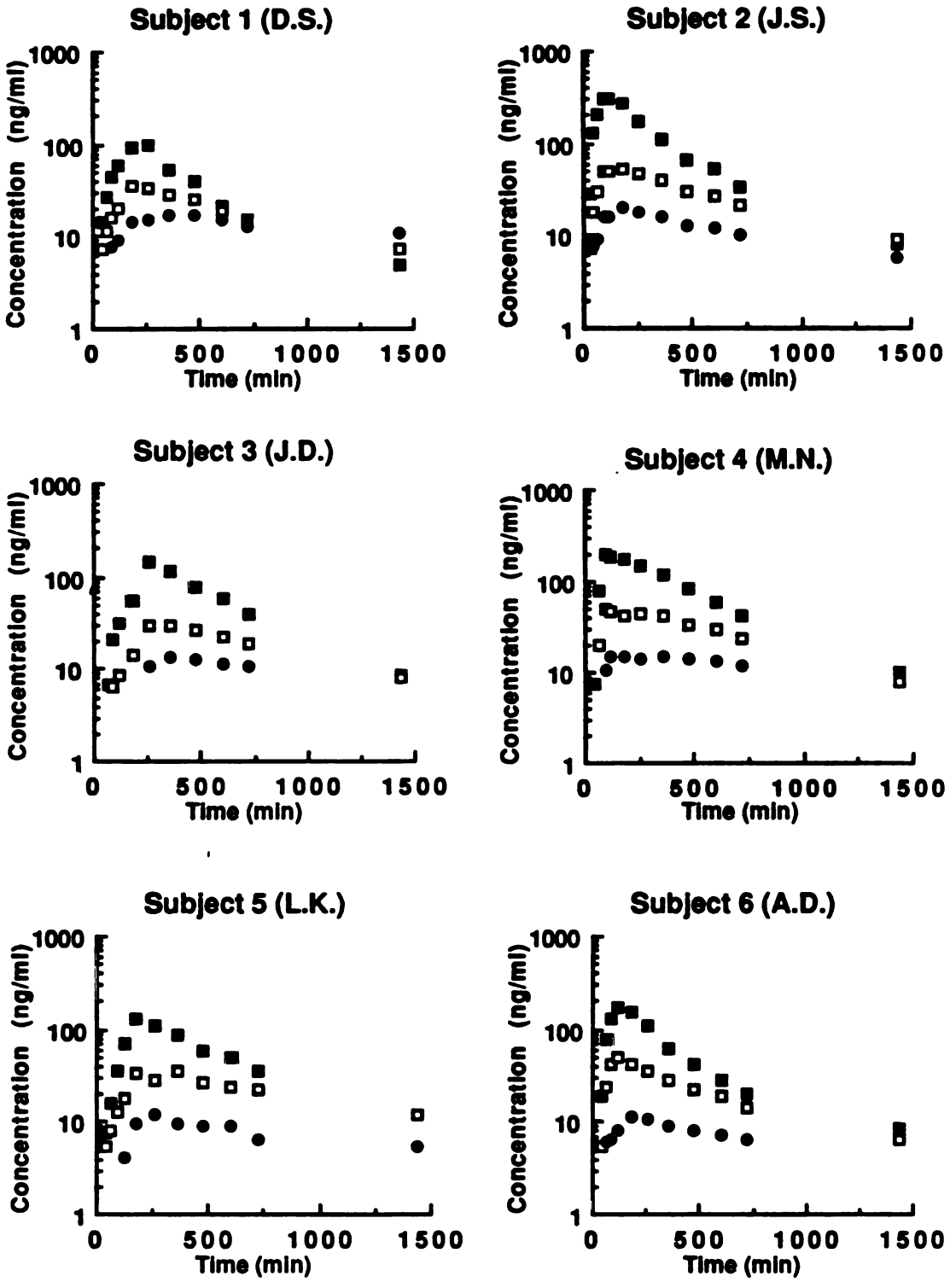

Figure 41. Semilogarithmic plots of the plasma concentrations of diltiazem (■), NDD (□) and DAD (●) *vs* time in each subject after administration of an oral dose of 120 mg of diltiazem.

Table 19. Half-lives of diltiazem, NDD and DAD

Subject	Diltiazem Half-Life[1] (h)	Diltiazem Half-Life[2] (h) (Model)[3]	NDD Half-Life[1] (h)	DAD Half-Life[1] (h)
1	6.7	3.0 (K01)	8.9	27.0
2	5.5	6.5 (K02)	8.3	12.6
3	5.3	5.0 (K01)	9.6	20.2
4	5.5	4.6 (K01)	7.7	15.8
5	7.2	5.0 (K01)	13.7	21.9
6	8.8	372 (K02)	8.3	10.5
Mean	**6.5**		**9.4**	**18.0**
S.D.	**1.4**		**2.2**	**6.2**

[1]Determined from linear regression analysis of the terminal portion of the ln concentration-time curve as 0.693/slope

[2]Determined from the estimate of λ_z from the nonlinear regression fit of the concentration-time data as $0.693/\lambda_z$

[3]K01 is a one-compartment model with zero order input; K02 is a two-compartment model with zero order input

independent method. The mean apparent oral clearance of diltiazem in the six subjects was 1728 ± 592 (S.D.) ml/min.

The total amounts of diltiazem, NDD and DAD excreted unchanged in the urine in 24 h (mean ± S.D. for the six subjects) were 2.71 ± 0.99 mg, 3.71 ± 0.82 mg and 0.25 ± 0.10 mg, representing 2.3%, 3.2% and 0.23% of the dose. These values probably do not represent the total amount that would be excreted at time infinity because the cumulative

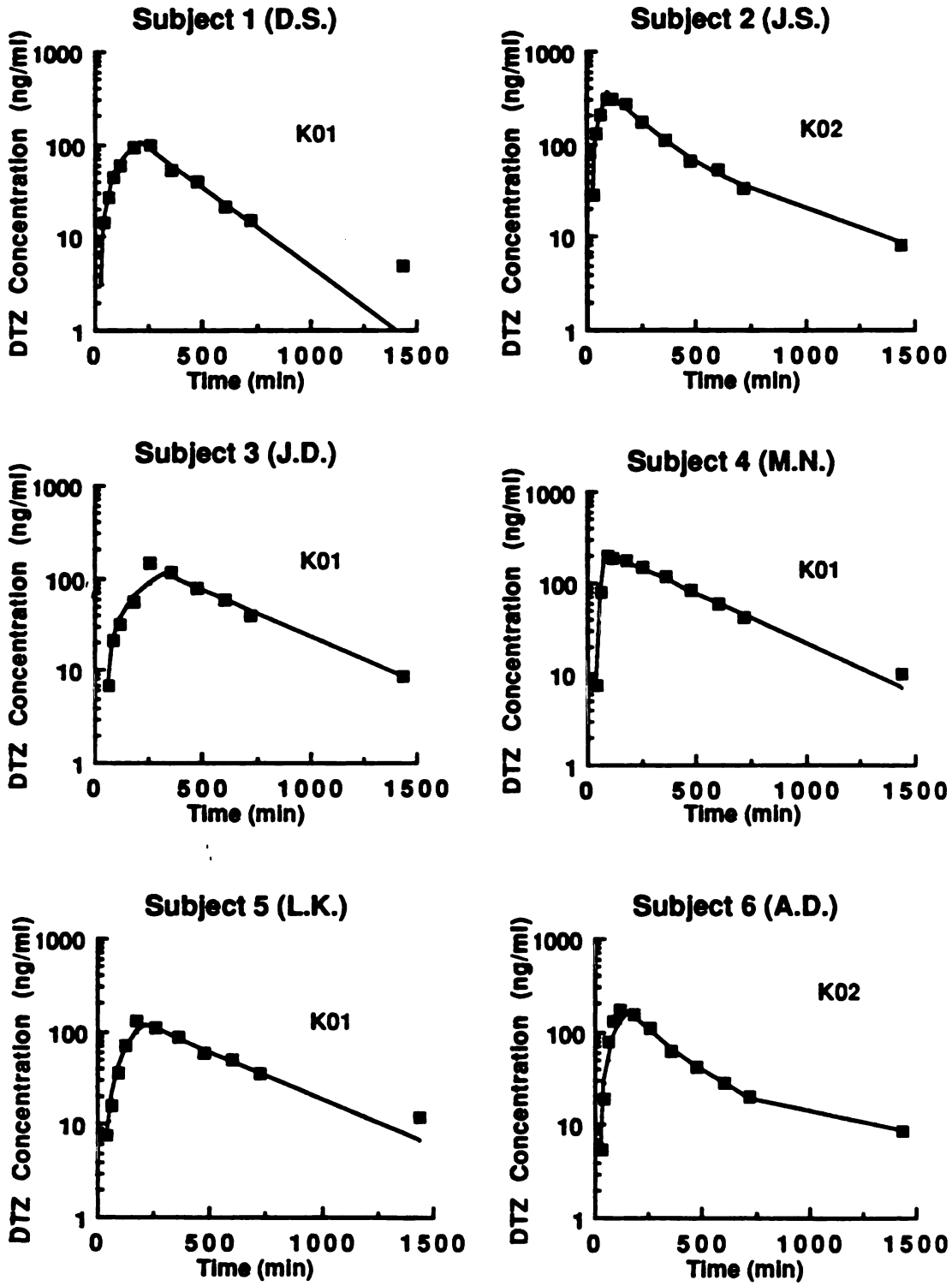

Figure 42. Semilogarithmic plots of the plasma concentrations of diltiazem (DTZ) *vs* time in each subject with the curves generated from the pharmacokinetic model of best fit. (K01 = one-compartment model, zero order input; K02 = two-compartment model, zero order input)

Table 20. Area under the diltiazem plasma concentration-time curve

Subject	$AUC_{0\rightarrow1440}$[1] (ng-min/ml)	$AUC_{0\rightarrow\infty}$[2] (ng-min/ml)	$AUC_{0\rightarrow\infty}$[3] (ng-min/ml)
1	40,146	40,368	42,923
2	103,847	108,613	107,825
3	65,490	69,185	69,497
4	90,974	93,812	95,693
5	64,106	67,035	71,664
6	59,910	345,139	66,577
Mean	**70,746**	**120,692**	**75,696**
S.D.	**22,936**	**112,453**	**22,996**

[1]Area under the curve from 0 to 1440 min calculated using the linear trapezoidal rule for increasing concentrations and the logarithmic trapezoidal rule for decreasing concentrations
[2]Area under the curve from 0 to infinity where the AUC from 1440 min to infinity was calculated as the concentration at 1440 min divided by the terminal elimination rate constant, both estimated from the model of best fit (Figure 42, Table 19)
[3]Area under the curve from 0 to infinity where the AUC from 1440 min to infinity was calculated as the measured concentration at 1440 min divided by the terminal elimination rate constant, estimated from linear regression of the terminal points (Table 19)

amount was still increasing at 24 h. The renal clearances of diltiazem, NDD, and DAD for each subject, calculated as the slope of the line from the least squares linear regression (forced through the origin) of plots of excretion rate into the urine *vs* plasma concentration at the midpoint of the urine collection interval, are shown in Table 21. The mean renal clearances for diltiazem, NDD and DAD (± S.D.) were 48.0 ± 15.9 ml/min, 152.4 ± 16.4 ml/min and 26.1 ± 9.5 ml/min, respectively. The values were very consistent between

Table 21. Renal clearances of diltiazem, NDD and DAD[1]

Subject	Diltiazem Renal Clearance (ml/min)	NDD Renal Clearance (ml/min)	DAD Renal Clearance (ml/min)
1	43.2	134.7	15.6
2	39.4	142.5	27.4
3	24.2	142.1	12.9
4	50.6	169.2	33.5
5	63.3	150.4	34.0
6	67.0	175.7	32.9
Mean	**48.0**	**152.4**	**26.1**
S.D.	**15.9**	**16.4**	**9.5**

[1]Obtained from the slope of the linear regression (forced through zero) of excretion rate *vs* the plasma concentration at the midpoint of the urine collection

individuals. Of note is the more than three-fold higher mean renal clearance of NDD compared to diltiazem and DAD. The detailed data on urine concentrations of diltiazem, NDD and DAD, and urine volume and pH for each subject are presented in Appendix K.

Plasma Protein Binding

The fractions unbound (fu) of diltiazem, NDD and DAD, corrected for volume shifts, for each subject, are shown in Table 22. Also shown is the fractional increase in the volume of the plasma compartment of the dialysis cell for each subject (δ), calculated from the protein concentration in the plasma samples before and after dialysis. The mean ($\pm$ S.D.) fu for diltiazem, NDD and DAD from all six subjects was 0.254 ($\pm$ 0.027), 0.323 ($\pm$ 0.035) and 0.230 ($\pm$0.021), respectively. When the concentrations of diltiazem were

Table 22. Unbound fraction (fu) of diltiazem, NDD and DAD in plasma from six subjects

Subject	fu Diltiazem	fu NDD	fu DAD	δ[1]
1	0.290[2]	0.300[3]	0.252	0.16
2	0.224	0.360	0.215	0.12
3	0.225	0.364	0.251	0.10
4	0.268	0.273	0.240	0.11
5	0.271	0.311	0.217	0.10
6	0.244	0.330	0.203	0.13
Mean	**0.254**	**0.323**	**0.230**	**0.12**
S.D.	**0.027**	**0.035**	**0.021**	**0.02**

[1] Fractional increase in the volume of the plasma compartment of the dialysis cell

[2] Values represent means of duplicates

[3] Value is the mean of triplicate samples

measured by HPLC after dialysis against pooled plasma, the mean fu (± S.D.) was 0.256 (±0.031). This value is in very close agreement with the value obtained using radiolabeled diltiazem, suggesting that [^{3}H]diltiazem was stable during the dialysis procedure. The mean recovery of [^{3}H]diltiazem from 12 dialysis cells was 84 ± 5%.

Determination of the unbound fraction of diltiazem and its metabolites allows the unbound renal clearances to be calculated as the renal clearance divided by fu. The unbound renal clearances of diltiazem, NDD and DAD for each subject are presented in Table 23. Although glomerular filtration rate (GFR) was not measured in these subjects, the

Table 23. Unbound renal clearances of diltiazem, NDD and DAD

Subject	Diltiazem Unbound Renal Clearance (ml/min)	NDD Unbound Renal Clearance (ml/min)	DAD Unbound Renal Clearance (ml/min)
1	149	449	62
2	176	396	127
3	108	390	51
4	189	620	140
5	234	484	157
6	275	532	162
Mean	**188**	**478**	**116**
S.D.	**60**	**88**	**48**

unbound renal clearance of NDD is approximately four fold greater then the average GFR for a 20 year old male (125 ml/min) demonstrating the NDD is eliminated by net renal secretion. Diltiazem also appears to actively secreted.

Pharmacodynamics

The values for heart rate, mean arterial pressure and PR interval obtained at each blood sampling time for each subject are listed in Appendix K. The measurements of heart rate, diastolic and systolic blood pressure, mean arterial pressure and the change in PR interval were plotted *vs* time for each subject. The change in PR interval was the only pharmacologic measurement that showed a change with time. When heart rate and mean arterial pressure were plotted against the total plasma concentration of diltiazem, there was no apparent positive or negative relationship.

However, when the change in PR interval was plotted against the plasma concentration of diltiazem, there was an obvious positive relationship. Furthermore, when the points on the plot were connected in chronological order, there was a prominent clockwise hysteresis in four out of six subjects (Subjects 1,3,4 and 5) (Figure 43). In the other two subjects, the connecting lines crossed over several times so that there were portions of both clockwise and counterclockwise hysteresis. Because of the time-dependence of this concentration-effect relationship, the traditional pharmacodynamic models cannot be applied to the data. Therefore, no further quantitative analysis was performed.

Discussion

Although the effectiveness of diltiazem in the therapy of angina pectoris and certain cardiac arrhythmias has been demonstrated, many questions remain unanswered about its pharmacokinetics and pharmacodynamics. The situation became more complex with the recent discovery of a new metabolite, NDD (Sugihara *et al.*, 1984), that is present in plasma along with DAD after oral administration of diltiazem (Goebel and Kölle, 1985; Montamat and Abernethy, 1987; Smith *et al.*, 1983). Although evidence of pharmacologic activity of NDD and DAD in animal studies has suggested possible pharmacologic effect in humans, no information is available on the influence of NDD and DAD on the pharmacokinetics or pharmacodynamics of diltiazem.

In the present study, both the pharmacokinetics and pharmacodynamics of diltiazem and these two metabolites, NDD and DAD, were studied in healthy adult subjects after a 120 mg oral dose. Administration of this high single dose and the use of a sensitive assay for diltiazem, NDD and DAD in both plasma and urine allowed us to monitor concentrations for 24 h after the dose. This enabled us to fully describe the pharmacokinetics of diltiazem, NDD and DAD, as much as is possible after an oral dose.

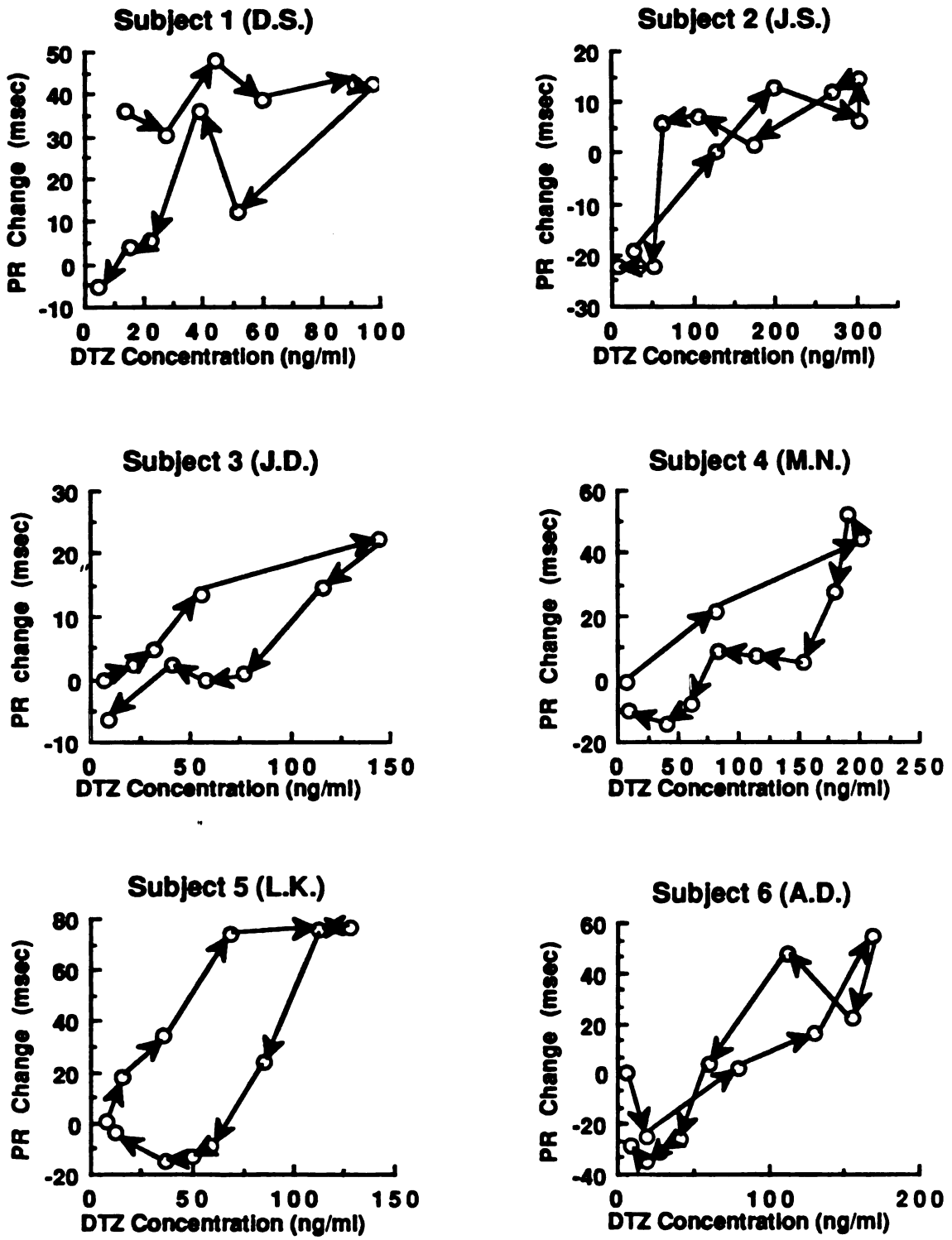

Figure 43. Plots of change in PR interval vs concentration of diltiazem (DTZ) for each of the six subjects. The direction of the arrows indicates the chronological order of the concentrations.

Pharmacokinetics

NDD achieved concentrations as high as 54 ng/ml and the concentrations declined more slowly than those of diltiazem, with a mean half-life of 9.4 h (Table 19). This value is in good agreement with previous estimates in the literature (Goebel and Kölle, 1985; Montamat and Abernethy, 1987). The half-life of DAD was longer than that of NDD, as reported previously (Goebel and Kölle, 1985; Montamat and Abernethy, 1987), but the mean value (18.0 h) was approximately two-fold greater. In this study, the concentrations of DAD in plasma were close to the lower limits of sensitivity of the assay, whereas in previous studies, estimates of the half-life of DAD were made after chronic oral dosing of diltiazem when the plasma levels of DAD were higher. Thus, it is possible that half-life values obtained in this study may be less reliable. Nevertheless, it appears that the half-lives of both metabolites are longer than the half-life of diltiazem and therefore the elimination of these metabolites is not formation rate limited (Rowland and Tozer, 1980).

Estimates of the half-life of diltiazem were very much dependent on the method of analysis of the data. Upon visual examination of the semilogarithmic plots of diltiazem concentration *vs* time, a slower terminal elimination rate constant was apparent at the later times in most cases (Figure 42). However, when the data were fit by one- and two-compartment models, the final points did not contribute much to the weighted sum of squares. As a result, a one-compartment model resulted in a significantly better fit than a two-compartment model, using the objective measure of the Schwartz criterion, in four of the six subjects. Therefore, use of the estimated elimination rate constant from a one-compartment fit to calculate the half-life resulted in a lower value than that obtained by linear regression of the final three points (Table 19). An even shorter half-life was estimated in these four subjects when a one-compartment model was used to fit the data and no weighting was used (results not shown). On the other hand, in the two subjects in which the data were better fit by a two-compartment model, a shorter half-life was obtained by linear regression of the final three points than from the parameter estimates. However, the problems associ-

ated with reliance only on objective measures of the best fit are illustrated by the data from subject 6. Although a two-compartment model provided a significantly better fit, the resulting half-life for the terminal phase is clearly excessive. (Figure 42, Table 19)

The results of our use of several different methods to estimate the half-life of diltiazem may help explain some of the variability in parameter estimates in the literature. The mean half-lives of diltiazem obtained from single dose studies reported in the literature have ranged from 3.1 to 11.2 h (Table 14, Chapter 6). The method of obtaining these estimates has been highly variable, and in many cases the specific details of the data analysis were not presented. Both model-independent and model-dependent methods have been used. Furthermore, one-, two- and three-compartment models have been used to describe diltiazem concentration-time data and to obtain estimates of the half-life using the terminal elimination rate constant from the equation of best fit.

The method of estimating half-life may also explain the apparent increase in half-life with chronic dosing found by Montamat and Abernethy (1987). They compared half-lives after chronic oral administration of diltiazem with half-lives after a single intravenous dose. The half-life after the intravenous dose was estimated using parameters from a compartmental fit of concentration-time data whereas the longer half-life estimated after chronic oral dosing was obtained by linear regression of the terminal portion of a plot of the logarithm of the concentration *vs* time. The differences were similar in magnitude to those we found by applying model-independent and model-dependent methods to our data (Table 19).

These considerations may also be important for clearance estimates of diltiazem obtained as a result of compartmental analysis. Even if the trapezoidal method is used to calculated the area under the curve (AUC), the extrapolated AUC from the final time point to infinity (AUC_{extrap}) is usually calculated using the final estimated time point from the equation of best fit, divided by the estimated terminal disposition rate constant. If multiple compartments are not detected, the extrapolated AUC, and therefore the total AUC ($AUC_{0\rightarrow\infty}$), may be underestimated and thus the clearance ($Cl = Dose/AUC_{0\rightarrow\infty}$) overesti-

mated when model-dependent methods are used. It is possible that at least two of the very high estimates for the clearance of diltiazem at variance with the estimated bioavailabilities (Hermann *et al.*, 1983; Schwartz and Abernethy, 1987) (Table 14, Chapter 6) might be explained in this way.

We calculated AUC_{extrap} by both model-dependent and model-independent methods (Table 20). In the four subjects whose plasma concentration-time data were fit by a one-compartment model, $AUC_{0\rightarrow\infty}$ was slightly lower when the model-dependent method was used. In the other two subjects, whose data were fit by a two-compartment model, $AUC_{0\rightarrow\infty}$ was higher using this method. In general, however, the estimates of $AUC_{0\rightarrow\infty}$ were similar using both methods. This was expected because we sampled for 24 hours and AUC_{extrap} represented only a small percentage of $AUC_{0\rightarrow\infty}$. However, in the studies of Hermann *et al.* (1983) and Schwartz and Abernethy (1987), plasma concentrations were measured for 12 hours and 9 to 10 hours, respectively, and it is not known what contribution AUC_{extrap} made to $AUC_{0\rightarrow\infty}$.

We also calculated the apparent oral clearance (Cl/F) of diltiazem using $AUC_{0\rightarrow\infty}$ determined by the model-independent method. The mean value of 1728 ± 592 (S.D.) ml/min agrees well with the apparent oral clearance after a single oral dose in young adults calculated from the data of Smith *et al.* (1983) (1191 ± 516 ml/min) and Kinney *et al.* (1981) (1524-1946 ml/min). However, the values for apparent oral clearance calculated from the data of Schwartz and Abernethy (1987), Fu *et al.* (1987) and Hermann *et al.* (1983) (based on a 70 kg person) were generally higher (mean values of 2478, 2742 and 4118 ml/min, respectively).

Although total clearance of diltiazem cannot be determined from data obtained after oral administration, an estimate of intrinsic hepatic clearance (Cl_i) can be obtained from the equation $AUC_{oral} = D/(Cl_i * fu)$, as described in Chapter 6. Using $AUC_{0\rightarrow\infty}$ calculated by model-independent methods (Table 20) and fu (Table 22) to calculate the apparent Cl_i in each subject, the mean apparent Cl_i is 6754 ± 1866 (S.D.) ml/min. As pointed out in

Chapter 6, however, the important assumptions made when using this equation are that diltiazem is completely absorbed intact from the gastrointestinal tract and that the blood to plasma concentration ratio for diltiazem is equal to 1. To test the second assumption, we carried out preliminary experiments in blood from three healthy volunteers. The results demonstrated that the mean ratio was not significantly different from 1, in agreement with the previous report in the literature (Kölle *et al.*, 1983).

The present study provides new information on the distribution and renal elimination of diltiazem and its two metabolites, NDD and DAD. Although previous metabolite studies have indicated that very little of a dose of diltiazem or either of these metabolites is excreted unchanged in the urine (Rovei *et al.*, 1980; Sugihara *et al.*, 1984), their concentrations have not been followed with time. The data presented here confirm that very little is excreted unchanged and the total amounts agree well with previous estimates. Because fu for each compound was determined in each subject, clearance by filtration could be calculated and compared to the total renal clearance. Although the creatinine clearances were not determined for these subjects, if one assumes an average value of glomerular filtration rate (GFR) of 125 ml/min for a 20 year old male, then the clearance of these compounds by filtration is equal to fu * GFR. Interestingly, the renal clearances of NDD and diltiazem exceeded clearance by filtration, indicating that they are excreted by net tubular secretion. The renal clearance of DAD, on the other hand, did not exceed clearance by filtration . Because renal excretion of unchanged drug represents such a minor elimination pathway for diltiazem, changes in renal function or competition for tubular transport would not be expected to have a significant effect on plasma concentrations of diltiazem. Pozet *et al.* (1983) observed no changes in the pharmacokinetics or effect of diltiazem in patients with GFRs less than 50% of normal. The percentage of a single 120 mg oral dose that was excreted in 24 hours as unchanged diltiazem in these patients was 1.35%, slightly less than what we observed. It is not known if either NDD or DAD concentrations would be sensitive to changes in renal function because the relative contributions of further metabolism

and renal excretion to the elimination of the metabolites are unknown.

The fu of diltiazem determined in this study (mean, 0.254) was within the range of values reported in the literature. The extent of plasma protein binding of NDD and DAD at 37° has not previously been reported. The fu of DAD was slightly lower than that of diltiazem (0.230 vs 0.254), consistent with previous reports obtained at 22° C (Morselli *et al.*, 1978). The fu of NDD (0.323), on the other hand, was higher than that of diltiazem. Consideration of the relative unbound concentrations of these metabolites in plasma may become important in determining the contribution of these metabolites to the effect of diltiazem.

Pharmacodynamics

The pharmacodynamic data were of particular interest. Significant effects on AV conduction were observed in all subjects as manifested by the prolonged PR interval. This appears to be a direct effect of the treatment. There is a known inverse relationship between heart rate and PR interval (Carruthers *et al.*, 1987), and diltiazem could have indirectly increased the PR interval by decreasing heart rate. However, no effect on heart rate or blood pressure could be discerned in any of the subjects.

Of note is the clockwise hysteresis observed in four of six subjects. This is an indication of decreasing effect with time for the same concentration of diltiazem. Previously, only a counterclockwise hysteresis has been noted after an intravenous dose of diltiazem (Ellenbogen *et al.*, 1986; Joyal *et al.*, 1986; Smith *et al.*, 1983). Counterclockwise hysteresis is usually an indication of a delay before equilibrium between plasma concentrations and concentrations at the site of the effect is reached (Holford and Sheiner, 1982).

There are a number of possible explanations for the clockwise hysteresis observed here in four of the six subjects as proposed by Holford and Sheiner (1982). These include: 1) tolerance to the effect of diltiazem, 2) arterio-venous differences in time to equilibrium with drug concentrations at the effect site (Stanski *et al.*, 1984), and 3) the presence of an inhibitory metabolite and an increase in the metabolite to parent concentration ratio with

time.

Without further study, it is not possible to determine which mechanism is responsible for the time-dependence we observed. Tolerance to the conduction effects of diltiazem has not been previously reported. Compensating physiological mechanisms that could lead to tolerance would be expected if diltiazem had decreased blood pressure and therefore indirectly increased heart rate, but this was not the case. The arterio-venous equilibrium differences normally would be expected to result in time-dependence over short intervals, but the hysteresis we observed was produced over a period of many hours.

The possibility that one or both of the metabolites may have an inhibitory action on the electrophysiologic effect of diltiazem is intriguing. *In vivo* and *in vitro* studies in animal tissues suggested that these compounds have equal or lower hemodynamic activity than diltiazem (Cavero *et al.*, 1979; Narita *et al.*, 1986; Yabana *et al*, 1985). However, these relative potency determinations were based on doses and it is not known how their potencies compare when unbound concentrations producing an effect are compared. Furthermore, there has been no study of their comparative electrophysiologic effects *in vitro* or *in vivo*. Although the concentrations of NDD and DAD appear to follow the concentrations of diltiazem (Figure 42), in fact, the ratios of the unbound concentration of metabolite to unbound concentration of diltiazem increase with time. Therefore, it is possible that one or both are reducing the effect of diltiazem on AV conduction either by competing for receptor sites and having no or only partial calcium channel blocking activity, or by having calcium channel agonist activity. Clearly, to determine if one of these possibilities provides the explanation for the time-dependence of the effect of diltiazem after a single oral dose, further *in vitro* and *in vivo* studies are necessary in which the metabolites are studied separately.

In summary, this study has demonstrated that two metabolites of diltiazem, NDD and DAD, reach significant plasma levels after a single oral dose of diltiazem. Furthermore, all three compounds are bound to plasma proteins to a similar extent. Although representing only a minor pathway of elimination for diltiazem, all three compounds are

excreted unchanged in the urine and both NDD and diltiazem are excreted by net tubular secretion. Of particular interest was the finding that diltiazem has a significant inhibitory effect on AV conduction in healthy young adults and that this effect is related to the plasma concentrations of diltiazem. However, the concentration-effect relationship exhibits a clockwise hysteresis. A number of mechanisms could explain this observation. One possibility of particular interest is that either NDD or DAD, or both, have an effect that is antagonistic to the effect of diltiazem. To explore this hypothesis, both *in vitro* and *in vivo* studies of the electrophysiologic effects of these metabolites in the presence and absence of diltiazem are necessary.

CHAPTER 8

Summary and Conclusions

The class of drugs known as calcium channel blockers is an important new addition to the therapy of cardiovascular disease. The discovery that the effects of these compounds are elicited by a unique mechanism involving inhibition of calcium influx into myocardial and vascular smooth muscle cells (Fleckenstein, 1977) generated much interest. Subsequently, calcium channel blockers have also become important tools to study the role of calcium in the control of a wide variety of cellular events.

Considerable effort has been spent to determine the mechanism and site of action of these compounds. At the time this work began, the 1,4-dihydropyridine class of calcium channel blockers was of particular interest because a high affinity binding site for these compounds had been identified in various animal tissues. This finding suggested that their effect was mediated through a specific receptor. Additional evidence from *in vitro* pharmacologic response studies supported this hypothesis in smooth muscle (Bolger *et al.*, 1983) but it was not clear that the high affinity binding site identified in myocardium was a receptor. In the first part of this dissertation, we carried out studies to address specific questions related to the site and mechanism of action of the 1,4-dihydropyridine calcium channel blockers in myocardium.

In the second part of the dissertation we addressed questions regarding the pharmacokinetics and pharmacodynamics of diltiazem, a representative compound from another chemical class of calcium channel blockers, the benzothiazepines. Despite the fact that diltiazem has been used clinically for a decade, information about its pharmacokinetics and pharmacodynamics is limited and often contradictory. Furthermore, a potential complicating factor is the relatively recent discovery of a potentially active metabolite (Sugihara *et al.*, 1984; Yabana *et al.*, 1985) that appears in the plasma after oral administration of dil-

tiazem. The pharmacokinetics of this metabolite and another major metabolite, DAD, have not been well described. In addition, it is not known if these metabolites contribute to the pharmacologic effect of diltiazem.

A summary of the major findings of this dissertation are presented in the following sections.

Comparison of Binding Affinities and Negative Inotropic Potencies of the 1,4-Dihydropyridine Calcium Channel Blockers in Rabbit Myocardium

To address the question of whether the high affinity binding site for the 1,4-dihydropyridine calcium channel blockers is a receptor, based on classical receptor theory, we compared the binding affinities and potencies of negative inotropic response for a series of twelve 1,4-dihydropyridine analogues in rabbit myocardium. Binding affinities were determined as the IC_{50} for displacement of the radiolabeled 1,4-dihydropyridine compound, [^{3}H]nitrendipine, from binding sites in isolated membrane particulates from rabbit myocardium. The negative inotropic response was measured in isolated contracting right ventricular papillary muscles from the rabbit heart and expressed as the IC_{50}. A statistically significant rank order correlation between binding affinities and potencies of inhibitory response was obtained, but the absolute values of the potencies of response were consistently lower than the binding affinities by one to three orders of magnitude. These results confirmed the discrepancy that had been reported for a few of these compounds and extended the finding to many more compounds.

Among the most likely theories that could explain this discrepancy are: 1) a low affinity binding site is the receptor and 2) the activity of these compounds is governed by the modulated receptor hypothesis and therefore binding affinity is higher in depolarized, disrupted membranes than in intact, polarized cells. We examined the binding of [^{3}H]nitrendipine at high concentrations, but did not observe a low affinity binding site. Although there is considerable evidence from electrophysiologic studies in support of the modulated

receptor hypothesis (Bean, 1984; Hamilton *et al.*, 1987; Sanguinetti and Kass, 1984a, Uehara and Hume, 1985), and our data were clearly consistent with this hypothesis, we could not confirm that it provided the explanation for our results.

Three compounds demonstrated a much weaker inotropic effect, relative to their binding affinities, than the other compounds. Structural features that may favor this very low myocardial activity were identified. These included the presence of a meta nitro substituent on the phenyl ring and/or the size of the ester substituents. Two of these three compounds also were very potent in relaxing vascular smooth muscle (Gordon *et al.*, 1986) and thus demonstrated the greatest degree of vascular smooth muscle selectivity among this group of 1,4-dihydropyridines.

Species Differences in the Negative Inotropic Response of 1,4-Dihydropyridine Calcium Channel Blockers in Myocardium

Myocardial excitation-contraction coupling is known to be different in different species (Bers, 1985). In particular, there is considerable evidence that rat myocardium differs from other mammalian myocardium in that : 1) it exhibits a negative force-frequency relationship, whereas a positive relationship exists for most other mammals, and 2) its action potential is of a shorter duration (Forester and Mainwood, 1974). These differences between the rat and other animals may arise because of a greater dependence on intracellular stores of calcium than on influx of extracellular calcium for contraction.

To address the question of whether there are differences between rat and other mammalian species in the activity of the 1,4-dihydropyridine calcium channel blockers, we carried out binding and response experiments similar to those done in rabbit myocardium and the results from the two species were compared. The negative inotropic effect of these compounds was significantly lower in rat myocardium and the slope of the concentration-response curves was significantly more shallow. These differences were not due to a difference in the high affinity binding site and we did not observe a low affinity binding site in

rat myocardium. Three further hypotheses could explain the data. The first is that the modulated receptor hypothesis is operational and less effect is observed in rat myocardium because of its abbreviated action potential and the correspondingly short time the rat myocardial cells spend in the depolarized, high affinity state. This hypothesis predicts that higher concentrations of 1,4-dihydropyridine compounds would be necessary to elicit an effect in rat myocardial cells than in cells that were depolarized for longer periods.

The second hypothesis is that the rat myocardium is less dependent on influx of calcium for contraction so that inhibition of calcium influx would have minimal effect on the force of contraction. Although we found that the steady state contractions in both rat and rabbit myocardium were equally dependent on the concentration of extracellular calcium, it could not be determined if this calcium was directly or indirectly responsible for contraction and therefore if contraction would be sensitive to inhibition of calcium influx.

Finally, it is possible that these agents possess agonistic as well as antagonistic effects and the agonist potency (relative to antagonist potency) is greater in rat than in rabbit myocardium. Although we could not distinguish among these hypotheses to explain our results, the data illustrate the importance of considering species differences when examining the effect of calcium channel blockers.

Characterization of Affinity Labels for the 1,4-Dihydropyridine Calcium Channel Blocker Receptor

Although receptor binding and pharmacologic response studies can provide much information on the mechanism and site of action of the 1,4-dihydropyridine calcium channel blockers, in order to fully understand the molecular mechanism of action it is necessary to isolate and characterize the macromolecules to which these compounds bind. One approach is the use of affinity labels, analogue compounds that covalently bind to the receptor and that can be radiolabeled to allow the isolation and further characterization of the receptor molecule.

Our objective in these studies was to use affinity labels to obtain information on the molecular characteristics of the 1,4-dihydropyridine receptor in myocardium. We first carried out experiments to determine if the compound, GK-III-120D, an azido derivative of nifedipine, was a specific high affinity photoaffinity label for the 1,4-dihydropyridine receptor. The compound was incubated with rat myocardial particulates, exposed to UV or visible light, and the maximum number of specific binding sites for [^{3}H]nitrendipine was determined and compared against various control preparations. After extensive study, it was concluded that GK-III-120D did not covalently bind to 1,4-dihydropyridine sites to an appreciable extent. After UV exposure, any reduction of specific binding could be attributed to a combination of a direct destructive effect of the UV radiation and incomplete washing out of noncovalently bound compound. Visible light appeared to photoactivate the compound in solution, but failed to cause any loss of specific [^{3}H]nitrendipine binding when GK-III-120D was exposed in the presence of tissue. The most probable explanation for the lack of covalent binding was that GK-III-120D, in addition to being photoactivated, was degraded to the nitrosopyridine derivative, which has a very low affinity for the binding site. Thus the compound was removed too rapidly for covalent binding to occur. Consequently, GK-III-120D was not a suitable compound with which to carry out isolation studies.

We then decided to use a chemoaffinity label analogue of the 1,4-dihydropyridine compounds in an attempt to isolate the 1,4-dihydropyridine receptor in rat myocardium. The compound was a radiolabeled isothiocyanate 1,4-dihydropyridine derivative (*o*-NCS) that had been reported to covalently bind to the 1,4-dihydropyridine binding site in ileal, myocardial and skeletal muscle (Horne *et al.*, 1984; Kirley and Schwartz, 1984; Venter *et al.*, 1983). We incubated this compound with rat myocardial membrane particulates and carried out SDS-PAGE gel electrophoresis to isolate and characterize the macromolecule to which the chemoaffinity label was attached.

The results from these experiments indicated that no radioactivity was associated

with any of the bands in the electrophoresis lanes. We therefore investigated whether *o*-NCS was actually covalently binding by carrying out dissociation experiments. From preliminary experiments, it appeared that the addition of a high concentration of nifedipine to an incubation mixture of *o*-NCS in myocardial membrane particulates resulted in dissociation of *o*-NCS, with a half-life of less than 20 min. Subsequent reports in the literature confirmed our preliminary findings that *o*-NCS does not appear to covalently bind to the 1,4-dihydropyridine binding site (Ferry *et al.*, 1986; Greenberg *et al.*, 1985; Kozlowski *et al.*, 1986).

It appears that in theory, the use of affinity labels would be a useful method to isolate the specific macromolecule to which the 1,4-dihydropyridine compounds bind. Unfortunately, it appears that a suitable affinity label has yet to be developed for the 1,4-dihydropyridine receptor. Consequently, our planned molecular characterization studies were abandoned.

The Pharmacokinetics and Pharmacodynamics of Diltiazem and its Metabolites in Healthy Adults after a Single Oral Dose

To address some of the unanswered questions regarding the pharmacokinetics and pharmacodynamics of diltiazem and its two metabolites, NDD and DAD, a clinical study was conducted in which six healthy male subjects received a 120 mg oral dose of diltiazem. Concentrations of diltiazem, NDD and DAD were measured in plasma and urine collected at specified intervals for 24 hours after the dose and measures of pharmacologic response were obtained at each blood sampling time. In addition, plasma protein binding studies were carried out to determine the unbound fraction for each of these compounds in each subject.

We demonstrated that the plasma concentration-time profile of diltiazem exhibited two-compartment characteristics, although this model did not provide the best fit of the data in most cases. Therefore, differences between estimates of diltiazem half-life determined

by model-dependent and model-independent methods occurred and these results may help explain some of the inconsistencies in the estimated parameters reported in the literature.

The renal elimination of diltiazem, NDD and DAD has been characterized for the first time. Although the amount of each compound excreted unchanged in the urine is small, we were able to obtain good estimates of renal clearance. Both NDD and diltiazem were eliminated by net renal secretion whereas the renal clearance of DAD did not exceed clearance by filtration.

The estimate of unbound fraction that we obtained for diltiazem is in good agreement with values reported in the literature. In addition, we demonstrated that both NDD and DAD are bound to plasma proteins, with unbound fractions similar to that of diltiazem.

No significant effect of diltiazem on blood pressure or heart rate was noted in this study. However, a prolongation of the PR interval was noted in all six subjects. Furthermore, temporal changes were observed for the concentration-effect relationship, resulting in an apparent clockwise hysteresis in four of six subjects when change in PR interval was plotted against diltiazem concentration. Such a phenomenon suggests that some form of tolerance develops. This could occur as a result of changes in receptors, the effects of physiologic homeostatic reflex mechanisms, or the presence of inhibitory metabolites (Holford and Sheiner, 1982). Although we could not determine which mechanism was responsible, the present results provide an interesting focus for further research.

Although many questions remain to be answered regarding the site and mechanism of action of the 1,4-dihydropyridine calcium channel blockers in myocardium, the studies in this dissertation have contributed to our understanding of how binding to the high affinity site in myocardium is related to pharmacological effect of these compounds. In addition, knowledge of the species differences in the activity of these compounds may help us to better understand their mechanism of action. The results of the clinical study carried out as part of this dissertation have contributed to the body of knowledge about the pharmaco-

kinetics of diltiazem and have added important new information related to the relationship between plasma concentrations and electrophysiologic effects.

References

Ames GF-L: Resolution of bacterial proteins by polyacrylamide gel electrophoresis on slabs. Membrane, soluble and periplasmic fractions. J Biol Chem **249**: 634-644, 1974.

Antman EM, Stone PH, Muller JE and Braunwald E: Calcium channel blocking agents in the treatment of cardiovascular disorders. Part I: Basic and clinical electrophysiologic effects. Ann Intern Med **93**: 875-885, 1980.

Balwierczak JL, Johnson CL and Schwartz A: The relationship between the binding site of [^{3}H]*d-cis*-diltiazem and that of other non-dihydropyridine calcium entry blockers in cardiac sarcolemma. Mol Pharmacol **31**: 175-179, 1987.

Balwierczak JL and Schwartz A: Specific binding of [^{3}H]*d-cis*-diltiazem to cardiac sarcolemma and its inhibition by calcium. Eur J Pharmacol **116**: 193-194, 1985.

Bauer LA, Stenwall M, Horn JR, Davis R, Opheim K and Greene L: Changes in antipyrine and indocyanine green kinetics during nifedipine, verapamil, and diltiazem therapy. Clin Pharmacol Ther **40**: 239-242, 1986.

Bayley H and Knowles JR: Photoaffinity labeling. Methods Enzymol **46**: 69-114, 1977.

Bean BP: Nitrendipine block of cardiac calcium channels: high-affinity binding to the inactivated state. Proc Natl Acad Sci USA **81**: 6388-6392, 1984.

Bellemann P, Ferry D, Lubbecke F and Glossmann H: [^{3}H]Nitrendipine, a potent calcium antagonist, binds with high affinity to cardiac membranes. Arzneim Forsch **31**: 2064-2067, 1981.

Bellemann P, Schade A and Towart R: Dihydropyridine receptor in rat brain labeled with [^{3}H]nimodipine. Proc Natl Acad Sci USA **80**: 2356-2360, 1983.

Bennett JP Jr and Yamamura HI: Neurotransmitter, hormone, or drug receptor binding methods, in Yamamura HI, Enn SJ, and Kuhar MJ (eds.), Neurotransmitter Receptor Binding, 2nd ed., Raven Press, New York, 1985, p. 61-89.

Bers DM: Ca influx and sarcoplasmic reticulum Ca release in cardiac muscle activation during postrest recovery. Am J Physiol **248**: H366-H381, 1985.

Berson JA and Brown E: Studies on dihydropyridines. II. The photochemical disproportionation of 4-(2'-nitrophenyl)-1,4-dihydropyridines. J Am Chem Soc **77**: 447-450, 1955.

Bighley LD, Dimmitt DC and McGraw BF: Bioavailability of diltiazem hydrochloride formulations. Clin Res **28**: 587A, 1980.

Bloedow DC, Piepho RW, Nies AS and Gal J: Serum binding of diltiazem in humans. J Clin Pharmacol **22**: 201-205, 1982.

Bodem R and Sonnenblick EH: Mechanical activity of mammalian heart muscle: variable onset, species differences, and the effect of caffeine. Am J Physiol **228**: 250-261, 1975.

Bolger GT, Gengo P, Klockowski R, Luchowski E, Siegel H, Janis RA, Triggle AM and Triggle DJ: Characterization of binding of the Ca^{++} channel antagonist, [^{3}H]nitrendipine, to guinea-pig ileal smooth muscle. J Pharmacol Exp Ther **225**: 291-309, 1983.

Bolger GT, Gengo PJ, Luchowski EM, Siegel H, Triggle DJ and Janis RA: High affinity binding of a calcium channel antagonist to smooth and cardiac muscle. Biochem Biophys Res Commun **104**: 1604-1609, 1982.

Borsotto M, Barhanin J, Fosset M and Lazdunski M: The 1,4-dihydropyridine receptor associated with the skeletal muscle voltage-dependent Ca^{2+} channel. J Biol Chem **260**: 14255-14263, 1985.

Borsotto M, Barhanin J, Norman RI and Lazdunski M: Purification of the dihydropyridine receptor of the voltage-dependent Ca^{2+} channel from skeletal muscle transverse tubules using (+) [^{3}H]PN 200-110. Biochem Biophys Res Commun **122**: 1357-1366, 1984a.

Borsotto M, Norman RI, Fosset M and Lazdunski M: Solubilization of the nitrendipine

receptor from skeletal muscle transverse tubule membranes. Interactions with specific inhibitors of the voltage-dependent Ca^{2+} channel. Eur J Biochem **142**: 449-455, 1984b.

Bossert F: The chemistry of nifedipine, in Lochner W, Braasch W and Kroneberg G (eds.): 2nd International Adalat Symposium, Springer-Verlag, New York, 1975, p. 20-26.

Bossert F, Meyer H and Wehinger E: 4-Aryldihydropyridines, a new class of highly active calcium antagonists. Angew Chem Int Ed Engl **20**: 762-769, 1981.

Bristow MR, Ginsburg R, Laser JA, McAuley BJ and Minobe W: Tissue response selectivity of calcium antagonists is not due to heterogeneity of [^{3}H]-nitrendipine binding sites. Br J Pharmacol **82**: 309-320, 1984.

Brown AM, Kunze DL and Yatani A: Dual effects of dihydropyridines on whole cell and unitary calcium currents in single ventricular cells of guinea-pig. J Physiol **379**: 495-514, 1986.

Burt DR: Criteria for receptor identification, in Yamamura HI, Enn SJ, and Kuhar MJ (eds.), Neurotransmitter Receptor Binding, 2nd ed., Raven Press, New York, 1985, p. 41-60.

Campbell KP, Lipshutz GM and Denney GH: Direct photoaffinity labeling of the high affinity nitrendipine-binding site in subcellular membrane fractions isolated from canine myocardium. J Biol Chem **259**: 5384-5387, 1984.

Carrum G, Egan JM and Abernethy DR: Diltiazem treatment impairs hepatic drug oxidation: studies of antipyrine. Clin Pharmacol Ther **40**: 140-143, 1986.

Carruthers SG, McCall B, Cordell BA and Wu R: Relationships between heart rate and PR interval during physiological and pharmacological interventions. Br J Clin Pharmacol **23**: 259-265, 1987.

Catterall WA: The emerging molecular view of the sodium channel. Trends Neurosci **5**: 303-306, 1982.

Cauvin C, Loutzenhiser R and Van Breemen C: Mechanisms of calcium antagonist-induced vasodilation. Ann Rev Pharmacol Toxicol **23**: 373-396, 1983.

Cavalla D and Neff NH: Chemical mechanisms for photoaffinity labeling of receptors. Biochem Pharmacol **34**: 2821-2826, 1985.

Cavero I, Boudet JP, Lefèvre-Borg F and Roach AG: Pharmacological evaluation of diltiazem and its desacetylated metabolite in several animal species, in Bing RJ (ed.), New Drug Therapy with a Calcium Antagonist - Diltiazem, Excerpta Medica, Amsterdam, 1979, p. 61-88.

Chaffman M and Brogden RN: Diltiazem. A review of its pharmacological properties and therapeutic efficacy. Drugs **29**: 387-454, 1985.

Cheng Y-C and Prusoff WH: Relationship between the inhibition constant (K_I) and the concentration of inhibitor which causes 50 per cent inhibition (I_{50}) of an enzymatic reaction. Biochem Pharmacol **22**: 3099-3108, 1973.

Chin JH: Differential sensitivity of calcium channels to dihydropyridines. Biochem Pharmacol **35**: 4115-4120, 1986.

Clozel JP, Caillé G, Taeymans Y, Théroux P, Biron P and Trudel F: High-performance liquid chromatographic determination of diltiazem and six of its metabolites in human urine. J Pharm Sci **73**: 771-773, 1984.

Cooper CL, Vandaele S, Barhanin J, Fosset M, Lazdunski M and Hosey MM: Purification and characterization of the dihydropyridine-sensitive voltage-dependent calcium channel from cardiac tissue. J Biol Chem **262**: 509-512, 1987.

Creese I and Snyder SH: Receptor binding and pharmacological activity of opiates in the guinea-pig intestine. J Pharmacol Exp Ther **194**: 205-219, 1975.

Curtis BM and Catterall WA: Solubilization of the calcium antagonist receptor from rat brain. J Biol Chem **258**: 7280-7283, 1983.

Curtis BM and Catterall WA: Purification of the calcium antagonist receptor of the voltage-sensitive calcium channel from skeletal muscle transverse tubules. Biochemistry

23: 2113-2118, 1984.

Curtis BM and Catterall WA: Reconstitution of the voltage-sensitive calcium channel purified from skeletal muscle transverse tubules. Biochemistry **25**: 3077-3083, 1986.

De Lean A, Munson PJ and Rodbard D: Simultaneous analysis of families of sigmoidal curves: application to bioassay, radioligand assay, and physiological dose-response curves. Am J Physiol **235**: E97-E102, 1978.

DePover A, Grupp IL, Grupp G and Schwartz A: Diltiazem potentiates the negative inotropic action of nimodipine in heart. Biochem Biophys Res Commun **114**: 922-929, 1983.

DePover A, Matlib MA, Lee SW, Dubé GP, Grupp IL, Grupp G and Schwartz A: Specific binding of [^{3}H]nitrendipine to membranes from coronary arteries and heart in relation to pharmacologic effects. Paradoxical stimulation by diltiazem. Biochem Biophys Res Commun **108**: 110-117, 1982.

Doble A, Benavides J, Ferris O, Bertrand P, Menager J, Vaucher N, Burgevin MC, Uzan A, Gueremy C and Le Fur G: Dihydropyridine and peripheral type benzodiazepine binding sites: subcellular distribution and molecular size determination. Eur J Pharmacol **119**: 153-167, 1985.

Ebel VS, Schütz H and Hornitschek A: Untersuchungen zur Analytik von Nifedipin unter besonderer Berücksichtigung der bei Lichtexposition entstehenden Umwandlungsprodukte. Arzneim Forsch **28**: 2188-2193, 1978.

Echizen H and Eichelbaum M: Clinical pharmacokinetics of verapamil, nifedipine and diltiazem. Clin Pharmacokinet **11**: 425-449, 1986.

Ehlert FJ, Roeske WR, Itoga E and Yamamura HI: The binding of [^{3}H]nitrendipine to receptors for calcium channel antagonists in the heart, cerebral cortex, and ileum of rats. Life Sci **30**: 2191-2202, 1982.

Eisner U and Kuthan J: The chemistry of dihydropyridines. Chem Rev **72**: 1-42, 1972.

Ellenbogen KA, Roark SF, Smith MS, McCarthy EA, Bjornsson TD, Pritchett ELC:

Effects of sustained intravenous diltiazem infusion in healthy persons. Am J Cardiol **58**: 1055-1060, 1986.

Fabiato A and Fabiato F: Calcium-induced release of calcium from the sarcoplasmic reticulum of skinned cells from adult human, dog, cat, rabbit, rat, and frog hearts and from fetal and new-born rat ventricles. Ann NY Acad Sci **307**: 491-522, 1978.

Fedan JS, Hogaboom GK and O'Donnell JP: Photoaffinity labels as pharmacological tools. Biochem Pharmacol **33**: 1167-1180, 1984.

Feld G and Singh: Diltiazem: pharmacologic properties and therapeutic uses. Hosp Formul **20**: 814-821, 1985.

Ferry DR and Glossmann H: Identification of putative calcium channels in skeletal muscle microsomes. FEBS Lett **148**: 331-337, 1982.

Ferry DR, Goll A and Glossmann H: Calcium channels: evidence for oligomeric nature by target size analysis. EMBO J **2**: 1729-1732, 1983a.

Ferry DR, Goll A and Glossmann H: Putative calcium channel molecular weight determination by target size analysis. Naunyn-Schmiedeberg's Arch Pharmacol **323**: 292-297, 1983b.

Ferry DR, Goll A and Glossmann H: (-)-[^{3}H]Azidopine is a specific, irreversible label for heart calcium channels - a [^{3}H]isothiocyanate 1,4 dihydropyridine is not. Naunyn-Schmiedeberg's Arch Pharmacol **334** (Suppl): R27, 1986.

Ferry DR, Kämpf K, Goll A and Glossmann H: Subunit composition of skeletal muscle transverse tubule calcium channels evaluated with the 1,4-dihydropyridine photoaffinity probe, [^{3}H]azidopine. EMBO J **4**: 1933-1940, 1985.

Ferry DR, Rombusch M, Goll A and Glossmann H: Photoaffinity labelling of Ca^{2+} channels with [^{3}H]azidopine. FEBS Lett **169**: 112-118, 1984.

Finch MB and Johnston GD: The peripheral vascular effects of diltiazem – dose-response characteristics. Br J Clin Pharmacol **20**: 447-451, 1985.

Fleckenstein A: Specific pharmacology of calcium in myocardium, cardiac pacemakers,

and vascular smooth muscle. Ann Rev Pharmacol Toxicol **17**: 149-166, 1977.

Fleckenstein A: Calcium antagonists and calcium agonists: fundamental criteria and classification, in Fleckenstein A, Van Breemen C, Groß R, and Hoffmeister F (eds.), Cardiovascular Effects of Dihydropyridine-Type Calcium Antagonists and Agonists, Springer-Verlag, Berlin, 1985, p. 3-31.

Flockerzi V, Oeken H-J and Hofmann F: Purification of a functional receptor for calcium-channel blockers from rabbit skeletal-muscle microsomes. Eur J Biochem **161**: 217-224, 1986a.

Flockerzi V, Oeken H-J, Hofmann F, Pelzer D, Cavalié A and Trautwein W: Purified dihydropyridine-binding site from skeletal muscle t-tubules is a functional calcium channel. Nature **323**: 66-68, 1986b.

Forester GV and Mainwood GW: Interval dependent inotropic effects in the rat myocardium and the effect of calcium. Pflügers Arch **352**: 189-196, 1974.

Fosset M, Jaimovich E, Delpont E and Lazdunski M: [^{3}H]Nitrendipine receptors in skeletal muscle. Properties and preferential localization in transverse tubules. J Biol Chem **258**: 6086-6092, 1983.

Fox RR: The rabbit as a research subject. Physiologist **27**: 393-402, 1984.

Fu M, Hung J-S, Yeh S-J, Lin F-C, Hsu RS and Wu D: Pharmacokinetics and pharmacodynamic effects of aqueous diltiazem in healthy humans. J Clin Pharmacol **27**: 106-110, 1987.

Galizzi J-P, Borsotto M, Barhanin J, Fosset M and Lazdunski M: Characterization and photoaffinity labeling of receptor sites for the Ca^{2+} channel inhibitors *d-cis*-diltiazem, (±)-bepridil, desmethoxyverapamil, and (+)-PN 200-110 in skeletal muscle transverse tubule membranes. J Biol Chem **261**: 1393-1397, 1986.

Garcia ML, King VF, Siegl PKS, Reuben JP and Kaczorowski GJ: Binding of Ca^{2+} entry blockers to cardiac sarcolemmal membrane vesicles. Characterization of diltiazem-binding sites and their interaction with dihydropyridine and aralkylamine receptors.

J Biol Chem **261**: 8146-8157, 1986.

Giacomini KM, Wong FM and Tozer TN: Correction for volume shift during equilibrium dialysis by measurement of protein concentration. Pharm Res **1**: 179-181, 1984.

Glossmann H and Ferry DR: Solubilization and partial purification of putative calcium channels labelled with [^{3}H]-nimodipine. Naunyn-Schmiedeberg's Arch Pharmacol **323**: 279-291, 1983.

Glossmann H, Ferry DR, Goll A, Striessnig J and Zernig G: Calcium channels and calcium channel drugs: recent biochemical and biophysical findings. Arzneim Forsch **35**: 1917-1935, 1985.

Glossmann H, Ferry DR, Lübbecke F, Mewes R and Hofmann F: Calcium channels: direct identification with radioligand binding studies. Trends Pharmacol Sci **3**: 431-437, 1982.

Glossmann H, Ferry DR, Striessnig J, Goll A and Moosburger K: Resolving the structure of the Ca^{2+} channel by photoaffinity labelling. Trends Pharmacol Sci **8**: 95-100, 1987.

Goebel K-J and Kölle EU: High-performance liquid chromatographic determination of diltiazem and four of its metabolites in plasma. Application to pharmacokinetics. J Chromatogr **345**: 355-363, 1985.

Goll A, Ferry DR and Glossmann H: Target size analysis of skeletal muscle Ca^{2+} channels. Positive allosteric heterotropic regulation by d-*cis*-diltiazem is associated with apparent channel oligomer dissociation. FEBS Lett **157**: 63-69, 1983.

Goll A, Glossmann H and Mannhold R: Correlation between the negative inotropic potency and binding parameters of 1,4-dihydropyridine and phenylalkylamine calcium channel blockers in cat heart. Naunyn-Schmiedeberg's Arch Pharmacol **334**: 303-312, 1986.

Gordon HJ, Dave B, Boyd R, Giacomini KM, Zobrist RH and Giacomini JC: Correlation of binding affinity and pharmacologic potency for the dihydropyridine calcium an-

tagonists in vascular smooth muscle. Clin Res **34**: 399A, 1986.

Gould RJ, Murphy KMM and Snyder SH: Tissue heterogeneity of calcium channel antagonist binding sites labeled by [^{3}H]nitrendipine. Mol Pharmacol **25**: 235-241, 1984.

Green FJ, Farmer BB, Wiseman GL, Jose MJL and Watanabe AM: Effect of membrane depolarization on binding of [^{3}H]nitrendipine to rat cardiac myocytes. Circ Res **56**: 576-585, 1985.

Greenberg DA, Cooper EC and Carpenter CL: Reversible dihydropyridine isothiocyanate binding to brain calcium channels. J Neurochem **44**: 319-321, 1985.

Guillory RJ and Jeng SJ: Photoaffinity labeling: theory and practice. Fed Proc **42**: 2826-2830, 1983.

Gurney AM, Nerbonne JM and Lester HA: Photoinduced removal of nifedipine reveals mechanisms of calcium antagonist action on single heart cells. J Gen Physiol **86**: 353-379, 1985.

Haas VH and Härtfelder G: α-Isopropyl-α-[(N-methyl-N-homoveratryl)-γ-amino-propyl]-3,4-dimethoxyphenylacetonitril, eine Substanz mit coronargefäßerweiternden Eigenschaften. Arzneim Forsch **12**: 549-558, 1962.

Hamilton SL, Yatani A, Brush K, Schwartz A and Brown AM: A comparison between the binding and electrophysiological effects of dihydropyridines on cardiac membranes. Mol Pharmacol **31**: 221-231, 1987.

Hanstein WG: Photoaffinity labeling of membrane components. Methods Enzymol **56**: 653-683, 1979.

Harrison RA and Lunt GG: Biological membranes. Their structure and function, 2nd ed., Blackie & Sons Limited, Glasgow, 1980, p. 86-89.

Henry PD: Comparative pharmacology of calcium antagonists: nifedipine, verapamil and diltiazem. Am J Cardiol **46**: 1047-1058, 1980.

Hermann Ph, Rodger SD, Remones G, Thenot JP, London DR and Morselli PL:

Pharmacokinetics of diltiazem after intravenous and oral administration. Eur J Clin Pharmacol **24**: 349-352, 1983.

Hess H-J, Graham RM and Homcy CJ: Photoaffinity label for the α_1-adrenergic receptor: synthesis and effects on membrane and affinity-purified receptors. Proc Natl Acad Sci USA **80**: 2102-2106, 1983.

Hess P, Lansman JB and Tsien RW: Different modes of Ca channel gating behaviour favoured by dihydropyridine Ca agonists and antagonists. Nature (Lond) **311**: 538-544, 1984.

Hille B: Local anesthetics: hydrophilic and hydrophobic pathways for the drug-receptor reaction. J Gen Physiol **69**: 497-515, 1977.

Hof RP, Rüegg UT, Hof A and Vogel A: Stereoselectivity at the calcium channel: opposite action of the enantiomers of a 1,4-dihydropyridine. J Cardiovasc Pharmacol **7**: 689-693, 1985.

Holck M, Thorens S and Haeusler G: Characterization of [^{3}H]nifedipine binding sites in rabbit myocardium. Eur J Pharmacol **85**: 305-315, 1982.

Holck M, Thorens S and Haeusler G: Does [^{3}H]nifedipine label the calcium channel in rabbit myocardium? J Receptor Res **3**: 191-198, 1983.

Holford NHG: DRUGFUN, Prophet Public Procedures, Perry HM (ed), Bolt Berenek and Newman Inc., Cambridge, MA, 1982a, p. 4-63–4-80.

Holford NHG: MODELTEST, Prophet Public Procedures, Perry HM (ed), Bolt Berenek and Newman Inc., Cambridge, MA, 1982b, p. 4-139–4-145.

Holford NHG and Sheiner LB: Understanding the dose-effect relationship: clinical application of pharmacokinetic-pharmacodynamic models. Clin Pharmacokinet **6**: 429-453, 1981.

Homcy CJ and Graham RM: Molecular characterization of adrenergic receptors. Circ Res **56**: 635-650, 1985.

Hondeghem LM and Katzung BG: Time- and voltage-dependent interactions of anti-

arrhythmic drugs with cardiac sodium channels. Biochim Biophys Acta **472**: 373-398, 1977.

Hondeghem LM and Katzung BG: Antiarrhythmic agents: the modulated receptor mechanism of action of sodium and calcium channel-blocking drugs. Ann Rev Pharmacol Toxicol **24**: 387-423, 1984.

Hondeghem LM and Mason JW: Agents used in cardiac arrhythmias, in Katzung BG (ed.), Basic and Clinical Pharmacology, 3rd ed., Appleton & Lange, Norwalk, CT, 1987, p. 151-168.

Horne P, Triggle DJ and Venter CJ: Nitrendipine and isoproterenol induce phosphorylation of a 42,000 dalton protein that co-migrates with the affinity labeled calcium channel regulatory subunit. Biochem Biophys Res Commun **121**: 890-898, 1984.

Horne WA, Weiland GA, Oswald RE and Cerione RA: Rapid incorporation of the solubilized dihydropyridine receptor into phospholipid vesicles. Biochim Biophys Acta **863**: 205-212, 1986.

Janis RA, Krol GJ, Noe AJ and Pan M: Radioreceptor and high-performance liquid chromatographic assays for the calcium channel antagonist nitrendipine in serum. J Clin Pharmacol **23**: 266-273, 1983.

Janis RA, Maurer SC, Sarmiento JG, Bolger GT and Triggle DJ: Binding of [^{3}H]nimodipine to cardiac and smooth muscle membranes. Eur J Pharmacol **82**: 191-194, 1982.

Janis RA, Rampe D, Sarmiento JG and Triggle DJ: Specific binding of a calcium channel activator, [^{3}H]Bay K 8644, to membranes from cardiac muscle and brain. Biochem Biophys Res Commun **121**: 317-323, 1984a.

Janis RA, Sarmiento JG, Maurer SC, Bolger GT and Triggle DJ: Characteristics of the binding of [^{3}H]nitrendipine to rabbit ventricular membranes: modification by other Ca^{++} channel antagonists and by the Ca^{++} channel agonist Bay K 8644. J Pharmacol Exp Ther **231**: 8-15, 1984b.

Janis RA and Triggle DJ: New developments in Ca^{2+} channel antagonists. J Med Chem **26**: 775-785, 1983.

Janis RA and Triggle DJ: 1,4-Dihydropyridine Ca^{2+} channel antagonists and activators: a comparison of binding characteristics with pharmacology. Drug Develop Res **4**: 257-274, 1984.

Joyal M, Pieper J, Cremer K, Feldman RL and Pepine CJ: Pharmacodynamic aspects of intravenous diltiazem administration. Am Heart J **111**: 54-61, 1986.

Kanaya S, Arlock P, Katzung BG and Hondeghem LM: Diltiazem and verapamil preferentially block inactivated cardiac calcium channels. J Mol Cell Cardiol **15**: 145-148, 1983.

Kanaya S and Katzung BG: Effects of diltiazem on transmembrane potential and current of right ventricular papillary muscle of ferrets. J Pharmacol Exp Ther **228**: 245-251, 1984.

Katz AM: Physiology of the Heart, Raven Press, New York, 1977, p. 229-256.

Kazda S, Garthoff B, Meyer H, Schloßmann K, Stoepel K, Towart R, Vater W and Wehinger E: Pharmacology of a new calcium antagonist compound, isobutyl methyl 1,4-dihydro-2,6-dimethyl-4-(2-nitrophenyl)-3,5-pyridinedicarboxylate (Nisoldipine, Bay k 5552). Arzneim Forsch **30**: 2144-2162, 1980.

Kelly JJ and Hoffman BF: Mechanical activity of rat papillary muscle. Am J Physiol **199**: 157-162, 1960.

Kempner ES and Schlegel W: Size determination of enzymes by radiation inactivation. Anal Biochem **92**: 2-10, 1979.

Kenessey A, Cantor EH and Spector S: Low affinity dihydropyridine (DHP) binding site in rat heart membranes. Fed Proc **43**: 550, 1984.

Kinney EL, Moskowitz RM and Zelis R: The pharmacokinetics and pharmacology of oral diltiazem in normal volunteers. J Clin Pharmacol **21**: 337-342, 1981.

Kirley TL and Schwartz A: Solubilization and affinity labeling of a dihydropyridine bind-

ing site from skeletal muscle: effects of temperature and diltiazem on [^{3}H]dihydropyridine binding to transverse tubules. Biochem Biophys Res Commun **123**: 41-49, 1984.

Kitchen I: Textbook of *in vitro* Practical Pharmacology, Blackwell Scientific Publications, Boston, 1984, p. 101-118.

Koiwaya Y, Ashihara T, Nakamura M and Etoh A: Plasma concentration of diltiazem after oral administration in normal volunteers. Clin Ther **3**: 436-440, 1981a.

Koiwaya Y, Matsuguchi T and Nakamura M: Plasma concentrations of diltiazem after oral administration in coronary artery disease patients: a comparison with those in normal volunteers. Clin Ther **4**: 127-132, 1981b.

Kozlowski R, Ehrhard P, Fischli W, Osterrieder W and Holck M: *o*-Isothiocyanate dihydropyridine (oNCS-DHP), a long-acting, reversible inhibitor of the Ca^{++} channel. J Pharmacol Exp Ther **238**: 1084-1091, 1986.

Kroneberg G: Pharmacology of nifedipine, in Lochner W, Braasch W and Kroneberg G (eds.): 2nd International Adalat Symposium, Springer-Verlag, New York, 1975, p. 12-19.

Kugita H, Inoue H, Ikezaki M, Konda M and Takeo S: Synthesis of 1,5-benzothiazepine derivatives. Chem Pharm Bull **19**: 595-602, 1971.

Kwong TC, Sparks JD and Sparks CE: Lipoprotein and protein binding of the calcium channel blocker diltiazem. Proc Soc Exp Biol Med **178**: 313-316, 1985.

Laduron PM: Criteria for receptor sites in binding studies. Biochem Pharmacol **33**: 833-839, 1984.

Laemmli UK: Cleavage of structural proteins during the assembly of the head of bacteriophage T4. Nature **227**: 680-685, 1970.

Lee KS and Tsien RW: Mechanism of calcium channel blockade by verapamil, D600, diltiazem and nitrendipine in single dialysed heart cells. Nature (Lond) **302**: 790-794, 1983.

Lo MMS, Barnard EA and Dolly JO: Size of acetylcholine receptors in the membrane. An improved version of the radiation inactivation method. Biochemistry **21**: 2210-2217, 1982.

Loev B, Goodman MM, Snader KM, Tedeschi R and Macko E: "Hantzsch-type" dihydropyridine hypotensive agents. J Med Chem **17**: 956-965, 1974.

Lowry OH, Rosebrough NJ, Farr AL and Randall RJ: Protein measurement with the Folin phenol reagent. J Biol Chem **193**: 265-275, 1951.

Maguire ME, Wiklund RA, Anderson HJ and Gilman AG: Binding of [^{125}I]iodohydroxybenzylpindolol to putative β-adrenergic receptors of rat glioma cells and other cell clones. J Biol Chem **251**: 1221-1231, 1976.

Mannhold R, Rodenkirchen R and Bayer R: Qualitative and quantitative structure-activity relationships of specific Ca antagonists. Prog Pharmacol **5**: 25-52, 1982.

Marangos PJ, Patel J, Miller C and Martino AM: Specific calcium antagonist binding sites in brain. Life Sci **31**: 1575-1585, 1982.

Marsh JD, Loh E, Lachance D, Barry WH and Smith TW: Relationship of binding of a calcium channel blocker to inhibition of contraction in intact cultured embryonic chick ventricular cells. Circ Res **53**: 539-543, 1983.

McBride W, Mukherjee A, Haghani Z, Wheeler-Clark E, Brady J, Gandler T, Bush L, Buja LM and Willerson JT: Nitrendipine: effects on vascular responses and myocardial binding. Am J Physiol **247**: H775-H783, 1984.

Meshi T, Sugihara J and Sato Y: Metabolic fate of *d-cis*-3-acetoxy-5-[2-(dimethylamino)ethyl]-2,3-dihydro-2-(*p*-methoxyphenyl)-1,5-benzothiazepin-4(5H)-one hydrochloride (CRD-401). Chem Pharm Bull **19**: 1546-1556, 1971.

Meyer Von H, Bossert F, Wehinger E, Stoepel K and Vater W: Synthese und vergleichende pharmakologische Untersuchungen von 1,4-Dihydro-2,6-dimethyl-4-(3-nitrophenyl)pyridin-3,5-dicarbonsäureestern mit nicht-identischen Esterfunktionen. Arzneim Forsch **31**: 407-409, 1981.

Meyer H, Wehinger E, Bossert F, Böshagen H, Franckowiak G, Goldmann S, Seidel W and Stoltefuss J: Chemistry of dihydropyridines [1-4], in Fleckenstein A, Van Breemen C, Groß R, and Hoffmeister F (eds.), Cardiovascular Effects of Dihydropyridine-Type Calcium Antagonists and Agonists, Springer-Verlag, Berlin, 1985, p. 90-103.

Millard RW, Grupp G, Grupp IL, DiSalvo J, DePover A and Schwartz A: Chronotropic, inotropic, and vasodilator actions of diltiazem, nifedipine and verapamil. A comparative study of physiological responses and membrane receptor activity. Circ Res **52** (suppl I): 29-39, 1983.

Miller RJ and Freedman SB: Are dihydropyridine binding sites voltage sensitive calcium channels? Life Sci **34**: 1205-1221, 1984.

Montamat SC and Abernethy DR: N-monodesmethyldiltiazem is the predominant metabolite of diltiazem in the plasma of young and elderly hypertensives. Br J Clin Pharmacol **24**: 185-189, 1987.

Montamat SC, Abernethy DR and Mitchell JR: High-performance liquid chromatographic determination of diltiazem and its major metabolites, N-monodemethyldiltiazem and desacetyldiltiazem, in plasma. J Chromatogr **415**: 203-207, 1987.

Morad M, Goldman YE and Trentham DR: Rapid photochemical inactivation of Ca^{2+}-antagonists shows that Ca^{2+} entry directly activates contraction in frog heart. Nature **304**: 635-638, 1983.

Morselli PL, Rovei V, Mitchard M, Durand A, Gomeni R and Larribaud J: Pharmacokinetics and metabolism of diltiazem in man (observations on healthy volunteers and angina pectoris patients), in Bing RJ (ed.), New Drug Therapy with a Calcium Antagonist–Diltiazem, Excerpta Medica, Amsterdam, 1979, p. 152-167.

Mukherjee C, Caron MG, Mullikin D and Lefkowitz RJ: Structure-activity relationships of adenylate cyclase-coupled beta adrenergic receptors: determination by direct binding studies. Mol Pharmacol **12**: 16-31, 1976.

Murphy KMM and Snyder SH: Calcium antagonist receptor binding sites labeled with [^{3}H]nitrendipine. Eur J Pharmacol **77**: 201-202, 1982.

Nabata H: Effects of calcium-antagonistic coronary vasodilators on myocardial contractility and membrane potentials. Jpn J Pharmacol **27**: 239-249, 1977.

Nagao T, Sato M, Nakajima H and Kiyomoto A: Studies on a new 1,5-benzothiazepine derivative (CRD-401). II. Vasodilator actions. Jpn J Pharmacol **22**: 1-10, 1972.

Nakajima H, Hoshiyama M, Yamashita K and Kiyomoto A: Effect of diltiazem on electrical and mechanical activity of isolated cardiac ventricular muscle of guinea pig. Jpn J Pharmacol **25**: 383-392, 1975.

Nakajima H, Hoshiyama M, Yamashita K and Kiyomoto A: Electrical and mechanical responses to diltiazem in potassium depolarized myocardium of the guinea pig. Jpn J Pharmacol **26**: 571-580, 1976.

Nakamura S, Suzuki T, Sugawara Y, Usuki S, Ito Y, Kume T, Yoshikawa M, Endo H, Ohashi M and Harigaya S: Metabolic fate of diltiazem. Distribution, excretion and protein binding in rat and dog. Arzneim Forsch **37**: 1244-1252, 1987.

Nakayama K, Kurihara J, Miyajima Y, Ishii K and Kato H: Calcium antagonistic properties of nicardipine, a dihydropyridine derivative assessed in isolated cerebral arteries and cardiac muscle. Arzneim Forsch **35**: 687-693, 1985.

Narita H, Otsuka M, Yabana H and Nagao T: Hypotensive response of spontaneously hypertensive rats to centrally administered diltiazem and its metabolites: in relevance to the hypotensive action by oral administration. J Pharmacobio-Dyn **9**: 547-553, 1986.

Nerbonne JM, Richard S and Nargeot J: Calcium channels are 'unblocked' within a few milliseconds after photoremoval of nifedipine. J Mol Cell Cardiol **17**: 511-515, 1985.

Norman RI, Borsotto M, Fosset M, Lazdunski M and Ellory JC: Determination of the molecular size of the nitrendipine-sensitive Ca^{2+} channel by radiation inactivation.

Biochem Biophys Res Commun **111**: 878-883, 1983.

Norman RI, Burgess AJ, Allen E and Harrison TM: Monoclonal antibodies against the 1,4-dihydropyridine receptor associated with voltage-sensitive Ca^{2+} channels detect similar polypeptides from a variety of tissues and species. FEBS Lett **212**: 127-132, 1987.

Ochs HR and Knüchel M: Pharmacokinetics and absolute bioavailability of diltiazem in humans. Klin Wochenschr **62**: 303-306, 1984.

Pieper JA: Diltiazem binding to human serum proteins. Clin Pharmacol Ther **35**: 266 (abstract), 1984.

Piepho RW, Bloedow DC, Lacz JP, Runser DJ, Dimmit DC and Browne RK: Pharmacokinetics of diltiazem in selected animal species and human beings. Am J Cardiol **49**: 525-528, 1982.

Porzig H, Kokubun S, Prod'hom B, Becker C and Reuter H: Voltage-dependent cooperative interactions of calcium channel ligands in intact cardiac cells. Biomed Biochim Acta **46**: S370-S374, 1987.

Pozet N, Brazier JL, Hadj Aïssa A, Khenfer D, Faucon G, Apoil E and Traeger J: Pharmacokinetics of diltiazem in severe renal failure. Eur J Clin Pharmacol **24**: 635-638, 1983.

Quinn P, Briscoe MG, Nuttall A and Smith HJ: Species variation in arterial-myocardial sensitivity to verapamil. Cardiovasc Res **15**: 398-403, 1981.

Razzetti R, Bongrani S and Schiantarelli P: *In vitro* effects of nicardipine on vascular and cardiac muscle preparations. Pharmacol Res Commun **16**: 795-808, 1984.

Rengasamy A, Ptasienski J and Hosey MM: Purification of the cardiac 1,4-dihydropyridine receptor/calcium channel complex. Biochem Biophys Res Commun **126**: 1-7, 1985.

Renton KW: Inhibition of hepatic microsomal drug metabolism by the calcium channel blockers diltiazem and verapamil. Biochem Pharmacol **34**: 2549-2553, 1985.

Reuter H, Porzig H, Kokubun S and Prod'hom B: 1,4-Dihydropyridines as tools in the study of Ca^{2+} channels. Trends Neurosci **8**: 396-400, 1985.

Rhodes DG, Sarmiento JG and Herbette LG: Kinetics of binding of membrane-active drugs to receptor sites. Diffusion-limited rates for a membrane bilayer approach of 1,4-dihydropyridine calcium channel antagonists to their active site. Mol Pharmacol **27**: 612-623, 1985.

Rodenkirchen R, Bayer R, Steiner R, Bossert F, Meyer H and Möller E: Structure-activity studies on nifedipine in isolated cardiac muscle. Naunyn-Schmiedeberg's Arch Pharmacol **310**: 69-78, 1979.

Rogart RB, deBruyn Kops A and Dzau VJ: Identification of two calcium channel receptor sites for [^{3}H]nitrendipine in mammalian cardiac and smooth muscle membrane. Proc Natl Acad Sci USA **83**: 7452-7456, 1986.

Rovei V, Gomeni R, Mitchard M, Larribaud J, Blatrix Ch, Thebault JJ and Morselli PL: Pharmacokinetics and metabolism of diltiazem in man. Acta Cardiol (Brux) **35**: 35-45, 1980.

Rovei V, Mitchard M and Morselli PL: Simple, sensitive and specific gas chromatographic method for the quantification of diltiazem in human body fluids. J Chromatogr **138**: 391-398, 1977.

Rowland M, Benet LZ, and Graham GG: Clearance concepts in pharmacokinetics. J Pharmacokinet Biopharm **1**: 123-136, 1973.

Rowland M and Tozer TN: Metabolite kinetics, in Clinical Pharmacokinetics. Concepts and Applications, Lea & Febiger, Philadelphia, 1980, p. 124- 137.

Saikawa T, Nagamoto Y and Arita M: Electrophysiologic effects of diltiazem, a new slow channel inhibitor, on canine cardiac fibers. Jpn Heart J **18**: 235-245, 1977.

Sanguinetti MC and Kass RS: Voltage-dependent block of calcium channel current in the calf cardiac Purkinje fiber by dihydropyridine calcium channel antagonists. Circ Res **55**: 336-348, 1984a.

Sanguinetti MC and Kass RS: Photoalteration of calcium channel blockade in the cardiac Purkinje fiber. Biophys J **45**: 873-880, 1984b.

Sarmiento JG, Epstein PM, Rowe WA, Chester DW, Smilowitz H, Wehinger E and Janis RA: Photoaffinity labeling of a 33-35,000 Dalton protein in cardiac, skeletal and smooth muscle membranes using a new ^{125}I-labelled 1,4-dihydropyridine calcium channel antagonist. Life Sci **39**: 2401-2409, 1986.

Sarmiento JG, Janis RA, Katz AM and Triggle DJ: Comparison of high affinity binding of calcium channel blocking drugs to vascular smooth muscle and cardiac sarcolemmal membranes. Biochem Pharmacol **33**: 3119-3123, 1984.

Sato M, Nagao T, Yamaguchi I, Nakajima H and Kiyomoto A: Pharmacological studies on a new 1,5-benzothiazepine derivative (CRD-401). Arzneim Forsch **21**: 1338-1343, 1971.

Schmid A, Barhanin J, Coppola T, Borsotto M and Lazdunski M: Immunochemical analysis of subunit structures of 1,4-dihydropyridine receptors associated with voltage-dependent Ca^{2+} channels in skeletal, cardiac and smooth muscles. Biochemistry **25**: 3492-3495, 1986a.

Schmid A, Barhanin J, Mourre C, Coppola T, Borsotto M and Lazdunski M: Antibodies reveal the cytolocalization and subunit structure of the 1,4-dihydropyridine component of the neuronal Ca^{2+} channel. Biochem Biophys Res Commun **139**: 996-1002, 1986b.

Schoemaker H, Hicks PE and Langer SZ: Calcium channel receptor binding studies for diltiazem and its major metabolites: functional correlation to inhibition of portal vein myogenic activity. J Cardiovasc Pharmacol **9**: 173-180, 1987.

Schwartz A, Grupp IL, Grupp G, Williams JS and Vaghy PL: Effects of calcium channel modulators in the heart: pharmacological and radioligand binding correlations. Biochem Biophys Res Commun **125**: 387-394, 1984.

Schwartz A and Triggle DJ: Cellular action of calcium channel blocking drugs. Ann Rev

Med **35**: 325-329, 1984.

Schwartz JB and Abernethy DR: Responses to intravenous and oral diltiazem in elderly and younger patients with systemic hypertension. Am J Cardiol **59**: 1111-1117, 1987.

Siegl PKS and McNeill JH: The negative inotropic potency of compound D 600 in rat, guinea pig, and rabbit cardiac preparations. Can J Physiol Pharmacol **58**: 1406-1411, 1980.

Singer SJ, Ruoho A, Kiefer H, Lindstrom J and Lennox ES: The use of affinity labels in the identification of receptors, in Rang HP (ed.), Biological Council Symposium on Drug Receptors, MacMillan, London, 1973, p. 183-191.

Smith MS, Verghese CP, Shand DG and Pritchett ELC: Pharmacokinetic and pharmacodynamic effects of diltiazem. Am J Cardiol **51**: 1369-1374, 1983.

Spedding M and Cavero I: "Calcium antagonists": a class of drugs with a bright future. Part II. Determination of basic pharmacological properties. Life Sci **35**: 575-587, 1984.

Stanski DR, Hudson RJ, Homer TD, Saidman LJ and Meathe E: Pharmacodynamic modeling of thiopental anesthesia. J Pharmacokinet Biopharm **12**: 223-240, 1984.

Stone PH, Antman EM, Muller JE and Braunwald E: Calcium channel blocking agents in the treatment of cardiovascular disorders. Part II: Hemodynamic effects and clinical applications. Ann Intern Med **93**: 886-904, 1980.

Strauer BE: Inotropic effects of nifedipine: a new coronary dilating agent. Int J Clin Pharmacol **9**: 101-107, 1974.

Striessnig J, Moosburger K, Goll A, Ferry DR and Glossmann H: Stereoselective photoaffinity labelling of the purified 1,4-dihydropyridine receptor of the voltage-dependent calcium channel. Eur J Biochem **161**: 603-609, 1986.

Studier FW: Analysis of bacteriophage T7 early RNAs and proteins on slab gels. J Mol Biol **79**: 237-248, 1973.

Sugihara J, Sugawara Y, Ando H, Harigaya S, Etoh A and Kohno K: Studies on the metabolism of diltiazem in man. J Pharmacobio-Dyn **7**: 24-32, 1984.

Sutko JL and Willerson JT: Ryanodine alteration of the contractile state of rat ventricular myocardium. Comparison with dog, cat, and rabbit ventricular tissues. Circ Res **46**: 332-343, 1980.

Takahashi M and Catterall WA: Identification of an α subunit of dihydropyridine-sensitive brain calcium channels. Science **236**: 88-91, 1987.

Takemori AE and Portoghese PS: Affinity labels for opioid receptors. Ann Rev Pharmacol Toxicol **25**: 193-223, 1985.

Talvenheimo JA: The purification of ion channels from excitable cells. J Membrane Biol **87**: 77-91, 1985.

Thomas G, Groß R and Schramm M: Calcium channel modulation: ability to inhibit or promote calcium influx resides in the same dihydropyridine molecule. J Cardiovasc Pharmacol **6**: 1170-1176, 1984.

Tozer TN, Gambertoglio JG, Furst DE, Avery DS and Holford NHG: Volume shifts and protein binding estimates using equilibrium dialysis: application to prednisolone binding in humans. J Pharm Sci **72**: 1442-1446, 1983.

Triggle CR, Agrawal DK, Bolger GT, Daniel EE, Kwan CY, Luchowski EM and Triggle DJ: Calcium-channel antagonist binding to isolated vascular smooth muscle membranes. Can J Physiol Pharmacol **60**: 1738-1741, 1982.

Tung L and Morad M: Voltage- and frequency-dependent block of diltiazem on the slow inward current and generation of tension in frog ventricular muscle. Pflügers Arch **398**: 189-198, 1983.

Turro NJ: Structure and dynamics of important reactive intermediates involved in photobiological systems. Ann NY Acad Sci **346**: 1-15, 1980.

Uehara A and Hume JR: Interactions of organic calcium channel antagonists with calcium channels in single frog atrial cells. J Gen Physiol **85**: 621-647, 1985.

Vaghy PL, Dubé GP, Grupp IL, Grupp G, Williams JS, Baik YH and Schwartz A: A proposed pharmacological role for dihydropyridine binding sites in heart and coronary smooth muscle, in Fleckenstein A, Van Breemen C, Groß R, and Hoffmeister F (eds.), Cardiovascular Effects of Dihydropyridine-Type Calcium Antagonists and Agonists, Springer-Verlag, Berlin, 1985, p. 156-184.

Vaghy PL, Grupp IL, Grupp G, Balwierczak JL, Williams JS and Schwartz A: Correlation of nitrendipine and Bay K 8644 binding to isolated canine heart sarcolemma with their pharmacological effects on the canine heart. Eur J Pharmacol **102**: 373-374, 1984.

Vandaele S, Fosset M, Galizzi J-P and Lazdunski M: Monoclonal antibodies that coimmunoprecipitate the 1,4-dihydropyridine and phenylalkylamine receptors and reveal the Ca^{2+} channel structure. Biochemistry **26**: 5-9, 1987.

Velena AH, Dubur GJ, Vitolina RO, Kimenis AA, Selga MJ, Zarinsh GV, Narusevicius EV, Macianskiene RA, Gendviliene VI and Simkhovich BZ: Effect of ryodipine on electromechanical parameters of heart and vessels, cAMP phosphodiesterase activity and swelling-contraction cycle of mitrochondria. Arzneim Forsch **35**: 907-914, 1985.

Venter JC, Fraser CM, Schaber JS, Jung CY, Bolger G and Triggle DJ: Molecular properties of the slow inward calcium channel. Molecular weight determinations by radiation inactivation and covalent affinity labeling. J Biol Chem **258**: 9344-9348, 1983.

Verghese C, Smith MS, Aanonsen L, Pritchett ELC and Shand DG: High-performance liquid chromatographic analysis of diltiazem and its metabolite in plasma. J Chromatogr **272**: 149-155, 1983.

Wei XY, Luchowski EM, Rutledge A, Su CM and Triggle DJ: Pharmacologic and radioligand binding analysis of the actions of 1,4-dihydropyridine activator-antagonist pairs in smooth muscle. J Pharmacol Exp Ther **239**: 144-153, 1986.

Weiland GA and Molinoff PB: Quantitative analysis of drug-receptor interactions: I. Determination of kinetic and equilibrium properties. Life Sci **29**: 313-330, 1981.

Westheimer FH: Photoaffinity labeling - retrospect and prospect. Ann NY Acad Sci **346**: 134-143, 1980.

Wilkinson GR and Shand DG: A physiological approach to hepatic drug clearance. Clin Pharmacol Ther **18**: 377-390, 1975.

Willerson JT, Wheelan S, Adcock RC, Templeton GH and Wildenthal K: Species differences in responses to hyperosmolality and D600 in cat and rat heart. Am J Physiol **235**: H276-H280, 1978.

Williams JS, Grupp IL, Grupp G, Vaghy PL, Dumont L and Schwartz A: Profile of the oppositely acting enantiomers of the dihydropyridine 202-791 in cardiac preparations: receptor binding, electrophysiological, and pharmacological studies. Biochem Biophys Res Commun **131**: 13-21, 1985.

Winegrad S: Calcium release from cardiac sarcoplasmic reticulum. Ann Rev Physiol **44**: 451-462, 1982.

Wouters W and Laduron PM: Isolation and molecular characterization of S_2-serotonin and D_2-dopamine receptors: solubilization and photoaffinity probes. Biochem Soc Trans **13**: 1103-1106, 1985.

Yabana H, Nagao T and Sato M: Cardiovascular effects of the metabolites of diltiazem in dogs. J Cardiovasc Pharmacol **7**: 152-157, 1985.

Yamamura HI and Snyder SH: Muscarinic cholinergic receptor binding in the longitudinal muscle of the guinea pig ileum with [^{3}H]quinuclidinyl benzilate. Mol Pharmacol **10**: 861-867, 1974.

Yousif FB, Bolger GT, Ruzycky A and Triggle DJ: Ca^{2+} channel antagonist actions in bladder smooth muscle: comparative pharmacologic and [^{3}H]nitrendipine binding studies. Can J Physiol Pharmacol **63**: 453-462, 1985.

Appendix A

NMR and Mass Spectra of Synthesized 1,4-Dihydropyridine Compounds

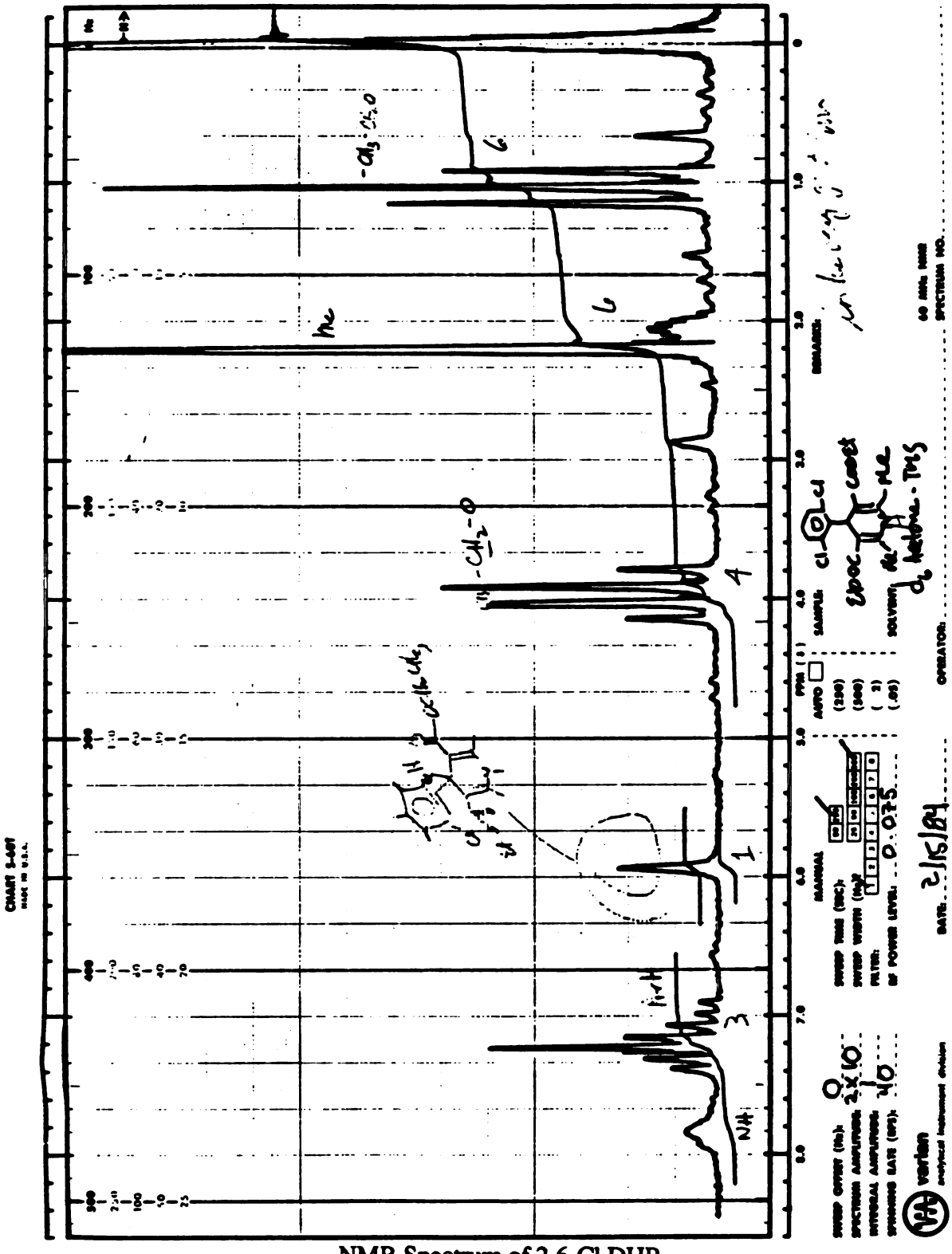

NMR Spectrum of 2,6-Cl DHP

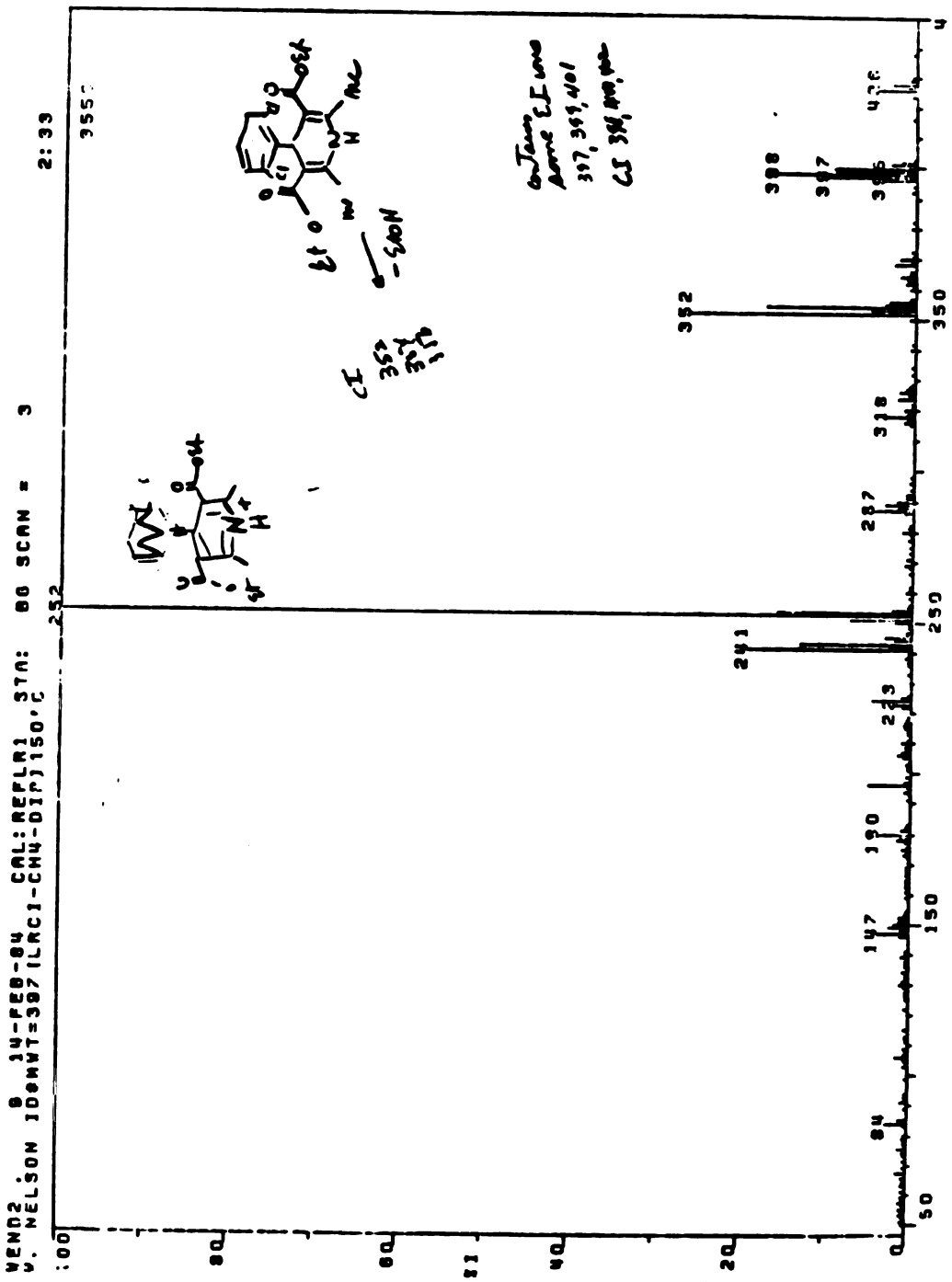

Mass Spectrum of 2,6-Cl DHP

Appendix A (cont'd)

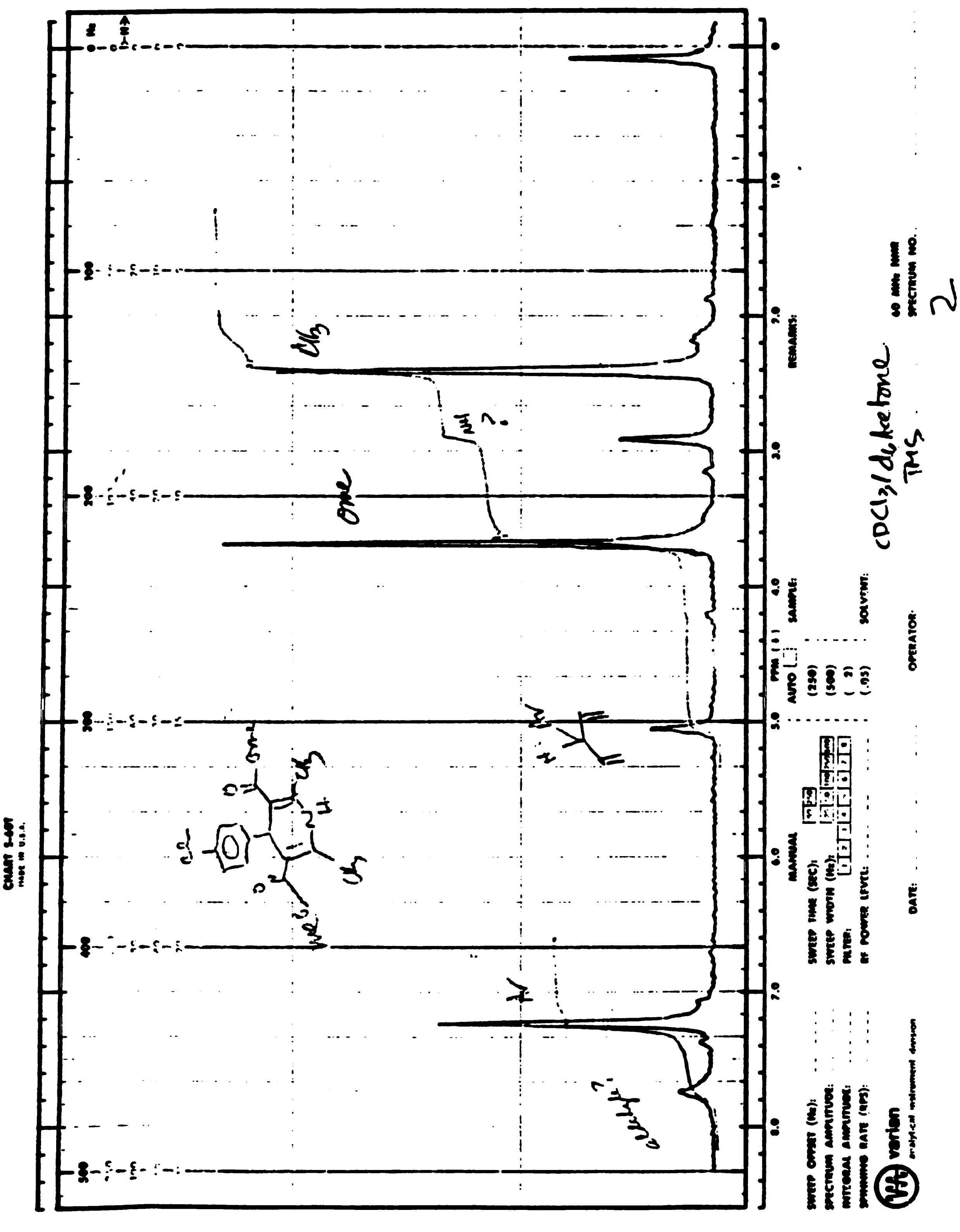

NMR Spectrum of 4-Cl DHP

Appendix A (cont'd)

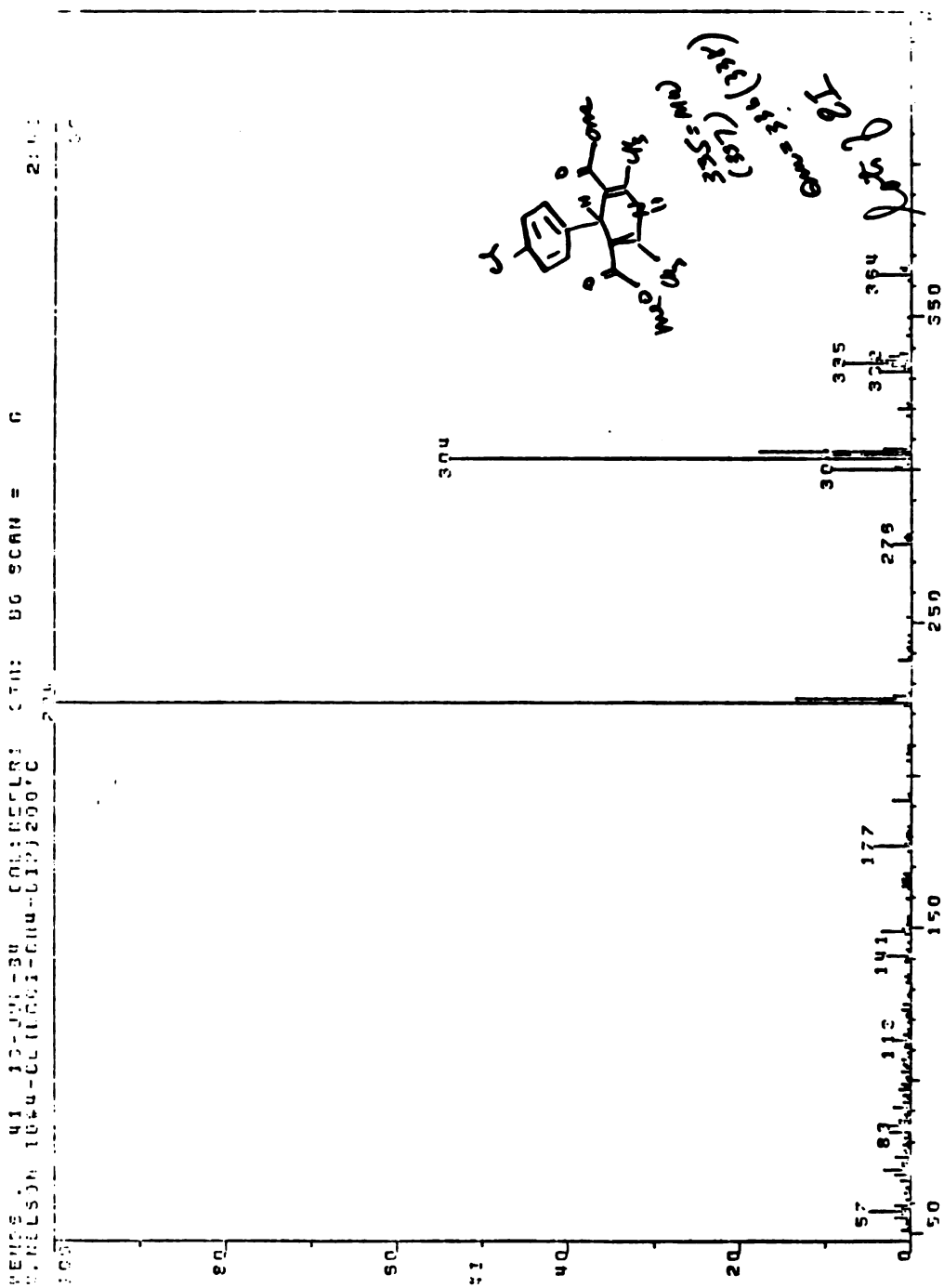

Mass Spectrum of 4-Cl DHP

Appendix A (cont'd)

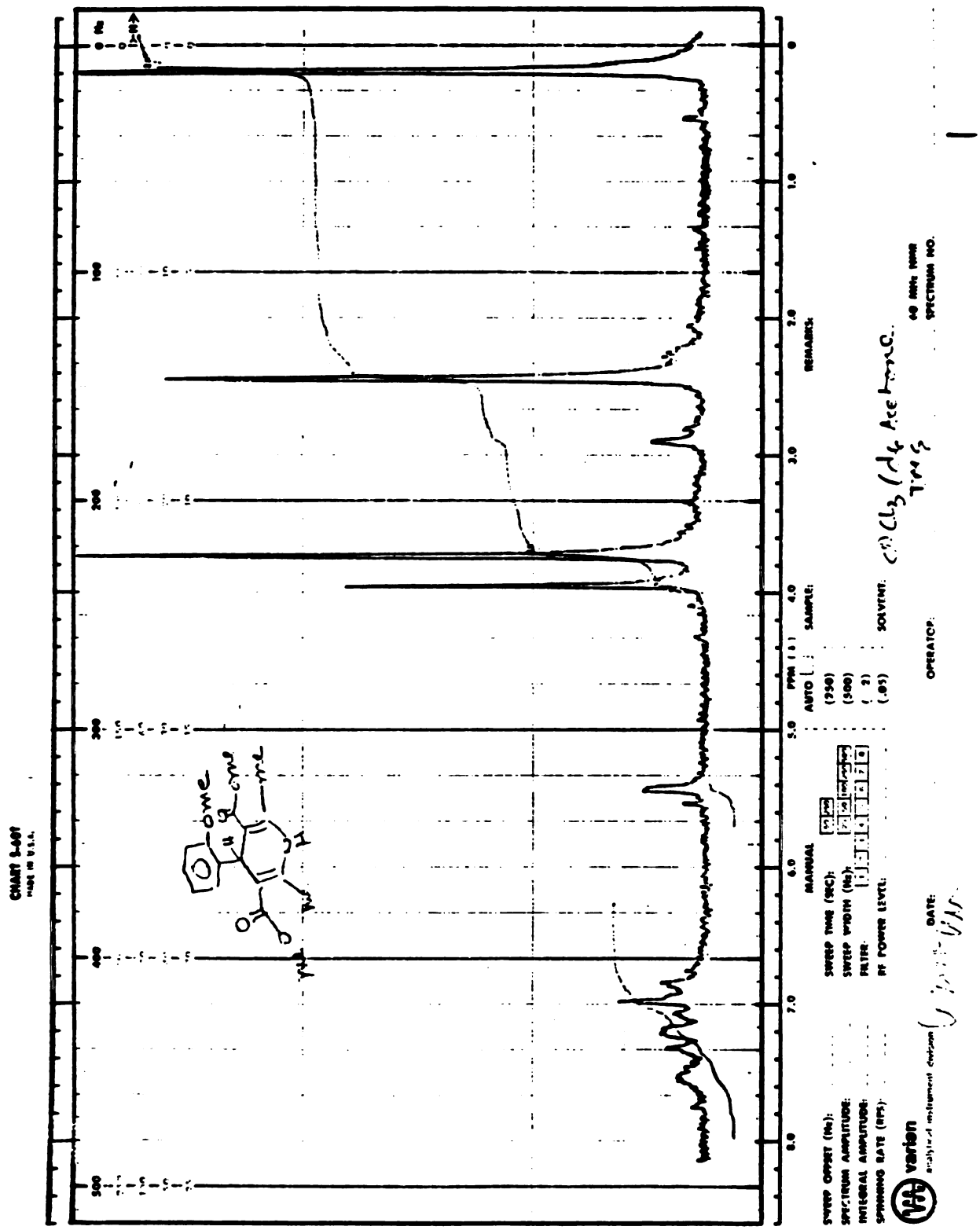

NMR Spectrum of 2-MeO DHP

Appendix A (cont'd)

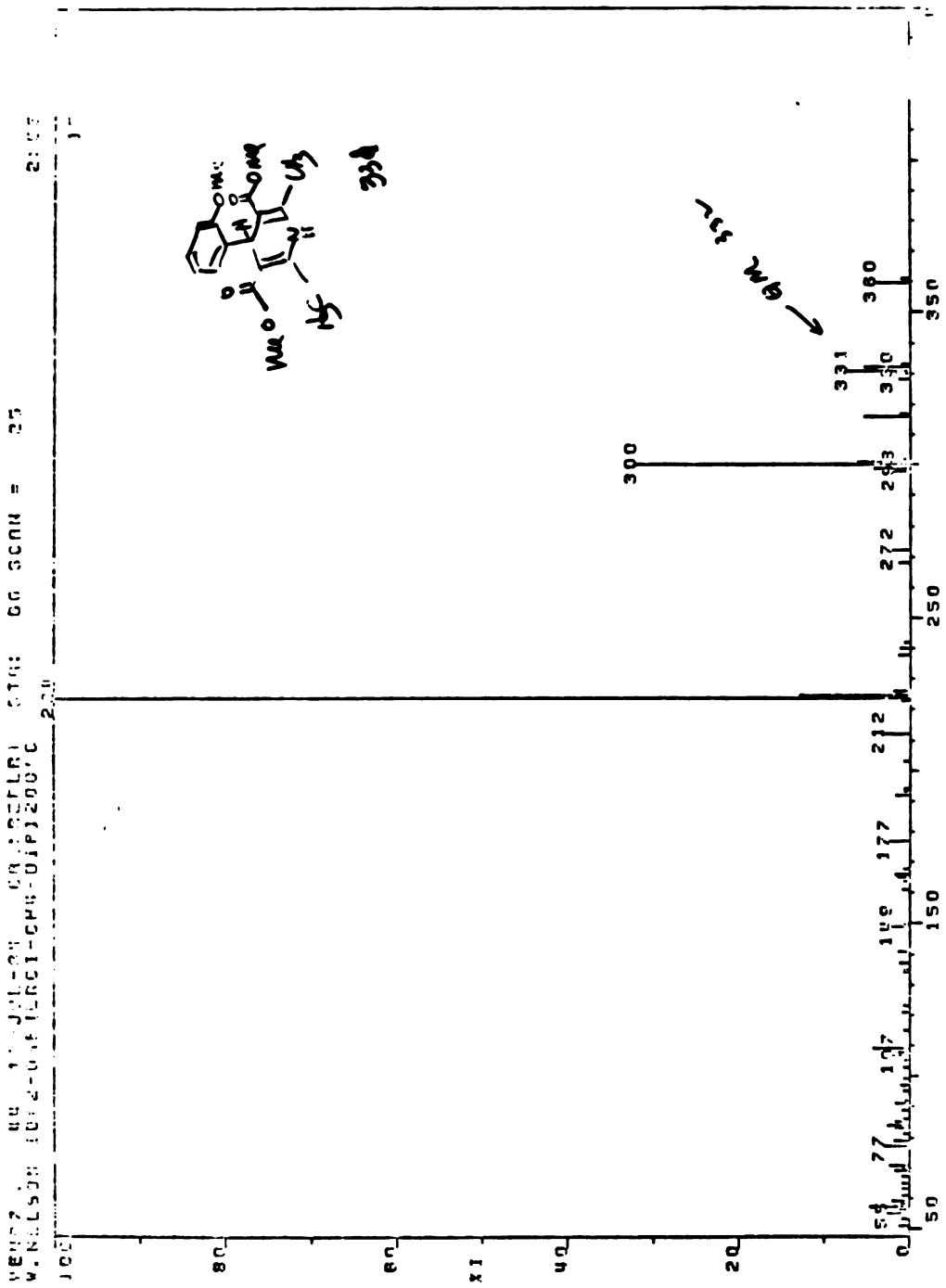

Mass Spectrum of 2-MeO DHP

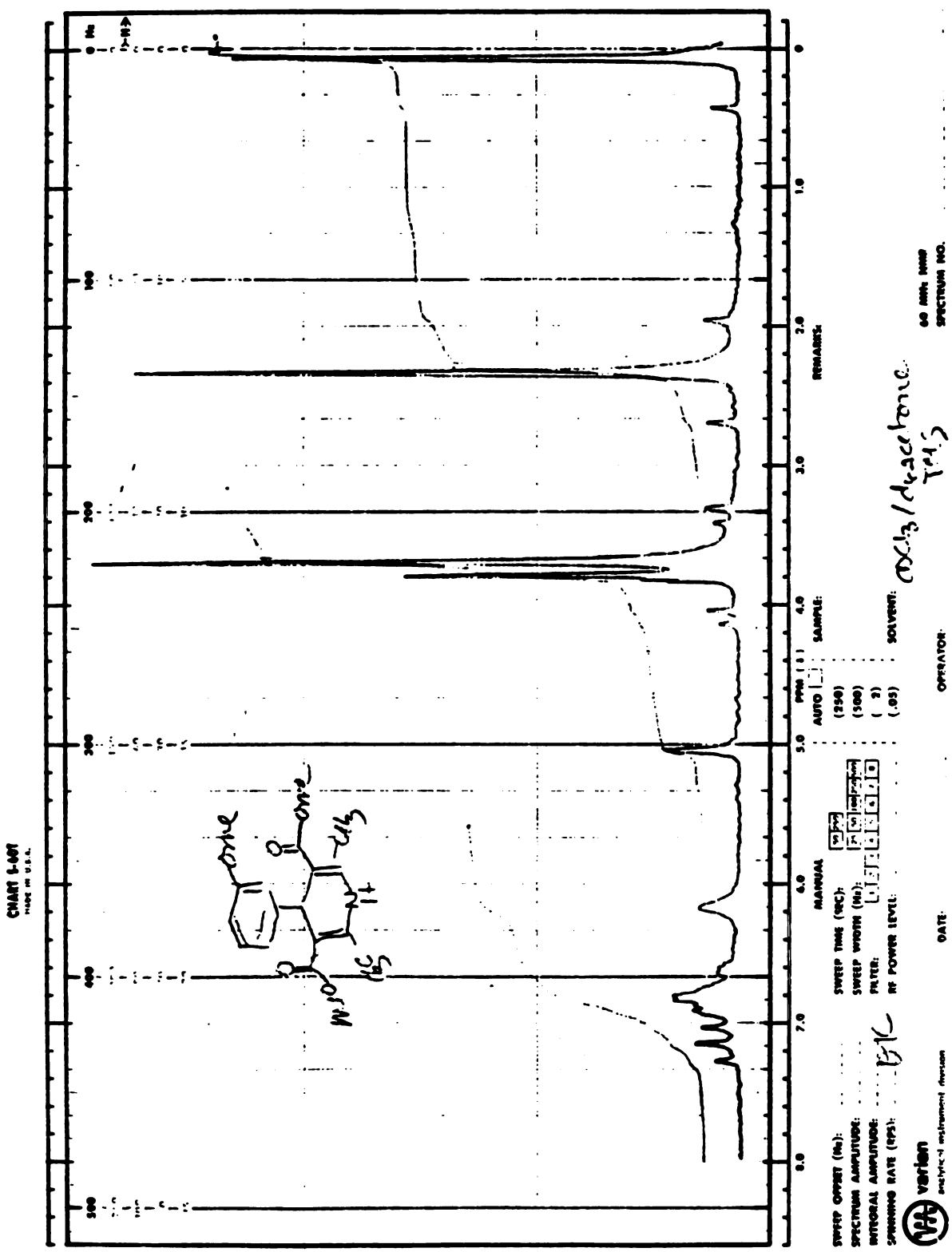

NMR Spectrum of 3-MeO DHP

Appendix A (cont'd)

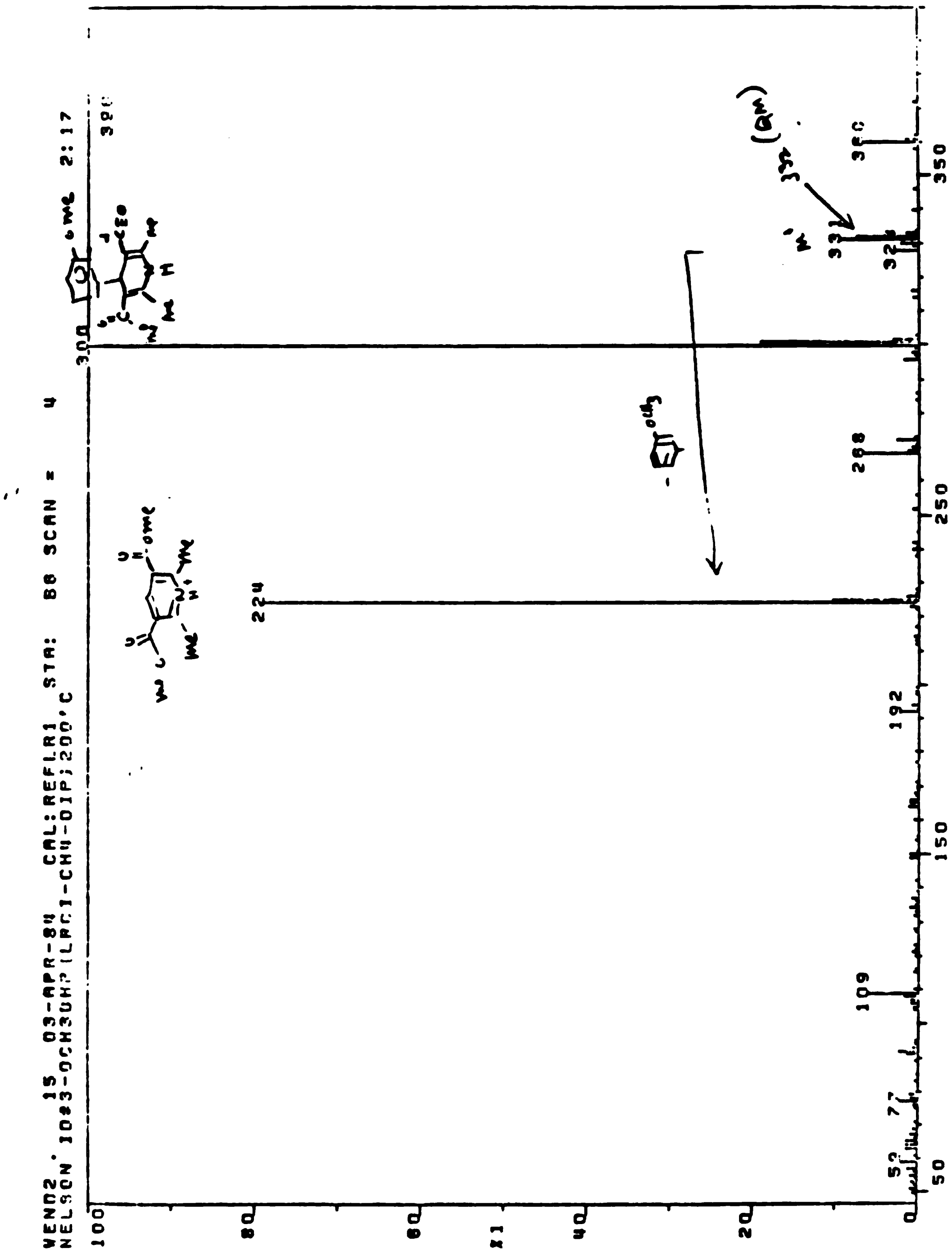

Mass Spectrum of 3-MeO DHP

Appendix A (cont'd)

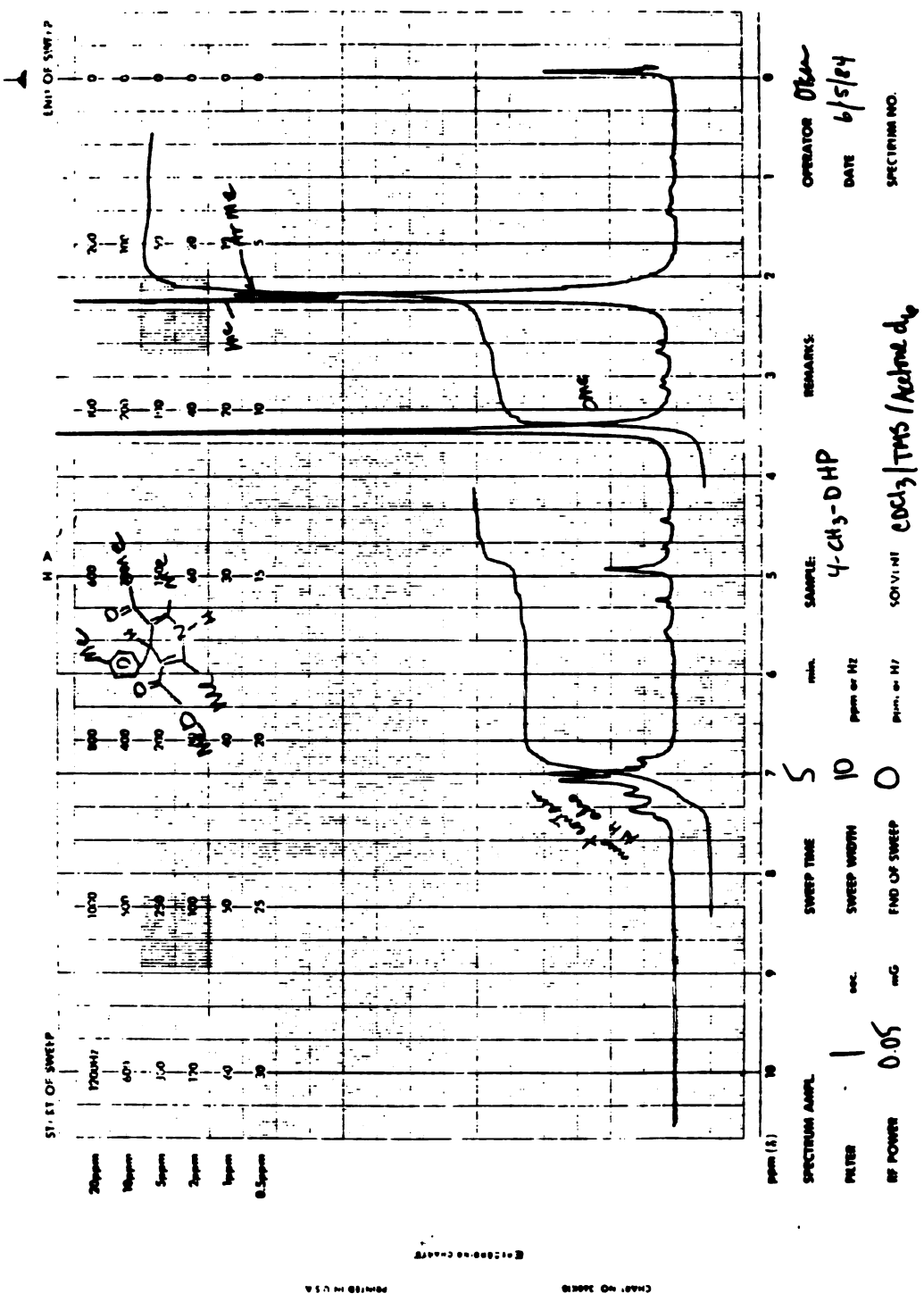

NMR Spectrum of 4-Me DHP

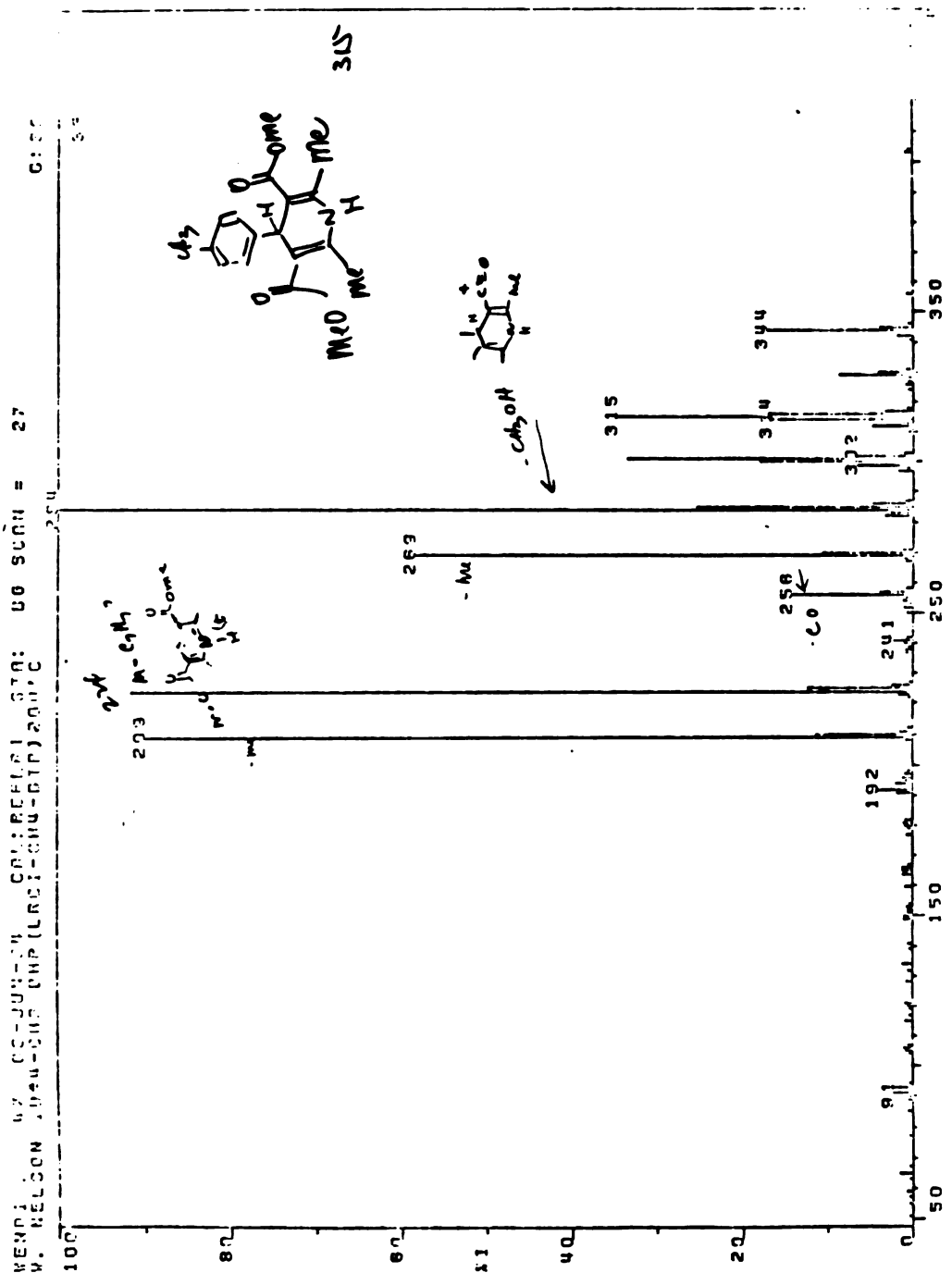

Mass Spectrum of 4-Me DHP

Appendix B

Derivation of Equations

Equation 1:

From the Law of Mass Action, the relationship between the concentration of a ligand (L), the concentration of a receptor (R) and the concentration of receptor-ligand complex (LR) is:

$$L + R \underset{k_2}{\overset{k_1}{\leftrightarrow}} LR \qquad \text{(i)}$$

where k_1 and k_2 are rate constants of the forward and reverse reactions, respectively. At equilibrium, the rate of the forward reaction ($k_1 * L * R$) equals the rate of the reverse reaction ($k_2 * LR$) and:

$$\frac{L * R}{LR} = \frac{k_2}{k_1} = K_d \qquad \text{(ii)}$$

where K_d is the dissociation constant. Also, at any time:

$$R_T = LR + R \qquad \text{(iii)}$$

where R_T is the total concentration of receptor. By rearranging equation (ii) to solve for R, and substituting the expression into equation (iii), equation (iii) becomes:

$$R_T = LR + \frac{K_d * LR}{L} \qquad \text{(iv)}$$

Solving for LR:

Appendix B (cont'd)

$$LR = \frac{R_T * L}{L + K_d} \qquad (v)$$

In addition to binding to receptors, the ligand can bind to sites with a K_d much higher than that of the receptor (K_d>>>L); or ligand can simply partition into membranes. In the former case, equation (v) reduces to:

$$LR = \frac{R_T}{K_d} * L \qquad (vi)$$

In the latter case, apparent binding also is directly proportional to the concentration of the ligand. Both types of apparent binding are included in the term "nonspecific" or "nonsaturable" binding, the magnitude of which is expressed as a proportionality constant. Therefore, by substituting B for LR, B_{max} for R_T, C for L and K_{ns} for the proportionality constant describing the extent of nonspecific binding, Equation 1 is obtained:

$$B = \frac{B_{max} * C}{C + K_d} + K_{ns} * C \qquad \text{Equation 1}$$

Equations 2 and 3:

For a single concentration of ligand (C_0), incubated with a single concentration of receptor, the value for total binding (B_0) from equation 1 would be:

$$B_0 = \frac{B_{max} * C_0}{C_0 + K_d} + K_{ns} * C_0$$

and the value for nonspecific binding (B_{ns}) would be:

$$B_{ns} = K_{ns} * C_0$$

with the difference between the two values (B_0-B_{ns}) equal to the total concentration of ligand-receptor complex at that concentration of ligand.

Appendix B (cont'd)

From the Law of Mass Action, if another ligand (I) that competes for the same receptor is present, the following interactions will take place:

$$R + \begin{matrix} L \leftrightarrow LR \\ I \leftrightarrow IR \end{matrix} \qquad \text{(vii)}$$

where I is the concentration of competing ligand (inhibitor) and IR is the concentration of the inhibitor-receptor complex. At equilibrium:

$$K_i = \frac{I * R}{IR} \qquad \text{(viii)}$$

where K_i is the dissociation constant for the inhibitor. In this case, the expression for the total concentration of receptors (R_T) is:

$$R_T = LR + IR + R \qquad \text{(ix)}$$

Solving for R in equation (ii) and for IR in equation (viii) and substituting these expressions into equation (ix) results in the following equation:

$$LR = \frac{R_T * L}{L + K_d\left(\frac{I}{K_i} + 1\right)} \qquad \text{(x)}$$

Experimentally, LR is determined as a function of I, and compared to LR in the absence of I (LR_0):

$$\frac{LR}{LR_0} = \frac{\dfrac{R_T + L}{L + K_d\left(\dfrac{I}{K_i + 1}\right)}}{\dfrac{R_T + L}{L + K_d}} = \frac{L + K_d}{L + K_d\left(\dfrac{I}{K_i} + 1\right)} \qquad \text{(xi)}$$

For equation (xi) to be valid, L in the absence of I must be approximately equal to L in the presence of I, necessitating that $R_T <<< K_d$.

If IC_{50} is defined as the concentration of I resulting in $LR/LR_0 = 0.5$, then equation

Appendix B (cont'd)

(xi) is reduced to:

$$IC_{50} = K_i\left(\frac{L}{K_d} + 1\right) \qquad \text{Equation 3}$$

Equation (xi) can be rearranged to:

$$\frac{LR}{LR_0} = \frac{1}{1 + \frac{I}{K_i\left(1 + \frac{L}{K_d}\right)}} = \frac{1}{1 + \frac{I}{IC_{50}}} \qquad \text{(xii)}$$

and therefore:

$$LR = LR_0 * \frac{1}{1 + \frac{I}{IC_{50}}} = \frac{B_0 - B_{ns}}{1 + \frac{I}{IC_{50}}} \qquad \text{(xiii)}$$

As for equation 1, the nonspecific binding of L (B_{ns}) must be included. In addition, a "slope factor" (n) is added as an exponential term to I and IC_{50} to allow for interactions between L and I such as positive ($n > 1$) and negative ($n < 1$) cooperativity of binding. This term also could have been included in Equation 1. The resulting equation is:

$$B = B_{ns} + \frac{B_0 - B_{ns}}{1 + \left(\frac{C}{IC_{50}}\right)^n} \qquad \text{Equation 2}$$

where C, in this case, is the concentration of I.

Equations 4 and 5:

Empirically, the relationship between concentrations of a drug and its response, either *in vitro* or *in vivo*, may be described by an equation of the general form:

$$E = \frac{E_{max} * C^n}{C^n + EC_{50}^n} \qquad \text{Equation 5}$$

where E is the effect or response, E_{max} is the maximum response and EC_{50} is the

concentration of drug at which 50% of the maximum effect is achieved. This equation allows for no response when the concentration is zero, an increase in response that is proportional to the concentration initially, and a leveling off of response as concentrations become very large. The steepness of the concentration-response relationship is described by n.

Many variations of equation 5 are possible. One such variation occurs when a drug causes a decrease in some baseline measurement, such as the force of contraction of muscle. The equation describing this inhibitory effect is:

$$E = E_0 - \frac{E_0 * C^n}{C^n + IC_{50}^n} = \frac{E_0 * IC_{50}^n}{C^n + IC_{50}^n} = \frac{E_0}{\left(\frac{C}{IC_{50}}\right)^n + 1} \qquad \text{Equation 4}$$

where E_0 is the initial response. Because the effect is inhibitory, IC_{50} is used instead of EC_{50}, but either term is appropriate.

In many cases, response to a drug can be related directly to the extent of receptor occupancy achieved by the drug and equations 4 and 5 can be related to the analogous equations relating drug concentration and receptor binding. If a compound has a receptor-mediated effect, then the following scheme may apply:

$$L + R \underset{k_2}{\overset{k_1}{\leftrightarrow}} LR \xrightarrow{k_3} E \qquad \text{(xiv)}$$

where E is the effect. If steady-state conditions are assumed for LR, then:

$$\frac{L * R}{LR} = \frac{k_2 + k_3}{k_1} = k_{act} = EC_{50} \qquad \text{(xv)}$$

Depending on the relative values of k_3 and k_2, EC_{50} may or may not be equal to K_d. If a compound is acting as a classical antagonist ($k_3 = 0$), then $IC_{50} = K_d$. In addition, if there

is an amplification system for response or spare receptors are present, then $EC_{50} < K_d$.

If a compound is an agonist, in addition to having affinity for a receptor, it also has efficacy or intrinsic activity. That is, although compounds may have the same affinity (K_d) for a receptor and the same rate of production of response (k_3*LR), they may have different levels of effectiveness in producing a response. This can be incorporated into the equilibrium binding equation as follows:

$$E = e * LR = \frac{e * B_{max} * C}{C + EC_{50}} = \frac{E_{max} * C}{C + EC_{50}} \qquad \text{(xvi)}$$

where e represents the efficacy.

Equation 6

Binding of a drug to plasma proteins can be described by the same equations developed for ligand-receptor interactions. Therefore, at equilibrium:

$$\frac{DP}{D * P} = K_A \qquad \text{(xvii)}$$

where D is the concentration of unbound drug, P is the concentration of free protein, DP is the concentration of bound drug, and K_A is the association constant. Because only the unbound drug is believed to exert a pharmacologic effect, the binding is usually expressed as the unbound fraction (fu):

$$fu = \frac{D}{D + DP} \qquad \text{(xviii)}$$

In equilibrium dialysis experiments, the unbound concentration of drug is equal to the concentration in the buffer at the end of dialysis (C'_b) and the bound concentration (C'_{bnd}) can be calculated from the plasma concentration (C'_p) minus the concentration in

buffer (C'_b). Therefore:

$$fu = \frac{C'_b}{C'_{bnd} + C'_b} \qquad \text{(xix)}$$

However, because of the higher osmotic pressure of the plasma, there is an osmotic water shift and at the end of the dialysis period the volume of the plasma exceeds the volume of the buffer. This volume shift is expressed as the fractional increase in volume (δ), determined independently. The unbound concentration should not be affected by this volume shift but the bound concentration will be lower. Therefore, C'_{bnd} is multiplied by $(1 + \delta)$ to obtain the concentration of bound drug in the original volume of plasma. Therefore, the equation describing fu after an equilibrium dialysis experiment is as follows:

$$fu = \frac{C'_b}{C'_{bnd}(1 + \delta) + C'_b} \qquad \text{Equation 6}$$

Appendix C. Results of Computer Fits of Data from Radioligand Binding Experiments in Rabbit Ventricular Membrane Particulates

Compound	IC_{50} (M)	Slope Factor (n)	-Log IC_{50}	p-value for IC_{50}	-Log K_i[1]
Nitrendipine	1.84E-10	0.84	9.74	0.0001	9.85
	7.04E-10	1.24	9.15	0.0001	9.33
	5.91E-10	1.08	9.23	0.045	9.33
Mean	**4.93E-10**	**1.05**	**9.37**		**9.50**
S.D.	**2.74E-10**	**0.20**	**0.32**		**0.30**
Nifedipine	6.58E-10	1.08	9.18	0.0001	9.34
	1.43E-09	1.31	8.84	0.0005	8.98
	1.15E-09	0.95	8.94	0.001	9.07
Mean	**1.08E-09**	**1.11**	**8.99**		**9.13**
S.D.	**3.91E-10**	**0.18**	**0.17**		**0.19**
Nimodipine	1.49E-09	1.16	8.83	0.003	9.00
	2.09E-09	1.02	8.68	0.018	8.83
	1.85E-09	1.96	8.73	0.0005	8.85
Mean	**1.81E-09**	**1.38**	**8.75**		**8.90**
S.D.	**3.02E-10**	**0.51**	**0.074**		**0.09**
Nicardipine	1.36E-09	1.92	8.87	0.002	8.99
	1.60E-09	1.91	8.80	0.0005	8.90
	1.17E-09	1.02	8.93	0.087	9.06
Mean	**1.38E-09**	**1.62**	**8.86**		**8.98**
S.D.	**2.15E-10**	**0.52**	**0.068**		**0.08**
Nisoldipine	1.17E-09	1.66	8.93	0.001	9.06
	1.24E-09	1.86	8.91	0.003	9.01
	1.81E-09	2.05	8.74	0.02	8.87
Mean	**1.41E-09**	**1.86**	**8.86**		**8.98**
S.D.	**3.51E-10**	**0.20**	**0.10**		**0.10**

Appendix C (cont'd)

Compound	IC_{50} (M)	Slope Factor (n)	-Log IC_{50}	p-value for IC_{50}	-Log K_i[1]
MR-I-12	4.91E-09	1.17	8.31	0.0001	8.49
	4.66E-09	0.99	8.33	0.001	8.46
	4.37E-09	0.97	8.36	0.003	8.48
Mean	**4.65E-09**	**1.04**	**8.33**		**8.48**
S.D.	**2.70E-10**	**0.11**	**0.025**		**0.02**
2,6-Cl DHP	3.58E-08	1.56	7.45	0.0001	7.62
	2.01E-08	1.55	7.70	0.0001	7.85
	7.75E-09	1.12	8.11	0.0001	8.23
Mean	**2.12E-08**	**1.41**	**7.75**		**7.90**
S.D.	**1.41E-08**	**0.25**	**0.34**		**0.31**
3-MeO DHP	8.09E-08	1.06	7.09	0.0001	7.27
	5.21E-08	1.14	7.28	0.0001	7.42
	5.77E-08	1.04	7.24	0.0005	7.36
Mean	**6.36E-08**	**1.08**	**7.20**		**7.35**
S.D.	**1.53E-08**	**0.05**	**0.10**		**0.07**
2-Cl DHP	1.49E-07	1.50	6.83	0.006	7.00
	1.78E-07	0.96	6.75	0.002	6.88
	2.01E-07	1.07	6.70	0.0001	6.82
Mean	**1.76E-07**	**1.18**	**6.76**		**6.90**
S.D.	**2.61E-08**	**0.29**	**0.065**		**0.09**
2-MeO DHP	3.16E-08	1.11	7.50	0.0001	7.62
	3.38E-08	0.99	7.47	0.0005	7.57
	6.18E-08	1.60	7.21	0.002	7.33
Mean	**4.24E-08**	**1.23**	**7.39**		**7.51**
S.D.	**1.68E-08**	**0.32**	**0.16**		**0.15**

Appendix C (cont'd)

Compound	IC_{50} (M)	Slope Factor (n)	-Log IC_{50}	p-value for IC_{50}	-Log K_i[1]
4-Cl DHP	2.00E-07	1.09	6.70	0.0005	6.82
	2.66E-07	1.15	6.58	0.001	6.71
	2.86E-07	1.19	6.54	0.0001	6.66
Mean	**2.51E-07**	**1.14**	**6.61**		**6.73**
S.D.	**4.50E-08**	**0.05**	**0.082**		**0.08**
4-Me DHP	1.20E-06	0.97	5.92	0.0001	6.04
	1.19E-06	1.12	5.92	0.0001	6.06
	1.60E-06	1.25	5.80	0.0005	5.91
Mean	**1.33E-06**	**1.11**	**5.88**		**6.00**
S.D.	**2.34E-07**	**0.14**	**0.073**		**0.08**

[1]K_i was calculated from IC_{50} using equation 3 (Chapter 3)

Appendix D. Results of Computer Fits of Data from Pharmacologic Response Experiments in Rabbit Right Ventricular Papillary Muscles

Compound	E_0 (% Control)	IC_{50} (M)	Slope Factor (n)	-Log IC_{50}	p-value for IC_{50}
Nitrendipine	92.2	2.62E-07	0.63	6.58	0.0001
	97.7	9.57E-07	0.68	6.02	0.0001
	105.0	7.71E-07	0.50	6.11	0.0001
Mean	**98.3**	**6.63E-07**	**0.60**	**6.24**	
S.D.	**6.4**	**3.60E-07**	**0.09**	**0.30**	
Nifedipine	103.4	6.98E-08	0.84	7.16	0.034
	98.1	5.87E-08	0.91	7.23	0.0001
	102.6	2.68E-08	0.67	7.57	0.006
Mean	**101.4**	**5.18E-08**	**0.81**	**7.32**	
S.D.	**2.9**	**2.23E-08**	**0.12**	**0.22**	
Nimodipine	84.7	9.71E-07	0.57	6.01	0.009
	92.7	1.33E-06	0.82	5.88	0.0005
	103.2	1.02E-06	0.58	5.99	0.008
Mean	**93.5**	**1.11E-06**	**0.66**	**5.96**	
S.D.	**9.3**	**1.95E-07**	**0.14**	**0.07**	
Nicardipine	106.4	1.12E-06	0.49	5.95	0.0005
	106.4	5.00E-06	0.49	5.30	0.001
	98.0	9.15E-07	0.39	6.04	0.053
Mean	**103.6**	**2.35E-06**	**0.46**	**5.76**	
S.D.	**4.8**	**2.30E-06**	**0.06**	**0.40**	
Nisoldipine	102.5	1.12E-07	0.50	6.95	0.003
	96.9	1.38E-07	0.64	6.86	0.0001
	110.7	3.30E-08	0.59	7.48	0.0005
Mean	**103.4**	**9.43E-08**	**0.58**	**7.10**	
S.D.	**6.9**	**5.47E-08**	**0.07**	**0.34**	

Appendix D (cont'd)

Compound	E_0 (% Control)	IC_{50} (M)	Slope Factor (n)	-Log IC_{50}	p-value for IC_{50}
MR-I-12	100.0	1.66E-06	0.87	5.78	0.0005
	95.4	3.57E-07	0.46	6.45	0.029
	88.0	1.93E-07	0.64	6.71	0.004
Mean	**94.5**	**7.37E-07**	**0.66**	**6.31**	
S.D.	**6.1**	**8.04E-07**	**0.21**	**0.48**	
2,6-Cl DHP	82.6	1.60E-06	0.70	5.80	0.0005
	113.3	9.69E-07	0.52	6.01	0.002
	91.4	1.64E-06	0.68	5.79	0.004
Mean	**95.8**	**1.40E-06**	**0.63**	**5.86**	
S.D.	**15.8**	**3.76E-07**	**0.10**	**0.13**	
3-MeO DHP	92.9	2.36E-06	1.12	5.63	0.0001
	91.9	5.19E-07	0.67	6.28	0.006
	90.3	1.79E-06	0.64	5.75	0.001
Mean	**91.7**	**1.56E-06**	**0.81**	**5.89**	
S.D.	**1.3**	**9.42E-07**	**0.27**	**0.35**	
2-Cl DHP	98.0	1.08E-05	0.83	4.97	0.001
	103.4	3.29E-06	0.49	5.48	0.009
	107.0	5.90E-06	0.73	5.23	0.002
Mean	**102.8**	**6.66E-06**	**0.68**	**5.23**	
S.D.	**4.5**	**3.81E-06**	**0.17**	**0.26**	
2-MeO DHP	103.2	1.61E-06	1.25	5.79	0.0001
	97.2	1.61E-06	1.09	5.79	0.0005
	116.8	1.19E-06	1.16	5.92	0.001
	93.6	1.17E-06	1.01	5.93	0.003
Mean	**102.7**	**1.40E-06**	**1.13**	**5.86**	
S.D.	**10.2**	**2.48E-07**	**0.10**	**0.08**	

Appendix D (cont'd)

Compound	E_0 (% Control)	IC_{50} (M)	Slope Factor (n)	-Log IC_{50}	p-value for IC_{50}
4-Cl DHP	96.7	1.70E-05	0.88	4.77	0.0005
	95.8	1.81E-05	1.05	4.74	0.0005
	96.3	1.34E-05	0.85	4.87	0.002
Mean	**96.3**	**1.62E-05**	**0.93**	**4.79**	
S.D.	**0.5**	**2.46E-06**	**0.11**	**0.07**	
4-Me DHP	100.9	3.32E-05	0.74	4.48	0.004
	106.3	4.34E-06	0.51	5.36	0.001
	102.8	2.63E-05	0.89	4.58	0.0005
	106.2	5.36E-06	0.49	5.27	
Mean	**104.1**	**1.73E-05**	**0.66**	**4.92**	
S.D.	**2.7**	**1.47E-05**	**0.19**	**0.46**	

Appendix E. Results of Radioligand Binding and Pharmacologic Response Experiments in Rabbit Aorta[1]

Compound	K_i, Binding (M)	IC_{50}, Response (M)
Nitrendipine	1.26E-9	2.10E-9
2,6-Cl DHP	2.39E-8	5.71E-8
Nimodipine	3.33E-8	7.76E-9
MR-I-12	5.85E-8	1.53E-8
2-MeO DHP	8.40E-8	3.55E-8
4-Cl DHP	4.73E-7	2.08E-7
4-Me DHP	2.31E-6	2.01E-7

[1] From Gordon *et al.*, Clin Res **34**: 399A, 1986.

Appendix F. Results of Computer Fits of Data from Radioligand Binding Experiments in Rat Myocardial Membrane Particulates

Compound	IC_{50} (M)	Slope Factor (n)	-Log IC_{50}	p-value for IC_{50}	-Log K_i[1]
Nitrendipine	6.76E-10	1.15	9.17	0.0005	9.26
	6.88E-10	0.90	9.16	0.0005	9.25
	4.24E-10	1.21	9.37	0.0001	9.46
Mean	**5.96E-10**	**1.09**	**9.24**		**9.32**
S.D.	**1.49E-10**	**0.16**	**0.12**		**0.12**
Nifedipine	1.17E-09	1.22	8.93	0.003	9.03
	8.85E-10	1.08	9.05	0.0001	9.15
	9.49E-10	1.11	9.02	0.0001	9.12
Mean	**1.00E-09**	**1.14**	**9.00**		**9.10**
S.D.	**1.50E-10**	**0.07**	**0.06**		**0.06**
Nimodipine	8.87E-10	0.96	9.05	0.0001	9.15
	1.81E-09	1.05	8.74	0.0005	8.83
	1.25E-09	1.41	8.90	0.0005	9.01
Mean	**1.32E-09**	**1.14**	**8.90**		**9.00**
S.D.	**4.65E-10**	**0.24**	**0.15**		**0.16**
Nicardipine	1.23E-09	1.46	8.91	0.002	9.01
	1.73E-09	1.80	8.76	0.0001	8.85
	1.35E-09	1.46	8.87	0.0001	8.97
Mean	**1.44E-09**	**1.57**	**8.85**		**8.94**
S.D.	**2.61E-10**	**0.20**	**0.08**		**0.08**
Nisoldipine	7.97E-10	1.82	9.10	0.0001	9.19
	1.31E-09	2.12	8.88	0.0005	8.97
	7.62E-10	1.31	9.12	0.0005	9.21
Mean	**9.56E-10**	**1.75**	**9.03**		**9.12**
S.D.	**3.07E-10**	**0.41**	**0.13**		**0.13**

Appendix F (cont'd)

Compound	IC_{50} (M)	Slope Factor (n)	-Log IC_{50}	p-value for IC_{50}	-Log K_i[1]
MR-I-12	3.94E-09	0.78	8.40	0.001	8.52
	5.86E-09	1.17	8.23	0.0001	8.33
	5.73E-09	1.09	8.24	0.002	8.34
Mean	**5.18E-09**	**1.01**	**8.29**		**8.40**
S.D.	**1.07E-09**	**0.21**	**0.10**		**0.11**
2,6-Cl DHP	7.92E-09	0.97	8.10	0.003	8.20
	2.11E-08	1.08	7.68	0.001	7.77
	1.21E-08	1.15	7.92	0.0005	8.01
Mean	**1.37E-08**	**1.07**	**7.90**		**7.99**
S.D.	**6.74E-09**	**0.09**	**0.21**		**0.21**
3-MeO DHP	7.09E-08	0.96	7.15	0.0001	7.24
	6.51E-08	1.08	7.19	0.003	7.28
	6.96E-08	0.86	7.16	0.001	7.27
Mean	**6.85E-08**	**0.97**	**7.16**		**7.26**
S.D.	**3.04E-09**	**0.11**	**0.02**		**0.02**
2-Cl DHP	2.13E-07	1.06	6.67	0.0005	6.76
	2.20E-07	1.22	6.66	0.0001	6.75
	2.11E-07	1.61	6.68	0.0005	6.79
Mean	**2.15E-07**	**1.30**	**6.67**		**6.77**
S.D.	**4.73E-09**	**0.28**	**0.01**		**0.02**
2-MeO DHP	5.09E-08	1.14	7.29	0.0005	7.38
	5.23E-08	1.00	7.28	0.001	7.37
	3.92E-08	0.88	7.41	0.0001	7.50
Mean	**4.75E-08**	**1.01**	**7.33**		**7.42**
S.D.	**7.19E-09**	**0.13**	**0.07**		**0.07**

Appendix F (cont'd)

Compound	IC_{50} (M)	Slope Factor (n)	-Log IC_{50}	p-value for IC_{50}	-Log K_i[1]
4-Cl DHP	3.34E-07	1.06	6.48	0.0001	6.58
	2.22E-07	1.17	6.65	0.0005	6.74
	1.91E-07	0.83	6.72	0.002	6.81
Mean	**2.49E-07**	**1.02**	**6.62**		**6.71**
S.D.	**7.52E-08**	**0.17**	**0.13**		**0.12**
4-Me DHP	1.81E-06	1.09	5.74	0.002	5.84
	1.64E-06	1.17	5.79	0.0001	5.88
	1.81E-06	1.19	5.74	0.0005	5.83
Mean	**1.75E-06**	**1.15**	**5.76**		**5.85**
S.D.	**9.81E-08**	**0.05**	**0.02**		**0.03**

[1]K_i was calculated from IC_{50} using equation 3 (Chapter 3)

Appendix G. Results of Computer Fits of Data from Pharmacologic Response Experiments in Rat Right Ventricular Strips

Compound	E_0 (% Control)	IC_{50} (M)	Slope Factor (n)	-Log IC_{50}	p-value for IC_{50}
Nitrendipine	104.4	3.41E-06	0.26	5.47	0.191
	111.0	4.66E-05	0.84	4.33	0.002
	124.4	1.52E-03	0.06	2.82	0.912
Mean	**113.3**	**5.23E-04**	**0.39**	**4.21**	
S.D.	**10.2**	**8.63E-04**	**0.40**	**1.33**	
Nifedipine	107.1	1.82E-07	0.37	6.74	0.005
	101.2	4.24E-07	0.18	6.37	0.096
	110.2	1.43E-05	0.25	4.84	0.073
Mean	**106.2**	**4.97E-06**	**0.27**	**5.99**	
S.D.	**4.6**	**8.08E-06**	**0.10**	**1.01**	
Nimodipine	115.8	2.30E-05	0.86	4.64	0.0001
	89.2	1.94E-06	0.19	5.71	0.364
	86.9	5.10E-06	0.60	5.29	0.006
Mean	**97.3**	**1.00E-05**	**0.55**	**5.21**	
S.D.	**16.1**	**1.14E-05**	**0.34**	**0.54**	
Nicardipine	117.6	6.78E-05	0.36	4.17	0.001
	107.7	9.08E-05	0.29	4.04	0.018
	113.3	1.18E-04	0.47	3.93	0.027
Mean	**112.9**	**9.22E-05**	**0.37**	**4.05**	
S.D.	**5.0**	**2.51E-05**	**0.09**	**0.12**	
Nisoldipine	90.8	1.10E-06	0.45	5.96	0.006
	98.1	2.10E-06	0.39	5.68	0.0005
	98.4	2.16E-06	0.11	5.67	0.669
Mean	**95.8**	**1.79E-06**	**0.32**	**5.77**	
S.D.	**4.3**	**5.95E-07**	**0.18**	**0.17**	

Appendix H

Summary of Calcium Concentration Response Experiments

Results of Computer Fits of Data from Calcium Concentration-Response Experiments in Rabbit Papillary Muscle and Rat Right Ventricular Strips

	Rabbit		Rat	
Experiment	**EC_{50} (mM) (p-value)**	**n (p-value)**	**EC_{50} (mM) (p-value)**	**n (p-value)**
1[1]	1.31 (.0001)	2.29 (.0001)	1.60 (.0001)	2.89 (.0001)
2	1.69 (.186)	1.05 (.11)	1.33 (.0001)	2.02 (.0001)
3	6.08 (.038)	1.58 (.0001)	3.54 (.178)	1.29 (.009)
4	1.54 (.0001)	2.39 (.0001)	1.93 (.0001)	2.50 (.0001)
5	1.52 (.0001)	2.98 (.0001)	1.49 (.0001)	2.85 (.0001)
Mean[2]	**2.43**	**2.06**	**1.98**	**2.31**
S.D.	**2.05**	**0.75**	**0.90**	**0.67**

[1]Graphs shown in Chapter 4

[2]No statistically significant difference between species for either parameter

Appendix H (cont'd)

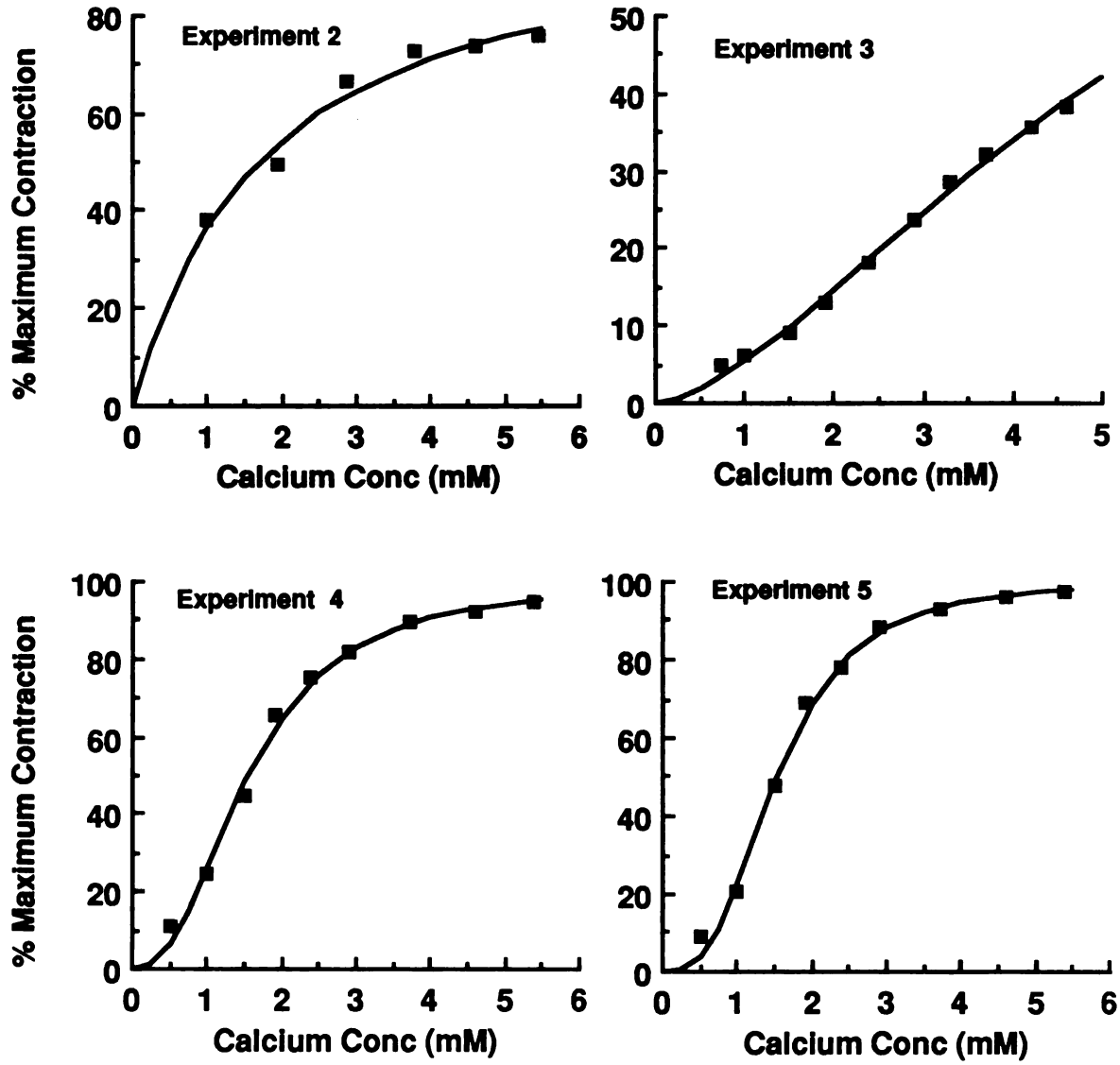

Data from calcium concentration-response experiments in rabbit myocardium showing both the experimental points and the computer fits of the data using Equation 5 (Chapter 4).

Appendix H (cont'd)

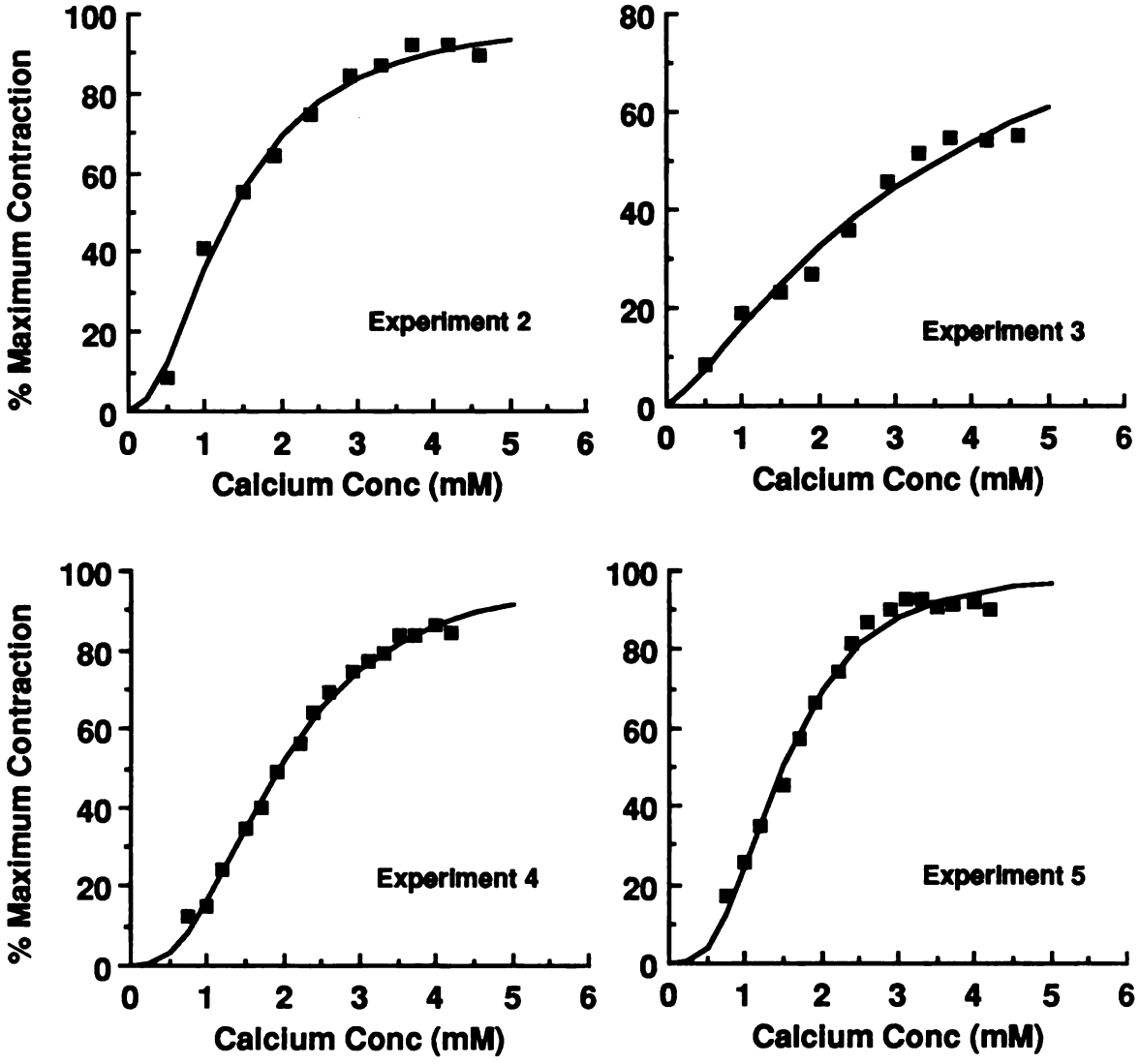

Data from calcium concentration-response experiments in rat myocardium showing both the experimental points and the computer fits of the data using Equation 5 (Chapter 4).

Appendix I

Chemical Structures of Additional 1,4-Dihydropyridine Compounds

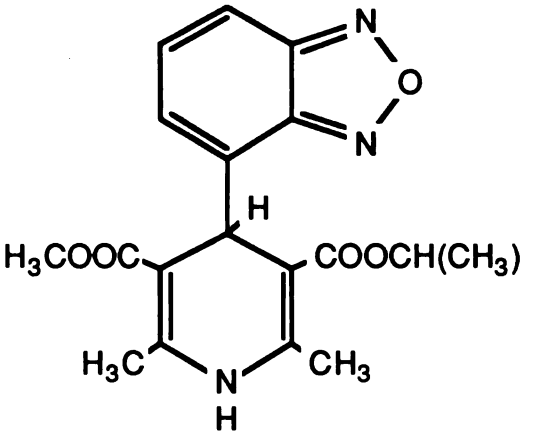

PN 200-110

Chemical structure of PN 200-110 (Isopropyl 4-(2,1,3-benzoxadiazol-4-yl)-1,4-dihydro-2,6-dimethyl-5-methoxycarbonylpyridine-3-carboxylate)

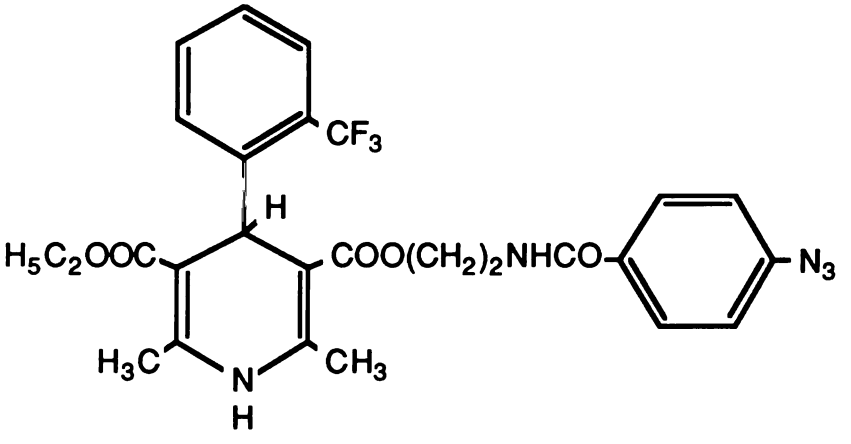

Azidopine

Chemical structure of azidopine (2-(4-azidobenzyl)aminoethyl ethyl 1,4-dihydropyridine-2,6-dimethyl-4(2-trifluoromethyl)-pyridine-3,5-dicarboxylate)

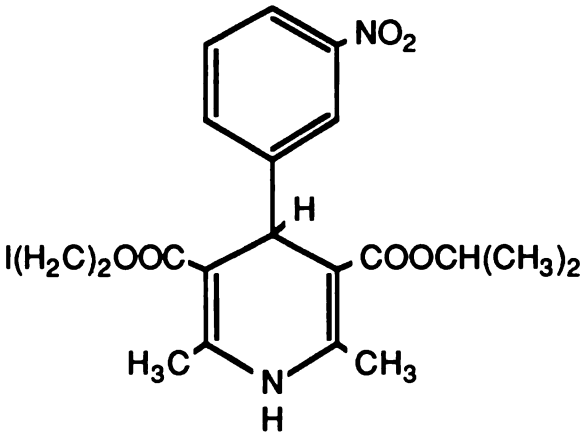

BAY P 8857

Chemical structure of Bay P 8857 (2-iodoethyl isopropyl 1,4-dihydro-pyridine-2,6-dimethyl-4-(3-nitrophenyl)-pyridine-3,5-dicarboxylate)

Appendix J

SDS-PAGE Stock Solutions
Laemmli Discontinuous Buffer System

1. Acrylamide Solution

Acrylamide	30 g
Bisacrylamide	0.8 g
DDW qs to	100 ml

Store at 4° C in dark bottle after filtering through Whatman #1 filter. Stable for 1 month.

2. Separating Gel Buffer

Tris	6.81 g (0.562 M)
SDS	0.1 g
DDW qs to ≈	90 ml
Adjust pH to 8.8 with	1 N HCl
DDW qs to	100 ml

Store at 4° C. Stable for 2 weeks.

3. Stacking Gel Buffer

Tris	1.682 g (0.139 M)
SDS	0.1 g
DDW qs to ≈	80 ml
Adjust pH to 6.8 with	1N HCl
DDW qs to	100 ml

Store at 4° C. Stable for 2 weeks.

Appendix J (cont'd)

4. Electrode Buffer

Tris	6.05 g (0.025 M)
Glycine	28.8 g (0.192 M)
SDS	2.0 g (0.1%)
DDW qs to	2 L

Check that pH is ≈ 8.3

5. Solubilizing Buffer (Dilute 1:1 with protein sample)

Tris	1.51 g (0.125 M)
Glycerol	20 ml **or**
Sucrose	20 g
DDW qs to ≈	50 ml
Adjust pH to 6.8 with	1 N HCl
SDS	4.0 g
2-Mercaptoethanol	10 ml
Bromophenol Blue	0.01 g
DDW qs to	100 ml

Store at 4° C. Stable for 1 month

6. TEMED (N,N,N',N'-Tetramethylethylenediamine)

Use as is

7. Ammonium persulfate

100 mg/ml in DDW

Make fresh

8. Staining/Fixative Solution

Coomassie Blue	1.25 g
Methanol	200 ml
Glacial Acetic Acid	35 ml
DDW	265 ml

9. Destaining Solution

Methanol	50 ml
Glacial Acetic Acid	70 ml
DDW	880 ml

Preparation of Polyacrylamide Gels

1. Separating Gel

Final Concentrations:

Acrylamide	10%
Bisacrylamide	0.27%
Tris	0.375 M, pH 8.8
SDS	0.07%

Method of Preparation:

Acrylamide Solution (# 1)	10 ml
Separating Buffer (#2)	20 ml
Degas using water aspirator.	
Add:	8 µl TEMED (0.025%)
	80 µl Ammonium persulfate solution (0.027%)

Gently mix and pour between glass plates.

Appendix J (cont'd)

2. Stacking Gel

Final Concentrations:

Acrylamide	3%
Bisacrylamide	0.08%
Tris	0.125 M, pH 6.8
SDS	0.09%

Method of Preparation

Acrylamide Solution (#1)	1 ml
Stacking Buffer (#3)	9 ml
Degas using water aspirator	
Add:	5 µl TEMED
	75 µl Ammonium persulfate solution

Gently mix and pour on top of separating gel

Appendix K

Summary of Data for Each Volunteer in Diltiazem Study

Volunteer 1 (D.S.)- Concentration-Time Data for Diltiazem, NDD and DAD and Measures of Pharmacologic Response

Time (min)	Diltiazem Conc. (ng/ml)	NDD Conc. (ng/ml)	DAD Conc. (ng/ml)	PR Interval (msec)	MAP[1] (mm Hg)	HR[2] (beats/min)
0	n.d.[3]	n.d.	n.d.	156.0	83	64
30	n.d.	n.d.	n.d.	167.2	90	75
45	14.0	7.3	n.d.	192.0	100	66
60	27.1	11.5	n.d.	186.4	93	61
90	44.0	16.1	7.5	204.0	99	65
120	60.3	20.1	9.3	194.4	101	60
180	91.3	36.1	14.7	198.4	82	70
255	97.9	33.0	15.3	198.4	79	66
360	52.2	28.8	16.8	168.0	88	68
480	38.8	25.5	16.6	192.0	84	64
600	21.8	18.6	15.5	161.6	81	57
720	15.1	14.4	12.7	160.0	84	68
1440	4.8	7.3	10.7	150.4	89	70

[1]Mean arterial pressure, obtained from the Dinamap-845XT Vital Signs Monitor

[2]Heart rate, obtained from the Dinamap-845XT Vital Signs Monitor

[3]Not detected

Appendix K (cont'd)

Volunteer 1 (D.S.)-Summary of Urinary Data

Time (min)	Urine Volume (ml)	pH	Diltiazem Conc. (ng/ml)	NDD Conc. (ng/ml)	DAD Conc. (ng/ml)
30	15	6.00	n.d.[1]	83	n.d.
90	175	6.82	1034	1436	44
150	355	6.74	309	311	73
210	465	6.79	853	989	48
300	370	6.94	769	1394	62
420	21	7.13	605	2207	96
540	265	6.88	424	498	62
660	355	6.70	284	958	65
780	373	6.14	236	522	109
1440	390	6.03	902	1826	496

[1]Not detected

Appendix K (cont'd)

Volunteer 2 (J.S.)- Concentration-Time Data for Diltiazem, NDD and DAD and Measures of Pharmacologic Response

Time (min)	Diltiazem Conc. (ng/ml)	NDD Conc. (ng/ml)	DAD Conc. (ng/ml)	PR Interval (msec)	MAP[1] (mm Hg)	HR[2] (beats/min)
0	n.d.[3]	n.d.	n.d.	142.4	81	59
30	28.6	7.1	n.d.	123.2	98	63
45	129.0	17.6	7.6	142.4	83	65
60	200.3	29.2	9.0	155.2	70	64
90	303.8	50.0	15.9	148.8	74	65
120	302.4	51.0	15.9	156.8	81	68
180	271.3	53.7	20.1	154.4	94	59
255	174.6	47.6	17.5	144.0	83	56
360	107.4	38.7	16.4	149.6	86	59
480	64.2	29.4	12.9	148.0	90	56
600	51.4	27.3	12.4	120.0	86	53
720	33.3	21.1	10.2	120.0	81	68
1440	8.3	9.0	5.9	120.0	83	76

[1]Mean arterial pressure, obtained from the Dinamap-845XT Vital Signs Monitor

[2]Heart rate, obtained from the Dinamap-845XT Vital Signs Monitor

[3]Not detected

Appendix K (cont'd)

Volunteer 2 (J.S.)-Summary of Urinary Data

Time (min)	Urine Volume (ml)	pH	Diltiazem Conc. (ng/ml)	NDD Conc. (ng/ml)	DAD Conc. (ng/ml)
30	158	6.70	45.6	n.d.[1]	n.d.
90	730	6.87	1014	401	40
150	365	6.90	1936	1663	89
210	345	6.68	1504	977	73
300	145	6.68	2918	3929	222
420	640	6.53	1126	1032	131
540	100	7.11	523	3743	89
660	340	6.75	697	1237	81
780	505	6.46	557	795	106
1440	360	5.99	1100	2249	172

[1]Not detected

Appendix K (cont'd)

Volunteer 3 (J.D.)- Concentration-Time Data for Diltiazem, NDD and DAD and Measures of Pharmacologic Response

Time (min)	Diltiazem Conc. (ng/ml)	NDD Conc. (ng/ml)	DAD Conc. (ng/ml)	PR Interval (msec)	MAP[1] (mm Hg)	HR[2] (beats/min)
0	n.d.[3]	n.d.	n.d.	137.6	85	56
30	n.d.	n.d.	n.d.	140.0	89	60
45	n.d.	n.d.	n.d.	140.0	89	50
60	7.0	n.d.	n.d.	137.6	91	44
90	21.8	6.5	n.d.	140.0	85	49
120	31.7	8.7	n.d.	142.4	94	48
180	55.1	14.2	n.d.	151.2	94	45
255	144.8	29.6	10.9	160.0	96	44
360	116.5	29.8	13.9	152.0	88	51
480	77.0	26.5	12.5	138.4	98	46
600	57.7	22.4	11.5	137.6	91	41
720	40.4	19.1	10.9	140.0	96	43
1440	8.8	8.0	n.d.	131.2	80	57

[1]Mean arterial pressure, obtained from the Dinamap-845XT Vital Signs Monitor

[2]Heart rate, obtained from the Dinamap-845XT Vital Signs Monitor

[3]Not detected

Appendix K (cont'd)

Volunteer 3 (J.D.)-Summary of Urinary Data

Time (min)	Urine Volume (ml)	pH	Diltiazem Conc. (ng/ml)	NDD Conc. (ng/ml)	DAD Conc. (ng/ml)
30	130	6.63	n.d.[1]	n.d.	n.d.
90	105	7.14	n.d.	118	n.d.
150	120	7.04	294	534	n.d.
210	300	6.85	494	607	n.d.
300	250	6.83	1372	1797	78
420	240	6.81	1314	2164	89
540	210	6.94	544	1861	60
660	195	6.35	763	1693	71
780	185	6.50	630	1224	108
1440	553	6.00	510	1184	83

[1]Not detected

Appendix K (cont'd)

Volunteer 4 (M.N.)- Concentration-Time Data for Diltiazem, NDD and DAD and Measures of Pharmacologic Response

Time (min)	Diltiazem Conc. (ng/ml)	NDD Conc. (ng/ml)	DAD Conc. (ng/ml)	PR Interval (msec)	MAP[1] (mm Hg)	HR[2] (beats/min)
0	n.d.[3]	n.d.	n.d.	184.8	81	77
30	n.d.	n.d.	n.d.	198.4	75	58
45	7.5	n.d.	n.d.	184.0	74	61
60	81.4	19.4	n.d.	206.4	80	66
90	202.3	51.3	10.3	229.6	77	65
120	191.6	47.0	14.6	236.8	77	62
180	180.1	42.1	15.1	213.6	76	61
255	153.6	44.2	14.0	190.4	81	60
360	115.5	42.6	15.3	192.0	85	61
480	83.5	34.2	14.3	193.6	80	63
600	60.6	29.7	13.4	176.8	70	55
720	41.4	23.3	12.0	170.4	82	68
1440	9.9	8.1	n.d.	174.4	92	88

[1]Mean arterial pressure, obtained from the Dinamap-845XT Vital Signs Monitor

[2]Heart rate, obtained from the Dinamap-845XT Vital Signs Monitor

[3]Not detected

Appendix K (cont'd)

Volunteer 4 (M.N.)-Summary of Urinary Data

Time (min)	Urine Volume (ml)	pH	Diltiazem Conc. (ng/ml)	NDD Conc. (ng/ml)	DAD Conc. (ng/ml)
30	41	7.25	n.d.[1]	n.d.	n.d.
90	100	7.59	1257	2666	126
150	355	7.03	1896	1480	225
210	900	6.88	1001	731	79
300	740	7.09	652	806	30
420	285	7.34	842	2077	62
540	250	7.22	656	2391	41
660	225	6.90	791	2060	59
780	160	7.00	839	2134	68
1440	205	6.41	975	2626	147

[1]Not detected

Appendix K (cont'd)

Volunteer 5 (L.K.)- Concentration-Time Data for Diltiazem, NDD and DAD and Measures of Pharmacologic Response

Time (min)	Diltiazem Conc. (ng/ml)	NDD Conc. (ng/ml)	DAD Conc. (ng/ml)	PR Interval (msec)	MAP[1] (mm Hg)	HR[2] (beats/min)
0	n.d.[3]	n.d.	n.d.	188.0	86	53
30	n.d.	n.d.	n.d.	181.6	80	53
45	7.6	5.4	n.d.	188.8	83	50
60	16.0	8.1	n.d.	205.6	83	52
90	35.6	12.9	n.d.	222.4	77	52
120	68.8	18.1	4.1	261.6	80	52
180	128.3	34.0	9.8	264.8	78	49
255	112.6	27.9	12.0	264.0	73	49
360	85.8	35.5	9.6	212.0	79	51
480	59.3	27.2	9.0	179.2	73	48
600	49.6	24.3	9.1	175.2	83	51
720	36.2	22.3	6.5	173.6	82	46
1440	12.2	12.1	5.5	184.8	78	46

[1]Mean arterial pressure, obtained from the Dinamap-845XT Vital Signs Monitor

[2]Heart rate, obtained from the Dinamap-845XT Vital Signs Monitor

[3]Not detected

Appendix K (cont'd)

Volunteer 5 (L.K.)-Summary of Urinary Data

Time (min)	Urine Volume (ml)	pH	Diltiazem Conc. (ng/ml)	NDD Conc. (ng/ml)	DAD Conc. (ng/ml)
30	46	5.96	n.d.[1]	n.d.	n.d.
90	125	6.17	1398	995	69
150	325	6.48	1706	978	81
210	150	6.23	3791	2682	161
300	335	6.36	1749	1581	129
420	140	5.98	3064	4028	224
540	235	6.93	310	1126	0
660	145	6.72	458	2045	61
780	65	6.84	258	1422	n.d.
1440	1140	6.86	224	717	n.d.

[1]Not detected

Appendix K (cont'd)

Volunteer 6 (A.D.)- Concentration-Time Data for Diltiazem, NDD and DAD and Measures of Pharmacologic Response

Time (min)	Diltiazem Conc. (ng/ml)	NDD Conc. (ng/ml)	DAD Conc. (ng/ml)	PR Interval (msec)	MAP[1] (mm Hg)	HR[2] (beats/min)
0	n.d.[3]	n.d.	n.d.	173.6	89	55
30	5.6	n.d.	n.d.	173.6	89	64
45	19.1	5.5	n.d.	148.8	86	56
60	79.8	24.3	6.0	176.0	92	63
90	130.0	42.8	6.5	189.6	82	60
120	168.5	49.3	8.2	228.0	86	56
180	155.2	42.5	11.2	196.0	79	53
255	112.5	34.8	10.8	221.6	87	54
360	61.2	28.3	9.3	177.6	75	67
480	41.7	22.2	8.2	147.2	79	55
600	28.1	19.5	7.3	142.4	82	58
720	19.7	14.4	6.4	139.2	82	59
1440	8.7	6.6	n.d.	144.8	76	66

[1]Mean arterial pressure, obtained from the Dinamap-845XT Vital Signs Monitor

[2]Heart rate, obtained from the Dinamap-845XT Vital Signs Monitor

[3]Not detected

Appendix K (cont'd)

Volunteer 6 (A.D.)-Summary of Urinary Data

Time (min)	Urine Volume (ml)	pH	Diltiazem Conc. (ng/ml)	NDD Conc. (ng/ml)	DAD Conc. (ng/ml)
30	48	5.53	n.d.[1]	n.d.	n.d.
90	63	5.95	5366	4197	166
150	390	6.43	2109	1372	109
210	240	6.30	2771	2271	131
300	280	6.37	1536	1732	92
420	68	5.84	4332	7586	317
540	90	6.29	736	3658	90
660	130	5.90	1116	2765	115
780	120	6.39	591	2084	88
1440	860	6.06	442	1061	87

[1]Not detected